Defining and Manipulating the Epigenetic stability of Human Embryonic Stem Cells

Kee-Pyo Kim, B.Sc., M.Sc.

Thesis submitted to the University of Nottingham for the degree of Doctor of Philosophy

March 2009

ABSTRACT

This thesis aimed to define and manipulate epigenetic stability of human embryonic stem cells (hESCs). The allele-specific expression of 22 imprinted genes was examined in 22 hESC lines by distinguishing parental single nucleotide polymorphisms in genomic DNA and cDNA. Half of the genes examined (*PEG10*, *PEG1*, *MESTIT1*, *IGF2*, *H19*, *GTL2*, *NESP55*, *PHLDA2* and *ATP10C*) showed variable allele-specific expression between cell lines, indicating vulnerability to disrupted imprinting. However, 8 genes (*KCNQ1OT1*, *NDN*, *NDNL1*, *SNRPN*, *IPW*, *PEG3*, *KCNQ1* and *CDKN1C*) showed consistent monoallelic expression. Moreover, 4 genes (*TP73*, *IGF2R*, *WT1* and *SLC22A18*) known to be monoallelically expressed or to exhibit polymorphic imprinting in human tissues were always biallelically expressed. *MEST isoform 1*, *PEG10* and *NESP55* showed an association between the variability observed in interline allele-specific expression status and DNA methylation at their imprinting regulatory regions. These evidences demonstrate gene-specific differences in the stability of imprinted loci in hESC lines and identify disrupted DNA methylation as one potential mechanism.

hESOD1 (human embryonic stem cells overexpressing *DNMT1*) cell lines were established to manipulate epigenetic stability of hESCs. Of ~ 2,200 CpG loci examined by restriction landmark genomic scanning (RLGS), cell lines (cultured over 23 passages) having only endogenous *DNMT1* showed *in vitro* culture induced DNA methylation alterations at 6 loci. However, hESOD1 cell lines showed DNA methylation alterations at only 1 or 2 loci, indicating that overexpression of exogenous *DNMT1* resulted in increased epigenetic stability. Of 14 imprinting regulatory regions, 10 tumour-suppressor gene promoters and 3 repetitive sequences examined, 3 loci (*DAPK-1*, *MGMT* and *TIMP-3*) were indentified to be hypermethylated in hESOD1 cell lines, whereas other 21 loci showed normal methylation levels. These evidences demonstrate that overexpression of exogenous *DNMT1* can prevent hESCs from accumulating DNA methylation changes upon *in vitro* culture and cause locus-specific hypermethylation.

DECLARATION

I hereby declare that this thesis has been composed by myself and has not been submitted for any other degree previously. Acknowledgements of specific procedures not performed by myself are clearly stated; otherwise, the work described is my own

Kee-Pyo Kim

Date: 20th March 2009

ACKNOWLEDGEMENTS

I would like to extend my sincere gratitude to Prof. Lorraine Young for her continual guidance and encouragements during my Ph.D study. I would also like to thank Prof. Chris Denning for his support and helpful discussions.

I would also like to acknowledge all lab colleagues for sharing their knowledge and technical wisdoms with me. Particularly, Dr. Alexandra Thurston, William Steele and Jayson Bispham for practical assistance in analysing genomic imprinting and DNA methylation, Maria D. Barbadillo Munoz, Dr. Cinzia Allegrucci, Dr. David Anderson, Dr. Helen Priddle and Elena Matsa for their advices and helpful discussions for culturing human embryonic stem cells, and Dr. Hazel Cruickshanks and Dr. Christina Tufarelli for providing HCT116 and MCF7 cell lines and the LINE1 probe.

I would also like to thank Prof. Christine Mummery (Hubrecht Institute), Prof. Chad Cowan (Harvard University) and Prof. Douglas Melton (Harvard University) for providing human embryonic stem cell lines, and Prof. David G. Skalnik (Indiana University) and Dr. Jeong-Heon Lee (Indiana University) for performing the DNMT activity assay.

I am also indebted to former supervisors, Prof. Yong-Mahn Han (KAIST) and Prof. Hoon-Taek Lee (Kon-Kuk University). They encouraged and supported me to get involved in this Ph.D. study. Furthermore, I would like to thank the Korea Science and Engineering Foundation (KOSEF) and Inter Disciplinary Training Centre (Regenerative Biology, Stem Cells, University of Nottingham) for providing scholarships of my Ph.D. study.

I would like to thank my family, especially my parents (Ho-Seob Kim and Eh-Sook Chang), grandmother (Seoul-Kang Yoon), sister (Dr. Eun-Hee Kim), parents-in law (Jong-Kyo Shin and Myung-Hee Yoon) and brother-in law (Gun Shin) for their encouragements and supports. Finally, I would like to thank my wife (Borami Shin) and 2-year old daughter (Hye-Won Kim) whose support and patience over the past few years has been greatly appreciated.

PUBLICATION

Kim K-P., Thurston A., Mummery C., Ward-van Oostwaard D., Priddle H., Allegrucci C., Denning, C. and Young L. (2007) Gene-specific vulnerability to imprinting variability in human embryonic stem cell lines *Genome Research* **17**(12), 1731-1742 (see Appendix 3)

CONTENTS

LIST OF FIGURES

LIST OF TABLES

LIST OF ABBREVIATIONS

Abbreviation	Explanation
%	Per cent
℃	Degree Celsius
5mC	5-methylcytosine
aa	Amino acids
ART	Assisted reproductive technology
bp	Base pair
BSA	Bovine serum albumin
BWS	Beckwith-Wiedemann syndrome
CM	Conditioned medium
CO_2	Carbon Dioxide
COBRA	Combined bisulphite restriction analysis
CpG	Cytosine-Guanine dinucleotide
CTCF	CCCTC-transcription factor
DKO	Double knockout
DMR	Differentially methylated region
DMSO	Dimethyl sulfoxide
DNA	Deoxyribonucleic acid
DNMT	DNA methyltransferase
dpc	Days post coitum
EC	Embryonal carcinoma
EG	Embryonic germ
EpiSC	Epiblast stem cell
ESC	Embryonic stem cell
FACS	Fluorescence activated cell sorting
FBS	Foetal bovine serum
FISH	Fluorescence *in situ* hybridisation
FITC	Fluorescein isothiocyanate
GFP	Green fluorescent protein
H_2O	Water
hESOD1	Human embryonic stem cells overexpressing DNMT1
IAP	Intracisternal (A) Particle
ICF	Immunodeficiency, centromeric instability and facial anomalies
ICM	Inner cell mass
ICSI	Intracytoplasmic sperm injection
iPS	Induced pluripotent stem
IVF	*in vitro* fertilisation
KO	Knockout
KSR	Knockout serum replacement
LIF	Leukaemia Inhibitory Factor
LOI	Loss of imprinting
LOM	Loss of methylation
LOS	Large offspring syndrome
M	Molar
Mb	Megabase
MEF	Mouse embryonic fibroblast
MMC	Mitomycin C
mRNA	Messenger RNA
MSP	Methylation-specific PCR
NEAA	Non essential amino acids

PFA	Paraformaldehyde
PBS	Phosphate buffered saline
PCNA	Proliferating cell nuclear antigen
PCR	Polymerase chain reaction
RFLP	Restriction fragment length polymorphism
PGC	Primordial germ cell
PWS	Prader-Willi syndrome
RLGS	Restriction landmark genome scanning
RNA	Ribonucleic acid
RNAi	RNA interference
RT	Reverse transcription
SCID	Severe combined immunodeficiency disease
SCNT	Somatic cell nuclear transfer
SD	Standard deviation
SNP	Single nucleotide polymorphism
T-DMR	Tissue-specific differentially methylated region
TE	Trophectoderm
TKO	Triple knockout
UTR	Untranslated Region
UV	Ultraviolet
V	Volt
ZP	Zona pellucida

GENE NOMENCLATURE

All mouse gene abbreviations are written with a capitalised first letter, and subsequent lower case letters, while for all other species abbreviations are fully capitalised. Italics are used for gene names *per se*, whereas protein names are not italicised.

1. INTRODUCTOIN

In the last two decades, several pluripotent cell lines (embryonal carcinoma cell lines, embryonic stem cell lines, embryonic germ cell lines and induced pluripotent cell lines) have been established in the human (Andrews et al., 1984; Park et al., 2008; Shamblott et al., 1998; Takahashi et al., 2007; Thomson et al., 1998; Yu et al., 2007). Regardless of their origins, all cell lines share similar morphological characteristics, express key pluripotency markers (e.g. OCT4 and NANOG), are capable of long-term self-renewal *in vitro* and have an ability to differentiate into multi-lineages *in vitro* and *in vivo*. Thus, these cell lines are thought to be a model for understanding mechanisms of differentiation of human tissues, and a material for pharmaceutical screening and for human therapeutic applications (reviewed by Fenno et al., 2008; Pera, 2001; Thomson and Odorico, 2000).

Despite these merits, however, several limitations have been exposed while human embryonic stem cells (hESCs) are propagated and differentiated *in vitro*. Firstly, in order to grow them *in vitro*, animal-derived compounds have typically added into culture media that are not acceptable for safe human transplantation (Amit et al., 2004; Ludwig et al., 2006b; Xu et al., 2001). Secondly, in terms of differentiation, optimised protocols and conditions have not been discovered to yield homogeneous populations (Anderson et al., 2007; Burridge et al., 2007; Denning et al., 2006). Thirdly, they are prone to accumulate karyotypic abnormalities (especially gain of chromosomes 17q and 12) over extended culture (Baker et al., 2007; Draper et al., 2004). Finally, there are indicators of epigenetic variations in hESCs upon *in vitro* culture (Allegrucci et al., 2004; Bibikova et al., 2008; Pannetier and Feil, 2007; Rugg-Gunn et al., 2007), the consequences of which are not yet defined.

A larger number of studies in various species have suggested that epigenetic errors in at least some imprinted genes of preimplantation stage embryos and their derived foetuses, placentae (Khosla et al., 2001a; Mann et al., 2004; Sato et al., 2007; Young et al., 2001) and ESCs (Dean et al., 1998; Fujimoto et al., 2006; Humpherys et al., 2001; Mitalipov et al., 2007) can occur when assisted reproduction technology (ART) procedures including superovulation, *in vitro* maturation (IVM), *in vitro* culture (IVC), *in vitro* fertilisation (IVF) are applied. These errors cause phenotypic abnormalities, growth defects and Large offspring syndrome (LOS) during prenatal and postnatal

development (Dean et al., 1998; Fernandez-Gonzalez et al., 2004; Young et al., 2001). Current methods for establishing and culturing hESC lines rely on ART procedures (reviewed by Fenno et al., 2008; Hoffman and Carpenter, 2005), implicating that at least some hESC lines may have epigenetic errors at imprinted loci.

Because epigenetic errors at imprinted loci are known to be closely associated with tumourigenesis and several congenital disorders in the human (reviewed by Feinberg, 2007; Horsthemke and Ludwig, 2005; Jelinic and Shaw, 2007; Robertson, 2005), comprehensive studies are required to indentify whether hESC lines are epigenetically stable while they are *in vitro* cultured. There are conflicting data about the epigenetic stability of *in vitro* cultured hESCs (Allegrucci et al., 2007; Bibikova et al., 2006; Calvanese et al., 2008; Maitra et al., 2005; Mitalipov, 2006; Plaia et al., 2006; Rugg-Gunn et al., 2005; Sun et al., 2006). Preliminary studies of a limited number of imprinted genes in few hESC lines detect little or no epigenetic variations and disruptions (Mitalipov, 2006; Plaia et al., 2006; Rugg-Gunn et al., 2005; Sun et al., 2006). However, recent studies have detected epigenetic instability at certain CpG islands, ribosomal DNA and tumour-suppressor gene promoters by increasing the number of hESC lines and genes examined (Allegrucci et al., 2007; Bibikova et al., 2006; Calvanese et al., 2008; Maitra et al., 2005).

1.1 Human embryonic stem cell line

1.1.1 Derivation

The first derivation of hESC lines was reported by Thomson et al., (1998). hESC lines were established from inner cell masses (ICMs) of human blastocyst stage embryos that were *in vitro* fertilised and cultured (Thomson et al., 1998). Embryos were donated from infertile couples who underwent IVF procedures. The zona pellucidae (ZP) of 20 blastocysts were removed by pronase, and 14 ICMs were isolated by immunosurgery and plated onto mouse embryonic fibroblasts (MEFs) mitotically inactivated by irradiation. Following 9 to 15 days in culture, ICM-derived outgrowths were dissociated into clumps either by exposure to Ca^{2+}/Mg^{2+}-free PBS or dispase, or mechanical dissociation, and then re-plated onto fresh MEFs to continue their expansion. Finally, 5 hESC lines (H1, H7, H9, H13 and H14) were established

(Thomson et al., 1998). hESCs showed prominent nucleoli and a high ratio of nucleus to cytoplasm and express high levels of telomerase activity and cell-surface markers (e.g. SSEA-3, SSEA-4) (Thomson et al., 1998). They were capable of prolonged symmetrical self-renewal *in vitro* and had a capacity to differentiate into derivatives of all primitive embryonic germ layers (ectoderm, mesoderm and endoderm) *in vivo*, as demonstrated from teratoma formation (Thomson et al., 1998).

Based on initially designed conditions by Thomson et al., (1998), numerous hESC lines have been established. Currently, ~ 400 hESC lines are presumed to be established in over 20 countries (reviewed by Allegrucci and Young, 2007). The majority of cell lines are generated from the ICMs of blastocyst stage embryos. However, some cell lines are generated from single blastomeres of 8- to 10- cell stage embryos or morula stage embryos (Chung et al., 2008; Klimanskaya et al., 2006; Strelchenko et al., 2004). Very recently, 6 patient-specific hESC lines have been established from pathenogenetic derived blastocyst stage embryos (Revazova et al., 2007). Furthermore, it has been clearly confirmed that SCNT-hES-1, previously shown to be derived by somatic cell nuclear transfer (SCNT) (Hwang et al., 2004), is a pathenogenetically derived-stem cell line, as determined by genome-wide single nucleotide polymorphisms (SNPs) and DNA methylation analyses at three imprinted loci (*KvDMR1*, *H19* DMR and *SNRPN* DMR) (Kim et al., 2007a).

1.1.2 Characterisation

Established hESC lines need to be characterised within at least six criteria (reviewed by Hoffman and Carpenter, 2005; Laslett et al., 2003). The criteria are (1) the expression of hESC-specific cell surface makers (e.g. SSEA-3, SSEA-4, TRA-1-60, TRA-1-60, TRA-1-81 and alkaline phosphatase), (2) high level of telomerase activity, (3) a normal euploid karyotype over extended culture, (4) the expression of pluripotent transcription factors (e.g. OCT3/4 and NANOG), (5) teratoma formation (with components of all three germ layers) after injection into severe combined immunodeficient (SCID) mice, and (6) spontaneous differentiation into three germ layers under *in vitro* conditions. These criteria are important to determine whether hESC lines have proliferative, pluripotency, differentiative capacities and karyotypic stability (reviewed by Hoffman and Carpenter, 2005; Laslett et al., 2003). Although investigators realise the importance of characterisation for maintaining hESC lines,

some of newly derived cell lines have not been fully characterised. For example, teratoma formation, karyotyping and telomerase activity analyses are frequently omitted (Chung et al., 2008; Ludwig et al., 2006b; Richards et al., 2002). Importantly, each laboratory uses different protocols and materials to characterise their derived cell lines, implicating batch-to-batch and data variations between laboratories. Thus, a recent study by the international stem cell initiative (ISCI) has compared 59 hESC lines derived from 17 laboratories using same protocols and materials (e.g. antibodies) to identify common characteristics between lines (Adewumi et al., 2007) that can define the hESCs characteristics.

1.1.3 Culture conditions

hESC lines are usually derived and cultured on MEFs as feeder cells in medium containing foetal bovine serum (FBS) (Thomson et al., 1998). Importantly, FBS is a complex mixture containing undefined compounds, has a batch-to-batch variation and may contain factors to induce differentiation of hESCs (reviewed by Unger et al., 2008). Furthermore, to isolate ICM from the blastocyst stage embryo, immunosurgery needs to be performed using antibodies raised from animal species (Solter and Knowles, 1975). Therefore, current methods and materials for deriving and culturing hESC lines are not independent of animal-derived components and hence the transfer of animal pathogens to hESC lines can be a potential risk. In fact, a study by Martin et al., (2005) has demonstrated that hESC lines can incorporate an immunogenic nonhuman sialic acid, N-glycolylneuraminic (Neu5Gc), from mouse feeder cells, FBS and/or KnockOut SR (KSR) that they are cultured with. Thus, new culture conditions (serum-, animal product- and feeder cell-free) are required for safe human transplantation.

1.1.3.1 Serum-free

A study by Amit et al. (2000) has suggested that basic fibroblast growth factor (bFGF) is an essential component to maintain an undifferentiated state of hESCs in serum-free condition. Thus, FBS was replaced with the bFGF and KSR (serum replacement) (Amit et al., 2000). Based on above condition, 17 HUES-lines (HUES1 to HUES17) and HS293 and HS306 cell lines were established (Cowan et al., 2004; Inzunza et al., 2005). However, feeder cells such as MEFs and postnatal human fibroblasts are still required to support hESCs self-renewal in this condition. Furthermore, KSR contains

AlbuMAX which is a lipid-enriched bovine serum albumin (BSA) (Amit et al., 2000; Unger et al., 2008). Thus, this system is not animal-derived component independent.

1.1.3.2 Feeder cell-free

A feeder cell-free culture condition was firstly introduced by Xu et al., (2001). The feeder cells were replaced with either matrigel, which was a solubilised basement membrane preparation extracted from mouse Engelbreth-Holm-Swarm (EHS) sarcoma (Kleinman and Martin, 2005), or human laminin (Xu et al., 2001). Thus, hESCs can be maintained on either matrigel or laminin in the MEF-conditioned medium (CM) containing KSR and bFGF. Within this condition, hESCs exhibit long-term maintenance *in vitro* with the inhibition of spontaneous differentiation (Xu et al., 2001). However, MEFs need to be cultured in the medium containing FBS to obtain MEF-CM, and KSR still needs to be added. Thus, this condition is also not animal-derived component independent.

1.1.3.3 KSR-free

Recently, two cell lines (WA15 and WA16) have been derived in a serum- and KSR-independent culture medium which is named as TeSR1 (Ludwig et al., 2006a; Ludwig et al., 2006b). Five factors, bFGF, LiCl (lithium chloride), GABA (γ-aminobutyrid acid), pipecolic acid and TGFβ, are components of TeSR1 (Ludwig et al., 2006a; Ludwig et al., 2006b). However, several limitations have been exposed in this condition. The WA15 cell line has a karyotypic abnormality over extended culture (Ludwig et al., 2006a; Ludwig et al., 2006b). Moreover, the costs of some components are very expensive for everyday research use generally. Therefore, a new variant, mTeSR1, that contains BSA and cloned zebrafish basic fibroblast growth factor (zbFGF) has been developed for culture of hESCs on Matrigel (Ludwig et al., 2006a).

1.1.4 Differences between mouse and human ESCs

Morphological differences between human and mouse ESCs have been reported on the basis of manual passage methods (Ginis et al., 2004). mESCs form thick layers up to ten cells over feeder cells, whereas hESCs form thin layers from two to four cells (Ginis et al., 2004). Moreover, hESCs form round, flat and loose colonies with well-defined edges, whereas mESCs form more spherical and tight colonies (Ginis et al.,

2004; Reubinoff et al., 2000). The population-doubling (PD) time of hESCs (24h to 72h) is much longer than that of mESCs (~ 12h) (Cowan et al., 2004). Although almost all stem cell markers including SSEA-3/4, TRA-1-60/81/254, GTCM-2, TG-30/343 and alkaline phosphatase are expressed in hESCs, only SSEA-1 and alkaline phosphatase are present in mESCs (Henderson et al., 2002; Laslett et al., 2003). In addition, class 1 major histocompatbility (MHC) and Thy1 antigens are expressed only in hESCs (Draper et al., 2002).

The pluripotency of both mESCs and hESCs is guided by distinct signalling pathways. Activin/Nodal/TGFβ (transforming growth factor β) pathways are essential for maintaining the undifferentiated state of hESCs (Beattie et al., 2005; James et al., 2005; Vallier et al., 2005; Xiao et al., 2006), and thus bFGF needs be added in the hESC culture medium (Xu et al., 2005). However, mESCs rely on JAK (janus-associated tyrosine kinase)/STAT (signal transducers and activators of transcription)/BMP (bone morphogenetic protein) pathways to maintain an undifferentiated state without feeder cells (Williams et al., 1988; Ying et al., 2003a), and thus LIF (leukemia inhibitory factor) should be added in the mESC culture medium (Williams et al., 1988). BMP4 in combination with LIF has shown to be sufficient to maintain mESCs (serum- and feeder-free) in an undifferentiated state (Ying et al., 2003a). However, LIF and BMPs are not able to maintain an undifferentiated state of hESCs in the feeder-free culture condition (Pera et al., 2004; Reubinoff et al., 2000; Xu et al., 2002).

Recently, mouse and rat epiblast stem cells (EpiSCs) have been derived from the late epiblast layer of postimplantation embryos (5.75 dpc and 7.5 dpc, respectively) (Brons et al., 2007). Interestingly, the Activin/Nodal signalling pathway was required for maintaining pluripotency of EpiSCs within the chemically defined medium, indicating similarity to hESCs. Also, EpiSCs were morphologically distinct from mESCs but similar to hESCs, showing compacted and round colonies (Brons et al., 2007). However, SSEA-1 is expressed in EpiSCs which is not present in hESCs (Brons et al., 2007).

1.1.5 Differences between human pluripotent cell lines

Years before the derivation of hES and human embryonic germ (hEG) cell lines (Shamblott et al., 1998; Thomson et al., 1998), the human embryonal carcinoma (hEC) cell line provides a *in vitro* model to understand mechanisms of differentiation of human tissues (Przyborski et al., 2000). The hEC cell line is derived from a testicular germ cell tumour (Andrews et al., 1984). This cell line contains undifferentiated stem cell components of teratocarcinomas (Pal and Ravindran, 2006; Sperger et al., 2003). Thus, the hEC cell line is generally considered as malignant counterparts of embryonic stem cells. hEG cell lines are derived from primordial germ cells (PGCs) isolated from the developing gonadal ridges and mesenteries of 5- to 9-week embryos (Shamblott et al., 1998). Very recently, induced pluripotent stem (iPS) cell lines are derived from somatic cells by viral introduction of transcriptional factors including OCT3/4 and SOX2 with either NANOG and LIN28 (Yu et al., 2007), or MYC and KLF4 (Park et al., 2008; Takahashi et al., 2007). Although they are derived from different sources, they share many parts of common features including pluripotency, and *in vivo* and *in vitro* differentiative capacity. However, they have distinct differences between cell lines.

hES, hEC and iPS cells share a similar morphology that is distinct from hEG cells (Andrews et al., 1984; Ginis et al., 2004; Shamblott et al., 1998; Takahashi et al., 2007; Thomson et al., 1998). hEG cells form tight and more spherical colonies that are difficult to be dissociated into single cells, whereas hES, hEC and iPS cells form relatively flat, loose and round colonies that are easily dissociated into single cells by trypsin and other enzymes. At the molecular level, hES, hEC and iPS cells express all cell-surface markers except for SSEA-1, but hEG cells express all makers including SSEA-1 (Andrews et al., 1984; Thomson et al., 1998; Thomson et al., 1995). OCT3/4 and NANOG are expressed in hES, hEC and iPS cells, but their expression are still unknown in hEG cells (Andrews et al., 1984; Shamblott et al., 1998; Takahashi et al., 2007; Thomson et al., 1998). Furthermore, hEC cells frequently contain karyotypic abnormalities, often with gain of chromosome 17q and the presence of one or more isochromosomes 12p (Andrews et al., 1984; Draper et al., 2004). hES cells retain normal karyotypes at earlier passages but have similar karyotypic abnormities of hECs under the feeder-free condition (Baker et al., 2007; Draper et al., 2004). hEG and iPS cells retain normal karyotypes at earlier passages, but it has not confirmed yet at later passages (Park et al., 2008; Shamblott et al., 1998; Yu et al., 2007). Finally, hEC cells

form teratoma containing simple structures, whereas hES and iPS cells form teratoma with the variety of tissues representative of all three embryonic germ layers (Andrews et al., 1984; Park et al., 2008; Thomson et al., 1998; Yu et al., 2007). Teratoma formation has not been examined in hEG cells (Shamblott et al., 1998).

Table 1-1. Comparison of human pluripotent stem cells

Marker	hES cells	hEC cells	iPS cells	hEG cells
Morphology	Flat, loose and round colony	Flat, loose and round colony	Flat, loose and round colony	Tight and spherical colony
SSEA-1	-	-	-	+
SSEA-3	+	+	+	+
SSEA-4	+	+	+	+
TRA-1-60	+	+	+	+
TRA-1-81	+	+	+	+
Alkaline phosphatase	+	+	+	+
OCT3/4	+	+	+	Unknown
NANOG	+	+	+	Unknown
Karyotype	Normal	Abnormal	Normal	Normal
Teratoma formation	+	+	+	Unknown

+; expresssed, -; not expresssed

1.2 Epigenetic modifications

In the last decade, epigenetic mechanisms have been extensively studied with different model systems to understand how gene transcription is regulated and mediated in nuclei of mammalian cells. Genes need to be inactive or active depending on the tissue type, and this process is guided by epigenetic modifications. DNA methylation and histone modifications are known to be critical epigenetic modifications of the genome that can directly modulate chromatin structure (e.g. heterochromatin and euchromatin) and regulate gene expression in mammalian cells (reviewed by Bird, 2002).

The term “epigenetic” describes heritable changes in gene expression that occur without genotypic changes during development (reviewed by Jaenisch and Bird, 2003; Li, 2002; Reik, 2007; Surani, 2001). In mammals, epigenetic marks inherited from parents are thought to be erased at the early stages of germ cell development (reviewed by Constancia et al., 2004; Ferguson-Smith and Surani, 2001; Reik et al., 2001). Subsequently, neo epigenetic marks at DNA and histones are differentially set up among lineages, resulting in differential gene expression of each cell. Lineage-

specific gene expression allows stem cells to be differentiated into various types of tissues, together with the production of tissues-specific transcriptional factors.

Recently, the 'Human epigenome project (see http://www.epigenome.org/)' has emerged (2008; Brena et al., 2006) and 'Human genome project (see http://genomics.energy.gov/)' has been completed (Lander et al., 2001; Venter et al., 2001). A number of techniques have been newly developed to investigate epigenetic modifications in detail, revealing that aberrant epigenetic modifications in the genome might be associated with many types of human diseases (reviewed by Feinberg, 2007; Robertson, 2005).

1.2.1 DNA methylation

DNA methylation is known to be a major epigenetic process in the mammalian genome and is responsible for diverse biological phenomena including embryonic development, genomic imprinting, X-inactivation, host-defence against transposable elements and tissue-specific gene expression (reviewed by Bird, 2002; Feinberg, 2007; Jaenisch and Bird, 2003; Reik, 2007; Surani, 2001). DNA methylation occurs by covalent addition of a methyl group (CH_3) from the methyl donor, *S*-adenosy-L-methionine (AdoMet) to the 5-position of cytosine in the pyrimidine ring of a symmetrical cytosine-guanine (CpG) dinucleotide, resulting in the formation of 5-methylcytosine (m^5C) (Figure 1-1) (reviewed by Bestor, 2000; Cheng and Blumenthal, 2008). Less frequently, DNA methylation can also occur in non-CpG dinucleotides such as CpNpG and non-symetrical CpA and CpT (Ramsahoye et al., 2000). The enzymatic reaction of DNA methylation is carried out by DNA methyltranferases (DNMTs) (Bestor et al., 1988; Okano et al., 1998a).

In the human genome, 60 ~ 90% of cytosine residues are located in CpG dinucleotides and approximately 50 million CpG dinucleotides are present (Lander et al., 2001; Venter et al., 2001; Zhao and Zhang, 2006). Over 10% of CpG dinucleotides are concentrated on CpG rich regions designated as CpG islands which are normally unmethylated, whereas over 80 % of CpG dinucleotides are not associated with CpG islands and highly methylated (Zhao and Zhang, 2006). Takai and Jones (2002) have defined that a CpG island is a region of 500 base pairs in size with GC content of at least 55% and a ratio of observed/expected CpG frequency of at least 0.65. By

computational analysis of the human genome sequence, 29,000 CpG islands are predicted in the human genome (Lander et al., 2001; Venter et al., 2001). Most human chromosomes contain between 5 to 15 CpG islands per megabase (Mb), but some chromosomes including Y chromosome, chromosome 16, 17, 22 and 19 contain more or less CpG islands in a range 2.9 to 43 CpG islands per Mb (Lander et al., 2001).

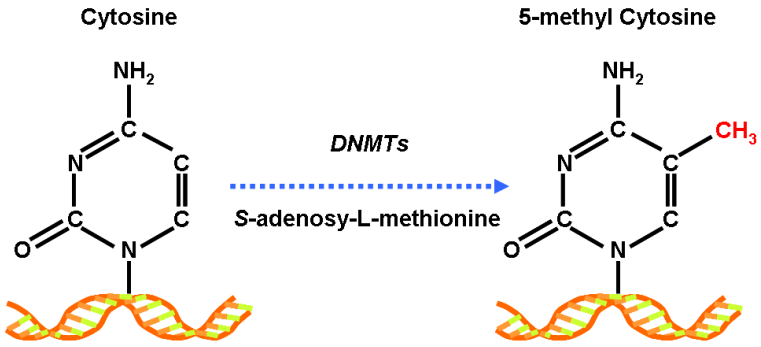

Figure 1-1. The formation of 5-methylcytosine
The *DNA methyltransferases* (*DNMTs*) catalyses the methylation of the 5 position of the cytosine ring by using *S*-adenosy-L-methionine (AdoMet) as the donor molecule for the methyl group (CH_3).

1.2.2 DNA methylation and transcriptional control

Methylated CpG islands are not randomly distributed in the genome but are clustered in the specific chromatin, heterochromatin, containing repetitive sequences and transposable elements (Yoder et al., 1997b). This is to ensure transcriptional silencing of potentially harmful transposons or viral sequences (reviewed Bird, 2002; Jaenisch and Bird, 2003). In the euchromatin regions, however, unmethylated CpG islands are typically found near 5' end regions of genes such as untranslated regions (UTRs), promoters and the first exon and intron (Marino-Ramirez et al., 2004), and most of them overlap the transcriptional start sites, resulting in gene expression (Figure 1-2 A).

1.2.2.1 Monoallelic methylation

Exceptions are CpG islands involved in genomic imprinting and genes on the inactive X chromosome in females. Genomic imprinting is monoallelic expression of a subset of genes that can be mediated by methylation of one parental allele at specific regulatory regions (reviewed by Constancia et al., 2004; Ferguson-Smith and Surani, 2001; Reik and Walter, 2001; Surani, 2001). Thus, the imprinted allele is generally (but not always) silenced by methylation, but the other allele of imprinted genes is expressed and unmethylated. In terms of X inactivation, the promoter region of the

transcriptionally active *Xist* allele on the inactive X chromosome is unmethylated, whereas that of the transcriptionally inactive *Xist* allele on the active X chromosome is methylated (reviewed by Avner and Heard, 2001). Thus, gene loci related to genomic imprinting and X chromosome inactivation are monoallelically methylated on their regulatory regions to result in monoallelic expression.

1.2.2.2 Hypermethylation

Hypermethylation has frequently been found at the promoter regions of tumour-suppressor genes (TSGs) and miRNA genes in various types of cancers, resulting in transcriptional silencing (Figure 1-2 B) (reviewed by Bibikova et al., 2008; Esteller, 2007; Feinberg, 2007; Reik, 2007). For instance, *ESR1* (*Estrogen receptor*), *CDH1* (*E-Cadherin*) and *TIMP-3* (*tissue inhibitor of metalloproteinase-3*) promoters are hypermethylated in cancers derived over 15 different human tissues and in most cases these genes are transcriptionally silenced, although they are expressed and unmethylated in normal tissues (Ohm et al., 2007). Furthermore, *mir-9-1*, *mir124a3*, *mir-148a*, *mir-152* and *mir-663* promoters are hypermethylated in human breast cancers that is associated with transcriptional silencing of these genes (Lehmann et al., 2008).

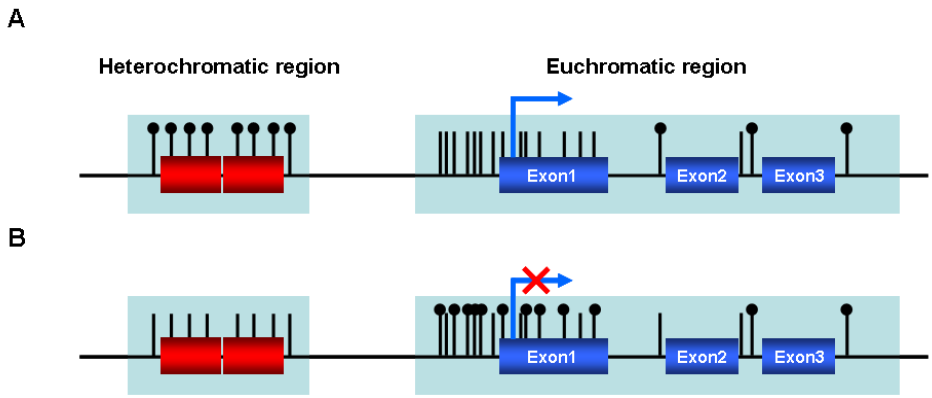

Figure 1-2. Typical DNA methylation patterns of CpG dinucleotides in the human genome
(A) In normal cells, CpG islands at the promoter region of gene are unmethylated permitting gene expression, whereas CpG islands at repetitive sequences within the heterochromatic region are hyper-methylated. (B) In cancer cells, the promoter region of the gene is hyper-methylated resulting in gene silencing, whereas CpGs within repetitive sequences are hypo-methylated. Red rectangles indicate repetitive sequences in heterochromatin. Blue rectangles indicate exons of a tumour suppressor gene in euchromatin. Vertical bars indicate CpG dinucleotides. Filled circles represent methylated CpG dinucleotides. Arrows indicate transcription. Adapted from Esteller (2007).

1.2.2.3 Mechanisms

At least three mechanisms are thought to be involved in transcriptional regulation mediated by DNA methylation. Firstly, transcription factors such as major late transcription factor (MLTF) and upstream transcription factor (USF) are not able to access their binding sites in some genes due to the epigenetic modification of cytosine bases to 5-methylcytosine (Watt and Molloy, 1988). This prevents these genes from being transcribed. Secondly, particular transcriptional insulators, CTCF (CCCTC-biding factor) and YY1, bind to only unmethylated DNA (Donohoe et al., 2007; Fedoriw et al., 2004; Kim et al., 2006; Schoenherr et al., 2003). Their bindings do not allow enhancers to access to promoter regions of genes, resulting in gene silencing. Finally, methyl-CpG binding domain proteins (MBD1, MBD2, MBD3, MBD4 and MeCP2) bind only methylated DNA and recruit chromatin remodelling complexes to form a transitionally repressive structure that leads to gene silencing (Fujita et al., 2003).

1.2.3 DNA methyltransferases (DNMTs)

DNA methylation is enzymatically catalysed by DNA methyltransferases (DNMTs) (reviewed by Bestor, 2000; Li, 2002). So far, three active DNMTs (DNMT1, DNMT3A and DNMT3B) have been identified in both the human and mouse (Bestor et al., 1988; Okano et al., 1998a). DNMT1 maintains DNA methylation patterns during the progression of replication at the S phase using hemimethylated CpG dinucleotides as substrates in the nascent strand of DNA (reviewed by Bestor, 2000; Li, 2002). Thus, it is popularly known as a maintenance methyltransferase. DNMT3A and DNMT3B are thought to be involved in the creation of new methylation patterns at unmethylated CpG dinucleotides as substrates (Okano et al., 1999; Okano et al., 1998a). Thus, they are generally named as *de novo* methyltransferases. Additionally, DNMT3L and DNMT2 have been identified, but no methyltransferase enzymatic activities have been confirmed yet in mammals (Aapola et al., 2000; Aapola et al., 2002; Okano et al., 1998b). Instead, DNM3L acts as a methylation mediator by stimulating the methylation activity of DNMT3A and DNMT3B (Hata et al., 2002; Suetake et al., 2004). DNMT2 acts as a RNA methyltransferase which methylates $tRNA^{Asp}$ (Goll et al., 2006; Jurkowski et al., 2008).

1.2.3.1 DNMT1

1.2.3.1.1 Alternative transcripts

The first mammalian *Dnmt1* cDNA was identified from mouse by Bestor et al., (1988). Dnmt1 encodes for a protein of 1620 amino acids and 190 kDa in molecular weight (Bestor et al., 1988). *Dnmt1* has tissue-specific splicing transcripts, somatic- (*Dnmt1s*), pachytene spermatocyte- (*Dnmt1p*) and oocyte-specific *Dnmt1* (*Dnmt1o*) isoforms, which are derived from sex-specific promoters (Mertineit et al., 1998). Dnmt1o (175 kDa in molecular weight) is a truncated form 118 N-terminal amino acids of Dnmt1s (Mertineit et al., 1998). Dnmt1o has an enzymatic activity and is present in unfertilised oocytes and preimplantation embryos (Mertineit et al., 1998). Dnmt1o protein is localised in the cytoplasm of the metaphase II oocyte and preimplantation stage embryos, but it is in the nucleus at the 8-cell stage only (Cardoso and Leonhardt, 1999; Howell et al., 2001; Mertineit et al., 1998). In human, expression of an oocyte-specific *DNMT1* mRNA is detected in mature oocytes and embryos at the 2-cell, 4-cell and blastocyst stages, but not in somatic tissues (Hayward et al., 2003). The expression and distribution of DNMT1o protein has not been examined yet in human oocytes and preimplantation stage embryos.

In initial studies, no DNMT1s protein is detected in mouse oocytes and preimplantation stage embryos, although its transcript is present (Cardoso and Leonhardt, 1999; Mertineit et al., 1998). Thus, it is believed that only Dnmt1o can maintain DNA methylation patterns during preimplantation stage development. However, recent studies by Kurihara et al. (2008) and Cirio et al. (2008) have found that Dnmt1s protein is present in the nucleus of mouse oocytes and preimplantation stage embryos. Moreover, Kurihara et al. (2008) has demonstrated that inactivation of *Dnmt1s* in mouse embryos by either RNA-mediated knockdown or antibody neutralisation leads to loss of methylation at the *H19* DMR and intracisternal A-type particle (IAP), indicating that *Dnmt1s* can be involved in the maintenance of DNA methylation patterns at imprinted loci and repetitive sequences during preimplantation development (Kurihara et al., 2008).

1.2.3.1.2 *de novo* methylation

DNMT1 can also act as a *de novo* methyltrasferase to methylate unmethylated CpG dinucleotides, although *in vitro* assays have indicated a 10 to 50 fold preference for hemimethylated CpG sites (Bacolla et al., 1999; Pradhan et al., 1999; Yoder et al., 1997a). For example, the over-expression of *Dnmt1* in mESCs and human lung fibroblasts (IMR90/SV40) shows a significant increase in both maintenance and *de novo* DNA methyltransferase activities, resulting in hypermethylation of repetitive elements, tumour-suppressor gene promoters and imprinted loci (Biniszkiewicz et al., 2002; Vertino et al., 1996). Furthermore, of 1749 CpG loci examined by restriction landmark genomic scanning (RLGS), an additional 373 loci (21%) are *de novo* methylated in human lung fibroblasts overexpressing *DNMT1* (HMT17, HMT19 and HMT1E1 lines) (Feltus et al., 2003).

1.2.3.1.3 Role in development and differentiation

Gain- and loss-of-function studies of *DNMT1* in the mouse and human have demonstrated that appropriate *DNMT1* expression is essential for embryonic development and lineage-specific differentiation. mESCs overexpressing *Dnmt1* exhibit hypermethylation at repetitive sequences (centromeres and IAP) and loss of imprinting of *Igf2* and *H19* (but not *Igf2r*, *Peg3*, *Snrpn* and *Grf1*) that leads to embryonic lethality after diploid and tetraploid blastocyst injection (Biniszkiewicz et al., 2002). Moreover, the inactivation of *Dnmt1* in mESCs show extensive perturbations of DNA methylation (at repetitive sequences, sub-telomeric domains and imprinted loci) and genomic imprinting that leads to elongated telomeres, failure of differentiation towards hematopoietic and cardiomyocyte lineages, and embryonic lethality (Chen et al., 2003; Gonzalo et al., 2006; Jackson et al., 2004). Furthermore, *Dnmt1* knockout (KO) MEFs show demethylation at IAP elements and loss of imprinting that gives rise to growth retardation and cell death mediated by *p53* (Jackson-Grusby et al., 2001). In the human, complete deletion of *DNMT1* in the human colon cancer cell line (HCT116) leads to chromosomal defects, cell cycle arrest and cell death (Chen et al., 2007).

1.2.3.2 Overlapping functions of DNMTs

If one of *DNMTs* is functionally lost by mutation or deletion, it appears that they can compensate for each other to maintain DNA methylation patterns, although the

supporting data is contradictory. Single KOs of *Dnmt3a* and *Dnmt3b* in mESCs and MEFs show no apparent changes in global methylation levels (Okano et al., 1999; Dodge et al., 2005). Only certain classes of minor satellite sequences are demethylated (Okano et al., 1999). In contrast to single KOs, however, *Dnmt3a* and *Dnmt3b* double knockout (DKO) mESCs and *Dnmt1*, *Dnmt3a* and *Dnmt3b* triple knockout (TKO) mESCs show substantial loss of methylation at imprinted loci, retroviral sequences, and major and minor satellite repeats (Okano et al., 1999; Tsumura et al., 2006). In the human, *DNMT1* and *DNMT3B* DKO in HCT116 show significantly reduced methyltransferase activity and loss of genomic DNA methylation (about 95%), but single KOs of *DNMT1* and *DNMT3B* in HCT116 exhibit only 20% and 3% loss of methylation, respectively (Rhee et al., 2002; Rhee et al., 2000). The methylation of promoter regions of $p16^{INK4a}$ (*a prototypic INK4 protein*), *TIMP-3* and *IGF2* is not or little changed in single KO cells, whereas these regions were completely demethylated in DKO cells (Rhee et al., 2002). Importantly, single KOs of *Dnmt3a* and *Dnmt3b* in mESCs have no perturbation of undifferentiated stem cell states, showing normal morphology and expected expression and promoter unmethylation of transcriptional factors (*Oct4* and *Nanog*) (Jackson et al., 2004; Li et al., 2007; Okano et al., 1999). These cells retain an ability to differentiate into hematopoietic and cardiomyocyte lineages and *Oct4* and *Nanog* promoters are methylated after differentiation (Jackson et al., 2004; Li et al., 2007). Unlike in single KOs, *Dnmt3a* and *Dnmt3b* DKO mESCs show reduced ability to form embryo bodies and differentiate into hematopoietic and cardiomyocyte lineages (Jackson et al., 2004; Li et al., 2007). This has been defined by abnormal expression of trophoblast-, mesodermal- and endodermal markers (Jackson et al., 2004; Li et al., 2007). The promoter regions of *Oct4* and *Nanog* remain unmethylated and the genes are still expressed after differentiation (Jackson et al., 2004; Li et al., 2007). Collectively, the inactivation of one of the *DNMTs* does not affect global DNA methylation and cellular differentiation capacity. This may be due to the fact that *DNMTs* can compensate for each other to maintain normal DNA methylation patterns in the mammlian genome. This also indicates that they may share the target sites to be methylated.

Notably, there are contrasting data. Chen et al., (2003) has showed that in *Dnmt3a* and *Dnmt3b* DKO J1 mESCs, endogenous C-type retrovirus (pMO), minor satellite and IAP repeats are demethylated. These demethylated loci can be remethylated by

overexpression of either *Dnmt3a* or *Dnmt3b* cDNA, but not with *Dnmt1* cDNA (Chen et al., 2003). Furthermore, loci demethylated by inactivation of *Dnmt1* can be remethylated by overexpression of *Dnmt1* cDNA, but not with *Dnmt3a* and *Dnmt3b* cDNA, respectively (Chen et al., 2003). Thus, Chen et al., (2003) has suggested that the role of *Dnmt1*, *Dnmt3a* and *Dnmt3b* can not be overlapped and their target sites are different, and thereby they are required cooperative expression to maintain normal DNA methylation patterns in the mammalian genome. On the other hand, of 1300 CpG sites examined by RLGS, an additional 236 loci are detected, indicating demethylation in *Dnmt1* KO cells (Hattori et al., 2004). In addition, the same loci are identified to be demethylated in *Dnmt3a* and *Dnmt3b* DKO cells, suggesting *Dnmt1*, *Dnmt3a* and *Dnmt3b* can share same target sites to be methylated (Hattori et al., 2004).

1.2.3.3 Structure of DNMTs and associated functional domains

1.2.3.3.1 DNMT1

DNMT1 consists of two domains namely a regulatory, N-terminal domain and a catalytic, C-terminal domain (reviewed by Bestor, 2000; Cheng and Blumenthal, 2008). Both domains are linked by a short stretch of repeated Gly-Lys (GK) dipeptides (Figure 1-3). The C-terminal domain of *DNMT1* contains six conserved motifs (I, IV, VI, VIII, IX and X) that allows transfer of methyl groups from AdoMet to cytosine, mostly within CpG dinucleotides (Bacolla et al., 1999; Posfai et al., 1989; Pradhan et al., 1999). In detail, motifs I and X fold together to form AdoMet binding sites, motif IV contains the prolylcysteinyl dipeptide providing the cytosine thiolate at active sites, motif VI contains the glutamyl residue that protonates the 3 position of the target cytosine, motif IX maintains the structure of the target recognition domain that makes base-specific contacts in the major groove, and VIIIs' function is not clear yet (Lauster et al., 1989; Posfai et al., 1989; Yoder et al., 1997a). The N-terminal domain of *DNMT1* contains a number of functional domains including a proliferating cell nuclear antigen (PCNA) binding domain (PBD), a nuclear localisation signal (NLS), a DNA replication foci targeting sequence (RFT or TS), a cysteine-rich Zn^{2+} binding motif (ATRX), and a polybromo homology domain (PBHD) (Bestor, 2000; Cheng and Blumenthal, 2008). Thus, the N-terminal domain allows targeting to replication foci, discriminating between hemimethylated and unmethylated CpG dinucleotides, and associating with chromatin modifiers, while DNA is replicated

(reviewed by Bestor, 2000; Cheng and Blumenthal, 2008). Furthermore, the N-terminal domain is responsible for recruiting *Dnmt1* to DNA repair sites (Mortusewicz et al., 2005).

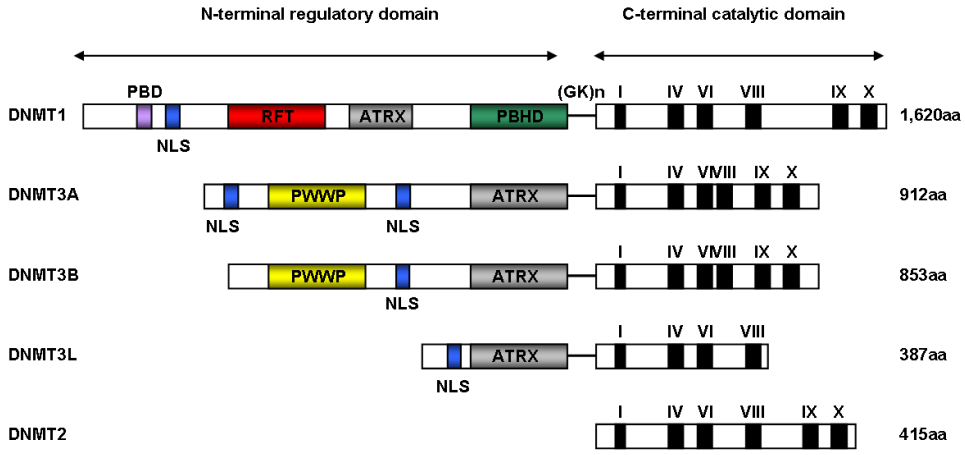

Figure 1-3. The structure of the member of the mammalian DNMT family
The N-terminal domain contains a proliferating cell nuclear antigen (PCNA)-binding domain (PBD) shown as a purple rectangle, a nuclear localisation signal (NLS) shown as a blue rectangle, an a cysteine-rich Zn^{2+} binding motif (ATRX) shown as a grey rectangle, a polybromo homology domain (PBHD) shown as a green rectangle, a DNA replication foci targeting sequence (RFT or TS) shown as a red rectangle and a tetrapeptide (proline-tryptophan-tryptophan-proline) motif (PWWP) shown as a yellow rectangle. The C-terminal domain contains six conserved motifs (I, IV, VI, VIII, IX and X). Both domains are linked by a short stretch of repeated Gly-Lys (GK) dipeptides. I is involved in the formation of the AdoMet binding sites, IV binds to substrate cytosine at the active site, VI contains the glutamyl residue serving as a proton donor, IX maintains the structure of the substrate-biding sites, X participates in the formation of the AdoMet binding sites. VIIIs' function is not clear yet. aa is as amino acids. Adapted from Bestor (2002), and Cheng and Blumenthal (2008)

The N-terminal domain of DNMT1 possesses the capability of transcriptional repression, independent of catalyzing DNA methylation (Rountree et al., 2000). The transcriptional repression activity can be enhanced by interacting with histone deacetylases (HDAC1 and HDAC2) which remove acetyl groups from the tail of histones and help to maintain condensed chromatin structure and transcriptional silenced states (Fuks et al., 2000; Rountree et al., 2000). Moreover, DNMT1 interacts with the number of proteins, including heterochromatin protein 1β (HP1β), histone methyltransferases (SUV39H1 and G9A), tumour suppressor protein 53 (p53), retinoblastoma (Rb), DNMT3A/3B and DNA methyltransferase 1 associated protein 1 (DMAP1) (Esteve et al., 2005; Esteve et al., 2006; Fuks et al., 2000; Fuks et al., 2003; Kim et al., 2002; Pradhan and Kim, 2002; Rountree et al., 2000) that enhances transcriptional repression activity of DNMT1. For example, DMAP1 (encoding for

467 amino acids and 53 kDa in molecular weight) was isolated as a DNMT1 interacting protein by yeast two-hybrid screening (Rountree et al., 2000). A luciferase activity assay has demonstrated that transcriptional repression activity of DNMT1 can be stimulated by a direct interaction of 212 - 422 amino acids of DMAP1 with the first 120 amino acids of DNMT1 (Liu and Fisher, 2004; Rountree et al., 2000). Therefore, a specific interaction between DNMT1 and other proteins related to histone modifications, cell cycle and apoptosis might be essential to mediate transcriptional regulation of genes in mammalian nuclei.

1.2.3.3.2 DNMT3A and DNMT3B

DNMT3A and DNMT3B share a structural similarity with DNMT1 (reviewed by Bestor, 2000; Cheng and Blumenthal, 2008) (Figure 1-3). Both DNMT3A and DNMT3B proteins are organised into a large regulatory N-terminal domain and a smaller catalytic C-terminal domain (Figure 1-3). Two domains are linked by a short stretch of repeated Gly-Lys (GK) dipeptides (reviewed by Bestor, 2000; Cheng and Blumenthal, 2008). The C-terminal domain of DNMT3A and DNMT3B contains six conserved motifs (I, IV, VI, VIII, IX and X). Their regulatory N-terminal domains contain NLS, ARTX and PWWP (proline-tryptophan-tryptophan-proline motif) (Bestor, 2000; Cheng and Blumenthal, 2008).

A truncation mutant study of Dnmt3a and Dnmt3b has suggested that the PWWP domain is essential for the association with heterochromatin at the S phase to maintain DNA methylation patterns at pericentric heterochromain regions (Chen et al., 2004). Moreover, the PWWP domain of Dnmt3a and Dnmt3b is associated with transcriptioanlly silenced and condensed mitotic chromatin during mitosis (Ge et al., 2004). Recently, point mutation (serine 270) of the PWWP domain has been found in Japanese patients who suffering from the ICF (immunodeficiency, centromeric instability, and facial anomalies) syndrome (Shirohzu et al., 2002), which is characterised by loss of methylation at pericentromeric heterochromatin of chrosomosomes 1, 9 and 16 (Chen et al., 2004; Xu et al., 1999).

DNMT3A and DNMT3B can repress gene transcription by means, independent of catalyzing *de novo* DNA methylation (Bachman et al., 2001; Fuks et al., 2001; Fuks et al., 2003). Their transcriptional repression activities are mediated by ARTX-like

PBHD of the N-terminal domain (Bachman et al., 2001; Fuks et al., 2001). The transcriptional repression activity of DNMT3A and DNMT3B can be enhanced by interacting with each other, histone-modifying enzymes, histone-remodelling enzymes or other co-repressors. Specifically, DNMT3A and DNMT3B interact with DNMT1/3L, HDACs, RP58 (sequence-specific transcriptional repressor), hSNF2H (ATP-dependent chromatin remodelling enzyme), HP1β and SUV39H1 (Bachman et al., 2001; Fuks et al., 2000; Fuks et al., 2001; Fuks et al., 2003; Geiman et al., 2004; Kim et al., 2002). These interactions allow forming of heterochromatin and stimulating of transcriptional repression activity.

1.2.3.3.3 DNMT3L

Another methyltransferase like protein (DNMT3L) has been identified in the human and mouse (Aapola et al., 2000; Aapola et al., 2001). Like *Dnmt3a* and *Dnmt3b*, *Dnmt3l* is highly expressed in the germ cell and embryonic stem cell (Bourc'his et al., 2001; Kaneda et al., 2004; La Salle et al., 2004). *Dnmt3l* is essential for establishing and maintaining DNA methylation patterns at imprinted loci, unique nonpericentric heterochromatic sequences and repetitive sequences (Arnaud et al., 2006; Bourc'his et al., 2001; Hata et al., 2002; Webster et al., 2005). DNMT3L also consist of two domains as same as other DNMTs have, and both domains are linked by GK dipeptides (Figure 1-3). However, *DNMT3L* has only few components in both domains. The N-terminal domain of *DNMT3L* contains only ARTX and NLS, and only four conserved motifs (I, IV, VI and VIII) are present in the C-terminal domain. Thus, this can be explained why *DNMT3L* lacks the enzymatic activity to transfer methyl groups to DNA (Bestor, 2000; Margot et al., 2003; Suetake et al., 2004). Interestingly, even if *DNMT3L* has a NLS domain (156-159 amino acid), it is shown to be localised in both the cytoplasm and nucleus of NIH3T3, COS-7 and human rhabdomyosarcoma (RD) cell line (Aapola et al., 2002; Hata et al., 2002).

1.2.3.3.4 DNMT2

DNMT2 is the smallest methyltransferase and has only the C-terminal domain containing six conserved motifs (reviewed by Bestor, 2000). In contrast to the other DNMTs, DNMT2 is localised to the cytoplasm of transfected NIH3T3, indicating that it does not directly contact with genomic DNA (Goll et al., 2006). No methylation or

phenotypic changes are detected in *Dnmt2* KO mice and no endogenous DNA methyltransferase activity has been confirmed yet (Okano et al., 1998b). However, interestingly, transgenic flies and *Drosophila* S2 cells overexpressing mouse and *Drosophila Dnmt2* cDNA show an increased methylation activity and hypermethylation at two loci (CG8547 and CG8553) (Narsa Reddy et al., 2003; Tang et al., 2003). Furthermore, recently it has been reported that *DNMT2* can methylate to C5 position of cytosine 38 (C38) in $tRNA^{Asp}$, suggesting that it may function as an active RNA methyltransferase (Goll et al., 2006). Conserved motifs IV, VI and VII of DNMT2 catalyses methylation to $tRNA^{Asp}$ (Jurkowski et al., 2008).

1.2.4 Histone modifications

Within eukaryotic nuclei, genomic DNA needs to be tightly compacted and organised into a structure, chromatin (Bernstein et al., 2005; Lachner et al., 2003). The nucleosome (the fundamental unit of chromatin) is composed of 146 base pairs of DNA wrapped around an octamer that consists of two copies each of core histone H2A, H2B, H3 and H4 (Bernstein et al., 2005; Lachner et al., 2003). The nucleosomes are linked together by the linker DNA and histone H1. Although the core region of the histone octamer remains inside the nucleosome, the N-terminal tails of histones are exposed and post-translationally modified by acetylation, methylation, phosphorylation, ubiquitylation and sumoylation (Bernstein et al., 2005; Lachner et al., 2003). For example, histone H3 can be methylated at lysines 4, 9, 27, 36, and 79, and histone H4 can be methylated at lysine 20 (Lachner et al., 2003).

Histone modifications co-operate to form a specific chromatin structure and to regulate gene transcription (reviewed by Jaenisch and Bird, 2003; Li, 2002; Reik, 2007). For instance, both acetylation of H3 and H4, and methylation of H3 at lysine 4 (H3-K4), at lysine 36 (H3-K36) and at lysine 79 (H3-K79) are closely associated with active genes and frequently found in euchromatin regions, whereas methylation of H3 at lysine 27 (H3-K27) and methylation of H3 at lysine 9 (H3-K9) and at lysine 20 (H3-K20) are co-related with transcriptional repression of genes and the formation of large constitutive heterochromatin domains (Bernstein et al., 2005; Peters et al., 2001; Rice et al., 2003; Schotta et al., 2004).

Different degrees of methylation at the same residue may influence different degrees of chromatin structures. Histone methylation takes place on the lysine (K) residues. Lysine residues can be mono-, di-, and try-methylated (Peters et al., 2003; Rice et al., 2003; Schotta et al., 2004; Wu et al., 2005). H3-K9 trimethylation is predominantly localised in pericentric heterochromatin regions, whereas H3-K9 mono- and dimethylation are enriched at early replicating euchromatin regions (Rice et al., 2003; Wu et al., 2005). In addition, H3-K27 monomethylation and H4-K20 trimethylation are largely localised in heterochromatin regions, whereas H3-K27 di- and trimethylation, and H4-K20 mono- and dimethylation are present in euchromatin regions (Peters et al., 2003; Schotta et al., 2004).

1.2.5 Histone methyltransferases (HMTs)

Histone methylation is catalysed by the number of histone methyltransferases (HMTs). Five histone methyltransferases (Suv39h1, Suv39h2, G9a, Eset and Eu-HMTase) have been identified in mammals (Dodge et al., 2004; Peters et al., 2001; Tachibana et al., 2001). Interestingly, although all histone methyltransferases can transfer methyl groups at K residues of histone H3 and H4, they have distinct enzymatic activities and localisation patterns in mammalian nuclei. Suv39h1 and Suv39h2 tend to be localised in the pericentric heterochromatin region, whereas G9a and Eset are localised in the euchromatic region (Dodge et al., 2004; Lehnertz et al., 2003; Tachibana et al., 2001; Tachibana et al., 2002). An *in vitro* activity assay has demonstrated that G9a has a 10- to 20-fold strong enzymatic activity, compared to Suv39h1 (Tachibana et al., 2001). In addition, G9a can methylate both H3-K27 and H3-K9, whereas Suv39h1 and Suv39h2 preferentially methylates only H3-K9 (Rice et al., 2003; Tachibana et al., 2001; Tachibana et al., 2002).

KO studies in mice have suggested that *Suv39h1*, *Suv39h2*, *G9a* and *Eset* are essential for early embryonic development and germ cell differentiation (Dodge et al., 2004; Lehnertz et al., 2003; Peters et al., 2003; Peters et al., 2001; Tachibana et al., 2002). *G9a* KO mice showed loss of H3-K9 methylation in the euchromatic region and apoptosis that leads to embryonic lethality between 9.5 - 12.5 dpc (Peters et al., 2003; Tachibana et al., 2002). *Eset* KO mice also result in embryonic lethality between 3.5 and 5.5 dpc (Dodge et al., 2004). *Suv39h1/2* DKO mice show loss of H3-K9

methylation in the heterochromatin region, chromosomal instability and impaired spermatogenesis (Lehnertz et al., 2003; Peters et al., 2001).

1.2.6 Histone modifications associated with DNA methylation

Histone modifications have an important role to maintain DNA methylation patterns in the genome. In the fungus (*Neurospora crassa*), inactivation of *DIM-5* (*defective in methylation 5*; encoding a H3-K9 methyltransferase) leads to loss of DNA methylation at ζ-η, Ψ63, 1D21, 9A20 and rDNA (Tamaru and Selker, 2001). Moreover, in *Arabidopsis thaliana*, the mutation of *KRYPTONITE* (a H3-K9 methyltransferase) shows loss of DNA methylation at CpNpG trinucleotides (but not CpG dinucleotides) (Jackson et al., 2002) and the deletion of *DDM1* (*decrease in DNA methylation*), a SWI2/SNF2-like protein, causes 70% reduction of genomic methylation at repetitive sequences (Jeddeloh et al., 1999). In mammals, *Suv39h1* and *Suv39h2* DKO mESCs show loss of DNA methylation at pericentric satellite repeats (but not at minor satellites or endogenous C-type retroviruses) (Lehnertz et al., 2003). Furthermore, *G9a* KO mESCs show loss of maternal methylation at the *Snrpn* DMR, resulting in loss of imprinting of *Snrpn* (Xin et al., 2003). The mutation of *Lsh* (*lymphoid specific helicase*, a member of the SNF2 chromatin remodelling family) in mice shows substantial loss of DNA methylation at the repetitive sequences, promoter regions of single copy genes (*b-Globin* and Pgk-2), and an imprinted locus (*H19* DMR) (Dennis et al., 2001). These evidences indicate DNA methylation and histone modifications (chromatin remodelling) are interdependent and the interplay between them is required for regulating gene transcription in mammals.

1.3 Genomic imprinting

1.3.1 Imprinted genes

Genomic imprinting describes an epigenetic process, resulting in the parent of origin-specific monoallelic expression of a subset of genes (reviewed by Constancia et al., 2004; Reik and Walter, 2001; Surani, 2001). Although most genes in mammals are expressed from both parental alleles, imprinted genes are preferentially expressed from either the paternal or maternal allele (reviewed by Ferguson-Smith and Surani 2001). Since the first imprinted genes, mouse *insulin-like growth factor 2* (*Igf2*), its

neighbouring gene *H19*, and *Igf2 receptor* (*Igf2r*) have been discovered (Barlow et al., 1991; Bartolomei et al., 1991; DeChiara et al., 1991), so far ~ 80 imprinted genes in mice and ~ 50 imprinted genes in humans have been identified (Morison et al., 2005). This number is continually increasing. A study by using large-scale expression profiling has estimated that a larger number of candidate transcripts (over 2,000) in the mouse and human genome are imprinted (Nikaido et al., 2003), although allele-specific expression of these candidates has not been examined. Table 1-1 summarises known human imprinted genes. Briefly, human imprinted genes have been identified on at least 10 human chromosomes. Most of them are clustered in specific chromosomes (e.g. chromosomes 7, 11, 15), whereas some of them are randomly disributed in the rest of chromosomes. Approximately, half of genes are expressed from the maternal allele and the other half are expressed from the paternal allele.

Table 1-2. Known human imprinted genes

locus	Transcript	Functional component	Imprinting status	Expressed allele
1p36	*TP73*		I	M
1p31	*ARHI*		I	P
6q24	*HYMAI*		I	P
	PLAGL1		I	P
6q25	*IGF2R*		PI	M
7p12	*GRB10*		I	P or M[a]
7q21	*CALCR*		PD	M
	SGCE		I	P
	PEG10		I	P
	PPP1R9A		I	M
	PON1		PD	P
	DLX5		I	M
7q32	*CPA4*		I	M
	MEST		I	P or M[a]
	MESTIT1		I	P
	COPG2IT1		I	P
10q22	*CTNNA3*		PD	M
11p15	*H19*		I	M
	IGF2		I	P
	IGF2AS		I	P
	INS		I	P
	TRPM5		PD	P
	KCNQ1		I	M
	KCNQ1OT1		I	P
	CDKN1C		I	M
	SLC22A1LS		PD	M
	SLC22A18		I	M
	PHLDA2		I	M
	OSBPL5		I	M
	ZNF215		PD	M

11p13	*WT1*		I	P
	WT1AS		I	P
14q32	*DLK1*		I	P
	MEG3		I	M
15q11	*MKRN3*		I	P
	MAGEL2		I	P
	NDN		I	P
	SNURF-SNRPN	*SNURF*	I	P
		SNRPN	I	P
		HBII-436	I	P
		HBII-13	I	P
		HBII-437	I	P
		HBII-438A	I	P
		PWCR1	I	P
		HBII-52	I	P
		HBII-438B	I	P
		UBE3A-AS	I	P
	UBE3A		I	M
	ATP10A		I	M
18q21	*TCEB3C*		I	M
19q13	*PEG3*		I	P
	ZIM2		I	P
20q11	*NNAT*		I	P
20q13	*L3MBTL*		I	P
	GNAS1	*NESP55*	I	M
		GNASXL	I	P
		Exon-1A	I	P
		GS-α	I	M
	SANG		I	P

I, imprinted; NI, not imprinted; PI, polymorphic imprinted; PD, provisional data; M, maternal; P, paternal; [a] imprinting is isoform dependent. Adopted from Morison et al., (2005).

Detailed summaries of known imprinted genes, their functions and expression patterns are available in following websites; (1) Mammalian Genetics Unit, MRC, Harwell, Oxfordshire, UK; (http://www.har.mrc.ac.uk/research/genomic_imprinting/), (2) Cancer Genetic Laboratory, Department of Biochemistry, University of Otago, Dunedin, New Zealand; (http://igc.otago.ac.nz/home.html), (3) Jirtle Laboratory, Duke University, Durham, USA, the Geneimprint; (http://www.geneimprint.com/), and (4) Laboratory for Genome Exploration Research Group, RIKEN Genomic Research Center, Yokohama, Japan; (http://fantom2.gsc.riken.go.jp/imprinting/).

1.3.2 Human chromosome 11p15

Most imprinted genes (at least 80%) are not randomly distributed within the genome but are clustered in specific chromosomes, which is thought to influence their

coordinated transcriptional regulations within clusters (Reviewed by Ferguson-Smith and Surani, 2001; Reik and Walter, 2001; Surani, 2001). Some clusters are very large (several megabases in size) and are highly conserved between the human and mouse. Within clusters, maternally and paternally imprinted genes, as well as non-imprinted genes are localised together. For example, 10 imprinted genes (6 maternally expressed genes and 4 paternally expressed genes) and 7 non-imprinted genes have been identified on human chromosome 11p15 (Table 1-1 and Figure 1-4). This cluster consists of two independent imprinting sub-domains, domain 1 containing *MRPL23*, *H19*, *IGF2*, *IGF2AS* and *INS* genes and domain 2 containing *NAPIL4*, *TSSC3*, *TSSC5*, *CDKN1C*/*p57*^{KIP2}, *KCNQ1*, *KCNQ1OT1*/*LIT1*, *TSSC4* and *CD81*. The allele-specific expression of these genes are guided by two imprinting control regions (ICRs; ICR1 and ICR2) located on *KCNQ1-KCNQ1OT1* and *IGF2-H19* loci, and differentially methylated regions (DMRs) located on the upstream of the *IGF2* gene (reviewed by Reik and Walter, 2001; Robertson, 2005; Surani, 2001).

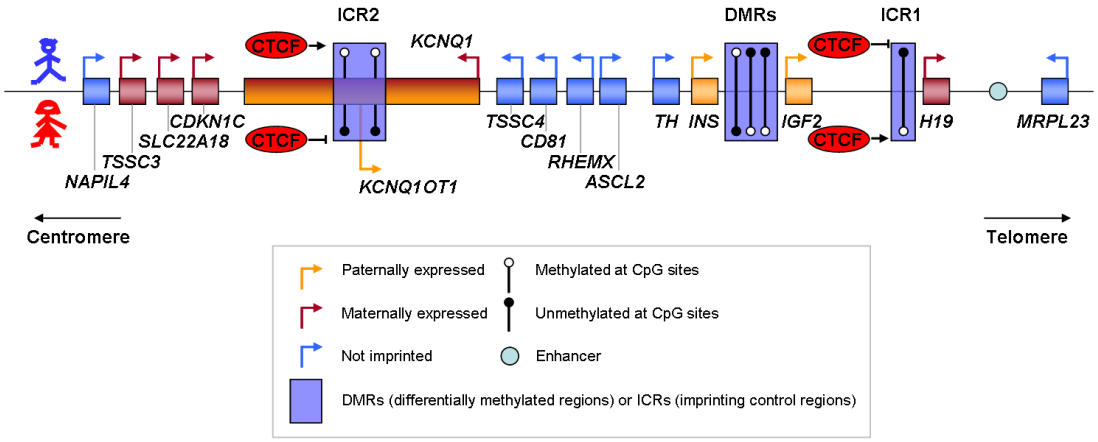

Figure 1-4. Human chromosome 11p15
7 non-imprinted genes (*NAPL4*, *TSSC4*, *CD81*, *RHEMX*, *ASCL2*, *TH*, *MRPL23*) and 10 imprinted genes can be found within this locus. Within the 10 imprinted genes, 6 (*OSBPL5*, *TSSC3*, *SLC22A18*, *CDKN1C*, *KCNQ1*, *H19*) are maternally expressed and 4 (*KCNQ1OT1*, *INS*, *IGF2*, *IGF2AS*) are paternally expressed. Imprinted gene expression in this locus is controlled by ICRs (imprinting control regions), DMRs (differentially methylated regions), CTCF (CCCTC-binding factor) proteins and enhancers. ICR2 is also known as *KvDMR1* and is maternally methylated and paternally unmethylated. ICR1 is also known as *H19* CTCF and is paternally methylated and maternally unmethylated. Upstream of *IGF2*, three DMRs (DMR0, DMR1, DMR2) have been characterised in the human. DMR0 is maternally methylated, whereas DMR1 and DMR2 are paternally methylated. Adapted from Robertson (2005).

The CTCF (CCCTC-binding factor) proteins are also involved in the regulation of imprinted gene expression within two domains. They bind to only unmethylated

alleles of both ICR1 and ICR2 and act as insulators to prevent enhancers from binding to the promoter region of corresponding genes (Fitzpatrick et al., 2007; Prawitt et al., 2005; Sparago et al., 2004). For example, once the CTCF protein binds to the unmethylated maternal allele of ICR1, enhancers are not able to access to the promoter region of *IGF2*. Thus, *IGF2* is transcriptionally silenced from the maternal allele, whereas the *H19* gene can be expressed. On the paternal allele of ICR1, DNA methylation blocks CTCF binding that allows enhances to access to the promoter regions of *IGF2*, resulting in *IGF2* expression from the paternal allele and *H19* silenced (Reviewed by Ferguson-Smith and Surani, 2001; Reik and Walter, 2001).

1.3.3 Differentially methylated regions (DMRs)

The allele-specific expression of imprinted genes is controlled by DNA methylation at their regulatory regions (reviewed by Li, 2002; Reik and Walter, 2001). In imprinted loci, DNA methylation usually occurs in a specific region named as differentially methylated region (DMR). The DMR is differentially methylated between parental alleles to direct monoallelic expression of its corresponding imprinted genes. For example, the *SNRPN* gene is paternally expressed and maternally silenced in association with paternal unmethylation and maternal methylation at the *SNRPN* DMR (El-Maarri et al., 2001; Geuns et al., 2003; Lucifero et al., 2002). So far, at least 15 DMRs have been identified in the human and mouse and they are largely conserved between species (Table 1-2). Most of them are localised in promoter regions of their relevant imprinted genes. However, some DMRs are localised in intronic regions (e.g. *KvDMR1* and *Igf2r* DMR2) that are associated with the expression of antisense transcripts (e.g. *KCNQ1OT1* and *Air*) (Horike et al., 2000; Lee et al., 1999; Smilinich et al., 1999; Vu et al., 2004; Wutz et al., 1997). Not all DMRs are associated with allele-specific expression of imprinted genes. For instance, *IGF2R* DMR2 is differentially methylated, but biallelic expression of *IGF2R* is frequently found in human tissues, indicating that other epigenetic mechanisms such as hisone modifications may be involved in *IGF2R* imprinting (Monk et al., 2006a; Vu et al., 2004).

Table 1-3. Known DMRs and timing of establishment of their imprints

Gene	Imprinting marks		Reference
	Human	Mouse	
IGF2R-AIR locus	-	S (DMR1), G (DMR2; M in oocyte, U in sperm)	(Arnaud et al., 2006; Lucifero et al., 2002; Stoger et al., 1993)
PEG1	G (M in oocyte, U in sperm)	G (M in oocyte, U in sperm)	(Kerjean et al., 2000; Li et al., 2002; Lucifero et al., 2002; Sato et al., 2007)
SLC22A18	-	S	(Lewis et al., 2004)
CDKN1C	-	S	(Lewis et al., 2004)
KvDMR1	G (M in oocyte, U in sperm)	G (M in oocyte, U in sperm)	(Geuns et al., 2007b; Khoureiry et al., 2008; Lewis et al., 2004; Sato et al., 2007; Umlauf et al., 2004)
IGF2	S (DMR0, DMR2)	S (DMR0, DMR2)	(Murrell, 2006; Oswald et al., 2000)
RASFRF1		G (M in sperm, U in oocyte)	(Yoon et al., 2002)
U2AF1-RS1	-	S and G[a]	(Shibata et al., 1997)
IGF-H19 locus	G (M in sperm, U in oocyte)	G (M in sperm, U in oocyte)	(Borghol et al., 2006; Davis et al., 2000; Hartmann et al., 2006; Kerjean et al., 2003; Kerjean et al., 2000; Lucifero et al., 2002; Olek and Walter, 1997; Sato et al., 2007; Ueda et al., 2000)
DLK1-GTL2 locus	G (M in sperm, U in oocyte)	G (M in sperm and U in oocyte)	(Geuns et al., 2007a; Lin et al., 2003)
NDN	G (PM in oocyte, U in sperm)	G (PM in oocyte, U in sperm)	(El-Maarri et al., 2001; Hanel and Wevrick, 2001)
SNRPN	G[b] (M in oocyte, U in sperm)	G (M in oocyte, U in sperm)	(El-Maarri et al., 2001; Geuns et al., 2003; Lucifero et al., 2002)
PEG3	-	G (M in oocyte, U in sperm)	(Arnaud et al., 2006; Lucifero et al., 2002)
NESP55	-	S or G[c]	(Hayward et al., 2001; Liu et al., 2000)

[a] dependent on regions examined; [b] conflicting data; [c] dependent on isoforms; -, Not examined yet; M, methylated; U, unmethylated; PM, partially methylated; G, germline DMRs; S, somatic DMRs

Histone modifications can also occur at DMRs and ICRs that may regulate imprinted gene expression (Fournier et al., 2002; Grandjean et al., 2001; Gregory et al., 2001; Hu et al., 2000; Lewis et al., 2004). Repressive histone marks such as methylation at histone H3 lysine 9 (H3-K9) and lysine 27 (H3-K27) tend to be found in the methylated allele of ICRs and DMRs, whereas active histone marks such as H3 and H4 acetylation can be found in the unmethylated allele of ICRs and DMRs. For example, in *Igf2r*, *Igf2-H19*, *Snrpn*, and *U2af1-rs1* locus, acetylation of H3 and H4 are present on the unmethylated alleles of their DMRs, whereas methylation of H3-K9 can be found in the methylated alleles (Fournier et al., 2002; Grandjean et al., 2001; Gregory et al., 2001; Hu et al., 2000; Lewis et al., 2004).

1.3.4 The life cycle of imprint

1.3.4.1 Erasure

In gametes, before the acquisition of differential DNA methylation patterns on both parental alleles, pre-existing DNA methylation patterns from the previous generation require to be erased (reviewed by Constancia et al., 2004; Ferguson-Smith and Surani, 2001; Reik and Walter, 2001; Surani, 2001). In the mouse, this occurs when primordial germ cells (PGCs) migrate from the genital ridge to the gonad (at approximately days 10.5 to 13.5 of gestation) (Hajkova et al., 2002; Li et al., 2004; Szabo et al., 2002). This timing corresponds to the 5- to 11-weeks in the human (Onyango et al., 2002). A study by Hajkova et al., (2002) has examined DNA methylation patterns at DMRs of *Peg3*, *Lit1*, *Snrpn*, *H19* and non-imprinted gene (*α-actin*) in developing germ cells. All of above genes are demethylated between 10.5 and 13.5 dpc. This is associated with the allele-specific expression of imprinted genes (*Snrpn*, *Igf*2 and *H19*), showing that monoallelically expressed genes become biallelically expressed between 10.5 and 13.5 dpc (Szabo et al., 2002). Furthermore, embryo cloning (SCNT, somatic cell nuclear transfer) using PGCs as donor cells shows that imprints at different loci examined including *Peg1*, *Meg3*, *Peg3* and *H19* are erased between 10.5 and 13.5 dpc (Lee et al., 2002; Yamazaki et al., 2003).

1.3.4.2 Establishment and maintenance

Following this erasure, DNA methylation imprints are established at two different developmental time points, during gametogenesis and during embryogenesis to result in monoalleleic expression of imprinted genes. At most DMRs, DNA methylation patterns are established when germ cells are differentiating (reviewed by Reik and Walter, 2001; Surani, 2001). These DMRs are termed as ‘germline DMRs or primary DMRs’. However, at ‘somatic DMRs’ (also known secondary DMRs or post-zygotic DMRs), DNA methylation patterns are established after fertilization or at post-implantation stages of development. Table 1-2 summaries the timing of establishment of imprints at known DMRs. For example, *Igf2r* DMR2 is methylated in oocytes and unmethylated in sperm, indicating that it is a germline DMR, whereas *Igf2r* DMR1 is considered as a somatic DMR that is unmethylated in both oocytes and sperm (Stoger et al., 1993).

In germline DMRs, the establishment of genomic imprints occurs at different developmental time points between female and male. In male germline, acquisition of methylation at *H19*, *Rasgrf1* and *Gtl2* DMRs begins to be initiated in prenatal prospermatogonia before the start of meiosis and is completed prior to the end of the pachytene phase of meiosis (between 13.5 and 18.5 dpc) (Davis et al., 2000; Li et al., 2004; Oakes et al., 2007; Ueda et al., 2000). In female germ line, DNA methylation begins to be acquired in the growing oocyte (10 ~ 25 days after birth) following the pachytene phase of meiosis, but this may continue after fertilization in the female pronulceus of the zygote (El-Maarri et al., 2001; Lucifero et al., 2002; Obata and Kono, 2002). Once imprints are established, they can be maintained throughout mammalian development.

This whole process termed as 'the life cycle of imprint' has been well reviewed by Constancia et al., (2004) and Ferguson-Smith and Surani, (2001). If this process does not progress properly during development and differentiation of gametes and embryos due to either mutation or deletion of imprinted regulatory regions, diseases such as congenital disorders and cancers occur in humans and animals (see section 1.3.5).

1.3.4.3 Imprint formation and *DNMTs*

During development of gametes, the PGCs genome is globally demethylated between 10.5 and 13.5 days of mouse gestation, although repetitive sequences including intracisternal A particle (IAP), long interspersed nuclear element 1 (LINE1) and minor satellites appear to be only partially demethylated (Hajkova et al., 2002; Kafri et al., 1992; Li et al., 2004; Szabo et al., 2002). At the same time, DNA methylation imprints are erased in PGCs. Following demethylation, genomes in PGCs are subsequently *de novo* methylated between 15.5 and 18.5 days of gestation, as determined by immunostaining against 5-methylcytosine (5mC) (Coffigny et al., 1999). At the same time, DMRs within imprinted loci begin to acquire DNA methylation in male germ cells (Davis et al., 2000; Li et al., 2004; Oakes et al., 2007; Ueda et al., 2000), although maternal imprints are acquired in growing oocytes after birth (El-Maarri et al., 2001; Lucifero et al., 2002; Obata and Kono, 2002). Thus, genome-wide demethylation and *de novo* methylation are associated with the erasure and establishment of imprints in developmental timeline.

During embryogenesis, in only few hours later after fertilisation (at the pronuclear stage), the paternal genome is actively demethylated, whereas the maternal genome is passively demethylated in a manner dependent of DNA replication and this may continue up to 16-cell stage (Mayer et al., 2000; Oswald et al., 2000; Santos et al., 2002). Following further cleavages of embryos, *de novo* methylation occurs to establish tissue-specific epigenetic marks (Mayer et al., 2000; Oswald et al., 2000; Santos et al., 2002). However, sex-specific imprints are preserved from genome-wide demethylation and *de novo* methylation, although almost all non-imprinted genes are demethylated and subsequently *de novo* methylated (Gaudet et al., 2004; Lane et al., 2003). It is unclear yet how imprints are resistant to the waves of DNA demethylation and *de novo* methylation in the genome. One possible explanation is that unmethylted alleles can be protected from *de novo* methylation by interaction with CTCF proteins or other proteins (e.g. YY1) recognising unmethylated CpG loci (Donohoe et al., 2007; Fedoriw et al., 2004; Fitzpatrick et al., 2007; Kim and Kim, 2008; Kim et al., 2006). Alternately, the methylated alleles can be protected from demethylation by interacting methyl-CpG biding domain proteins (e.g. MBDs) or other proteins recognising methylated CpG loci (reviewed by Bird, 2002).

Studies by the deletion and mutation of *Dnmts* have demonstrated that the acquisition and maintenance of DNA methylation patterns at imprinted loci are guided by *Dnmts* (Bourc'his et al., 2001; Howell et al., 2001; Kaneda et al., 2004; Kurihara et al., 2008; Lucifero et al., 2007). *Dnmt1o* KO in mice show loss of methylation at maternally methylated DMRs with biallelic expression of maternally imprinted genes in embryos, indicating that *Dnmt1o* is important for the maintenance of maternal imprints during early embryonic development (Howell et al., 2001). In addition, inactivation of *Dnmt1s* in preimplantation stage embryos leads to loss of methylation at the *H19* DMR (Kurihara et al., 2008). Moreover, *Dnmt3a* KO in germ cells show loss of methylation at both maternal and paternal imprinted loci (Kaneda et al., 2004). Inactivation of *Dnmt3L* in mice leads to loss of imprinting of all maternally imprinted genes including *Snrpn*, *Ndn*, *Zfp127*, *Kcnq1ot1* and *Peg3* in oocytes and preimplantation embryos (Bourc'his et al., 2001; Hata et al., 2002). Thus, all *Dnmts* are required to establish and maintain normal imprints during gametogenesis and embryogenesis.

1.3.5 Imprinting disruption associated with human disease

The disruption of imprinting and dysfunction of one or more imprinted loci are associated with a range of human congenital disorders, including Prader-Willi syndrome (PWS), Angelman syndrome (AS), Silver-Russel syndrome (SRS), and Beckwith-Wiedemann syndrome (BWS), Transient Neonatal Diabetes Mellitus (TNDM), Albrights hereditary osteodystrophy (AHO), Pseudohypothyroidism type 1a (PHP-1a) and type 1b (PHP-1b), Biparental complete hydatidiform mole (BiCHM) (reviewed by Robertson, 2005). In addition, imprinting disruption is also associated with human cancers (reviewed by Feinberg, 2007; Holm et al., 2005; Jelinic and Shaw, 2007). Table 1-3 summaries imprinted genes associated with human diseases.

Table 1-4. Known imprinted genes associated with human diseases

Location	Gene	Disease type
1p36	*TP73*	Cancer
6q24	*HYMAI*	TNDM
	PLAGL1	TNDM
6q25	*IGF2R*	Cancer
7p12	*GRB10*	SRS
7q21	*PEG10*	Cancer
	DLX5	Rett syndrome
7q32	*MEST*	SRS, Cancer, BiCHM, AgCHM
	MESTIT1	SRS
11p13	*WT1*	Cancer
11p15	*H19*	BWS, Cancer
	IGF2	BWS, Cancer
	KCNQ1	BWS, RWS, JLNS
	KCNQ1OT1	BWS, Cancer, TNDB, BiCHM, AgCHM
	CDKN1C	BWS, Cancer
	TSSC3	Cancer
	SLC22A18	Cancer
	ZNF215	BWS
14q32	*DLK1*	Cancer
	MEG3	Cancer
15q11	*NDNL1*	PWS
	NDN	PWS
	SNRPN	PWS, BiCHM, AgCHM
	IPW	PWS
	ATP10C	AS, Cancer
	UBE3A	AS
19q13.4	*PEG3*	Cancer, BiCHM, AgCHM
20q13	*L3MBTL*	Cancer
	GNAS1	AHO, PHP-IA, PHP-IB, BiCHM, AgCHM, MAS

PWS, Prader-Willi syndrome; AS, Angelman syndrome; SRS, Silver-Russel syndrome; BWS, Beckwith-Wiedemann syndrome; TNDM, Transient Neonatal Diabetes Mellitus; AHO, Albrights hereditary osteodystrophy; PHP-1A, Pseudohypothyroidism type 1B; PHP-1B, Pseudohypothyroidism type 1B; BiCHM,

Biparental complete hydatidiform mole; RWS, Romano-Ward syndrome; JLNS, Jervell and Lange-Nielsen syndrome; MAS, McCune-Albright syndrome

1.3.5.1 Beckwith-Wiedemann syndrome (BWS)

BWS is predominantly a maternally transmitted disorder that is characterised by congenital overgrowth with a large tongue (macroglossia), large organs (visceromegaly), large body size (macrosomia), as well as increased predisposition to develop of embryonal Wilms' tumours (Bliek et al., 2001; DeBaun et al., 2003; Lee et al., 1999; Robertson, 2005; Weksberg et al., 2003). Most BWS cases are due to epigenetic alternations at imprinted genes on chromosome 11p15 (reviewed by Robertson, 2005). Half of BWS patients have loss of methylation at *KvDMR1* and consequently loss of imprinting of *KCNQ1OT1* (Bliek et al., 2001; Lee et al., 1999; Smilinich et al., 1999; Weksberg et al., 2003). Less frequently, gain of methylation on the maternal allele of ICR1 (*IGF2*/*H19* locus) can be found in BWS patients that is associated with transcriptional silencing of *H19* and biallelic expression of *IGF2* (Reik et al., 1995; Weksberg et al., 1993). Moreover, altered gene expression and methylation of *CDKN1C* have been reported in some BWS patients (Diaz-Meyer et al., 2005).

1.3.5.2 Prader-Willi syndrome (PWS) & Angelman syndrome (AS)

PWS and AS known as neuro-developmental disorders are associated with genetic and epigenetic mutations on human chromosome 15q11-13 (reviewed by Robertson, 2005). PWS is characterised by weak muscle tone (hypotonia), incomplete sexual development, mental retardation, feeding difficulties in early infancy, followed in later infancy or early childhood by excessive eating and obesity. Genetic alterlations such as maternal uniparental disomy (UDP), chromosomal deletions and gene mutations have commonly found in PWS patients, (reviewed by Robertson, 2005). Less frequently, epigenetic alterations at the *SNRPN* DMR can be found that is associated with loss of imprinting of *SNRPN* and its neirboring genes, *ZNF127*, *IPW*, *NDN* and *NDNL1* (Reis et al., 1994; Sutcliffe et al., 1994). AS is characterised by developmental delay, severe mental retardation, absent speech, ataxia and aggressive behaviour (Orstavik et al., 2003; Robertson, 2005). The majority of AS patients is arisen by molecular defects such as deletions of maternal chromosome 15q11-13, paternal UPD and germline *UBE3A* (*ubiquitin protein ligase E3A*) mutation. In only

5% of AS patients, loss of methylation at the *SNRPN* DMR has been reported (Cox et al., 2002; Orstavik et al., 2003).

1.3.5.3 Cancers

Imprinting disruptions can be frequently found in tumours and cancer cell lines in the human (reviewed by Feinberg, 2007 ; Jelinic and Shaw, 2007 ; Robertson, 2005). A PCR-RFLP (Restriction Fragment Length Polymorphism) analysis using a *Mnl*I restriction enzyme site in exon 9 of *PEG3* (*paternally expressed gene 3*) has revealed that *PEG3* is monoallelically expressed in normal cell lines and tissues, but it is biallelically expressed in choriocarcinoma (JEG3 and BeWo), glioma (HTB-16, HTB-17, and CRL-1620) and endometrial cervical ovarian cell lines (RL-95, C33A, ME180, Ovcar-3 and Ovcar-5) (Dowdy et al., 2005; Maegawa et al., 2001). Loss of imprinting of *PEG3* is associated with loss of methylation at the *PEG3* DMR (Dowdy et al., 2005; Maegawa et al., 2001). Moreover, *PEG1* (*MEST*) is expressed from the paternal allele in normal tissues and cells, but biallelic expression can be detected in invasive breast carcinomas and lung caners (Nakanishi et al., 2004; Pedersen et al., 2002). *IGF2* and *H19* are the most commonly affected genes in the various human cancers (reviewed by Feinberg, 2007).

1.3.6 Imprinting disruption associated with ART

Assisted reproductive technology (ART) procedures are designed to overcome the human infertility (reviewed by Horsthemke and Ludwig, 2005; Lucifero et al., 2004a; Maher, 2005). ART procedures include isolation, manipulation, and culture of gametes and embryos in *in vitro*. Additionally, superovulation, cryopreservation and intracytoplasmic sperm injection (ICSI) are also involved in ART procedures. It has been reported that ART procedures have detrimental effects on the baby such as a higher frequency of preterm delivery, reduced birth weight, and increased perinatal mortality compared to natural singleton pregnancies (Schieve et al., 2002). Moreover, recent studies have suggested that ART procedures may cause genetic and epigenetic disruptions at imprinted loci (reviewed by Horsthemke and Ludwig, 2005; Maher, 2005; Maher et al., 2003). Currently, derivation and culture of hESC lines have relied on ART procedures (reviewed by Allegrucci et al., 2004), implicating that hESC lines can have epigenetic errors at imprinted loci.

1.3.6.1 Intracytoplasmic sperm injection (ICSI)

ICSI is a technique used to inject a spermatozoa into the cytoplasm of an oocyte using a micromanipulator that bypasses almost all of natural fertilisation (Cox et al., 2002; Manning et al., 2000). Thus, ICSI may have physically deleterious effects to oocytes and sperm. For example, to perform ICSI, cumulus cells around oocytes need be denuded prior to micromanipulation. Moreover the sperm acrosome reaction into oocytes is completely bypassed and this may disturb the oocyte activation (reviewed by Horsthemke and Ludwig, 2005; Maher, 2005).

1.3.6.1.1 Oligospermia

Spermatozoa used in ISCI often originate from infertile men who sometimes have abnormal semen parameters (Hartmann et al., 2006; Kobayashi et al., 2007). A study by Kobayashi et al., (2007) has demonstrated that of 97 infertile men analysed, 16 (16.4%) show moderate oligospermia (defined as sperm count, 5-20 $\times 10^6$/ml) and severe oligospermia ($<5\times10^6$/ml), although normal spermia is determined by $\geq 20\times10^6$/ml. Kobayashi et al., (2007) has compared the methylation status at 7 imprinting regulatory regions between normal spermia and oligospermia. Although *KvDMR1* and *PEG3* DMRs are normally methylated in both, aberrant methylation at *H19* (LOM), *GTL2* (LOM), *PEG1* (GOM), ZAC (GOM) and *SNRPN* (GOM) DMRs are detected in 16 oligospermia patients (Kobayashi et al., 2007). Margues et al., (2004) has examined that of 123 infertile men investigated, 96 patients show oligospermia (46 were moderately and 50 were severely affected). Of 96 oligospermia examined, 23 show gain of methylation at the *H19* DMR, although the *MEST* DMR is normally methylated in all oligospermia. Thus, impaired spermatogenesis is closely linked to imprinting disruption that should be carefully considered before a spermatozoa use for ISCI (Hartmann et al., 2006).

1.3.6.1.2 Superovulation

Oocytes used in ICSI usually originate from women who have undergone an ovarian hyperstimulation with gonadotrophin. Gonadotrophin is commonly used in superovulation to collect sufficient numbers of oocytes for ART in the human and for experimental research in various animal species. Recent studies have suggested that superovulation can be associated with epigenetic disruptions of imprinted loci in

oocytes and their derived embryos (Fortier et al., 2008; Kerjean et al., 2003; Sato et al., 2007). A study by Sato et al., (2007) has analysed the DNA methylation status at *PEG1* and *H19* DMRs in superovulated human oocytes. Of 16 human oocytes examined, 6 show loss of maternal methylation at the *PEG1* DMR and 2 show gain of methylation at the *H19* DMR (Sato et al., 2007). In mouse superovulated oocytes, gain of methylation is detected at the *H19* DMR, although other loci including *Peg1*, *Lit1* and *Zac* are normally methylated (Sato et al., 2007). Furthermore, a study by Kerjean et al., (2003) has examined the DNA methylation status at *Igf2r*, *Peg1* and *H19* DMRs in 2-cell mouse embryos generated from superovulated oocytes. All loci are aberrantly methylated in embryos, showing loss of methylation at *Peg1* and *Igf2r* DMRs and gain of methylation at the *H19* DMR (Kerjean et al., 2003). Thus, superovulation might disturb the establishment of imprints (Lucifero et al., 2004a; Sato et al., 2007) that may be due to artificially enforced oogenesis and folliculogenesis.

1.3.6.2 *In vitro* culture (IVC)

There is evidence from animal studies of preimplantation embryos that *in vitro* culture (IVC) of embryos in medium containing undefined factors (e.g. serum) influences not only epigenetic alterations of imprinted loci but also phenotypic abnormalities during prenatal and postnatal development (Dean et al., 1998; Doherty et al., 2000; Fernandez-Gonzalez et al., 2004; Khosla et al., 2001a; Mann et al., 2004; Young et al., 2001).

1.3.6.2.1 Serum

Studies by Khosla et al., (2001) and Fernandez-Gonzalez et al., (2004) have investigated the effect of fetal calf serum (FCS) during development of both preimplantation and postimplantation stage mouse embryos. Embryos are *in vitro* cultured up to the blastocyst stage in chemically defined M16 medium without and with 10% FCS and then transfer into the uterus of recipient mice (Khosla et al., 2001a). The foetuses (day 14 of gestation) derived from blastocyst stage embryos cultured in presence of FCS show decreased expression of *H19* and *Igf2* that is associated with gain of methylation on the maternal allele of *H19* ICR1 (Khosla et al., 2001a). In addition, aberrant expression of *Grb10* and *Grb7* genes is detected in theses foetuses (Khosla et al., 2001a). Khosla et al., (2001) has found that the weight of foetuses derived from blastocyst stage embryos cultured in presence of FCS is lighter

than foetuses derived from blastocyst stage embryos cultured in absence of FCS. Fernandez-Gonzalez et al., (2004) has also found that the levels of mRNA expression of growth-related imprinted genes (*Igf2*, *Mest*, *H19* and *Grb10*) are significantly down-regulated in blastocyst stage embryos cultured in presence of FCS, compared with blastocyst stage embryos cultured in absence of FCS. Fernandez-Gonzalez et al., (2004) has found that the weight of mice derived from blastocyst stage embryos cultured in presence of FCS is significantly heavier than mice derived from blastocyst stage embryos cultured in absence of FCS. In sheep, loss of methylation at *IGF2R* DMR has been reported as a consequence of *in vitro* culture of ovine embryos in medium containing serum that is associated with Large Offspring syndrome (LOS) (Young et al., 2001). Thus, poorly defined factors in serum can alter imprinted gene expression and methylation that causes phenotypic abnormalities during prenatal and postnatal development.

1.3.6.2.2 Amino acids

The allele-specific expression of imprinted genes and DNA methylation at their regulatory regions have been examined in mouse embryos *in vitro* cultured up to the blastocyst stage in two different media (Whitten's and $KSOM^{AA}$; KSOM supplemented with amino acids) (Doherty et al., 2000; Mann et al., 2004). The Whitten's medium is previously known to lack methionine and other amino acids supplements, compared to $KSOM^{AA}$ (Doherty et al., 2000; Mann et al., 2004; Rinaudo and Schultz, 2004). Over 60% of embryos cultured in the Whitten's medium have loss of imprinting of *H19* (associated with loss of methylation at the *H19* DMR) and loss of methylation at the *Snrpn* DMR (but monoallelic), whereas only 14% of embryos cultured in the $KSOM^{AA}$ medium have these imprinting defects (Doherty et al., 2000; Mann et al., 2004). In addition, a microarray analysis has revealed that embryos cultured in the Whitten's medium have aberrant expression of 114 genes, whereas only 29 genes are aberrantly expressed in blastocysts cultured in $KSOM^{AA}$ (Rinaudo and Schultz, 2004). Mann et al., (2004) has also examined the imprinting and DNA methylation status in foetuses (day 9.5 of gestation) derived from embryos cultured in the Whitten's medium. Aberrant imprinted gene expression and DNA methylation are detected at *H19*, *Snrpn*, *Ascl2* and *Peg3* loci (Mann et al., 2004). Thus, genetic and epigenetic changes in *in vitro* cultured embryos can be occurred due to the lack of key amino acids supplied in the culture medium.

1.3.6.3 *In vitro* fertilisation (IVF)

A study by Li et al., (2005) has demonstrated that of 23 *in vitro* fertilised mouse embryos examined, 9 embryos show loss of imprinting of *H19* and gain of DNA methylation at the maternal allele of the *H19* DMR. However, 1 of 14 *in vivo* fertilised embryos shows loss of imprinting of *H19* (Li et al., 2005b). Moreover, 2 of 23 IVF-derived embryos have aberrant imprinting of *Igf2*, whereas none of 14 *in vivo* fertilised embryos show aberrant imprinting of *Igf2* (Li et al., 2005b). Of other imprinted genes (*Cdkn1c* and *Slc22a1L*) examined, all have normal imprinting status in both *in vitro* and *in vivo* fertilised embryos. Furthermore, mESC lines derived from IVF embryos show gain of methylation at the *H19* DMR, whereas mESC lines derived from *in vivo* fertilised embryos show normal methylation at the *H19* DMR (Li et al., 2005b). Thus, IVF can also be associated with epigenetic disruption at some imprinted loci.

1.3.6.4 ART procedures associated with human congenital disorders

In the human, case-controlled cohort studies have demonstrated that children born from ART procedures (e.g. ICSI and IVF) have an increased incidence of imprinting defects (reviewed by Lucifero et al., 2004a; Maher, 2005). An initial study did not observe imprinting defects in ART-conceived children (Manning et al., 2000). However, recent studies of registered children with imprinting defects have demonstrated that ART-conceived BWS and AS children are associated with epigenetic disruption at three DMRs (*KvDMR1*, *H19* DMR and *SNRPN* DMR) on human chromosome 15q11-13 (Cox et al., 2002; DeBaun et al., 2003; Gicquel et al., 2003; Orstavik et al., 2003). For example, of 149 BWS patients examined, six were born following ART (2 were born by ICSI and 4 were born by IVF) and they have loss of methylation at *KvDMR1* (Gicquel et al., 2003). Moreover, Maher et al., (2003) has reported that 6 of 149 BWS patients are born following ART (3 were born by ISCI and 3 were born by IVF) and 2 of 6 have loss of methylation at *KvDMR1*. DeBaun *et al.,* (2003) has demonstrated that of 7 IVF and ICSI-conceived BWS children examined (5 were born by ICSI and 2 were born by IVF), 5 show loss of methylation at *KvDMR1* and gain of methylation at the *H19* DMR (DeBaun et al., 2003). In addition, loss of methylation on the maternal allele of the *SNRPN* DMR is found in ICSI-conceived AS children (Cox et al., 2002; Orstavik et al., 2003). Thus, overall,

ART procedures are associated with an increased susceptibility to epigenetic disruption at *KvDMR1*, *H19* and *SNRPN* DMRs that may lead to human congenital disorders.

1.3.7 Genomic imprinting in human oocytes and embryos

1.3.7.1 Maternal methylation imprint

The methylation status of *KvDMR1* in the human oocytes and preimplantation stage embryos has been examined (Geuns et al., 2007b; Khoureiry et al., 2008). *KvDMR1* is methylated in oocytes and unmethylated in sperm (Geuns et al., 2007b). A similar maternal methylation imprint has been reported in the *SNRPN* DMR (El-Maarri et al., 2001; Geuns et al., 2003). The *SNRPN* DMR is methylated in human oocytes (GV, MI and MII stages), but it is unmethylated in sperm (El-Maarri et al., 2001; Geuns et al., 2003). In fertilised embryos (day 2 to 6), the *SNRPN* DMR is differentially methylated that is associated with monoallelic expression of *SNRPN* (Geuns et al., 2003; Huntriss et al., 1998). *PEG1*, *LIT1* and *ZAC* DMRs are also methylated in human oocytes but unmethylated in sperm, indicating maternal methylation imprints (Kerjean et al., 2000; Li et al., 2002; Sato et al., 2007).

1.3.7.2 Paternal methylation imprint

Paternally inherited methylation imprints have been reported at *H19* and *GTL2* DMRs (Geuns et al., 2007a; Kerjean et al., 2000). The *H19* DMR is differentially methylated in primary germ cell lines obtained from the gonadal ridges of 5- to 11-week post-fertilisation of female embryos (Onyango et al., 2002). However, the *H19* DMR become unmethylated in fetal spermatogonia and oogonia (Kerjean et al., 2000). Then, the acquisition of methylation imprint at the *H19* DMR appears only in a subset of adult spermatogonia (Kerjean et al., 2000). This paternal methylation imprint is maintained up to mature spermatozoa (Kerjean et al., 2000). A similar paternal methylation imprint can be found at the *GTL2* DMR (Geuns et al., 2007a). The *GTL2* DMR is unmethylated in oocytes (GV, MI and MII stages), whereas it is methylated in sperm (Geuns et al., 2007a).

1.3.8 Genomic imprinting in embryonic stem cell lines

1.3.8.1 Mouse and monkey embryonic stem cells

Mouse and monkey studies have raised concerns about the stability of epigenetic marks at imprinted loci in *in vitro* cultured ESC lines (Dean et al., 1998; Feil et al., 1997; Fujimoto et al., 2006; Humpherys et al., 2001; Mitalipov et al., 2007; Mitalipov, 2006). *In vitro* cultured mESC lines show gain of methylation of *H19* ICR1 and *Igf2* DMR2 and loss of methylation at the *U2af1-rs1* DMR that leads to loss or gain of imprinting of their corresponding genes (Dean et al., 1998; Feil et al., 1997). A study by Humpherys et al., (2001) has demonstrated variable expression patterns of *H19* and *Mest* genes between individual mESC subclones. Moreover, *in vitro* cultured monkey ES cell lines show loss of imprinting of *IGF2* and *H19* mediated by aberrant methylation at the *IGF2* DMR (Fujimoto et al., 2006; Mitalipov et al., 2007; Mitalipov, 2006). Since *IGF2*, *H19* and *SNRPN* in monkey blastocyst stage embryos are monoallelically expressed (Fujimoto et al., 2006), imprinting errors in monkey ESC lines are most likely to originate during *in vitro* culture. Thus, imprinted gene expression and methylation patterns appear to be variable and unstable upon *in vitro* propagation of mouse and monkey ESC lines.

1.3.8.2 Human embryonic stem cells

Initial studies on hESCs regarding imprint stability reached different conclusions compared to mouse and monkey ESCs studies (Mitalipov, 2006; Plaia et al., 2006; Rugg-Gunn et al., 2005; Sun et al., 2006). The allele-specific expression of 6 imprinted genes (*IGF2*, *H19*, *KCNQ1OT1*, *TSSC5*, *IPW* and *NESP55*) and DNA methylation of three imprinting control regions (*KvDMR1*, *SNRPN* DMR and *H19* DMR) observed “normal” imprinting and methylation status in all 4 hESC lines studied (hSF-6, H9, H7 and HES-3) (Rugg-Gunn et al., 2005). Moreover, three additional studies made the same conclusions that hESCs have a substantial degree of imprinting stability in both the differentiated and undifferentiated states (Mitalipov, 2006; Plaia et al., 2006; Sun et al., 2006). For example, Sun *et al*., (2006) has examined the allele-specific expression of 4 imprinted genes (*PEG10*, *H19*, *KCNQ1* and *NDNL1*) in SHhES-1 and HUES7. All genes are monoallelically expressed (Sun et al., 2006). This monoallelic expression persists through differentiation into embryoid bodies (EBs) (Sun et al., 2006). Moreover, Mitalipov (2006) has examined the allele-specific expression of *IGF2* and *H19* in BGN2 and H1 and Plaia et al.,

(2006) has examined the DNA methylation status of *SNRPN*, *DLK1* and *H19* DMRs in BG01V. All genes are normally imprinted in both studies (Mitalipov 2006; Plaia et al., 2006).

1.4 Thesis aims

The overall aim of this thesis is to investigate the stability of a wider range of 22 imprinted genes and 3 non-imprinted genes in *in vitro* cultured 22 hESC lines (Chapter 3) and also to provide mechanistic insight into imprinting instability by analysing DNA methylation at potential imprinting regulatory regions (Chapter 4). Another aim is to determine whether overexpression of a full-length *DNMT1* cDNA in hESCs may increase the epigenetic stability upon *in vitro* prolonged culture (Chapter 5).

2 MATERIALS AND METHODS

2.1 Human embryonic stem cell lines

22 human embryonic stem cell (hESC) lines and 1 human embryonic carcinoma (hEC) cell line (NTERA2) were used for this thesis (Table 2-1). 16 HUES-lines (HUES1, HUES2, HUES3, HUES4, HUES5, HUES6, HUES7, HUES8, HUES9, HUES10, HUES12, HUES13, HUES14, HUES15, HUES16 and HUES17) were provided by Dr. Chad Cowan (Harvard University) and cultured as previously described in Cowan et al., (2004). BG01 was derived from the BresaGen, Inc. and cultured as previously described in Mitalipova et al., (2003). H1 was derived from the Wisconsin Alumni Research Foundation (WiCell Research Institute) and cultured as previously described in Thomson et al., (1998). Both NL-HESC1 and HES-2 cell pellets were provided by Dr. Christine Mummery (Hubrecht Laboratory) (Reubinoff et al., 2000; van de Stolpe et al., 2005). Both NOTT1 and NOTT2 were derived and cultured in University of Nottingham (Allegrucci et al., 2007; Burridge et al., 2007). NTERA2 was cultured as previously described in Andrews *et al*., (1984). Table 2-1 summarise the characteristics and culture methods of each cell line. A human colon cancer cell line, HCT116, was cultured and provided by Dr. Hazel Cruickshanks (University of Nottingham).

Table 2-1. Human embryonic stem cell lines

Cell line	Gender	Passage	passage method	Growth matrix	Reference
HUES1	Female	31	Trypsin	MEFs	(Cowan et al., 2004)
HUES2	Female	27	Trypsin	MEFs	
HUES3	Male	37	Trypsin	MEFs	
HUES4	Male	26	Trypsin	MEFs	
HUES5	Female	30	Trypsin	MEFs	
HUES6	Female	35	Trypsin	MEFs	
HUES7	Male	26	Trypsin	MEFs	
HUES8	Male	37	Trypsin	MEFs	
HUES9	Female	30	Trypsin	MEFs	
HUES10	Male	29	Trypsin	MEFs	
HUES12	Male	28	Trypsin	MEFs	
HUES13	Female	32	Trypsin	MEFs	
HUES14	Female	27	Trypsin	MEFs	
HUES15	Female	31	Trypsin	MEFs	
HUES16	Male	29	Trypsin	MEFs	
HUES17	Male	35	Trypsin	MEFs	
BG01	Male	45	Mechanical	MEFs	(Mitalipova et al., 2003)

H1	Male	26	Trypsin	Matrigel	(Thomson et al., 1998)
HESC-NL1	Female	22	Mech+Disp	MEFs	(van de Stolpe et al., 2005)
HES-2	Female	56	Mech+Disp	MEFs	(Reubinoff et al., 2000)
NOTT1	Female	25	Trypsin	Matrigel	(Allegrucci et al., 2007; Burridge et al., 2007)
NOTT2	Male	32	Trypsin	Matrigel	
NTERA2	Male	70	Mechanical	MEFs	(Andrews et al., 1984)

MEFs: mouse embryonic fibroblasts, Mech: mechanical passaging, Disp: dispase

2.2 Antibodies

Antibodies were used for Western blot and immunostaining analyses. Table 2-2 and 2-3 summarise suppliers, immunised hosts and dilution factors of each antibody.

Table 2-2. Primary antibodies

Antibody	Supplier	Cat. No.	Immunised host	Dilution factor	
				Western Blot	Immunostaining
DNMT1[a]	NEB	M0231	Rabbit	1:2000	-
DNMT3A	ABGENT	AP1034a	Rabbit	1:200	-
DNMT3B	ABGENT	AP1035a	Rabbit	1:200	-
α-Tubulin	Calbiochem	CP06	Mouse	1:2000	-
OCT3/4	Santa Cruz	SC-5279	Mouse	1:500	1:200
NANOG[a]	R&D system	AF1997	Goat	1:200	1:200
SSEA4	Chemicon	MAB4304	Mouse	1:100	1:100
SOX1[a]	R&D system	AF3369	Goat	1:1000	-
SOX17[a]	R&D system	AF1924	Goat	1:1000	-
BRACHYURY[a]	R&D system	AF2085	Goat	1:1000	-
5-Methylcytosine[a]	Calbiochem	NA81	Mouse	1:1000	1:1000

[a] Following initial thaw, aliquots were made to avoid freeze and thaw repeats and stored at -20 ºC. Other antibodies were stored in the 4 ºC fridge.

Table 2-3. Secondary antibodies

Antibody	Supplier	Cat. No.	Immunised host	Dilution factor	
				Western Blot	Immunostaining
Anti-rabbit-HRP	GE Healthcare	NA934	Donkey	1:17,500	-
Anti-mouse-HRP	GE Healthcare	NA931	Sheep	1:10,000	-
Anti-goat-HRP	Santa Cruz	G2704	Donkey	1:10,000	-
Cy3 conjugated anti-mouse	Jackson ImmunoResearch	115-165-068	Goat	-	1:250
FITC conjugated anti-mouse	Jackson ImmunoResearch	115-095-068	Goat	-	1:200
FITC conjugated anti-goat	Novus Biologicals	NB710-F	Rabbit	-	1:200

Horseradish Peroxidase (HRP) conjugated secondary antibodies were stored in the 4 ºC fridge. Other florescence antibodies were stored in the -20 ºC freezer under the dark condition.

2.3 Oligonucleotide

All oligonucleotides were synthesised and purchased from Sigma-Genosys (http://www.sigmaaldrich.com/Brands/Sigma_Genosys.html) in the 0.05 µmol synthesis scale and desalt purification. Particular oligonucleotides used for Southern blot (Table 2-7) were purified by high-performance liquid chromatography (HPLC). For Southern blot, oligonucleotides were resuspended in RNase/DNase free water (Sigma, W4502) to give a final mass of 100 ng. Other oligonucleotides for PCR (polymerase chain reaction) were resuspended in RNase/DNase free water to give a final concentration of 100 µM. Individual stock dilutions of forward and reverse primers were prepared to be a concentration of 10 µM. For PCR, 10 µM of forward primer and 10 µM of reverse primer were mixed at a 1:1 ratio to be a concentration of 5 µM. Oligonucleotides and optimal PCR conditions are summarised in Table 2-4, 2-5, 2-6, 2-7 and 2-8.

Table 2-4. Primers used for genotyping and allelic specific expression

Gene	Polymorphism	Primer sequence (5'→3')	Band size (bp)		Optimised PCR Condition			Reference
			gDNA	cDNA	$MgCl_2$ (mM)	Temp. (℃)	Cycle No.	
TP73	*Sty*I	Genotyping F:CAGGAGGACAGAGCACGAG R:CGAAGGTGGCTGAGGCTAG Allele-specific expression F:GGGCTGCGACGGCTGCAGAGC R:GAGAGCTCCAGAGGTGCTC	229	161	1.5	gDNA: 55 cDNA: 58	40	(Mai et al., 1998a)
IGF2R	*Acl*I	F:TTCAACAACGTTAGGCCAGCTGGGTTAATTTC R:GTCCTCCCAGTTAAGGGAGGCTGA	178	178	2.5	60	38	(Vu et al., 2004)
	*Msc*I	F:TTTGATGGCCACACTGGTGCAAGATGGATGAG R:CGCTAAAACCACTACCTGCTGCGCT	120	120	2.5	60	38	
SLC22A1	C/T	Genotyping F:GCAAGCCTTCCTCATCTTATG R:GTTCCAGTCCACTTCATAGC Allele-specific expression Genotyping F R2:CAGGAGTCAGCACACACCAG	232	381	1.5	55	35	(Monk et al., 2006a)
PEG10	C/T	F:TCATTTTCCTGCCTGGTTGC R:GGAGCCTCTCATTCACAGC	406	406	1.5	63	38	(Sun et al., 2006)
PEG1	G/C	Genotyping F:AGTGTCGATTCTGGATGACC R:TCAACCTTAGTCAGAGCTCC Allele-specific expression (Isoform1) F:CATGGGATAACGCGGCCATG Genotyping R (Isoform2) F:GGTCTTACCTGAATCAGGATG Genotyping R	281	Isoform 1: 1209 Isoform 2: 1183	gDNA: 1.5 Isoform 1: 1.5 Isoform 2: 2.5	gDNA: 55 Isoform 1: 60 Isoform 2: 55	38	(Nakabayashi et al., 2002)
MESTIT1	G/A	Genotyping F:GATTCACAACAGTGGTATGG R:TCAGGGATATGTTGGGTGAA Allele-specific expression F:GAGGAAACTACCGCCTATAA Genotyping R	520	1359	1.5	55	38	
WT1	*Hinf*I	F:AATCAGAGAGCAAGGCATCG R:GTGCAAGGAGGTATGTACATC	319	319	2.5	62	40	(Mitsuya et al., 1997)

H19	*Alu*I	F:TACAACCACTGCACTACCTG R:TGGCCATGAAGATGGAGTCG or F:TGCTGCACTTTACAACCACTG R:GTGGCCATGAAGATGGAGTC	228 239	148 159	1.5	58	40	(Chen et al., 2000a; Hashimoto et al., 1995; Morison et al., 2000)
	*Rsa*I	F:CGGACACAAAACCCTCTAGCTTGGAAA R:GCGTAATGGAATGCTTGAAGGCTGCTC	704	624	1.5	60	38	
IGF2	*Apa*I	F:CTTGGACTTTGAGTCAAATTGG R:GGTCGTGCCAATTACATTTCA	292	292	2.5	58	38	(Cui et al., 1998; Hashimoto et al., 1995; Onyango et al., 2002)
TSSC4	G/A	Genotyping F:GAGATGGCCCAGCCTGACCCCACTGGC R:AACCTTTATTGTCCCTACCAGGGAGCC Allele-specific expression F:CCTTGAGCCGTTGAGCAGCTG Genotyping R	235	1410	1.5	60	35	(Monk et al., 2006a)
KCNQ1	G/A	Genotyping F:CTGTCACTGCCTGCACTTTG R:GCCGTTTGGCCGTGCCCAC Allele-specific expression F:CTTCGCCGAGGGACCTGGACCTG R:GATGAACAGTGAGGGCTTCC	190	271	1.5	58	38	
KCNQ1OT1	G/A	F:GATCCTCTCCAGGCAGCTTCTTCCACA R:CATAAGGTAGGTAAGTTTGTGTCCCTG	268	268	2.5	62	38	(Lee et al., 1999)
CDKN1C	G/A	F:CTAGCCAGCAGGCATCGAG R:CTCCATCGTGGATGTGCTG	270	270	1.5	58	40	(Monk et al., 2006a)
PHLDA2	T/C	Genotyping F:ATGAAATCCCCCGACGAGG R:TTGCAATGGGCACAGTGAT Allele-specific expression Genotyping F R:GGTCCGACTCGTCCAGCGT	916	494	1.5	58	40	(Qian et al., 1997)
NAP1L4	G/C	Genotyping F:GTTTCCAGCCCGCTGAATCTG R:CTCAGGGCACCAAGGTGGTTC Allele-specific expression F:GAGGAGGAATTAGAAGGTGAC Genotyping R	278	848	1.5	55	38	(Monk et al., 2006a)

SLC22A18	G/C	Genotyping F:CTTCAGCAGGGACAGCAGTCAGG R:GAGGAGGCTGCTCCACTCGCTGG Allele-specific expression F:GCTCTTCATGGTCATGTTCTCCA R:GGAGCAGTGGTTGTACAGAGG	260	365	1.5	62	40	(Onyango et al., 2002)
DLK1	C/T	F:CCGGCTTCATCGACAAGAC R:CACCACAAAGATTAGGACAGACC	640	640	1.5	63	38	(Kobayashi et al., 2000)
GTL2	A/G	F:GTGTGTACCTTGGTTGGTGACTC R:GAGGCATATATTTGAGTTACACATACCCCTTAGTCC	368	368	1.5	62	38	(Wylie et al., 2000)
NDN	*Mbo*I	F:GCCCGAATACGAGTTCTTTT R:CACACATCATCAGTCCCATA	540	540	2.5	60	38	(MacDonald and Wevrick, 1997)
NDNL1	C/A	F:AAGCCCTATCCAGGTCTCG R:TTGATAACCAAAGGCACACTC	453	453	1.5	60	40	(Sun et al., 2006)
SNRPN	*Bst*UI	F:AACCAGGCTCCATCTACTCTTTG R:TCTTGCAGGATACATCTCATTCTA	925	217	2.5	60	35	(Morison et al., 2000)
IPW	*Hph*I	F:CTGCATGATTTTTTTTCAAAAA R:ATATAGGGAGGTTCATTGCACA	390	390	1.5	56	38	(Wevrick et al., 1994)
ATP10C	*Ava*II	F:GGCTCAGTGTAGGTCCCAAG R:AGGCTGAGGAAACCAGGAC	204	204	1.5	65	40	(Meguro et al., 2001)
PEG3	*Mnl*I	F:CCCTCCCCTCGCATAATAACTA R:TCTTCTGTCTGTCTCCTCTCCC	338	338	2.5	58	38	(Dowdy et al., 2005)
NESP55	C/T	Genotyping F:GGCTCCTTGTGCTGTCTGTCTTGTAG R:CCACACAAGTCGGGGTGTAGCTTA Allele-specific expression F:TCGGAATCTGACCACGAGCA R:CACGAAGATGATGGCAGTCAC	233	1141	1.5	60	38	(Hayward et al., 2001)

Table 2-5. Primers used for bisulphite sequencing

Bisulphite region	Primer sequence (5'→3')	Band size (bp)	Optimised PCR Condition			Reference
			$MgCl_2$ (mM)	Temp. (℃)	Cycle No.	
TP73 promoter	F:GTTTGGGGGATAGTAGGGAGTT R:ACCCTAAACCTCCTACCTACAACC	552	1.5	55	38	(Dong et al., 2002)
PEG1 promoter	F:TYGTTGTTGGTTAGTTTTGTAYGGTT R:AAAAATAACACCCCCTCCTCAAAT	290	1.5	55	38	(Kerjean et al., 2000)

GTL2 CTCF biding site	F:ATTGATAGGTTATAAGTGTTAGTTGTGTG R:AAATTTCTACTTTTCCCATAACAAA	490	2.5	55	38	(Kawakami et al., 2006)
GTL2 CpG2	F:GTAAGTTTTATAGGTTGTAAAGGGGGTGTT R:CCACAACTAATAACTAAAAAAATAAACATT	216	2.5	55	38	
SLC22A18 promoter	F:GGGTAGGATTTAAGTTGGAGG R:CAACAAACACRTCAAAAACACC	427	1.5	55	40	(Monk et al., 2006a)
KCNQ1 promoter	F:GGGGTTGGTAGTAGTGGTTG R:CRCCCTCCRCCAACTCCAAC	233	1.5	55	40	
KvDMR1	F:TGATGTGTTTATTATTTYGGGG R:CCCTAAAATCCCAAATCCTC	304	2.5	55	38	
CDKN1C promoter	F:GTTTTAAATTGYGAGGAGAGGGG R:CCTCTCRAATCTCCRAAC	284	2.5	55	40	
NDN promoter	F1:TTAAATTAATTTTGGATATATTTAGGTAAG R1:TCAAATCCTTACTTTATTCTAACATATCT Nested PCR F2:TATATTTTTTTAGTTTAAATAGGAAAT R2:TCTAACAAAAACAAAACCTCTA	448 280	2.5	55	38	(El-Maarri et al., 2001)
NESP55 DMR	F:TTTTTGTAGAGTTAGAGGGTAGGT R:AAAAAAAACAACTCAAAATCTACC	344	2.5	55	38	(Judson et al., 2002)
IGF2 DMR0	F:TTGGTGTTGGAAAGTGTTTG R:CTATAACRTCCAAACCCTCTA	300	2.5	55	40	(Monk et al., 2006b)
IGF2 DMR2	F:GGGATTGGGTTAGGAGAAGTTT R:CCCCCAAAAATAACCAACAAT	164	2.5	57	40	(Kim et al., 2007b)
PEG3 DMR	F:GGAAAGAAAATTTTTATAGGTAGGATAGT R:AAACCCTAAACCTCCTAAACTAAATCTAA	173	2.5	57	40	
PEG10 DMR	F:GGTGTAATTTATATAAGGTTTATAGTTTG R:AACAAAAAAAATAAAATCCCACAC	234	2.5	55	38	
IGF2R DMR 1	F:AGGAGTTTTTGGGGTTTTTAAGT R:ACTAAAATTCCTACCTCCAACTTTC	287	2.5	57	40	
IGF2R DMR 2	F:GTAGTTTTTGTTTGGTTTTTGTTTG R:CCTATTCACACATAAAATAACCCCT	285	2.5	57	40	
H19 CTCF6	F:TATGGGTATTTTTGGAGGTTTTTT R:AAATCCCAAACCATAACACTAAAAC	311	2.5	57	40	
SNURF/*SNRPN* DMR	F:TAGGTTGTTTTTTGAGAGAAGTTAT R:AAAAAAACTAAAACCCCTACACTAC	236	2.5	57	40	

Table 2-6. Primers used for methylation-specific PCR

Gene	Primer sequence (5'→3')		Band size (bp)	Optimised PCR Condition			Reference
				$MgCl_2$ (mM)	Temp. (℃)	Cycle No.	
CDH1	Methylated F	TTAGGTTAGAGGGTTATCGCGT	116	2.5	60	41	(Herman et al., 1996)
	Methylated R	TAACTAAAAATTCACCTACCGAC					
	Unmethylated F	TAATTTTAGGTTAGAGGGTTATTGT	97				
	Unmethylated R	CACAACCAATCAACAACACA					
TIMP3	Methylated F	CGTTTCGTTATTTTTTGTTTTCGGTTTC	116	2.5	60	41	(Zochbauer-Muller et al., 2001)
	Methylated R	CCGAAAACCCCGCCTCG					
	Unmethylated F	TTTTGTTTTGTTATTTTTTGTTTTTGGTTTT	119				
	Unmethylated R	CCCCCAAAAACCCCACCTCA					
DAPK1	Methylated F	GGATAGTCGGATCGAGTTAACGTC	98	2.5	60	41	
	Methylated R	CCCTCCCAAACGCCGA					
	Unmethylated F	GGATAGTTGGATTGAGTTAATGTC	103				
	Unmethylated R	CAAATCCCTCCCAAACACCAA					
GATA4	Methylated F	GTATAGTTTCGTAGTTTGCGTTTAGC	102	2.5	60	41	(Akiyama et al., 2003)
	Methylated R	AACTCGCGACTCGAATCCCCG					
	Unmethylated F	TTTGTATAGTTTTGTAGTTTGTGTTTAGT	101				
	Unmethylated R	CCCAACTCACAACTCAAATCCCCA					
GATA5	Methylated F	AGTTCGTTTTTAGGTTAGTTTTCGGC	103	1.5	60	41	
	Methylated R	CCAATACAACTAAACGAACGAACCG					
	Unmethylated F	TGGAGTTTGTTTTTAGGTTAGTTTTTGGT	101				
	Unmethylated R	CAAACCAATACAACTAAACAAACAAACCA					
HIC1	Methylated F	TCGGTTTTCGCGTTTTGTTCGT	95	2.5	60	41	(Dong et al., 2001)
	Methylated R	AACCGAAAACTATCAACCCTCG					
	Unmethylated F	TTGGGTTTGGTTTTTGTGTTTTG	118				
	Unmethylated R	CACCCTAACACCACCCTAAC					
CCND1	Methylated F	TACGTGTTAGGGTCGATCG	276	2.5	55	41	(Evron et al., 2001)

	Methylated R	CGAAATATCTACGCTAAACG					
	Unmethylated F	GTTATGTTATGTTTGTTGTATG	222				
	Unmethylated R	TAAAATCCACCAACACAATCA					
ESR1	Methylated F	ATTTGTTTTCGTCGGGTC	107	2.5	55	41	(Imura et al., 2006)
	Methylated R	ATTAAAAACGACGCAACG					
	Unmethylated F	GTATTTGTTTTTGTTGGGTT	114				
	Unmethylated R	CCAAAATTAAAAACAACACA					
P16	Methylated F	TTATTAGAGGGTGGGGCGGATCGC	150	1.5	58	41	(Zochbauer-Muller et al., 2001)
	Methylated R	GACCCCGAACCGCGACCGTAA					
	Unmethylated F	TTATTAGAGGGTGGGGTGGATTGT	151				
	Unmethylated R	CAACCCCAAACCACAACCATAA					
MGMT	Methylated F	TTTCGACGTTCGTAGGTTTTCGC	81	2.5	60	41	(Zochbauer-Muller et al., 2001)
	Methylated R	GCACTCTTCCGAAAACGAAACG					
	Unmethylated F	TTTGTGTTTTGATGTTTGTAGGTTTTTGT	93				
	Unmethylated R	AACTCCACACTCTTCCAAAAACAAAACA					

Table 2-7. Oligonucleotides used for Southern blot

Gene	Oligonucleotide probe	Reference
α-Satellite	GAAACACTCTTTTTGTAGAATCTGCAAGTGGA	(Chen et al., 2007)
Satellite 2	TCGAGTCCATTCGATGAT	(Saito et al., 2001, 2002)
Satellite3	TCCACTCGGGTTGATT	

Table 2-8. Primers used for RT-PCR

Gene	Primer sequence (5'→3')		Band size (bp)	Optimised PCR Conditions			Reference
				$MgCl_2$ (mM)	Temp. (℃)	Cycle No.	
MGMT	Forward	GGCCGAAACTGAGTATGTGC	99	1.5	60	31	(Imura et al., 2006)
	Reverse	CCTTTAATACAGCGGTGCCT					
TIMP-3	Forward	GCAGCAAGCAGATAGACTCA	116	1.5	60	28	
	Reverse	CTTCCCTCCCTCACTCTTAC					

HIC-1	Forward	CGTGCGACAAGAGCTACAAG	304	1.5	60	33	(Kanai et al., 1999)
	Reverse	ATGTGGCTGATGAGGTTGCG					
GATA4	Forward	CTGGCCTGTCATCTCACTACG	263	1.5	60	30	(Bai et al., 2000)
	Reverse	GGTCCGTGCAGGAATTTGAGG					
GATA5	Forward	TCGCCAGCACTGACAGCTCAG	290	1.5	60	35	
	Reverse	TGGTCTGTTCCAGGCTGTTCC					
GAPDH	Forward	GACCACAGTCCATGCCATCAC	457	1.5	60	25	
	Reverse	GTCCACCACCCTGTTGCTGTA					

2.4 General methods

2.4.1 Genomic DNA extraction

Genomic DNA was isolated by either the standard phenol/chloroform extraction or DNeasy® Tissue kit (Qiagen: 69504). For the phenol/chloroform extraction, cell pellets were harvested by 0.05% Trypsin EDTA (Invitrogen: 25300-054), washed with PBS (Invitrogen: 14190) once, and centrifuged at 150 g for 4 min. Washed cell pellets were resuspended in 2 ml of lysis buffer (see section 8.1.1.22) and incubated at 37 °C overnight with agitation. The following day, an equal volume of phenol/chloroform (1:1, see section 8.1.1.13) was added to cell lysates and mixed with vortexing. To separate between organic and aqueous phases, centrifugation was performed at 800 g for 15 min. Only aqueous phases were taken out and placed into a new tube. The phenol/chloroform exaction was repeated until to get clean aqueous phases. Genomic DNA was precipitated by adding 1 in 10 of the volume of 3M NaOAc (see section 8.1.1.12) and 2 volumes of 100% ethanol (see section 8.1.1.16). Genomic DNA pellets were visualised by inverting the tube, placed into a new tube using a pipette tip, and centrifuged at 16,000 g for 15 min. DNA pellets were washed once with 70% ethanol and leaved to be air-dried. Dried pellets were resuspended in appropriate amounts of RNase/DNase free water (Sigma: W4502) with flicking. For the DNeasy® Tissue kit, genomic DNA was extracted according to the manufacturer's 'purification of total DNA from cultured animal cells' protocol (see the DNeasy® Tissue Handbook, March 2004). To elute genomic DNA, 100 ul of RNase/DNase free water was added into a column, incubated for 1 min and centrifuged at 8,000 g for 1 min. Genomic DNA was quantified by a NanoDrop® 1000 spectrophotometer (Thermo Scientific) and stored at -20 ºC.

2.4.2 RNA extraction and cDNA synthesis

Total RNA was extracted from cells using the RNeasy® Mini kit (Qiagen: 74104) with QIAshredder (Qiagen: 79654), following manufactuter's 'RNeasy mini protocol for isolation of total RNA from animal cells' protocol (see the RNeasy Mini Handbook, June 2001). Cell pellets were harvested using 0.05% Trypsin EDTA, washed with PBS once, centrifuged, and resuspended in the RLT buffer (provided in the kit)

containing 10 µl·ml^{-1} of β-Mercaptoethanol (Sigma: M3148). The small residual amounts of DNA were removed by the RNase-Free DNase Set kit (Qiagen: 79254). RNA was eluted in 30 µl of RNase-free water. The concentration of RNA was quantified by a NanoDrop® 1000 spectrophotometer. 1 µg of total RNA was reverse transcribed into complimentary DNA (cDNA). The reverse transcription (RT) was performed by the First-Strand cDNA Synthesis Kit (GE Healthcare: 27-9621-01) with pd(N)6 random hexamer primer (provided in the kit), according to the manufacturer's protocol. cDNA was stored at -20 ºC.

2.4.3 Polymerse chain reaction (PCR)

PCR was performed in a 25 µl reaction volume, with 0.625 Units of Hotstar Taq® DNA polymerase (Qiagen: 203205), 1X supplied reaction buffer, 0.5 µM of each primer (see Table 2-4, 2-5, 2-6, 2-7 and 2-8), 1.5 ~ 2.5 mM of $MgCl_2$, 0.25 mM of dNTP (Invitrogen: R725-01) and 50 ng of each template in a thermal cycler (TECHNE TC-512). The PCR cycling conditions were 95 ^{o}C for 15 min followed by 30 ~ 41 cycles (95 ^{o}C for 1 min, X ^{o}C for 30 s, 72 ^{o}C for 1 min) and a final extension step at 72 ^{o}C for 9 min. Optimised PCR conditions are summarised in Table 2-4, 2-5, 2-6, 2-7 and 2-8.

2.4.4 Gel electrophoresis

To visualise genomic DNA and PCR products, gel electrophoresis was performed in 0.8% ~ 3% agarose gels (Invitrogen: 15510-027) prepared in 1X TBE (see section 8.1.1.1) containing 0.2 µg·ml-1 ethidium bromide (Sigma: E1510) using the Scie-Plas Maxi Horizontal Gel Unit with removable casting trays (SLS Ltd: ELE8170). 1X TEB was used as a gel electrophoresis buffer. PCR products and genomic DNA were mixed with Gel Loading Dye (Sigma: G2526) and loaded into each lane of the gels. Gel electrophoresis was performed at 60 ~ 130 V using a Consort E835 power supply (SLS Ltd). PCR products and DNA were visualised by a Fujifilm LAS-100 Gel Documentation system and a CCD camera. Images were captured by a Fujifilm LAS-100 software and quantified by an Aida Image Analyser v.4.15 (Raytek Scientific Ltd, Sheffield) software. For the quantification of each band, a rectangular region of interest was drawn around each PCR band. The signal density was measured and

normalised with local background measurement around a rectangular region of interest. Then, normalised values were exported into Microsoft Excel for analysis.

2.4.5 Genotyping and allelic specific expression

Genotyping was performed by either PCR-RFLP (restriction fragment length polymorphism) or direct sequencing, according to previous publications described in Table 2-4. For PCR-RFLP, amplified PCR products were digested with appropriate restriction enzymes described in Table 2-4. 2% ~ 3% Agarose (Invitrogen: 15510-027) gels were used for gel electrophoresis. The predominantly monoallelic expression was defined when the allelic ratio was >3:1 (Cui et al., 1998). Direct sequencing was performed by either forward or reverse primer, as described in section 2.5.9.

2.4.6 Bisulphite modification

500 ng to 1 μg of genomic DNA was digested with either *BamHI* (Roche: 10 220 612 001) or *Eco*RI (Roch: 10 703 737 001) overnight at 37 ^{o}C. The digested DNA was placed into a sterile screw-cap tube, incubated at 100 ^{o}C for 5 min for DNA denaturation and then immediately placed on ice. 2.5 μl of 3 M NaOH (see section 8.1.1.8) was added to each tube and incubated at 37 ^{o}C for 20 min. During incubation, the bisulphite solution was prepared. 3.8 g of sodium bisulphite (BDH: 103564D) was mixed with 5.5 ml of RNase/DNase free water (Sigma: W4502) and 1 ml of 3 M NaOH using a tube roller under dark condition. At the same time, 110 mg of hydroquinone (Sigma: H9003) was dissolved in 1 ml of RNase/DNase free water by heating at 55 ^{o}C for 10 min. The dissolved hydroquinone was added to the bisulphite solution and mixed together. 270 μl of the freshly prepared bisulphite solution was added to denatured DNA. Incubation was performed at 55 ^{o}C for 5 h under dark condition. Following incubation, bisulphite treated DNA was added into a 2 ml sterile tube (Eppendorf: 0030 120.094) containing 600 μl of RNase/DNase free water (see section 8.1.1.20), 90 μl of 3 M sodium acetate (see section 8.1.1.12) and 1 μl of Pellet Paint^{TM} (Novagen: 69049-3). Then, 900 μl of ethanol (see section 8.1.1.16) was added and mixed by inversion. Centrifugation was performed at 14,000 g for 20 min. DNA pellets were washed with 500 μl of 70% ethanol and centrifuged for 10 min at 14,000 g. The pellets were air-dried for 10 min and resuspended in 50 μl of RNase/DNase

free water. 5 µl of 3 M NaOH was added into dissolved pellets for desulfonation of DNA and incubated at 37 ^{o}C for 15 min. Finally, bisulphite-converted DNA was purified using the QIAquick PCR purification kit (Qiagen: 28104) according to manufacturer's protocol. DNA was eluted in 30 µl of RNase/DNase free water. Bisulfite modified DNA was stored at -20 ^{o}C and used for PCR.

2.4.7 Combined bisulphite restriction analysis (COBRA)

2 µl of bisulphite modified DNA was used for PCR (see 2.5.6 and 2.5.3). Primers for COBRA are described in Table 2-5. Following PCR, PCR products were digested with appropriate restriction enzymes described in Table 2-9. Gel electrophoresis was performed and gel images were visualised, captured and analysed, as previously described in section 2.5.4.

Table 2-9. Restriction enzymes used for COBRA

Gene	Restriction enzyme	Supplier	Catalogue Number
TP73	*Acl*I	NEB	R0598S
IG2R	*Bst*UI	NEB	R0518S
PEG10	*Bst*UI	NEB	R0518S
	*Aci*I	NEB	R0551S
PEG1	*Acl*I	NEB	R0598S
	*Hpy*CH4IV	NEB	R0619S
SLC22A18	*Bst*UI	NEB	R0518S
CDKN1C	*Hpy*CH4IV	NEB	R0619S
KvDMR1	*Bst*UI	NEB	R0518S
	*Hpy*CH4IV	NEB	R0619S
IGF2 DMR0	*Hpy*CH4IV	NEB	R0619S
	*Aci*I	NEB	R0551S
IGF2 DMR2	*Acl*I	NEB	R0598S
	*Aci*I	NEB	R0551S
	*Hpy*CH4IV	NEB	R0619S
H19 CTCF	*Hpy*CH4IV	NEB	R0619S
	*Aci*I	NEB	R0551S
GTL2 CpG2	*Acl*I	NEB	R0598S
	*Hpy*CH4IV	NEB	R0619S
SNRPN	*Aci*I	NEB	R0551S
PEG3	*Hpy*CH4IV	NEB	R0619S
	*Aci*I	NEB	R0551S
NESP55	*Acl*I	NEB	R0598S
GNAS1 XLαs	*Aci*I	NEB	R0551S
	*Bst*UI	NEB	R0518S

2.4.8 Methylation-specific PCR (MSP)

2 µl of bisulphite modified DNA was used for MSP. Primers for MSP were described in Table 2-6. PCR and gel electrophoresis were performed as previously described in sections 2.5.3 and 2.5.4. For the positive control, genomic DNA was *in vitro* methylated by *Sss*I methylase (NEB: M0226S). 1 µl of *S*-adenosy-L-methionine (SAM) was added into 19 µl of RNase/DNase free water to give a final concentration of 1600 µM. In a 20 µl reaction volume, 5 µl of genomic DNA (1 µg), 2 µl of 10X buffer, 1 µl of *Sss*I methylase, 2 µl of SAM and 10 µl of RNase/DNase free water were added in the tube and mixed with flicking. Then, incubation was performed at 37 ^{o}C for 2 h, followed by enzyme inactivation at 60 ^{o}C for 20 min. DNA was purified using the QIAquick PCR purification kit (Qiagen: 28104) according to manufacturer's protocol.

2.4.9 Sequencing

For direct sequencing, PCR products were purified by the QIAquick Gel Extraction Kit (Qiagen: 28704) according to manufacturer's protocol (see QIAquick® spin Handbook, March 2006). Elution was performed in 20 µl of RNase/DNase free water. Purified PCR products were quantified by a NanoDrop® 1000 spectrophotometer. 20 ng of PCR products and either forward or reverse primer were sent to the DNA sequencing laboratory (University of Nottingham). For clonal sequencing, PCR products were purified by the QIAquick Gel Extraction Kit, cloned into PCR® XL-TOPO vector (Invitrogen: K4750-20), and subsequently transformed into One Shot® TOP10 Chemically Competent *E. coli* (Invitrogen: C4040-03). Individual colonies were inoculated into 2 ml of LB medium containing Kanamycin (50 µg/ml, see section 8.1.1.14) and cultured overnight in a 37^{o}C shaking incubator. The following day, plasmids were extracted using the QIAprep Spin Miniprep Kit (Qiagen: 27104) according to manufacturer's protocol (see QIAprep Miniprep Handbook, June 2005). 10 insert-containing colonies determined by *Eco*RI digestion were sequenced using the M13 forward primer. Sequencing results were analysed by a Chromas Lite v2.01 software (http://www.technelysium.com.au/chromas_lite.html).

2.4.10 Transformation

One Shot® TOP10 Chemically Competent *E. coli* (Invitrogen: C4040-03) for bisulfite clonal sequencing (see section 2.5.9) and Sub cloning Efficiency™

DH5α^{TM} Competent cells (Invitrogen: 18265-017) for the construction of pCAG-DNMT1-IRES-PAC and pCAG-DsRed2-C1-DNMT1-IRES-PAC plasmids (see section 2.5.14 and Chapter 5) were used. Once competent cells thawed, 0.5 µl of either PCR products or plasmids were added into cells and mixed by flicking the tube. The tube was incubated for 30 min on ice, followed by incubation for 1 min at 42 ºC. Then, 1 ml of SOC medium was added into the tube. The tube was incubated for 1 h at 37 ºC with shaking. Following incubation, 200 µl was spread onto an agar plate containing an antibiotic (see 2.4.1.14 and 2.4.1.15). A plate was placed upside down and incubated overnight at 37 ºC.

2.4.11 Protein extraction and quantification

Total proteins were extracted using the RIPA buffer (see section 8.1.2.14). Extracted proteins were quantified by the Bradford assay (see section 8.1.2.17). Trypsinized cell pellets were placed into an eppendorf tube, washed once with PBS and centrifuged at 150 g for 4 min. Cell pellets were resuspended in 20 ~ 50 µl of RIPA buffer containing Complete, EDTA-free Protease Inhibitor Cocktail (Roche: 11 873 580 001). Incubation was performed for 20 min on ice. Then, the tube was placed into liquid nitrogen (LN_2) for 30 sec for snap-freezing and placed into slushy water to thaw. The tube was grated in an eppendorf rack at least 5 times. Snap freezing and grating were repeated at least 3 times. Then, centrifugation was performed at 16,000 g for 30 min at 4 ºC. Only supernatant was taken out and placed into a new tube and stored at – 80 ºC.

2.4.12 Western blot

30 µg of each protein extract was mixed with the protein loading buffer (see section 8.1.2.15), boiled at 100 ºC for 5 min and loaded onto 4 ~ 8 % SDS-PAGE (sodium dodecyl sulphate-polyacrylamide gel electrophoresis) gels. 6 µl of Prestained Protein Marker, Broad Rage (6-175 kDa), (NEB: P7708S) was used for the determination of the molecular mass. Electrophoresis was performed at 80V ~ 100V for 2 h within 1X protein electrophoresis buffer (see section 8.1.2.1). The electrophoretically separated proteins on the gel were confirmed by Commassie blue gel staining (see section 8.1.2.8). Proteins were transferred to the Hybond ECL Nitrocellulose Membrane (GE Healthcare: RPN203D) by a wet-transfer system at 25V overnight. The membrane was stained by Poncea S (see section 8.1.2.18). The membrane was incubated in 5%

Skim milk (see section 8.1.2.5) for 3 h at room temperature and then probed with a primary antibody (see Table 2-2) for 3 h at room temperature with agitation. The membrane was washed 5 times for 1 h with TBST (see section 8.1.2.4), and incubated with a HRP-conjugated secondary antibody (see Table 2-3) for 1 h at room temperature with agitation. The membrane was washed 5 times with TBST for 1 h, treated with 1 ml of ECL Advance™ Western Blotting Detection reagent (GE Healthcare: RPN2135), and exposed to a Kodak BioMax XAR film (Sigma: F5388). Antibodies used in western blot and their dilution factors were described in Table 2-2 and 2-3.

2.4.13 Southern blot

Each 5 µg of genomic DNA was digested with either *Hpa*II (Roche: 10 239 291 001) or *Msp*I (Roche: 10 633 518 001) overnight at 37 ºC. Phenol/chloroform extraction and ethanol precipitation were performed to purify digested genomic DNA. DNA was resuspended in 20 µl of RNase/DNase free water and 5 µl of Gel Loading Dye (Sigma: G2526) was mixed into 20 µl DNA. Gel electrophoresis was performed at 60 V for 5 h. Then, the gel was stained by 0.2µg·ml^{-1} ethidium bromide (Sigma: E1510) for 10 min and subsequently destained for 10 min with distilled water. The electrophoretically separated genomic DNA was visualised by a Gel Documentation system and a CCD camera (see section 2.5.4). The membrane transfer was set-up as previously described (Southern, 2006). The membrane transfer was performed within 0.4 mM NaOH (see section 8.1.4.10) overnight. The membrane (Hybond-XL; Amersham RPN203S) was washed with 2X SSC (see section 8.1.4.2) for 2 min with agitation and air-dried between two filter papers (Fisher Scientific) for 20 min. The membrane was baked in a gel dryer (Bio-Rad: 165-1746) connected with a HydorTech™ vacuum pump (Bio-Rad: 165-1781) at 80 ºC for 2 h. For hybridisation, the membrane was placed in the hybridisation bottle and washed with 2X SSC once. 50 ml of pre-hybridisation solution (see 2.4.4.8) was added into the hybridisation bottle and incubated at 65 ºC for 4 h with rotation in a hybridisation oven. The probe was prepared, while incubation was in progress. In the first tube, 5 µl of 1 mg·ml^{-1} Random Hexamers (NEB: S1230S), 5 µl of 100 ng LINE probe provided by Dr. Hazel Cruickshanks (University of Nottingham), and 4 µl of RNase/DNase free water were added, mixed together with flicking several times, incubated at 100 ºC for 5 min and placed into ice for 2 min. In a second tube, 2.5 µl of 10X buffer, 5 µl of 0.5 mM ^{32}P-

dCTP (PerkinElmer), 2.5 µl of 0.5 mM dNTPs less dCTP, and 1 µl of Klenow (NEB: M0210S) were added and mixed together with flicking several times. The Klenow filled mixture in the second tube was placed into the first tube, mixed together with flicking several times and incubated at room temperature for 4 h in a perspex box. Before 1 h for probing, 25 ml of pre-hybridisation solution was taken out from the hybridisation bottle and placed into a new tube, and 2.25 g of Dextran sulphate (Sigma: D8906) was dissolved into this tube with rotation (see section 8.1.4.9). After 4 h incubation, 1 µl of 0.5 M EDTA (see 2.4.1.6) was added into in the tube to inactivate the Klenow enzyme. Then, unincorporated nucleotides were removed by a ProbeQuant^{TM} G-50 Micro Column (GE Healthcare: 27-5335-01), according to manufacturer's protocol. The probe was denatured at 100 ºC for 5 min and placed into ice for 2 min, added into the Dextran sulphate dissolved hybridisation solution, and mixed together. 25 ml of pre-hybridisation solution was poured off from the hybridisation bottle and this probe mixture was added into the bottle. Hybridisation was performed overnight at 65 ºC. Following day, the membrane was washed twice with a low stringency wash buffer, 2X SSC/0.1% SDS (see section 8.1.4.11), at room temperature for 20 min with rotation and washed twice with a high stringency wash buffer, 0.1X SSC/0.1%SDS (see section 8.1.4.12), at 65 ºC for 15 min. Finally, the membrane was washed once in 2X SSC (see section 8.1.4.2), exposed to a Kodak BioMax MS film (Sigma: Z363049).

2.4.14 Plasmid construction

pCAG-DNMT1-IRES-PAC and pCAG-DsRed2-C1-IRES-PAC plasmids were genereated. With the DsRed2 expression, it is easy to discriminate positive cell lines expressing exogenous *DNMT1* using fluorescence microscopy. Furthermore, immunocytochemistry and fluorescence-activated cell scanner (FACS) analyses are available for analysing living or fixed cells without a specific antibody (Liew et al., 2007; Ren et al., 2006; Smith et al., 2008; Zaragosi et al., 2007). However, due to the potential cytotoxic effect of fluorescent reporter proteins in mammalian cells (Liu et al., 1999; Vallier et al., 2004b), a plasmid without DsRed2 was also utilised in this thesis.

2.4.14.1 pCAG-DNMT1-IRES-PAC

The pDsRed2-C1-hDNMT1 plasmid was produced during a previous project in the laboratory of Prof. Yong-Mahn Han (KAIST). This plasmid contains a 5.2kb full-length human *DNMT1* cDNA. The pDsRed2-C1-hDNMT1 plasmid was digested with *Eco*RI (Roche: 11 175 084 001) and *Rsr*II (Roche: 11 292 595 001) with appropriate buffers. Then, gel electrophoresis was performed in a 0.8% agarose gel. A 5.2kb band of *DNMT1* cDNA was cut out by a blade. To purify *DNMT1* cDNA from the gel, gel extraction was performed using the QIAquick Gel Extraction Kit (Qiagen: 28704) according to manufacturer's protocol (see OIAquick® spin Handbook, March 2006).

The p336 plasmid (see section 5.2.1.1) provided by Prof. Chris Denning (University of Nottingham) was digested with *Eco*RI. Following gel electrophoresis on a 0.8% Agarose gel, the linearized p336 plasmid (6.3kb) was purified from the gel by the QIAquick Gel Extraction Kit (Qiagen: 28704). Shrimp Alkaline Phosphatase (SAP, Promega: M1821) was used to treat into the digested plasmid to prevent self-ligation.

Human *DNMT1* cDNA (*Eco*RI) and p336 (*Eco*RI-SAP) were ligated using the Quick Ligation™ Kit (NEB: M2200S) according to manufacturer's protocol. Transformation was performed with Sub cloning Efficiency™ DH5α™ Competent cells (Invitrogen: 18265-017) (see section 2.5.10). 20 colonies were handpicked up by pipette tips and inoculated into 2 ml of LB medium containing 100 $\mu g \cdot ml^{-1}$ Ampicillin. Then, incubation was performed at 37 ºC overnight with vigorous shaking. The following day, Miniprep was performed by the QIAprep Spin Miniprep Kit (Qiagen: 27104) according to manufacturer's protocol (see QIAprep Miniprep Handbook, June 2005). To elute each plasmid, 50 µl of RNase/DNase free water (Sigma: W4502) was added into the column. Following elution, 2 µl of each plasmid was subjected to restriction enzyme digestions with *EcoR*I (Roche: 11 175 084 001), *Pci*I (NEB: R0595S), *Xcm*I (NEB: R0533S) and *Sac*I (Roche: 10 669 792 001) to confirm the correct insertion of *DNMT1* cDNA into p336.

2.4.14.2 pCAG-DsRed2-C1-DNMT1-IRES-PAC

The pDsRed2-C1-hDNMT1 plasmid was digested with *Sal*I (NEB: R0138S), and Klenow (NEB: M0210S) was used to treat into *Sal*I sites to make blunt ends from sticky ends. Then, *Age*I (NEB: R0552S) digestion was performed with the *Sal*I-digested and Klenow-filled pDsRed2-C1-hDNMT1 plasmid. Gel electrophoresis was

performed in a 0.8% agarose gel. A 5.9 kb band of DsRed2-*DNMT1* cDNA was cut out from the gel by a blade. DsRed2-*DNMT1* cDNA was purified using the QIAquick Gel Extraction Kit (Qiagen: 28704).

The p336+linker (p388) plasmid (see section 5.2.1.1) provided by Prof. Chris Denning (University of Nottingham) was double digested with *Pme*I (NEB: 0560S) and *Age*I. Gel electrophoresis was performed on a 0.8% agarose gel. A 6,469 bp band of p388 was cut out from the gel by a blade. The digested plasmid was purified using the QIAquick Gel Extraction Kit (Qiagen: 28704). Then, ligation between DsRed2-*DNMT1* cDNA (*Sal*I-Klenow-*Age*I) and p388 (*Pme*I-*Age*I), and transformation were performed. Individual 12 colonies were handpicked up by pipette tips and inoculated into 2 ml of LB medium containing 100 $\mu g \cdot ml^{-1}$ Ampicillin. Incubation was performed at 37 ºC overnight with vigorous shaking. Then, Miniprep was performed. 12 plasmids were subjected to restriction enzyme digestions with *Bam*HI (Roche: 10 220 612 001), *Sac*I and *EcoR*I to confirm the correct insertion of DsRed2-*DNMT1* cDNA into p388.

2.4.15 Mouse embryonic fibroblasts (MEFs) culture

The MEFs 43 batch established in our laboratory was used for producing conditioned medium (BG-K CM). MEFs were cultured in the T75 flask (Fisher Scientific: TKT-130-190W) and split at a ratio of 1:3. Once MEFs were confluent, the MEFs medium was aspirated and MEFs were washed once with 10 ml of Dulbecco Phosphate Buffered Saline (DPBS, Invitrogen: 14190-169). Then, 2 ml of 0.05% Trypsin EDTA (Invitrogen: 25300-062) was added in the flask and incubated for 3 min at 37 ºC in an incubator. The flask was tapped gently to dislodge the cells and 8 ml of MEFs medium was added to inactivate Trypsin EDTA. The medium was pipetted over the flask surface vigorously and placed into the universal tube. Centrifugation was performed at 200 g for 4 min. The medium was aspirated and cell pellets were resuspended in 2 ml of MEFs medium. The cell suspension was added into a new T75 flask containing 13ml of MEFs medium. Then, MEFs were incubated in a 37 ºC incubator until they were confluent.

To prepare BG-K CM, MEFs were mitotically inactivated for 2.5 h at 37 ºC with 10 $\mu g \cdot ml^{-1}$ Mitomycin C (Sigma: M4287, see section 8.1.5.2). At the same time, 10 ml of

0.1% gelatine solution (see section 8.1.5.7) was added into a new T75 flask and incubated at 37 ºC for 2.5 h. Mitotically inactivated MEFs were washed with PBS three times and harvested by 0.05% Trypsin EDTA. Cells were counted by a Neubauer haemocytometer (Fisher scientific: MNK-504-020P). Cells were centrifuged at 150 g for 4 min and resuspended in appreciate amounts of MEF medium. 4.8 x 10^6 cells were seeded into a gelatine-coated T75 flask.

2.4.16 BG-K CM medium collection

The BG-K medium (see section 8.1.5.3) was conditioned by mitotically inactivated MEFs (see section 8.1.5.2). 25ml of the BG-K medium was added to mitotically inactivated MEFs in a T75 flask. Following incubation overnight, the BG-K CM medium was collected and placed into a 150 ml Sterilin Container (SLS Ltd: CON7572). bFGF (Sigma: F0291) was added into the BG-K CM medium to give a final concentration of 4 ng·ml^{-1}. 10 ml aliquots were stored at -80 ºC. BG-K CM was normally collected during 7 days.

2.4.17 HUES7 culture

To generate hESOD1 cell lines (see Chapter 5), HUES7 cells were cultured by trypsin-passaging on matrigel in the BG-K CM medium as previously described (Allegrucci et al., 2007; Anderson et al., 2007; Burridge et al., 2007). HUES7 cells were usually cultured in the T25 flask (Fisher Scientific: TKT-130-150L), and split at a ratio of 1:3. Once HUES7 cells were confluent, the medium was aspirated and cells were washed once with 5 ml of PBS. Then, 1 ml of 0.05% Trypsin EDTA (Invitrogen: 25300-062) was added in the flask and incubated for 1 min at 37 ºC in an incubator. Then, the flask was banged to dislodge the cells from the flask and 4 ml of the BG-K medium (see section 8.1.5.3) were added to inactivate Trypsin EDTA. The medium was pipetted up and down over the flask surface vigorously and placed into a universal tube. Centrifugation was performed at 150 g for 4 min. The medium was aspirated and cell pellets were resuspended in 3 ml of BG-K CM medium. 1 ml of cell suspension was added into a new T25 flask containing 4 ml of the BG-K CM medium. Cells were incubated in a 37 ºC incubator. The medium was changed everyday until cells were confluent.

2.4.18 OCT3/4, NANOG and SSEA4 staining

HUES7 cells were seeded at a density of 1×10^4 cells per well onto a 8-well chamber slide (Nunc Labtek: 177402). Cells were cultured for 24 ~ 48 h until fixation. The medium was aspirated, and cells were washed once with PBS and fixed with 4% PFA (see section 8.4.3.8) for 30 min at room temperature. Cells were washed three times with 0.2% Tween 20 in PBS. Then, cells were permeabilised with 0.2% Triton X-100 for 30 min at room temperature and washed once with 0.2% Tween 20 in PBS. Blocking was performed for 1 h at room temperature with 2% BSA/0.1% Tween 20 in PBS. Then, primary antibodies, OCT3/4 (Santa Cruz: SC-5279), NANOG (R&D system: AF1997) and SSEA4 (Chemicon: MAB4304), were treated at 1:200, 1:200 and 1:100 dilutions and incubated for 1 h at room temperature (see Table 2-2). Cells were washed three times with 0.2% Tween 20 in PBS. Secondary antibodies, FITC-conjugated anti-mouse secondary antibody (1:200 dilution, Jackson ImmunoResearch: 115-095-068), Cy3-conjugated anti-mouse secondary antibody (1:250 dilution, Jackson ImmunoResearch: 115-165-068), and FITC-conjugated anti-goat secondary antibody (1:200 dilution, Novus Biologicals: NB710-F) were treated and incubated at room temperature for 30 min (see Table 2-3). Cells were washed three times with 0.2% Tween 20 in PBS and mounted using VECTASHIELD® mounting medium with DAPI (Vector Laboratories: H1200).

2.4.19 Transfection and puromycin selection

Cells were harvested by 0.05% Trypsin EDTA. The number of cells was counted by a Neubauer haemocytometer (Fisher scientific: MNK-504-020P). 1×10^6 cells were resuspended in 750 µl of hypo-osmolar buffer (Eppendorf: 4308 070.501), and incubated at room temperature for 20 min. 50 µg of a linearized plasmid was added into the cell suspension and mixed together. The mixture was placed into a Geneflow Electroporation Cuvette (Geneflow: E6-0070). Electroporation was performed by using previously optimised conditions, 600V/30 µs (Anderson et al., 2007). Cells were seeded into one of 6 wells. The following day, the medium containing 300 $ng\cdot ml^{-1}$ of Puromycin (Sigma: P8833) was added into cells to select puromycin-resistant colonies. Following medium change everyday, puromycin-resistan colonies were handpicked up by pipette tips and transferred into one of 24 wells. Once cells were confluent in one of 24 wells, each colony was trypsinised, seeded into one of 24 wells (Fisher

scientific: TKT-190-010Y). Cells were expanded to be confluent in a T25 flask (Fisher scientific: TKT-130-150L).

Transiently transfection was performed by a GeneJammer^{TM} (Stratagene: 204130) according to manufacturer's protocol.

2.4.20 Cell cycle analysis

Cells harvested by 0.05% Trypsin EDTA were resuspended in 1 ml of PBS. To fix the cells, 2.5 ml of 100% ethanol was added into resuspended cells to give a final concentration of 70%. Incubation was performed on ice for 15 min to prevent clustering of cells during fixation. Cells were pelleted by centrifugation at 150 g for 4 min. The cell pellets were resuspended in 500 µl of the solution containing 50 $\mu g \cdot ml^{-1}$ Propidium Iodide (PI, Sigma P4170), 0.1 $mg \cdot ml^{-1}$ Ribonuclease A (RNase A, Sigma P6513), and 0.05% Triton X-100 and incubated at 37 ºC for 40 min. Following incubation, 3 ml of PBS was added into the solution to wash briefly. Cells were pelleted by centrifugation at 150 g for 4 min and resuspended in 500 µl of PBS. The cell cycle analysis was carried by a CYTOMICSTM FC500 Flow Cytometer (Beckmen Coulter). Data were analysed by WinMDI v2.8 (http://facs.scripps.edu/software.html) and Cylchred v1.0.2 programmes.

2.4.21 Statistical analysis

All statistically analyses were performed using SPSS 15.0 for windows (SPSS Inc., Chicago, USA). All results are presented as mean ± 1 standard deviation (SD) unless otherwise stated. The Post Hoc, Mann-Whitney and Kruskal-Wallis tests were performed on all samples. A non-parametric Kruskal-Wallis test and a Mann-Whitney test were used for between-groups analysis. Where a statistically significant result ($p<0.05$) was returned, a Post Hoc test was used to perform pairwise comparisons.

3 ALLELE-SPECIFIC EXPRESSION OF IMPRINTED GENES IN HUMAN EMBRYONIC STEM CELL LINES

3.1 Introduction

3.1.1 Allele-specific expression of imprinted genes

Although most autosomal genes are expressed from both parental alleles, imprinted genes are known be monoallelic expressed in a parent-of-origin-dependent manner (reviewed by Reik and Walter, 2001; Surani, 2001). The allele-specific expression of imprinted genes is guided by allele-specific differential epigenetic marks on their regulatory regions (reviewed by Constancia et al., 2004; Li, 2002). In the human, ~ 50 genes have been identified to be imprinted (see Table 1-1) (reviewed by Morison et al., 2005). However, imprinted genes are not always monoallelically expressed. Genes can be imprinted in a tissue-specific, isoform-specific, promoter-specific or polymorphic manner (reviewed by Constancia et al., 2004; Murrell, 2006). For most human imprinted genes, the allele-specific expression status in the inner cell mass (ICM) of blastocyst stage embryos is unknown and therefore the expected status of human embryonic stem cells (hESCs) is undefined yet.

3.1.1.1 Tissue-specific imprinting

Some imprinted genes show either monoallelic or biallelic expression depending on the tissue. This is defined as 'tissue-specific imprinting'. For example, *WT1* (*Wilms' tumour 1*) is monoallelically expressed in lymphocytes from peripheral blood, fibroblasts from fetal skin, body and umbilical cord, and placenta, whereas it is biallelically expressed in kidney and fetal brain (Jinno et al., 1994; Mitsuya et al., 1997). Furthermore, *UBE3A* (*ubiquitin protein ligase E3A*) is know to be imprinted in brain, but other tissues show biallelic expression (Rougeulle et al., 1997). Other imprinted genes including *ATP10C*/*ATP10A* (Meguro et al., 2001), *GNAS1* (*G protein α subunit 1*) (Hayward et al., 2001), *GRB10* (*growth factor receptor-bound 10*) (Blagitko et al., 2000) and *KCNQ1* (*potassium voltage-gated channel, KQT-like subfamily, member 1*) (Gould and Pfeifer, 1998) are previously known to have tissue-specific imprinting in the human.

3.1.1.2 Isoform-specific imprinting

Some genes can be imprinted in an isoform-specific manner. For example, *PEG1* (*paternally expressed gene 1*)/*MEST* (*mesoderm specific transcript*) has two isoforms (isoform 1 and 2) derived from their unique first exons (exon A and exon 1) in the human (Kosaki et al., 2000). *PEG1* isoform 1 is monoallelically expressed in most human tissues, whereas *PEG1* isoform 2 is biallelically expressed (Kosaki et al., 2000; Nakabayashi et al., 2002). Moreover, the *GRB10* gene consists of 4 different splicing variants (*GRB10β*, *GRB10γ*, *GRB10ε* and *GRB10σ*) and they have distinct allele-specific expression patterns (Blagitko et al., 2000; Hikichi et al., 2003). For instance, *GRB10γ1* is expressed from the maternal allele in the skeletal muscle, whereas other variants are expressed from two alleles (Blagitko et al., 2000).

3.1.1.3 Promoter-specific imprinting

Some genes can be imprinted in a promoter-specific manner. The *IGF2* (*Insulin-like growth factor 2*) gene was first identified to have promoter-specific imprinting (Ekstrom et al., 1995; Vu and Hoffman, 1994). In liver and chondrocytes, the *IGF2* transcript derived from the P1 promoter is expressed from both parental alleles, whereas other *IGF2* transcripts derived from P2, P3 and P4 promoters are monoallelically expressed (Ekstrom et al., 1995; Vu and Hoffman, 1994).

3.1.1.4 Polymorphic imprinting

Some genes can have polymorphic imprinting (defined as inter-individual variations of imprinting) in the same tissues (reviewed by Murrell 2006). For example, *IGF2R* (*insulin-like growth factor 2 receptor*) shows various expression patterns (monoallelic, predominant monoallelic and biallelic) between a range of term placentae examined (Monk et al., 2006a; Xu et al., 1993). Moreover, *PHLDA2* (*pleckstrin homology-like domain, family A, member 2*)/*TSSC3* (*tumor suppressing subtransferable candidate 3*)/*IPL* (*imprinted in placenta and liver*) is monoallelically or biallelically expressed in adult brain and blood (Muller et al., 2000; Qian et al., 1997). Other imprinted genes including and *TSSC5* (*tumour suppressing subtransferable candidate 5*)/*SLC22A18* (*Solute carrier family 22, member 18*) (Cooper et al., 1998) and *WT1* (Jinno et al., 1994) are previously known to have polymorphic imprinting in the human.

3.1.2 Determination of allele-specific expression

The allele-specific expression status of human imprinted genes can be determined by either polymerase chain reaction-restriction fragment length polymorphism (PCR-RFLP) or direct sequencing (Cui et al., 1998; Monk et al., 2006a; Onyango et al., 2002).

3.1.2.1 Genotyping

Genotyping is required to identify the sample having a heterogeneous genotype, because this type is only informative for analysing allele-specific expression of an imprinted gene. In this manner, DNA need to be amplified by PCR at the region containing a polymorphic site that allows determining a genotype followed by either a restriction enzyme digestion recognising a polymorphic site or direct sequencing (Cui et al., 1998; Monk et al., 2006a; Onyango et al., 2002).

3.1.2.2 Allele-specific expression

Once a sample has been determined as a heterozygous genotype and thus informative for an imprinted gene, allele-specific expression of the gene can be determined by PCR-RFLP and direct sequencing. In this time, cDNA need to be amplified by PCR and then either a restriction enzyme digestion or direct sequencing allows determining monoallelic, predominant monoallelic or biallelic expression of the gene (Cui et al., 1998; Monk et al., 2006a; Onyango et al., 2002). The allele-specific expression of the gene can be determined by the relative band intensity between two alleles in PCR-RFLP or the relative peak height between two alleles in direct sequencing (Cui et al., 1998; Monk et al., 2006a; Onyango et al., 2002). In PCR-RFLP, loss of imprinting is determined as a ratio of less than 3:1 between the more-abundant and less-abundant alleles, according to Cui et al., (1998). In direct sequencing, the electrophoretogram shows that both peaks are present at a polymorphic site with the same height. This is defined as loss of imprinting (Monk et al., 2006a; Onyango et al., 2002).

3.1.3 Allele-specific expression associated with biological consequences

The allele-specific expression of some imprinted genes identified in the human is closely associated with several biological consequences including congenital disorders,

PWS (Prader-Willi syndrome), BWS (Beckwith-Wiedemann syndrome) and AS (Angelman syndrome) (reviewed by Robertson, 2005; Weksberg et al., 2003) and cancer formation (reviewed by Feinberg, 2007; Jelinic and Shaw, 2007). Moreover, some imprinted genes are involved in embryonic and placental development, cell proliferation, cell death and behaviour (reviewed by Reik and Walter, 2001; Surani, 2001).

3.1.3.1 Genes related to human cancers

The allele-specific expression of *TP73*, *PEG1*, *IGF2*, *SLC22A18* and *PEG3* is associated with human tumourigenesis (Chi et al., 1999; Dowdy et al., 2005; Kaghad et al., 1997; Lee et al., 1998; Maegawa et al., 2001; Mai et al., 1998a; Mai et al., 1998b; Nakanishi et al., 2004; Pedersen et al., 2002; Schwienbacher et al., 2000). In detail, *TP73* (*tumour protein 73*) is located in human chromosome 1p 36.3 that is paternally imprinted (Kaghad et al., 1997). *TP73* is monoallelically expressed in normal tissues, whereas it is biallelically expressed in diverse human cancers, including lung, prostate and kidney carcinomas (Chi et al., 1999; Kaghad et al., 1997; Mai et al., 1998a; Mai et al., 1998b). *PEG1* is located in human chromosome 7q32 that is maternally imprinted (Kerjean et al., 2000; Kosaki et al., 2000; Riesewijk et al., 1997). Loss of imprinting of *PEG1* is often found in invasive breast and lung cancers (Nakanishi et al., 2004; Pedersen et al., 2002). *IGF2* is maternally imprinted on human chromosome 11p15 (Giannoukakis et al., 1993; Ohlsson et al., 1993). Loss and gain of imprinting of *IGF2* has been commonly found in ovarian, lung, liver and colon carcinomas (reviewed by Feinberg, 2007; Jelinic and Shaw, 2007). *SLC22A18*/*TSSC5* is located in human chromosome 11p15 that is imprinted in a tissue-specific manner (Lee et al., 1998). Gain of imprinting of *SLC22A18* has been found in hepatocarcinomas (Schwienbacher et al., 2000). *SLC22A18* is biallelically expressed in normal liver tissues, whereas it is predominatly monoallelically expressed in hepatocarcinomas (Schwienbacher et al., 2000). *PEG3* (*paternally expressed gene 3*) is maternally imprinted on human chromosome 19q13 (Dowdy et al., 2005; Maegawa et al., 2001). Loss of imprinting of *PEG3* is frequently found in glioma, ovarian, cervical and choriocarcinoma cell lines (Dowdy et al., 2005; Maegawa et al., 2001).

3.1.3.2 Genes related to human disorders

KCNQ1OT1 (*KCNQ1 overlapping transcript 1*)/*LIT1* (*long QT intronic transcript 1*), which is maternally imprinted in human chromosome 11p15, is an imprinted antisense RNA of the *KCNQ1* gene (Lee et al., 1999; Smilinich et al., 1999). Loss of imprinting of *KCNQ1OT1* mediated by loss of methylation at *KvDMR1* is frequently found in BWS patients (Lee et al., 1997; Smilinich et al., 1999). Less frequently, loss of imprinting of *IGF2* and *H19* can be found in BWS patients (Reik et al., 1995; Weksberg et al., 1993).

SNRPN (*small nuclear ribonucleoprotein-associated polypeptide N*) contains multiple discrete functional components including *SNURF* and *UBE3A-AS* (reviewed by Morison et al., 2005). *IPW* (*imprinted in Prader-Willi syndrome*) is an untranslated RNA (Wevrick et al., 1994) and *ATP10C* encodes for an aminophospholipid-transporting ATPase (Meguro et al., 2001). These genes are maternally imprinted and located in the PWS and AS critical region on human chromosome 15q11-13 (Figure 3-1). Loss of imprinting of *SNRPN*, *IPW* and *ATP10C* are closely associated with PWS and AS (Meguro et al., 2001; Orstavik et al., 2003; Reis et al., 1994; Sutcliffe et al., 1994; Wevrick et al., 1994). Furthermore, *NDN* and *NDNL1*, members of the MAGE (melanoma antigen) protein family, are also maternally imprinted on human chromosome 15q11-13, are potentially involved in PWS and AS (MacDonald and Wevrick, 1997).

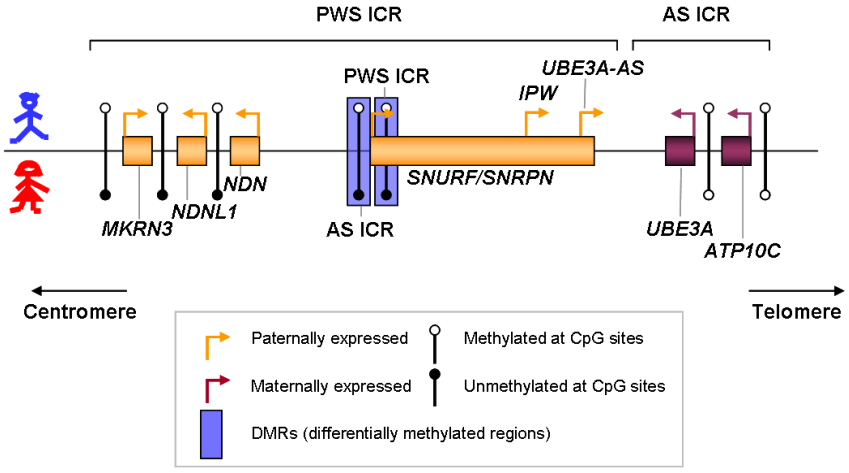

Figure 3-1. The Prader-Willi syndrome/Angelman syndrome locus

The *GNAS1* gene located in human chromosome 20q13 contains multiple discrete functional components including *NESP55* (*neuroendocrine secretory protein 55*), *NESP55AS* (*NESP55 antisense*), *XLas* (Golgi-specific $G_s\alpha$ isoform), *Exon 1A* (untranslated RNA), and $G_s\alpha$ (G protein alpha-subunit) (Hayward et al., 2001; Liu et

al., 2000). Loss of imprinting of *Exon 1A* and *NESP55* is associated with Pseudohypoparathyroidism type 1b (PHP-1b). Moreover, loss of imprinting of $G_s\alpha$ can be found in Albright hereditary osteodystrophy (AHO) and PHP-1a (Bastepe et al., 2005; Hayward et al., 2001; Patten et al., 1990).

3.1.3.3 Genes related to tissue development and differentiation

TP73 has an important role in the regulation of cell cycle and apoptosis (Kaghad et al., 1997). *CDKN1C* encodes for a cyclin-dependent kinase (CDK) inhibitor that plays an important role in the regulation of cell cycle (Hatada and Mukai, 1995; Matsuoka et al., 1995). *PEG10* (*paternally expressed gene 10*), a retrotransposon-derived gene, have an important role in liver regeneration and embryonic development (Okabe et al., 2003; Tsou et al., 2003). *WT1* plays an important role in urogenital development and hamatopoietic differentiation (Kreidberg et al., 1993; Park et al., 1993; Pritchard-Jones et al., 1990). *DLK1*, which encodes for a cell-surface transmembrane protein containing six epidermal growth factor (EGF) repeat motifs, plays an important role in the regulation of adipocyte differentiation, and hematopoietic differentiation and proliferation (Kawakami et al., 2006; Li et al., 2005a). *PEG3* has an important role in the regulation of apoptosis mediated by p53, embryonic development and differentiation of neuronal cells (Deng and Wu, 2000; Li et al., 1999). *NDN* and *NDNL1* have an important role in regulation of neuronal differentiation (Boccaccio et al., 1999; Kobayashi et al., 2002).

3.1.4 Allele-specific expression in human oocytes and embryos

Although allele-specific expression of imprinted genes has been extensively studied in mouse oocytes and preimplantation stage embryos, only few studies are available in the human. So far, allele-specific expression of 4 imprinted genes has been examined in human oocytes and preimplantation stage embryos. *IGF2* and *SNRPN* are monoallelically expressed in preimplantation stage embryos (Huntriss et al., 1998; Lighten et al., 1997; Salpekar et al., 2001) in association with differential methylation at the *SNRPN* DMR (El-Maarri et al., 2001; Geuns et al., 2003). *PEG1* is monoallelically expressed in preimplantation stage embryos (Monk and Salpekar, 2001) that is associated with differential DNA methylation at the *PEG1* DMR (Kerjean et al., 2000; Sato et al., 2007). However, *XIST* is expressed from both

parental alleles in human oocytes and preimplantation embryos (Daniels et al., 1997; Ray et al., 1997). Monoallelic DNA methylation at *KvDMR1* (Geuns et al., 2007b; Khoureiry et al., 2008), *H19* (Kerjean et al., 2000; Sato et al., 2007), *ZAC* (Sato et al., 2007), *GTL2* (Geuns et al., 2007a) DMRs has been reported in human oocytes and preimplantation stage embryos, implicating that their corresponding genes could be monoallelically expressed.

3.1.5 Allele-specific expression in human embryonic germ cell lines

The allele-specific expression of *H19*, *TSSC5*, *SNRPN* and *IGF2* has been examined in human embryonic germ (hEG) cell lines (LV.EB, SL.RC, EU.EE, SD.EP and SD.EC) derived from primordial germ cells (PGCs) isolated from the developing gonadal ridges and mesenteries of 5- to 9- weeks embryos (Onyango et al., 2002; Shamblott et al., 1998). All genes are monoallelic or predominant monoallelic expressed in 1 to 2 informative lines (see Table 3-1). In detail, *TSSC5* is monoallelically expressed in LV.EB (Onyango et al., 2002). *H19* is monoallelically expressed in SD.EP and SD.EC lines that is associated with differential methylation at the *H19* DMR (Onyango et al., 2002). *SNRPN* is monoallelically expressed in SL.RC. Predominant monoallelic expression of *IGF2* is observed in two cell lines, LV.EB and SL.RC, showing an allele ratio of 4:1 or 5:1. Thus, Onyango *et al*., (2002) has suggested hEG cell lines have stable imprinting status that may not be a significant barrier to hEG used in human therapeutic applications.

3.1.6 Allele-specific expression in human embryonic stem cell lines

The allele-specific expression of imprinted genes has been reported in human embryonic stem cell lines (Mitalipov, 2006; Plaia et al., 2006; Rugg-Gunn et al., 2005; Sun et al., 2006). Rugg-Gunn *et al*., (2005) has examined the allele-specific expression of 6 imprinted genes (*IGF2*, *IPW*, *KCNQ1OT1*, *H19*, *TSSC5* and *NESP55*) in 1 to 3 informative cell lines (total 4 cell lines examined; hSF-6, H9, H7 and HES-3) with a wide range of passages (passages from 42 to 155; see Table 3-1). Sun et al., (2006) has examined the allele-specific expression of 4 imprinted genes (*H19*, *KCNQ1*, *NDNL1* and *PEG10*) in sHhES-1 and HUES-7 cell lines at passages 21 to 62 (see Table 3-1). Mitalipov et al. (2006) has examined the allele-specific expression of *H19* and *IGF2* in BGN2 and H1. All genes studied are monoallelically or predominaly

monoreallically expressed in all cell lines examined (Mitalipov, 2006; Plaia et al., 2006; Rugg-Gunn et al., 2005; Sun et al., 2006).

In contrast to data from other mammalian ESC lines previously shown to exhibit imprinting errors (Dean et al., 1998; Feil et al., 1997; Fujimoto et al., 2006; Humpherys et al., 2001; Mitalipov et al., 2007; Mitalipov, 2006), hESC lines possess a substantial degree of imprinting stability (Mitalipov, 2006; Plaia et al., 2006; Rugg-Gunn et al., 2005; Sun et al., 2006). However, there are limitations in human hESC studies that preclude the general conclusion of imprint stability in hESC lines. Because over 400 hESC lines have been currently established, the few cell lines (total 9 cell lines) examined can not be extrapolated to generalise the imprinting status of all hESC lines. Within 9 cell lines, only one or two cell lines are informative for imprinted genes (Table 3-1) that is also difficult to generalise 'normal' imprinting status in hESC lines. Moreover, although ~ 50 imprinted genes have been identified in the human (Morison et al., 2005), only few imprinted genes are employed to determine imprinting stability of hESC lines (Table 3-1)

3.1.7 Chapter aims

The overall aim of this chapter is to perform the most comprehensive assessment to date of allele specific expression of 22 imprinted genes and 3 non-imprinted genes in 22 hESC lines, because imprinting disruptions in hESCs may induce spontaneous differentiation, prevent from *in vitro* and *in vivo* differentiation into a specific lineage, and form a certain type of cancers that are not acceptable for human safe transplantation (Allegrucci et al., 2004).

22 human imprinted genes were selected in this Chapter (see Table 3-2), because they are functionally known to be important for early embryonic development and differentiation, or to be closely associated with several human congenital disorders and tumours (see section 1.3.5 and 3.1.3).

In total, 22 hESC lines are examined in this Chapter (see Table 2-1). 16 HUES-lines were derived from the Harvard University and cultured (on MEFs with trypsin passage) under same protocols and materials, and passage numbers are similar (from 26 to 37) (Cowan et al., 2004). Additional 6 cell lines (BG01, H1, NOTT1, NOT2, HES-2 and NL-HES-1) were independently derived from five different laboratories

and cultured in various culture conditions and methods (Allegrucci et al., 2007; Burridge et al., 2007; Mitalipova et al., 2003; Reubinoff et al., 2000; Thomson et al., 1998; van de Stolpe et al., 2005). Their passage numbers were variable from 25 to 45. (Allegrucci et al., 2007; Burridge et al., 2007; Mitalipova et al., 2003; Reubinoff et al., 2000; Thomson et al., 1998; van de Stolpe et al., 2005).

Table 3-1. Imprinting status of mammalian embryonic stem cell lines

Species	Cell line		Imprinted genes													Reference
			PEG10	*IGF2*	*H19*	*KCNQ1*	*KCN1OT1*	*TSSC5*	*NDN*	*NDNL1*	*DLK1*	*SNRPN*	*IPW*	*NESP55*	*U2AF1-RS1*	*IGF2R*	
Human	EG	LV.EB	-	PM	-	-	-	M	-	-		-	-	-	-	-	(Onyango et al., 2002)
		SL.RC	-	PM	-	-	-	-	-	-		M	-	-	-	-	
		EU.EE	-	-	-	-	-	-	-	-		-	-	-	-	-	
		SD.EP	-	-	M	-	-	-	-	-		-	-	-	-	-	
		SD.EC	-	-	M	-	-	-	-	-		-	-	-	-	-	
	ES	hSF-6	-	M (p49~p86)	-	-	-	-	-	-		-	M (p49~p86)	-	-	-	(Mitalipov, 2006; Plaia et al., 2006; Rugg-Gunn et al., 2005; Sun et al., 2006)
		H9	-	-	M (p42 ~p62) PM, B (p66~p101)	-	M (p58~p96)	-	-	-		-	M (p61~p87)	-	-	-	
		H7	-	-	M (p58~p155)	-	M (p58~p155)	PM (p58~p155)	-	-		-	-	-	-	-	
		HES-3	-	-	M (p92~p101)	-	-	-	-	-		-	-	M, PM (p92~p101)	-		
		SHhES-1	M (p21~p47)	-	M (p24~p47)	M (p24~p47)	-	-	-	M (p24~p62)		-	-	-	-	-	
		HUES7	M (p21~p47)	-	M (p21~p47)	-	-	-	-	-		-	-	-	-	-	
		BGN2	-	-	M	-	-	-	-	-		-	-	-	-	-	
		H1	-	PM	-	-	-	-	-	-		-	-	-	-	-	
		BG01V	-	-	M	-	-	-	-	-	M	M	-	-	-	-	
Primate	ES	ORMES-1	-	B	-	-	-	-	-	-	-	M	-	-	-	-	(Fujimoto et al., 2006)
		ORMES-3	-	B	-	-	-	-	-	-	-	-	-	-	-	-	
		ORMES-5	-	B	M	-	-	-	-	-	-	-	-	-	-	-	
		ORMES-6	-	B	B	-	-	-	M	-	-	M	-	-	-	-	
		ORMES-7	-	B	-	-	-	-	M	-	-	M	-	-	-	-	
		ORMES-8	-	B	B	-	-	-	M	-	-	M	-	-	-	-	
		ORMES-10	-	B	B	-	-	-	M	-	-	-	-	-	-	-	
Mouse	ES	SF-1-1	-	PM	PM	-	-	-	-	-	-	-	-	-	PM	B	(Dean et al., 1998)
		SF-1-3	-	PM	PM	-	-	-	-	-	-	-	-	-	PM	B	
		SF-1-8	-	PM	PM	-	-	-	-	-	-	-	-	-	PM	B	
		SF-1-G	-	M	M	-	-	-	-	-	-	-	-	-	M	B	

M, monoallelic expression; PM, predominant monoallelic expression; B, biallelic expression; passage number in parenthesises

3.2 Results

To investigate the allele-specific expression of 22 imprinted genes and 3 non-imprinted genes (see Table 3-2), PCR-RFLP and direct sequencing were performed, according to previous publications described in Table 2-4.

Table 3-2. Imprinted genes and none-imprinted genes used in this chapter

Location	Gene	Imprinting	Expressed allele	Protein name or description	Accession number
1p36.33	*TP73*	I	Maternal	Tumour related protein	NM_005427
6q25.3	*SLC22A1*	PD or NR	-	Organic cation transporter	NM_003057
	IGF2R	PI	Biallelic	Insulin-like growth factor 2 receptor	NM_000876
7q21	*PEG10*	I	Paternal	Retroviral gag pol homologue	XM_496907
7q32	*PEG1*	I	Paternal	Alpha/β hydrolase fold family	NM_015068
	MESTIT1	I	Paternal	-	AF482998
11p13	*WT1*	I	Paternal	Zinc finger protein	AY245105
11p15.5	*NAPIL4*	NI	Biallelic	Nucleosome assembly protein	NM_005969
	PHLDA2	PD	Maternal	Pleckstrin homology-like domain	AF019953
	SLC22A18	I	Maternal	Organic cation transporter	AF059663
	CDKN1C	I	Maternal	Cyclin-dependent kinase inhibitor	NM_000076
	KCNQ1OT1	I	Paternal	-	AJ0006345
	KCNQ1	I	Maternal	Voltage-gated potassium channel	BC111847
	TSSC4	NI	Biallelic	Tumor suppressing candidate	AF125568
	IGF2	I	Paternal	Insulin-like growth factor 2	X07868
	H19	I	Maternal	-	AF087017
14q32	*DLK1*	I	Paternal	Delta-like 1 homolog	NM_003836
	GTL2	I	Maternal	Gene trap locus 2	AL117190
15q11-q13	*NDN*	I	Paternal	Necdin, neuronal growth suppressor	U35139
	NDNL1	I	Paternal	MAGE-like protein	NM_019066
	SNRPN	I	Paternal	Small nuclear ribonucleoprotein	NM_022806
	IPW	I	Paternal	-	U12897
	ATP10C	I	Maternal	ATPase, Class V	AH010630
19q13.4	*PEG3*	I	Paternal	Zinc-finger protein	NM_006210
20q13.2	*NESP55*	I	Maternal	Neuroendocrine secretory protein 55	M21741

Abbreviations: I, imprinted; NI, not imprinted; PI, polymorphic imprinting; PD, provisional data, NR, no reports of imprinting status, Adopted from Morison et al., (2005).

3.2.1 TP73

The allele-specific expression of TP73 was analysed by a *Sty*I polymorphism (Mai et al., 1998a). 9 informative cell lines (HUES1, HUES6, HUES7, HUES8, HUES10, HUES16, HES-2, NOTT2 and NTERA2) were identified by genotyping after genomic PCR amplification, followed by *Sty*I digestion (Figure 3-1 A). The allelic specific expression of *TP73* in 9 cell lines was determined by RT-PCR, followed by *Sty*I

digestion (Figure 3-1 B). Biallelic expression of *TP73* was detected in all informative cell lines, indicating an allele ratio of less than 3:1 of the two alleles. The biallelic expression of *TP73* was maintained during *in vitro* prolonged culture of HES-2 (passages 56, 65 and 96).

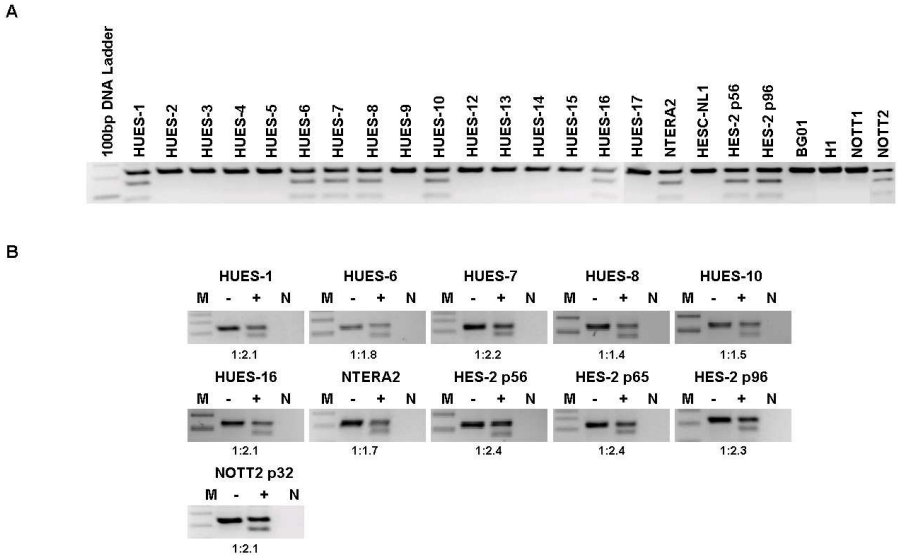

Figure 3-2. *TP73* imprinting in hESC lines
(A) Genotyping. PCR amplification with genomic DNA of each cell line, followed by *Sty*I digestion distinguished between heterozygous and homozygous cell line. (B) Allele-specific expression. RT-PCR with cDNA of informative heterozygous cell lines was carried out, followed by *Sty*I digestion. 50bp DNA ladder is denoted as the letter, M. Digestion with *Sty*I is indicated +, digested and -, not digested. The letter, N indicates a negative control of RT-PCR.

3.2.2 IGF2R

The allele-specific expression of *IGF2R* was analysed by both an *Acl*I polymorphism located in the promoter region and a *Msc*I polymorphism located in the intronic DMR (Vu et al., 2004). 12 informative cell lines (HUES1, HUES2, HUES3, HUES4, HUES5, HUES12, HUES13, HUES14, BG01, HESC-NL1, NOTT2 and H1) for an *Acl*I polymorphism and 3 informative cell lines (HUES5, HUES9 and HES-2) for a *Msc*I polymorphism were identified by PCR-RFLP (Figure 3-2 A and C). Of these informative cell lines examined, all cell lines showed biallelic expression, indicating an allele ratio of less than 3:1 of the two alleles (Figure 3-2 B and D). The biallelic expression retained during *in vitro* prolonged culture of HESC-NL1 (passages 22 and 58) and HES-2 (passages 56 and 96).

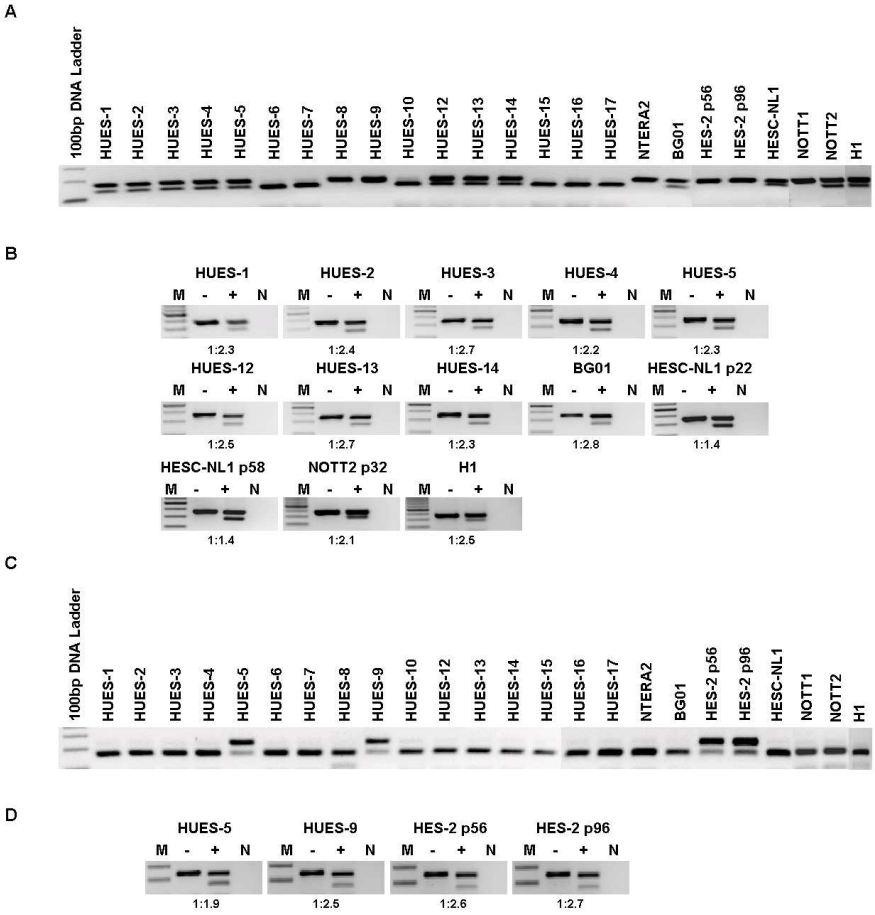

Figure 3-3. *IGF2R* imprinting in hESC lines
(A) Genotyping for an *Acl*I polymorphism. (B) Allele-specific expression of *IGF2R* for an *Acl* I polymorphism (C) Genotyping for a *Msc*I polymorphism. (D) Allele-specific expression of *IGF2R* for a *Msc*I polymorphism. (A and C) PCR amplification with genomic DNA of each cell line, followed by *Acl*I and *Msc*I digestion respectively distinguished between homozygous and heterozygous genotypes. (B and D) RT-PCR with cDNA of informative heterozygous cell lines, followed by *Acl*I and *Msc*I digestion respectively. 50bp DNA ladder is denoted by the letter, M. Digestion with *Acl*I or *Msc*I is indicated +, digested and -, not digested. The letter, N indicates negative control of RT-PCR.

3.2.3 PEG10

The allele-specific expression of *PEG10* was examined by a C/T polymorphism located in exon 12 (Sun et al., 2006). Of 4 informative cell lines (HUES5, HUES7, HUES10 and HUES12) examined, 3 showed monoallelic expression, indicated by only either the C or T allele at a polymorphic site (Figure 3-3 A and B). However, in HUES5, *PEG10* was biallelically expressed, indicated by both C and T peaks at a polymorphic site (Figure 3-3 B).

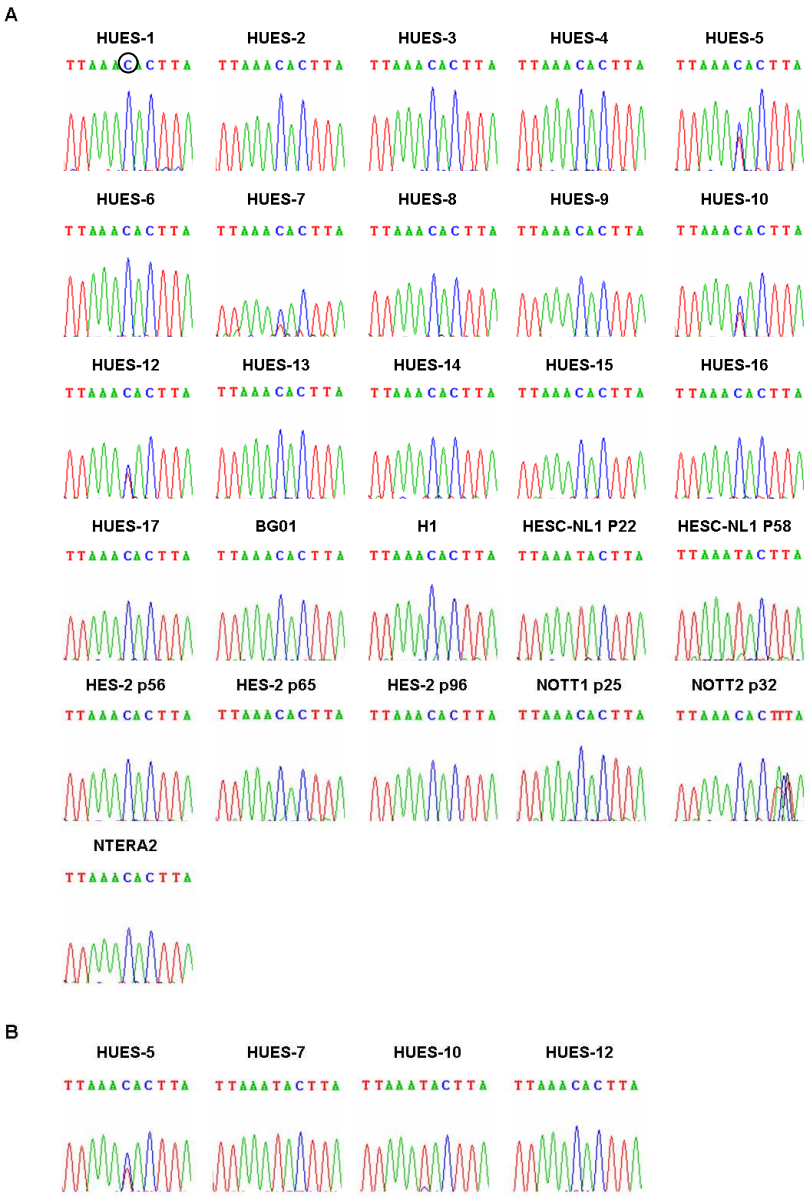

Figure 3-4. *PEG10* imprinting in hESC lines
(A) Genotyping. Chromatograms distinguished genotypes after PCR amplification of each cell line followed by direct sequencing. (B) Allele-specific expression. RT-PCR with cDNA of informative heterozygous cell lines, followed by direct sequencing. A circle indicates a polymorphic site.

3.2.4 PEG1 (MEST)

The isoform-specific imprinting of *PEG1* was examined by direct sequencing (Kosaki et al., 2000; Nakabayashi et al., 2002). 13 informative cell lines (HUES1, HUES2, HUES7, HUES10, HUES12, HUES15, HUES16, HUES17, BG01, NTERA2, HES-2, NOTT1 and NOTT2) were identified by a G/C polymorphism located in exon 12 of *PEG1* (Figure 3-4 A). Of 13 cell lines examined, 10 cell lines showed monoallelic expression and 1 cell line (HUES10) showed predominant monoallelic expression

indicated by a higher G peak than a C peak at a polymorphic site. NOTT2 and NTERA2 showed biallelic expression indicated by both G and C peaks at a polymorphic site (Figure 3-4 B). *PEG1* isoform 2 was expressed from two alleles in 10 of 13 informative cell lines examined (Figure 3-4 C). However, it was predominantly monoallelically expressed in HUES16 indicated by a higher C peak than a G peak at a G/C polymorphic site. NOTT1 and NTERA2 showed monoallelic expression indicated by only either the C or G allele at a polymorphic site (Figure 3-4 C). Isoform-specific imprinting status of *PEG1* persisted during *in vitro* prolonged culture of HES-2 (passages 56, 65 and 96) (Figure 3-4 B and C).

3.2.5 MESTIT1 (PEG1-AS)

The allele-specific expression of *MESTIT1* was examined by a G/A polymorphism located in exon 2 of *MESTIT1* (Nakabayashi et al., 2002). 12 informative cell lines (HUES2, HUES4, HUES7, HUES9, HUES10, HUES12, HUES15, HUES16, HUES17, HES-2, NOTT1 and NOTT2) were identified by genotyping (Figure 3-5 A). Of 12 informative cell lines examined, 9 cell lines showed monoallelic expression and 2 cell lines (HUES12 and NOTT1) showed predominantly monoallelic expression. However, *MESTIT1* was biallelically expressed in HUES15, indicated by both G and A peaks at a polymorphic site (Figure 3-5 B).

3.2.6 WT1

The allele-specific expression of *WT1* was determined by a *Hinf*I polymorphism located in exon 1 of *WT1* (Mitsuya et al., 1997). 6 cell lines (HUES2, HUES3, HUES5, HUES8, HUES9 and BG01) were informative (Figure 3-6 A). Of 6 cell lines examined, all cell lines showed biallelic expression, indicating an allele ratio of less than 3:1 of the two alleles (Figure 3-6 B).

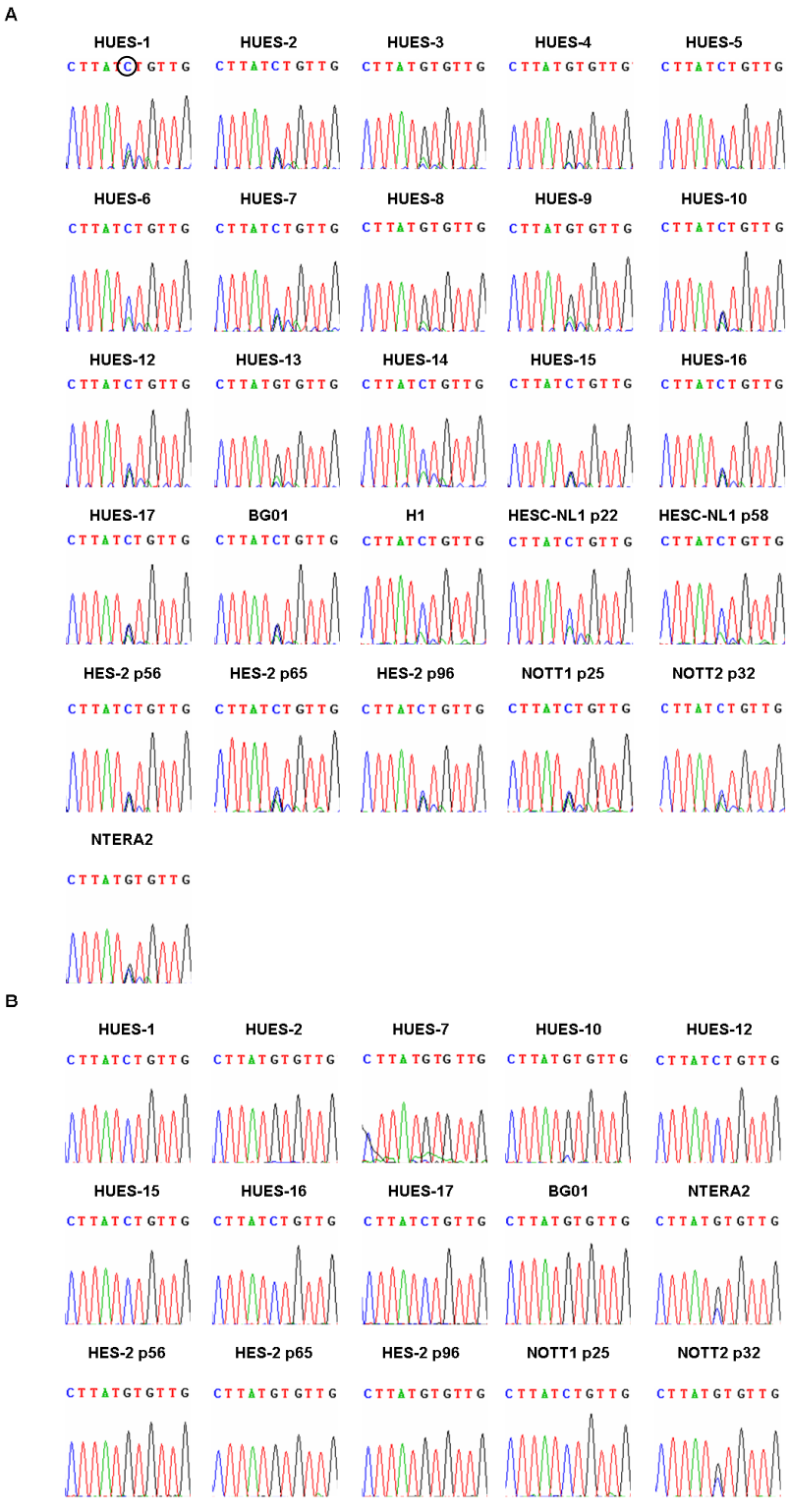
A
HUES-1
HUES-2
HUES-3
HUES-4
HUES-5
HUES-6
HUES-7
HUES-8
HUES-9
HUES-10
HUES-12
HUES-13
HUES-14
HUES-15
HUES-16
HUES-17
BG01
H1
HESC-NL1 p22
HESC-NL1 p58
HES-2 p56
HES-2 p65
HES-2 p96
NOTT1 p25
NOTT2 p32
NTERA2
B
HUES-1
HUES-2
HUES-7
HUES-10
HUES-12
HUES-15
HUES-16
HUES-17
BG01
NTERA2
HES-2 p56
HES-2 p65
HES-2 p96
NOTT1 p25
NOTT2 p32

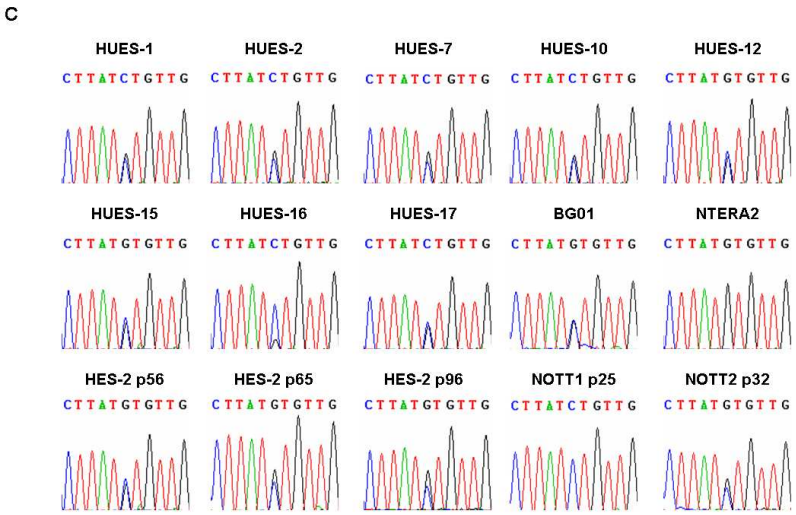

Figure 3-5. *PEG1* imprinting in hESC lines
(A) Genotyping. Chromatograms distinguished genotypes after PCR amplification of each cell line followed by direct sequencing (B) Allele-specific expression of *PEG1* isoform 1. (C) Allele-specific expression of *PEG1* isoform 2. (B and C) RT-PCR with cDNA of informative heterozygous cell lines, followed by direct sequencing. A circle indicates a polymorphic site.

3.2.7 H19

The allele-specific expression of *H19* was determined by both *Alu*I and *Rsa*I polymorphisms (Hashimoto et al., 1995; Morison et al., 2000). 11 informative cell lines (HUES1, HUES3, HUES5, HUES7, HUES9, HUES10, HUES14, HUES15, HES-2, NOTT1 and NOTT2) for a *Alu*I polymorphism and 13 informative cell lines (HUES1, HUES3, HUES4, HUES5, HUES7, HUES9, HUES10, HUES14, HUES15, BG01, HES-2, NOTT1 and NOTT2) for a *Rsa*I polymorphism were identified by PCR-RFLP (Figure 3-7 A). Of all informative cell lines examined, most cell lines sowed monoallelic expresion, except for NOTT2 and HES-2. NOTT2 and HES-2 showed biallelic expression (an allele ratio from 1.8:1 to 2.8:1) at both polymorphic sites (Figure 3-7 B). Biallelic expression of *H19* persisted during *in vitro* prolonged culture of HES-2 (passages 65 and 96).

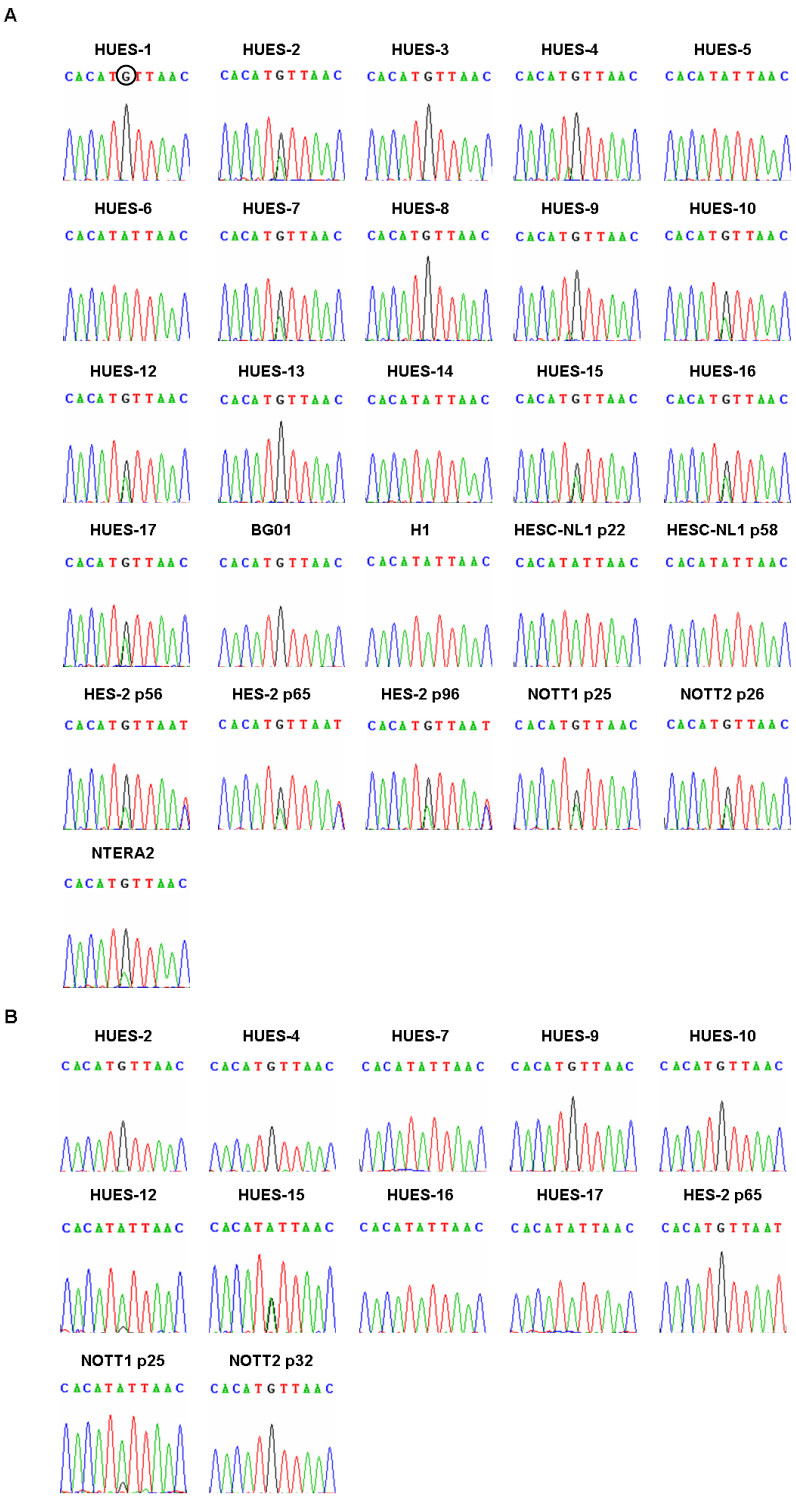

Figure 3-6. *MEST1OT1* imprinting in hESC lines

(A) Genotyping. Chromatograms distinguished genotypes after PCR amplification of each cell line followed by direct sequencing. (B) Allele-specific expression. RT-PCR with cDNA of informative heterozygous cell lines followed by direct sequencing. A circle indicates a polymorphic site.

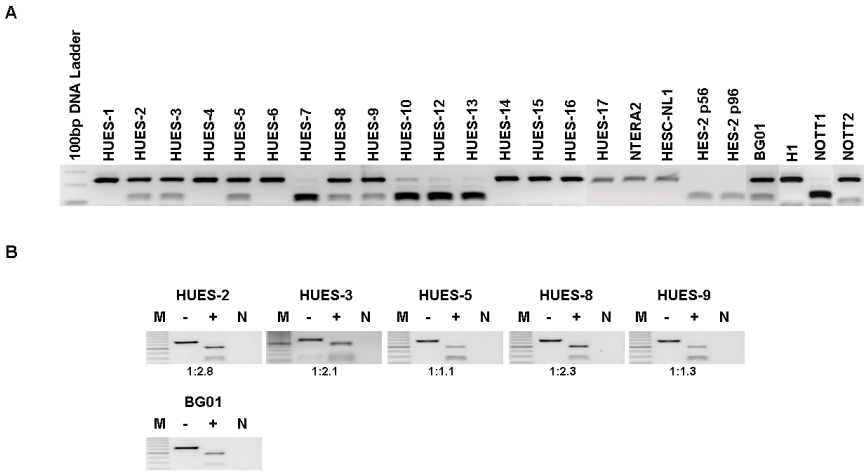

Figure 3-7. *WT1* imprinting in hESC lines
(A) Genotyping. PCR amplification with genomic DNA of each cell line followed by *Hif*I digestion distinguished between heterozygous and homozygous cell line. (B) Allele-specific expression. RT-PCR with cDNA of informative heterozygous cell lines followed by *Hif*I digestion. 50bp DNA ladder is denoted by the letter, M. Digestion with *Hif*I is indicated +, digested and -, not digested. The letter, N indicates a negative control of RT-PCR.

3.2.8 IGF2

The allele-specific expression of *IGF2* was determined by an *Apa*I polymorphism located in exon 9 (Hashimoto et al., 1995; Onyango et al., 2002). 10 cell lines (HUES1, HUES5, HUES6, HUES8, HUES9, HUES16, HUES17, HESC-NL1, HES-2 and NOTT2) were informative (Figure 3-8 A). Of 10 cell lines examined, 9 cell lines showed biallelic expression, indicating an allele ratio of less than 3:1 of the two alleles. However, HUES9 showed predominant monoallelic expression (an allele ratio 3.7:1) (Figure 3-8 B). The biallelic expression of *IGF2* persisted during *in vitro* prolonged culture of HES-2 (passages 56, 65 and 96).

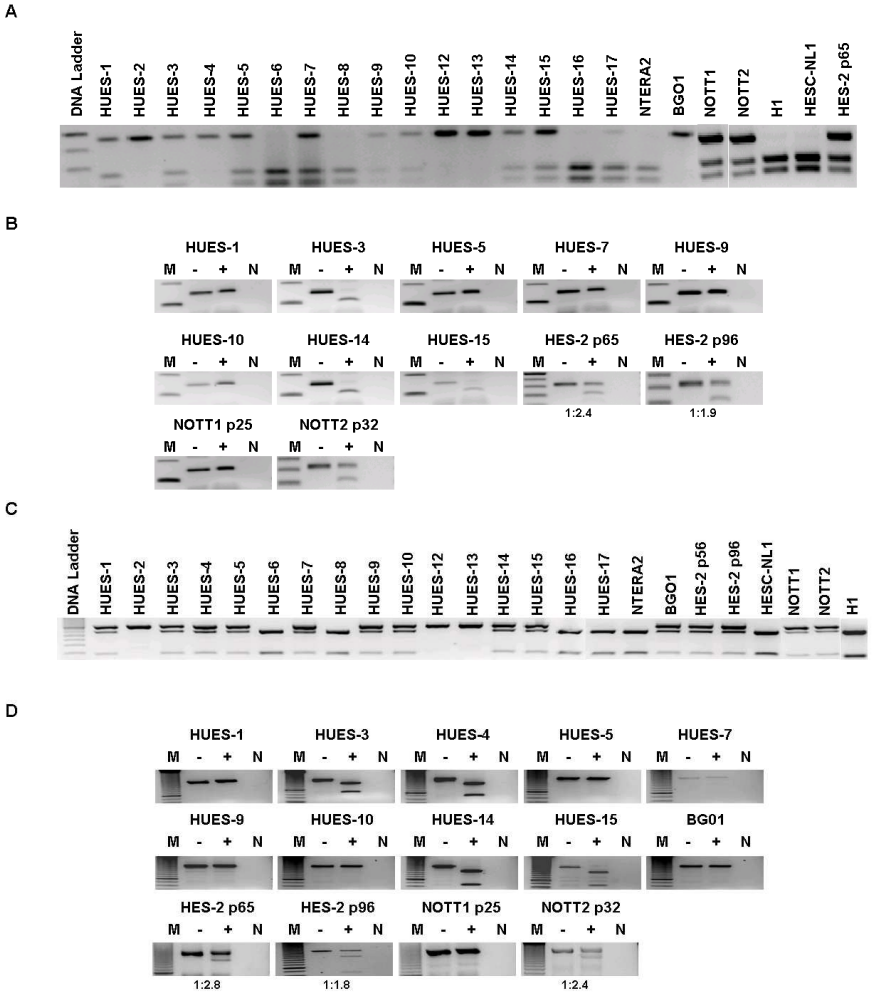

Figure 3-8. *H19* imprinting in hESC lines

(A) Genotyping for a *H19 Alu*I polymorphism. (B) Allele-specific expression of *H19 Alu*I RFLP. (C) Genotyping for a *H19 Rsa*I polymorphism. (D) Allele-specific expression of *H19 Rsa*I RFLP. (A and C) PCR amplification with genomic DNA of each cell line followed by *Alu*I and *Rsa*I digestion distinguished between heterozygous and homozygous cell line. (B and D) RT-PCR with cDNA of informative heterozygous cell lines followed by *Alu*I and *Rsa*I digestion. 50bp DNA ladder is denoted by the letter, M. Digestion with *Alu*I and *Rsa*I is indicated +, digested and -, not digested. The letter, N indicates negative control of RT-PCR.

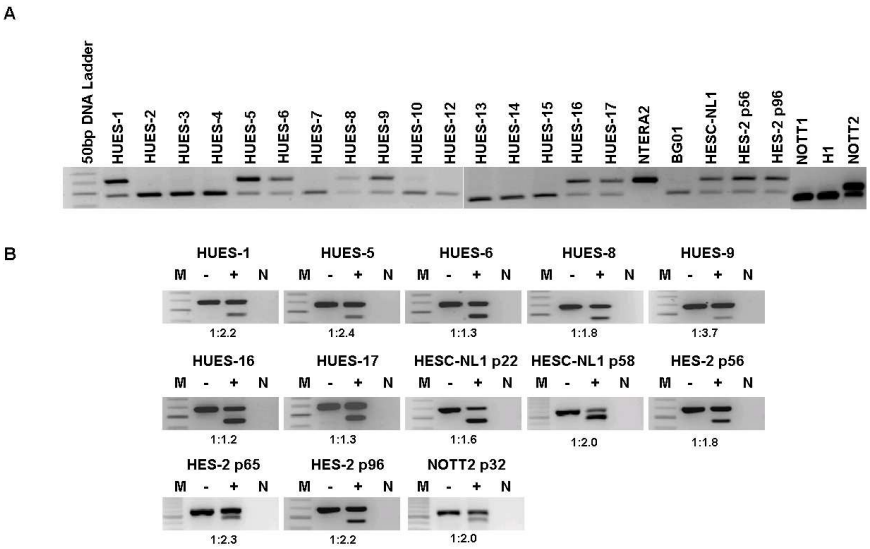

Figure 3-9. *IGF2* imprinting in hESC lines
(A) Genotyping. PCR amplification with genomic DNA of each cell line followed by *Apa*I digestion distinguished between heterozygous and homozygous cell line. (B) Allele-specific expression. RT-PCR with cDNA of informative heterozygous cell lines followed by *Apa*I digestion. 50bp DNA ladder is denoted by the letter, M. Digestion with *Apa*I is indicated +, digested and -, not digested. The letter, N indicates a negative control of RT-PCR.

3.2.9 KCNQ1 (KvLQT1)

The allele-specific expression of *KCNQ1* was determined by a G/A polymorphism (Sun et al., 2006). 8 informative cell lines (HUES1, HUES2, HUES6, HUES8, HUES9, HUES12, HUES13 and NOTT1) were identified by direct sequencing (Figure 3-9 A). Of 8 cell lines examined, all cell lines showed monoallelic expression, indicated by either G or A allele at a polymorphic site (Figure 3-9 B).

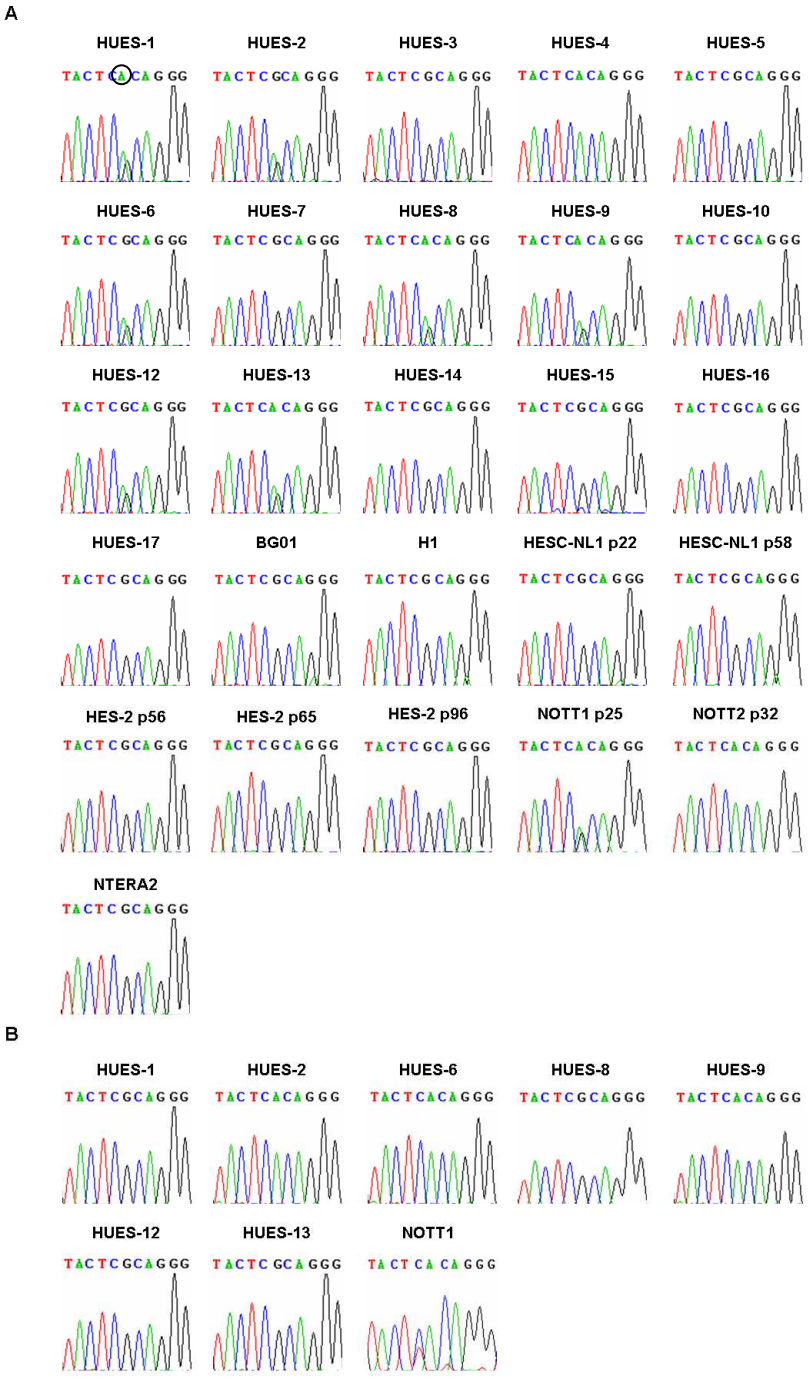

Figure 3-10. *KCNQ1* imprinting in hESC lines
(A) Genotyping at the G/A polymorphic site. Chromatograms distinguished genotypes after PCR amplification of each cell line followed by direct sequencing. (B) Allele-specific expression. RT-PCR with cDNA of informative heterozygous cell lines followed by direct sequencing. A circle indicates a polymorphic site.

3.2.10 KCNQ1OT1 (LIT1)

The allele-specific expression of *KCNQ1OT1* was examined by two G/A and C/T polymorphisms (Lee et al., 1999). 12 cell lines (HUES1, HUES2, HUES7, HUES8, HUES9, HUES10, HUES12, HUES13, HUES17, H1, BG01 and HES-2) were

informative for a G/A polymorphism (Figure 3-10 A). Other 12 cell lines (HUES2, HUES4, HUES7, HUES9, HUES10, HUES14, HUES15, HUES16, HUES17, BG01, HESC-NL1 and HES-2) were informative for a C/T polymorphism (Figure 3-11 A). Of all informative cell lines examined, all showed monoallelic expression (Figure 3-10 B and 3-11 B). Monoallelic expression of *KCNQ1OT1* is maintained during *in vitro* prolonged culture of HESC-NL1 (passages 22 and 58) and HES-2 (passages 56, 65 and 96).

3.2.11 CDKN1C ($p57^{KIP2}$)

The allele-specific expression of *CDKN1C* was examined by a G/A polymorphism of *CDKN1C* (Monk et al., 2006a). Of 3 informative cell lines (HUES04, HUES14 and HUES15) identified by direct sequencing (Figure 3-12 A), all showed predominantly monoallelically expression (Figure 3-12 B).

Figure 3-11. *KCNQ1OT1* imprinting in hESC lines (G/A polymorphism)
(A) Genotyping at the G/A polymorphic site. Chromatograms distinguished genotypes after PCR amplification of each cell line followed by direct sequencing. (B) Allele-specific expression of *KCNQ1OT1* at the G/A polymorphism. RT-PCR with cDNA of informative heterozygous cell lines followed by direct sequencing. A circle indicates a polymorphic site.

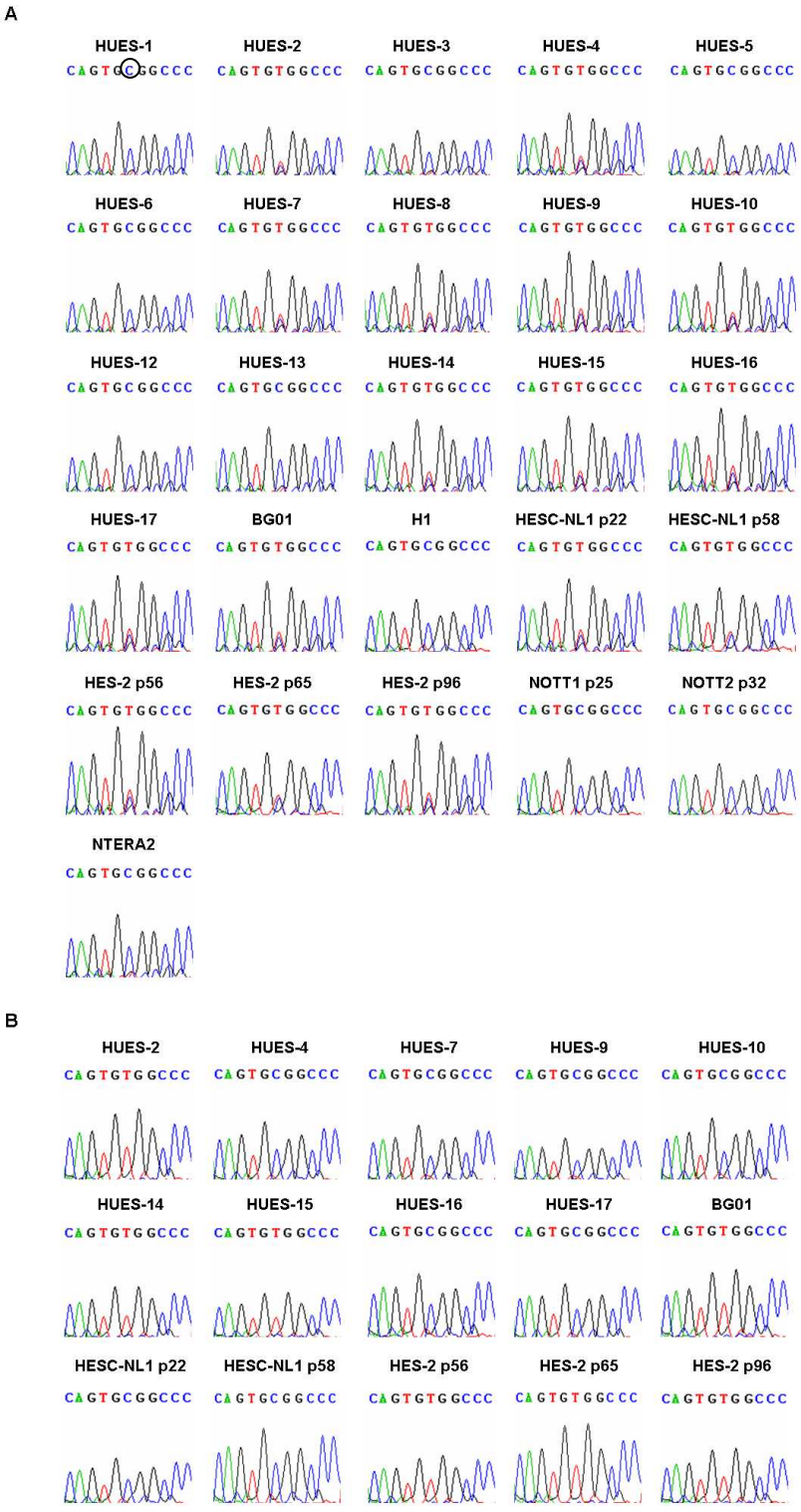

Figure 3-12. *KCNQ1OT1* imprinting in hESC lines (C/T polymorphism)
(A) Genotyping at the C/T polymorphic site. Chromatograms distinguished genotypes after PCR amplification of each cell line followed by direct sequencing. (B) Allele-specific expression. RT-PCR with cDNA of informative heterozygous cell lines followed by direct sequencing. A circle indicates a polymorphic site.

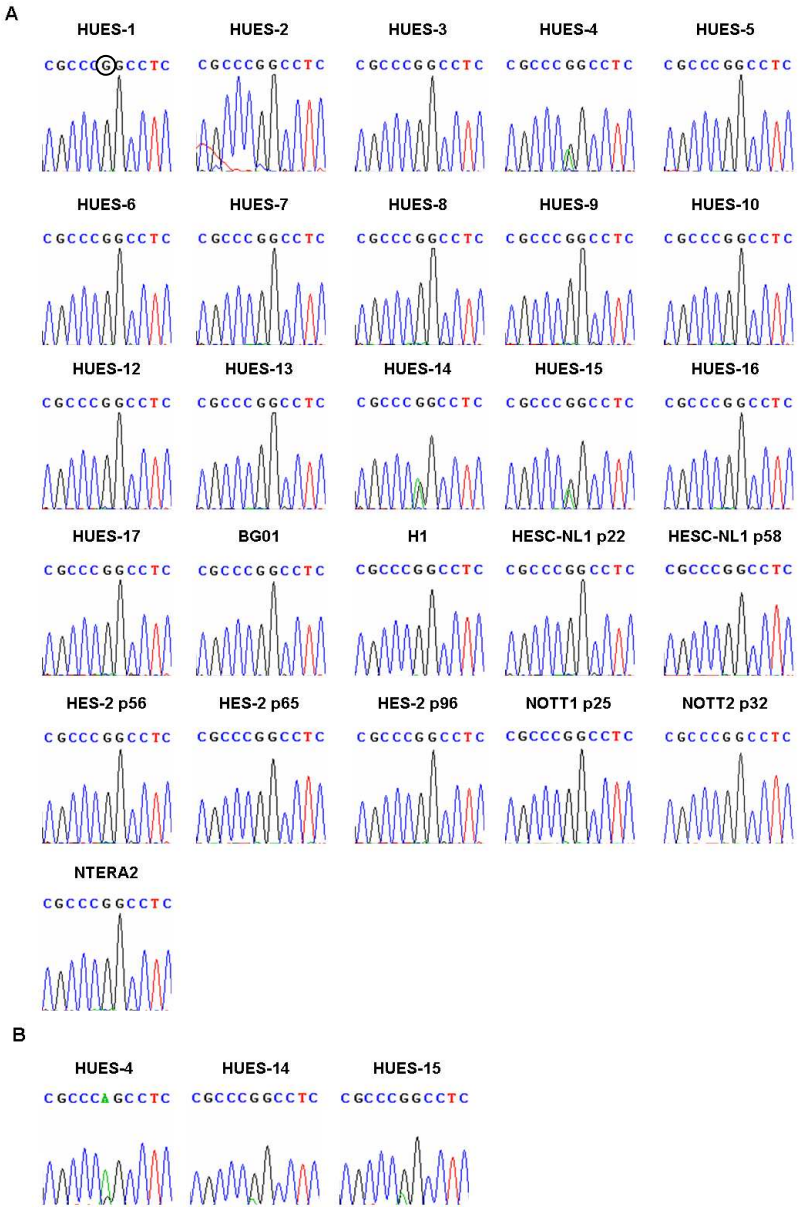

Figure 3-13 *CDKN1C* imprinting in hESC lines
(A) Genotyping at the G/A polymorphic site. Chromatograms distinguished genotypes after PCR amplification of each cell line followed by direct sequencing. (B) Allele-specific expression. RT-PCR with cDNA of informative heterozygous cell lines followed by direct sequencing. A circle indicates a polymorphic site.

3.2.12 PHLDA2 (TSSC3/IPL)

The allele-specific expression of *PHLDA2* was examined by a T/C polymorphism (Qian et al., 1997). 10 informative cell lines (HUES1, HUES2, HUES4, HUES5, HUES8, HUES14, HUES15, HUES16, HUES17 and HESC-NL1) were identified by direct sequencing (Figure 3-13 A). Of 10 cell lines examined, 4 cell lines (HUES1, HUES2, HUES8 and HESC-NL1) showed predominantly monoallelic expression but

6 cell lines (HUES4, HUES5, HUES14, HUES15, HUES16 and HUES17) showed biallelic expresion (Figure 3-13 B).

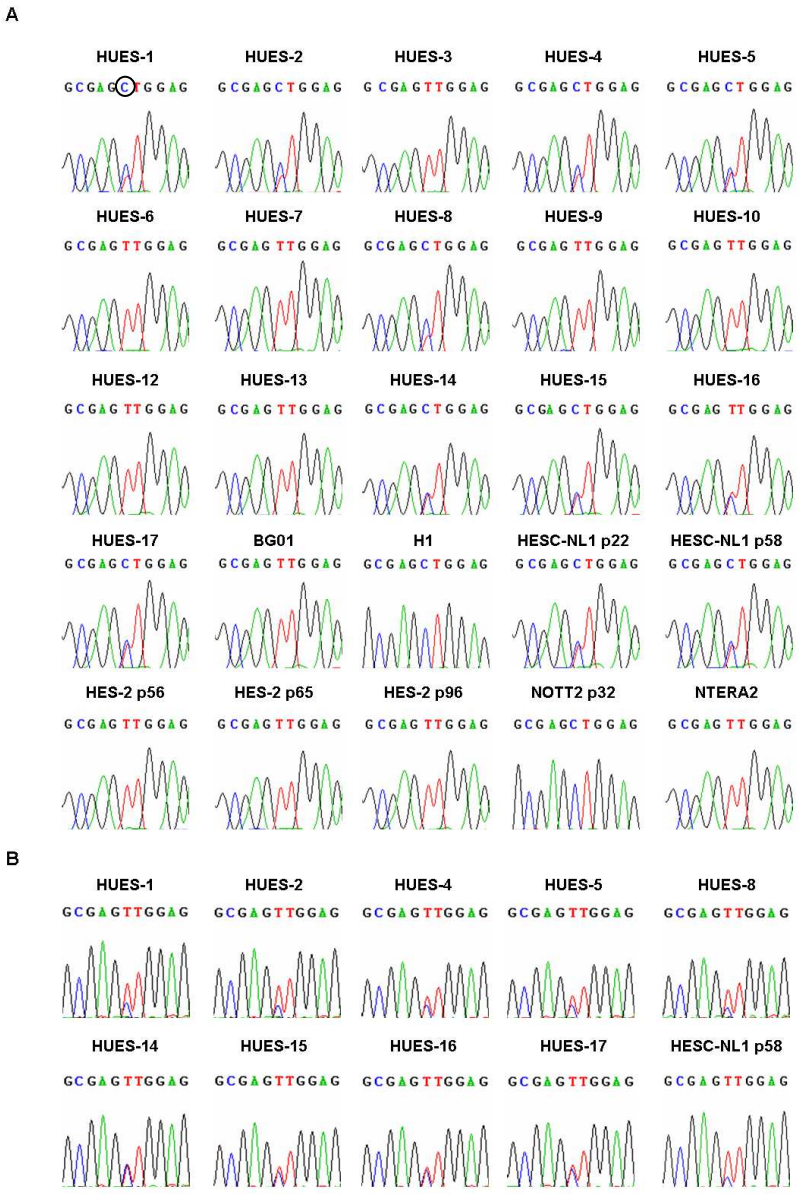

Figure 3-14. *PHLDA2* imprinting in hESC lines
(A) Genotyping at the T/C polymorphic site. Chromatograms distinguished genotypes after PCR amplification of each cell line followed by direct sequencing. (B) Allele-specific expression. RT-PCR with cDNA of informative heterozygous cell lines followed by direct sequencing. A circle indicates a polymorphic site.

3.2.13 SLC22A18 (TSSC5)

The allele-specific expression of *SLC22A18* was examined by a G/C polymorphism located in exon 11 (Onyango et al., 2002). 7 informative cell lines (HUES5, HUES12, HUES13, HUES14, HUES15, HESC-NL1 and NOTT2) were identified by direct

sequencing (Figure 3-14 A). Of 7 cell lines examined, all showed biallelic expression, indicated by both G and C peaks at a polymorphic site (Figure 3-14B).

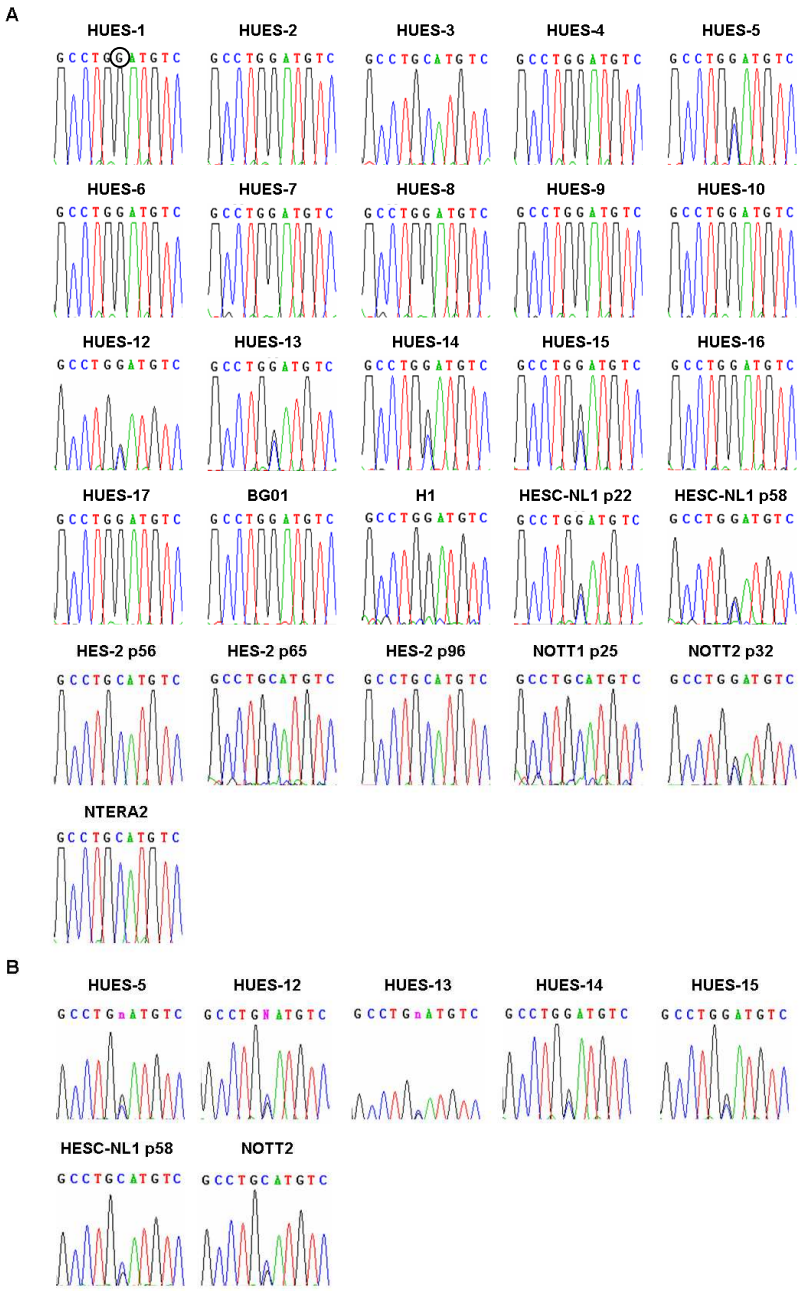

Figure 3-15. *SLC22A18* imprinting in hESC lines
(A) Genotyping at the G/C polymorphic site. Chromatograms distinguished genotypes after PCR amplification of each cell line followed by direct sequencing. (B) Allele-specific expression. RT-PCR with cDNA of informative heterozygous cell lines followed by direct sequencing. A circle indicates a polymorphic site.

3.2.14 DLK1 (PEG9)

The allele-specific expression of *DLK1* was determined by a C/T polymorphism located in the 3' UTR region (Kobayashi et al., 2000). By direct sequencing, no

informative cell lines were identified, showing all homozygous types, T/T (Figure 3-15). Thus, the allele-specific expression of this gene could not be determined.

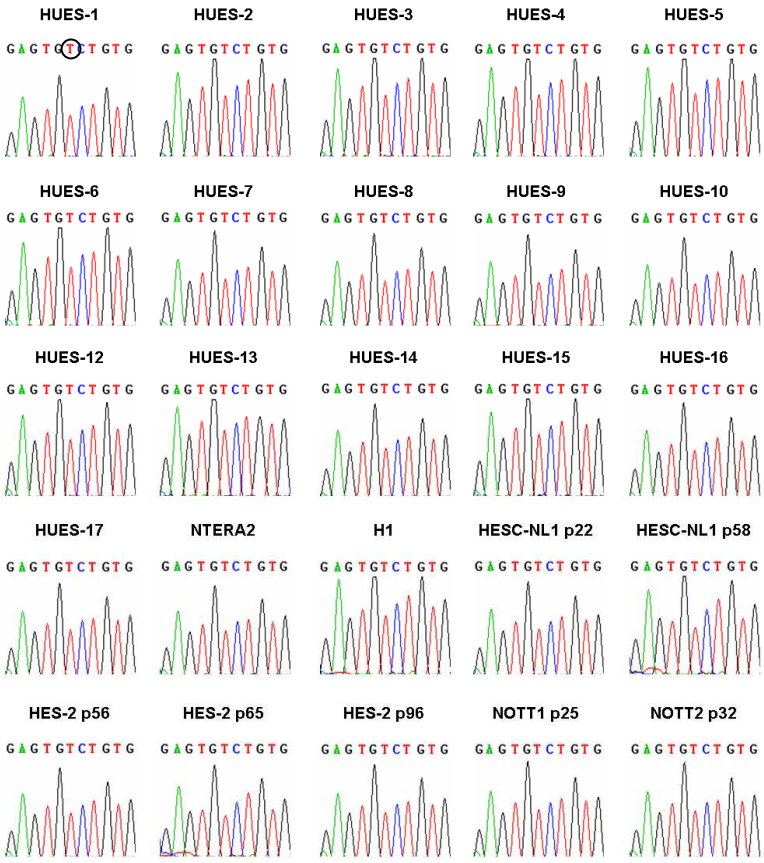

Figure 3-16. *DLK1* imprinting in hESC lines
Chromatograms showed all T/T genotypes in the hESC line and NTERA2 after PCR amplification, followed by direct sequencing. A circle indicates a polymorphic site.

3.2.15 GTL2 (MEG3)

The allele-specific expression of *GTL2* was determined by an A/G polymorphism located in exon 5 of *GTL2* (Wylie et al., 2000). 11 cell lines (HUES3, HUES7, HUES10, HUES12, HUES13, HUES14, HUES15, HUES17, HESC-NL1 and NOTT1) were informative (Figure 3-16 A). Of 10 cell lines examined, 8 cell lines showed monoallelic expression, 1 cell line (HUES14) showed predominant monoallelic expression, and 1 cell line (HUES15) showed biallelic expression (Figure 3-16 B).

Figure 3-17. *GTL2* imprinting in hESC lines

(A) Genotyping at the A/G polymorphic site. Chromatograms distinguished genotypes after PCR amplification of each cell line followed by direct sequencing. (B) Allele-specific expression. RT-PCR with cDNA of informative heterozygous cell lines followed by direct sequencing. A circle indicates a polymorphic site.

3.2.16 NDN

The allele-specific expression of *NDN* was examined by a *Mbo*I polymorphism (MacDonald and Wevrick, 1997). 7 cell lines (HUES4, HUES8, HUES15, HUES17, BG01, NOTT2 and H1) were informative, as determined by PCR-RFLP (Figure 3-17 A). Of 7 cell lines examined, all showed monoallelic expression (Figure 3-17 B).

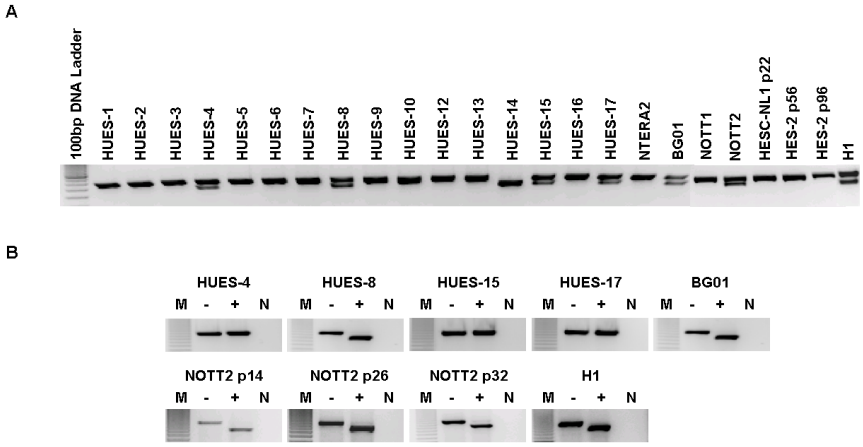

Figure 3-18. *NDN* imprinting in hESC lines
(A) Genotyping. PCR amplification with genomic DNA of each cell line followed by *Mbo*I digestion distinguished between heterozygous and homozygous cell line. (B) Allele-specific expression. RT-PCR with cDNA of informative heterozygous cell lines followed by *Mbo*I digestion. 50bp DNA ladder is denoted by the letter, M. Digestion with *Mbo*I is indicated +, digested and -, not digested. The letter, N indicates a negative control of RT-PCR.

3.2.17 NDNL1 (MAGEL2)

The allele-specific expression of *NDNL1* was determined by a C/A polymorphism (Sun et al., 2006). Only HUES9 was identified as an informative cell line (Figure 3-18 A). In this cell line, *NDNL1* was monoallelically expressed, indicated by only A peak at a polymorphic site (Figure 3-18 B).

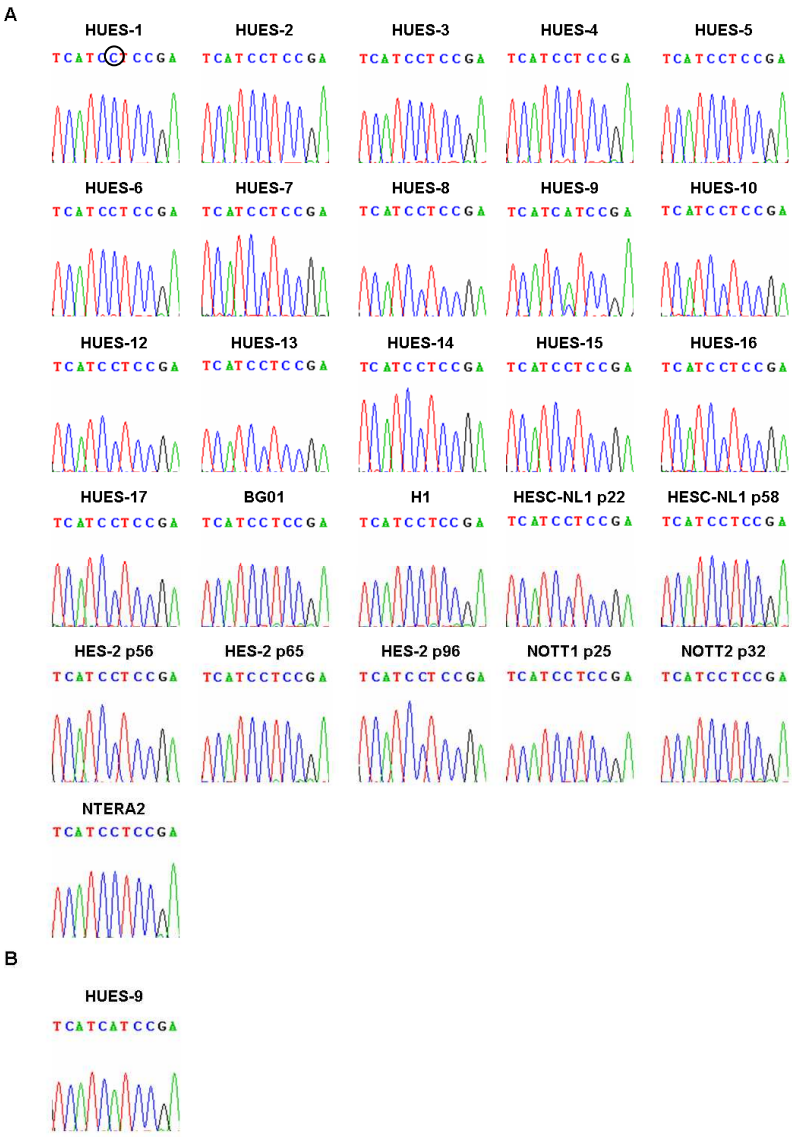

Figure 3-19. *NDNL1* imprinting in hESC lines
(A) Genotyping at the C/A polymorphic site. Chromatograms distinguished genotypes after PCR amplification of each cell line followed by direct sequencing. (B) Allele-specific expression. RT-PCR with cDNA of informative heterozygous cell lines followed by direct sequencing. A circle indicates a polymorphic site.

3.2.18 SNRPN

The allele-specific expression of *SNRPN* was determined by a *Bst*UI polymorphism located in the 5'UTR of exon 2 (Morison et al., 2000). 11 cell lines (HUES3, HUES4, HUES5, HUES6, HUES7, HUES10, HUES12, HUES17, BG01, NOTT1, NOTT2 and H1) were identified as informative cell lines (Figure 3-19 A). Of 11 cell lines examined, *SNRPN* was monoallelically expressed in all cell lines (Figure 3-19 B). To identify the possibility of PCR and restriction enzyme bias, monoallic expression of *SNRPN* was confirmed by direct sequencing (Figure 3-19 C).

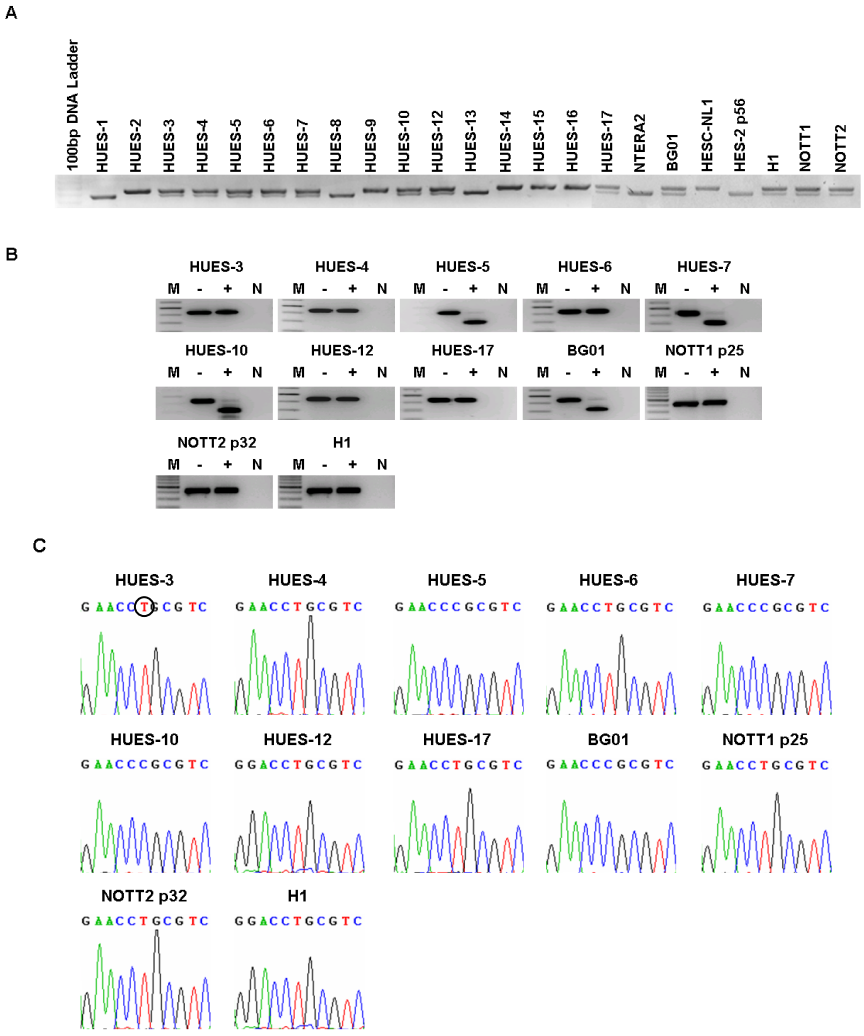

Figure 3-20. *SNRPN* imprinting in hESC lines
(A) Genotyping. PCR amplification with genomic DNA of each cell line followed by *BstU*I digestion distinguished between heterozygous and homozygous cell line. (B) Allele-specific expression. RT-PCR with cDNA of informative heterozygous cell lines followed by *Bst*UI digestion. 50bp DNA ladder is denoted by the letter, M. Digestion with *Bst*UI is indicated +, digested and -, not digested. The letter, N indicates a negative control of RT-PCR. (C) *SNRPN* imprinting confirmed by direct sequencing. RT-PCR with cDNA of informative heterozygous cell lines followed by direct sequencing. A circle indicates a polymorphic site.

3.2.19 IPW

The allele-specific expression of *IPW* was determined by a *Hph*I polymorphism located in exon 3 (Wevrick et al., 1994). 12 cell lines (HUES1, HUES3, HUES6, HUES7, HUES10, HUES12, HUES15, HUES17, BG01, HESC-NL1, HES-2 and NOTT2) were informative (Figure 3-20 A). Of 12 cell lines examined, 11 cell lines showed monoallelic expression and 1 cell line (HUES10) showed predominant monoallelic expression (Figure 3-20 B). The monoallelic expression of *IPW* was

stably maintained during *in vitro* prolonged culture of HESC-NL1 (passages 22 and 58), HES-2 (passages 56, 65 and 96) and NOTT2 (passages 14, 26 and 32).

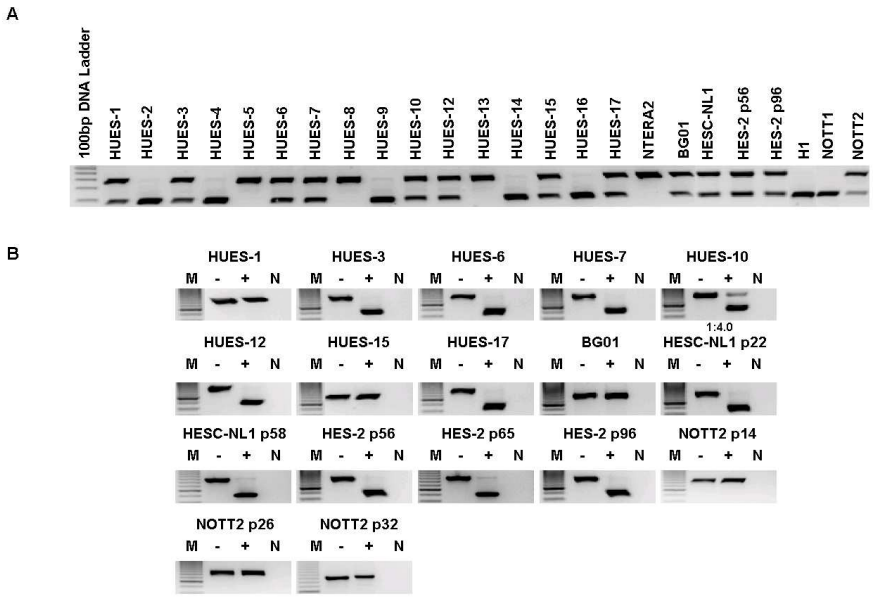

Figure 3-21. *IPW* imprinting in hESC lines
(A) Genotyping. PCR amplification with genomic DNA of each cell line followed by *Hph*I digestion distinguished between heterozygous and homozygous cell line. (B) Allele-specific expression. RT-PCR with cDNA of informative heterozygous cell lines followed by *Hph*I digestion. 50bp DNA ladder is denoted by the letter, M. Digestion with *Hph*I is indicated +, digested and -, not digested. The letter, N indicates a negative control of RT-PCR.

3.2.20 ATP10C (ATP10A)

The allele-specific expression of *ATP10C* was determined by an *Ava*II polymorphism (Meguro et al., 2001). 12 informative cell lines (HUES2, HUES5, HUES6, HUES7, HUES10, HUES15, HUES16, HUES17, HESC-NL1, NOTT1, NOTT2 and NTERA2) were identified by PCR-RFLP (Figure 3-21 A). Of 12 cell lines examined, 8 cell lines showed biallelic expression (an allelic ratio from 1.0:1 to 1.7:1), 2 cell lines (HUES6 and HUES16) showed predominant monoallelic expression (each allelic ratio, 5.0:1 and 6.6:1), and 2 cell lines (HUES5 and HUES7) showed monoallelic expression. The biallelic expression of *ATP10C* was maintained during *in vitro* prolonged culture of HL-HESC-1 (passages 22 and 58) and NOTT1 (passages 25 and 29).

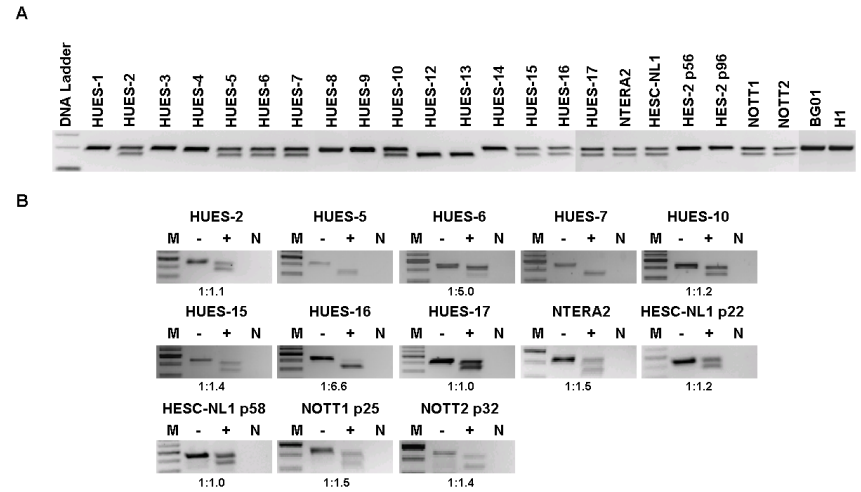

Figure 3-22. *ATP10C* imprinting in hESC lines
(A) Genotyping. PCR amplification with genomic DNA of each cell line followed by *Ava*II digestion distinguished between heterozygous and homozygous cell line. (B) Allele-specific expression. RT-PCR with cDNA of informative heterozygous cell lines followed by *Ava*II digestion. 50bp DNA ladder is denoted by the letter, M. Digestion with *Ava*II is indicated +, digested and -, not digested. The letter, N indicates a negative control of RT-PCR.

3.2.21 PEG3 (ZIM2)

The allele-specific expression of *PEG3* was determined by a *Mnl*I polymorphism located in exon 9 (Dowdy et al., 2005). 6 cell lines (HUES4, HUES6, BG01, HESC-NL1, NOTT2 and NTERA22) were informative (Figure 3-22 A). Of 6 cell lines examined, 5 cell lines showed monoallelic expression but one cell line (NTERA2) showed biallelic expression (Figure 3-22 B).

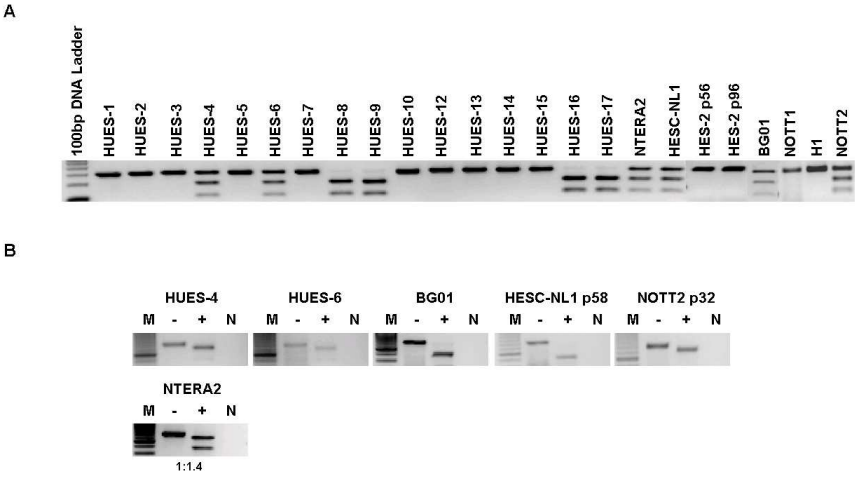

Figure 3-23. *PEG3* imprinting in hESC lines
(A) Genotyping. PCR amplification with genomic DNA of each cell line followed by *Mnl*I digestion distinguished between heterozygous and homozygous cell line. (B) Allele-specific expression. RT-PCR with cDNA of informative heterozygous cell lines followed by *Mnl*I digestion. 50bp DNA ladder is denoted by the letter, M. Digestion

with *Mnl*I is indicated +, digested and -, not digested. The letter, N indicates a negative control of RT-PCR.

3.2.22 NESP55

The allele-specific expression of *NESP55* was examined by a T/C polymorphism (Rugg-Gunn et al., 2005). 9 cell lines (HUES1, HUES4, HUES5, HUES9, HUES12, HUES14, HUES15, BG01 and HESC-NL1) were informative (Figure 3-23 A). Of 9 cell lines examined, 8 cell lines showed monoallelic expression, and one cell line (HUES5) showed biallelic expression, indicated by both C and T peaks at a polymorphic site (Figure 3-23 B). The monoallelic expression of *NESP55* is maintained during *in vitro* prolonged culture of HESC-NL1 (passage 22 to 58).

3.2.23 SLC22A1

The allele-specific expression of *SLC22A1* was determined by a C/T polymorphism (Monk et al., 2006a). 9 cell lines (HUES1, HUES7, HUES10, HUES13, HUES16, HUES17, H1, HESC-NL1 and HES-2) were informative (Figure 3-24 A). Of 9 cell lines examined, 4 cell lines (HUES1, HUES10, HUES13 and HES-2) showed monoallelic expression, 2 cell lines (HUES16 and HUES17) showed predominant monoallelic expression, and 2 cell lines (BG01 and HUES7) showed biallelic expression (Figure 3-24 B).

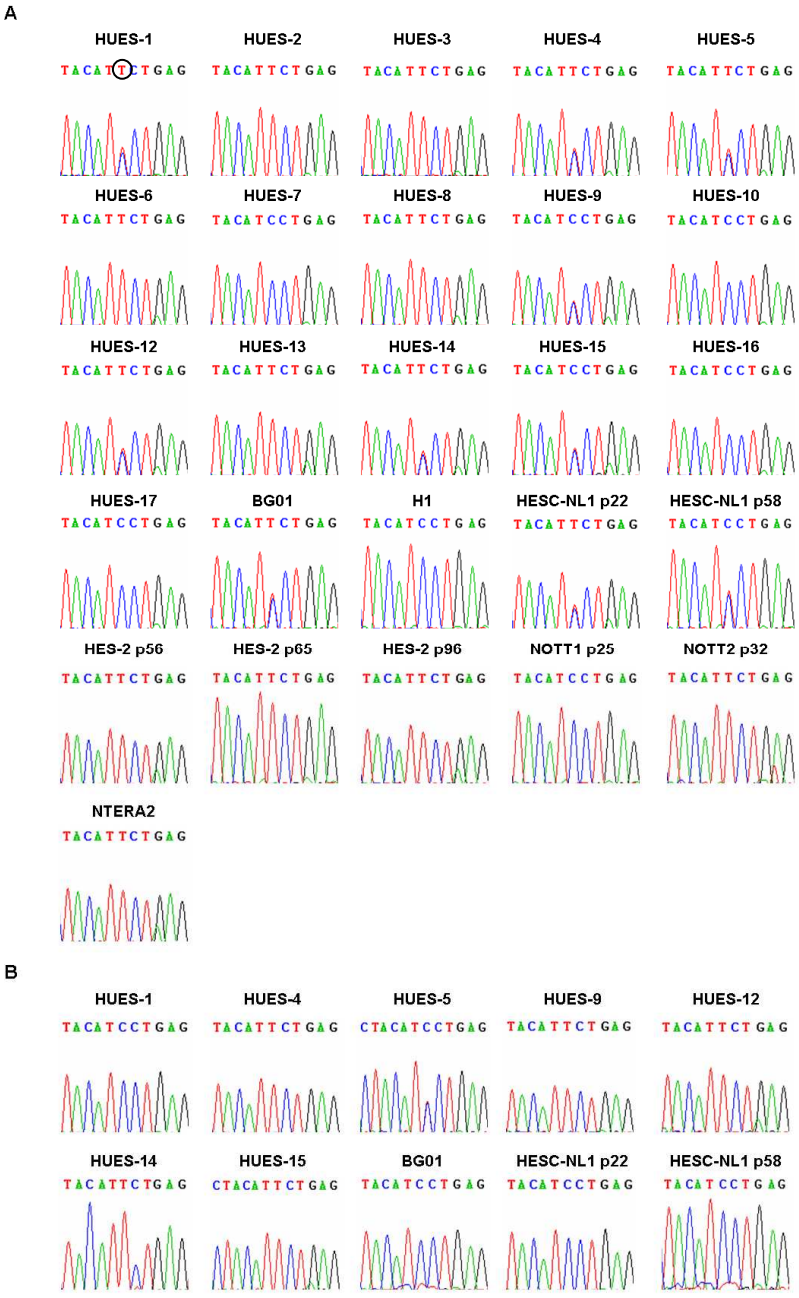

Figure 3-24. *NESP55* imprinting in hESC lines

(A) Genotyping at the T/C polymorphic site. Chromatograms distinguished genotypes after PCR amplification of each cell line followed by direct sequencing. (B) Allele-specific expression. RT-PCR with cDNA of informative heterozygous cell lines followed by direct sequencing. A circle indicates a polymorphic site.

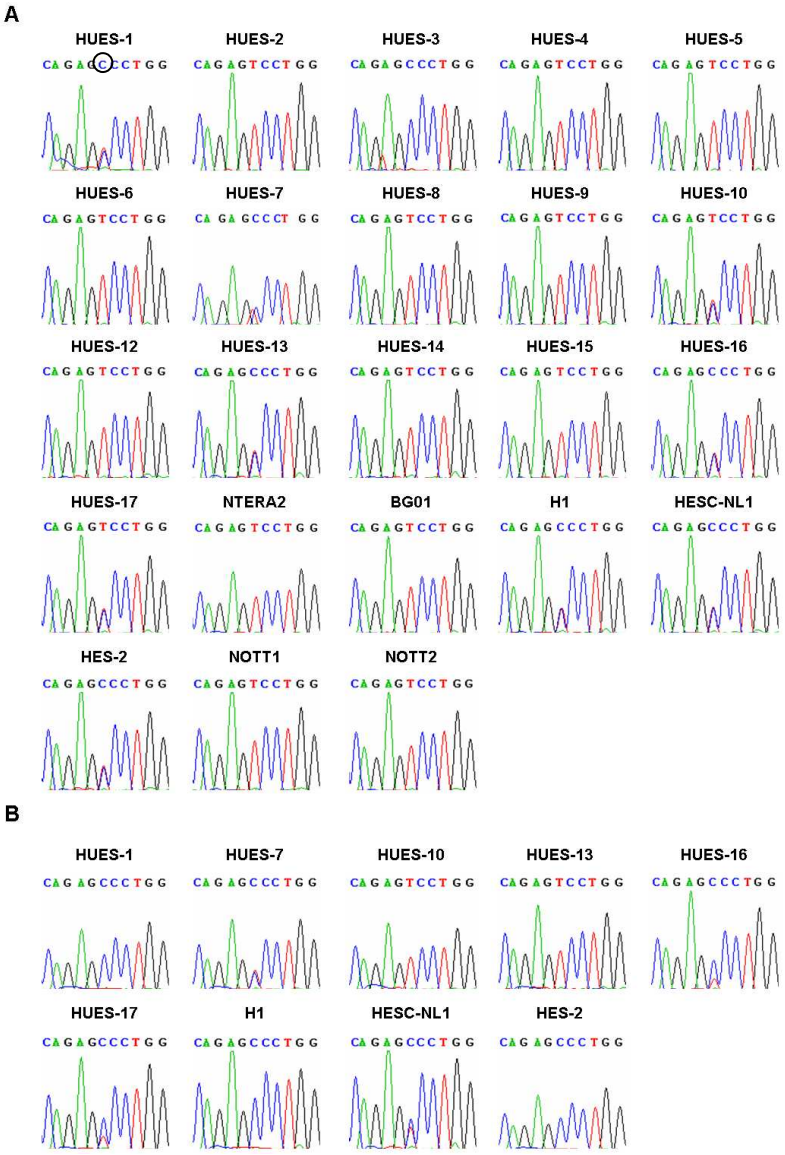

Figure 3-25. *SLC22A1* imprinting in hESC lines
(A) Genotyping at the C/T polymorphic site. Chromatograms distinguished genotypes after PCR amplification of each cell line followed by direct sequencing. (B) Allele-specific expression. RT-PCR with cDNA of informative heterozygous cell lines followed by direct sequencing. A circle indicates a polymorphic site.

3.2.24 TSSC4

The allele-specific expression of *TSSC4* was examined by a G/A polymorphism. 3 informative cell lines (HUES16, HUES17 and H1) were identified by direct sequencing (Figure 3-25 A). Of 3 cell lines examined, all showed biallelic expression (Figure 3-25 B).

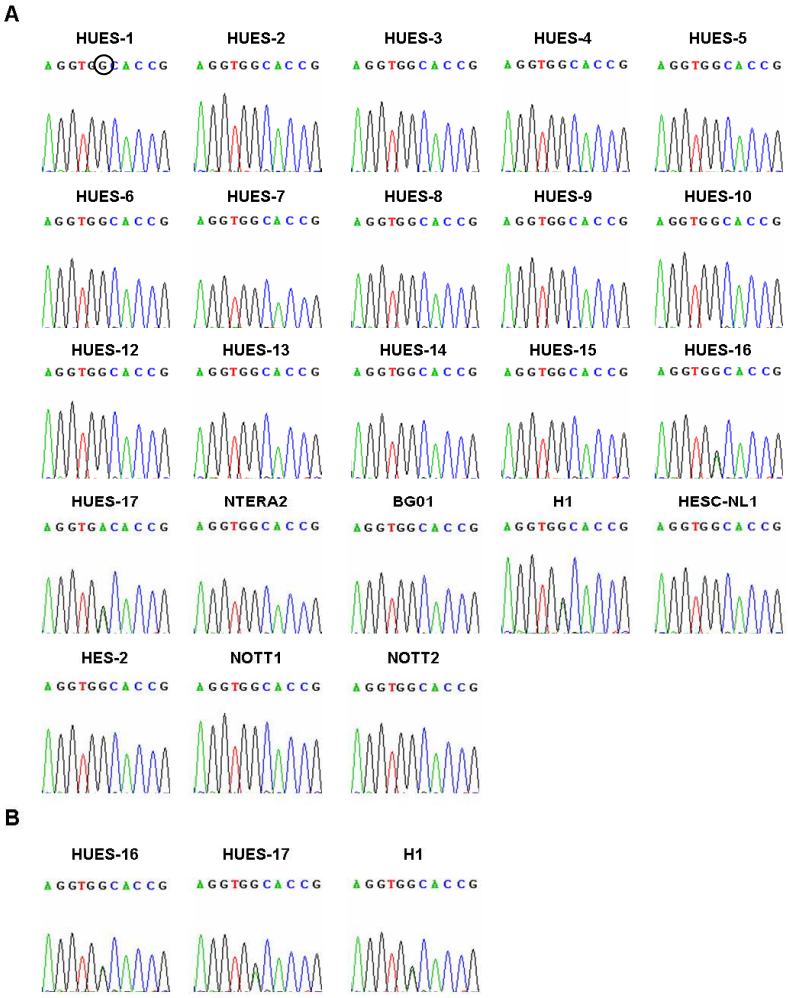

Figure 3-26. *TSSC4* imprinting in hESC lines
(A) Genotyping at the G/A polymorphic site. Chromatograms distinguished genotypes after PCR amplification of each cell line followed by direct sequencing. (B) Allele-specific expression. RT-PCR with cDNA of informative heterozygous cell lines followed by direct sequencing. A circle indicates a polymorphic site.

3.2.25 NAPIL4

The allele-specific expression of *NAPIL4* was determined by a G/C polymorphism (Monk et al., 2006a). 9 informative cell lines (HUES1, HUES2, HUES4, HUES5, HUES6, HUES12, HUES13, H1 and HES-2) were identified (Figure 3-26 A), Of 9 cell lines examined, all cell lines showed biallelic expression.

Figure 3-27. *NAPIL4* imprinting in hESC lines

(A) Genotyping. Chromatograms distinguished genotypes after PCR amplification of each cell line followed by direct sequencing. (B) Allele-specific expression. RT-PCR with cDNA of informative heterozygous cell lines followed by direct sequencing. A circle indicates a polymorphic site.

Table 3-3. Summary of genotyping and allele-specific expression of human embryonic stem cell lines

Loci	Gene	Polymorphism and DNA		Cell line																						
				HUES1	HUES2	HUES3	HUES4	HUES5	HUES6	HUES7	HUES8	HUES9	HUES10	HUES12	HUES13	HUES14	HUES15	HUES16	HUES17	BG01	H1	HESC-NL1	HES-2	NOTT1	NOTT2	NTERA2
1p36.33	*TP73*	*StyI*	gDNA	A/B	B/B	B/B	B/B	B/B	A/B	A/B	A/B	B/B	A/B	B/B	B/B	B/B	B/B	A/B	B/B	B/B	B/B	B/B	A/B	B/B	A/B	A/B
			cDNA	A/B					A/B	A/B	A/B		A/B					A/B					A/B		A/B	A/B
6q25.3	*SLC22A1*	*C/T*	gDNA	C/T	T/T	C/C	T/T	T/T	T/T	C/T	T/T	T/T	C/T	T/T	C/T	T/T	T/T	C/T	C/T	T/T	C/T	C/T	C/T	T/T	T/T	T/T
			cDNA	C/-						C/T			-/T		-/T			C>T	C>T		C/-	C/T	C/-			
	IGF2R	*AclI*	gDNA	A/B	A/B	A/B	A/B	A/B	A/A	A/A	B/B	B/B	A/A	A/B	A/B	A/B	A/A	A/A	A/A	A/B	A/B	A/B	B/B	B/B	A/B	B/B
			cDNA	A/B	A/B	A/B	A/B	A/B						A/B	A/B	A/B				A/B	A/B	A/B			A/B	
		MscI	gDNA	A/A	A/A	A/A	A/A	A/B	A/A	A/A	A/A	A/B	A/A	A/A	A/A	A/A	A/A	A/A	A/A	A/A	A/A	A/A	A/B	A/A	A/A	A/A
			cDNA					A/B				A/B											A/B			
7q21	*PEG10*	*C/T*	gDNA	C/C	C/C	C/C	C/C	C/T	C/C	C/T	C/C	C/C	C/T	C/T	C/C	C/C	C/C	C/C	C/C	C/C	C/C	T/T	C/C	C/C	C/C	C/C
			cDNA					C/T		-/T			-/T	C/-												
7q32	*PEG1*	*G/C*	gDNA	G/C	G/C	G/G	G/G	C/C	C/C	G/C	G/G	G/G	G/C	G/C	G/G	C/C	G/C	G/C	G/C	G/C	C/C	C/C	G/C	G/C	G/C	G/C
			cDNA[1]	-/C	G/-					G/-			G>C	-/C			-/C	-/C	-/C	G/-			G/-	-/C	G/C	G/C
			cDNA[2]	G/C	G/C					G/C			G/C	G/C			G/C	G<C	G/C	G/C			G/C	-/C	G/C	G/-
	MEST1OT1	*G/A*	gDNA	G/G	G/A	G/G	G/A	A/A	A/A	G/A	G/G	G/A	G/A	G/A	G/G	A/A	G/A	G/A	G/A	G/G	A/A	A/A	G/A	G/A	G/A	G/A
			cDNA		G/-		G/-			-/A		G/-	G/-	G<A			G/A	-/A	-/A				G/-	G<A	G/-	ND
11p13	*WT1*	*HinfI*	gDNA	B/B	A/B	A/B	B/B	A/B	B/B	A/A	A/B	A/B	A/A	A/A	A/A	B/B	B/B	B/B	B/B	A/B	B/B	B/B	A/A	A/A	A/B	B/B
			cDNA		A/B	A/B		A/B			A/B	A/B								A/B					ND	
11p15.5	*NAPIL4*	*G/C*	gDNA	G/C	G/C	G/G	G/C	G/C	G/C	C/C	G/G	C/C	C/C	G/C	G/C	G/G	G/G	G/G	G/G	C/C	G/C	G/G	G/C	G/G	G/G	G/G
			cDNA	G/C	G/C		G/C	G/C	G/C					G/C	G/C						G/C		G/C			
	PHLDA2	*C/T*	gDNA	C/T	C/T	T/T	C/T	C/T	T/T	T/T	C/T	T/T	T/T	T/T	T/T	C/T	C/T	C/T	C/T	T/T	C/C	C/T	T/T	ND	C/C	T/T
			cDNA	C<T	C<T		C/T	C/T			C<T					C/T	C/T	C/T	C/T			C<T				
	SLC22A18	*G/C*	gDNA	G/G	G/G	C/C	G/G	G/C	G/G	G/G	G/G	G/G	G/G	G/C	G/C	G/C	G/C	G/G	G/G	G/G	G/G	G/C	C/C	C/C	G/C	C/C
			cDNA					G/C						G/C	G/C	G/C	G/C					G/C			G/C	
	CDKN1C	*G/A*	gDNA	G/G	G/G	G/G	G/A	G/G	G/G	G/G	G/G	G/G	G/G	G/G	G/G	G/A	G/A	G/G	G/G	G/G	G/G	G/G	G/G	G/G	G/G	G/G
			cDNA				A>G									A<G	A<G									
	KCNQIOTI	*G/A*	gDNA	G/A	G/A	G/G	G/G	A/A	A/A	G/A	G/A	G/A	G/A	G/A	G/A	A/A	A/A	G/A	G/A	G/A	G/A	G/G	G/A	A/A	A/A	A/A
			cDNA	-/A	G/-					-/A	-/A	-/A	-/A	G/-	G/-			ND	-/A	G/-	-/A		G/-			
	KCNQ1	*G/A*	gDNA	G/A	G/A	G/G	A/A	G/G	G/A	G/G	G/A	G/A	G/G	G/A	G/A	G/G	G/G	G/G	G/G	G/G	G/G	G/G	G/G	G/A	A/A	G/G
			cDNA	G/-	-/A				-/A		G/-	-/A		G/-	G/-									-/A		
	TSSC4	*G/A*	gDNA	G/G	G/G	G/G	G/G	G/G	G/G	G/G	G/G	G/G	G/G	G/G	G/G	G/G	G/G	G/A	G/A	G/G	G/A	G/G	G/G	G/G	G/G	G/G
			cDNA															G/A	G/A		G/A					
	IGF2	*ApaI*	gDNA	A/B	A/A	A/A	A/A	A/B	A/B	A/A	A/B	A/B	A/A	A/A	A/A	A/A	A/A	A/B	A/B	A/A	A/A	A/B	A/B	A/A	A/B	B/B
			cDNA	A/B				A/B	A/B		A/B	A<B						A/B	A/B			A/B	A/B		A/B	
	H19	*AluI*	gDNA	A/B	B/B	A/B	B/B	A/B	A/A	A/B	A/A	A/B	A/B	B/B	B/B	A/B	A/B	A/A	A/A	B/B	A/A	A/A	A/B	A/B	A/B	A/A
			cDNA	-/B		A/-		-/B		-/B		-/B	-/B			A/-	A/-						A/B	-/B	A/B	
		RsaI	gDNA	A/B	B/B	A/B	A/B	A/B	A/A	A/B	A/A	A/B	A/B	B/B	B/B	A/B	A/B	A/A	A/A	A/B	A/A	A/A	A/B	A/B	A/B	A/A

			cDNA	-/B		A/-	A/-	-/B		-/B		-/B	-/B			A/-	A/-			-/B			A/B	-/B	A/B	
14q32	*DLK1*	*C/T*	gDNA	T/T	T/T	T/T	T/T	T/T	T/T	T/T	T/T	T/T	T/T	T/T	T/T	T/T	T/T	T/T	T/T	ND	T/T	T/T	T/T	T/T	T/T	T/T
			cDNA																							
	GTL2	*A/G*	gDNA	G/G	A/A	A/G	G/G	G/G	G/G	A/G	G/G	G/G	A/G	A/G	A/G	A/G	A/G	G/G	A/G	G/G	A/G	A/G	G/G	A/G	G/G	A/A
			cDNA			-/G				A/-			-/G	A/-	A/-	A>G	A/G		-/G		ND	A/-		-/G		
15q11-q13	*NDNL1*	*C/A*	gDNA	C/C	C/C	C/C	C/C	C/C	C/C	C/C	C/C	C/A	C/C	C/C	C/C	C/C	C/C	C/C	C/C	C/C	C/C	C/C	C/C	C/C	C/C	C/C
			cDNA									-/A														
	NDN	*MboI*	gDNA	B/B	B/B	B/B	A/B	B/B	B/B	B/B	A/B	B/B	B/B	B/B	B/B	A/A	A/B	B/B	A/B	A/B	A/B	B/B	B/B	B/B	A/B	B/B
			cDNA				-/B				A/-						-/B		-/B	A/-	A/-				A/-	
	SNRPN	*BstUI*	gDNA	A/A	B/B	A/B	A/B	A/B	A/B	A/B	A/A	B/B	A/B	A/B	A/A	B/B	B/B	B/B	A/B	A/B	A/B	B/B	A/A	A/B	A/B	A/A
			cDNA			-/B	-/B	A/-	-/B	A/-			A/-	-/B					-/B	A/-	-/B			-/B	-/B	
	IPW	*HphI*	gDNA	A/B	A/A	A/B	A/A	B/B	A/B	A/B	B/B	A/A	A/B	A/B	B/B	A/A	A/B	A/A	A/B	A/B	A/A	A/B	A/B	A/A	A/B	B/B
			cDNA	-/B		A/-			A/-	A/-			A>B	A/-			-/B		A/-	-/B		A/-	A/-		-/B	
	ATP10C	*AvaII*	gDNA	B/B	A/B	B/B	B/B	A/B	A/B	A/B	B/B	B/B	A/B	A/A	A/A	B/B	A/B	A/B	A/B	B/B	B/B	A/B	B/B	A/B	A/B	A/B
			cDNA		A/B			A/-	A<B	A/-			A/B				A/B	A>B	A/B			A/B		A/B	A/B	A/B
19q13.4	*PEG3*	*MnlI*	gDNA	B/B	B/B	B/B	A/B	B/B	A/B	B/B	A/A	A/A	B/B	B/B	B/B	B/B	B/B	A/A	A/A	A/B	B/B	A/B	B/B	B/B	A/B	A/B
			cDNA				-/B		-/B											A/-		A/-			-/B	A/B
20q13.2	*NESP55*	*C/T*	gDNA	T/C	T/T	T/T	T/C	T/C	T/T	C/C	T/T	T/C	C/C	T/C	T/T	T/C	T/C	C/C	C/C	T/C	C/C	T/C	T/T	C/C	T/T	C/C
			cDNA	-/C			T/-	T/C				T/-		T/-		T/-	T/-			-/C		-/C				

gDNA e.g. A/B: alleles are informative heterogeneous (A/B); alleles are homogenous wild type (A/A); alleles are homogeneous mutant type (B/B). cDNA e.g. A/B: monoallelic expression (A/- or -/B); predominant monoallelic expressions(A<B or A>B); biallelic expression (A/B) determined by Cui et al. (1998). [a] *PEG1* isoform 1, [b] *PEG1* isoform 2

3.3 Discussion

The purpose of this study was to investigate the imprinting stability in 22 *in vitro* cultured hESC lines by analysing the allele-specific expression of 22 imprinted genes and 3 non-imprinted genes. Of 23 imprinted genes examined, 9 genes (*PEG10*, *PEG1*, *MESTIT1*, *IGF2*, *H19*, *GLT2*, *NESP55*, *PHLDA2* and *ATP10C*) were variably imprinted between hESC lines, whereas other genes showed stable imprinting (Table 3-3 and 3-4), indicating gene-specific imprinting disruption. Moreover, of 22 hESC lines examined, 12 cell lines (HUES1, HUES2, HUES5, HUES6, HUES7, HUES9, HUES15, HUES16, HESC-NL1, HES-2, NOTT1 and NOTT2) showed that imprinting was disrupted at least one imprinted locus. Thus, in contrast to previous studies, which showed imprinting stability in hESC lines (Mitalipov, 2006; Plaia et al., 2006; Rugg-Gunn et al., 2005; Sun et al., 2006), imprinting instability can be detected by increasing the number of cell lines and imprinted genes examined.

Table 3-4. Imprinting stability of human embryonic stem cell lines

Imprinted gene		Monoallelic	Partial-allelic	Biallelic	No. of cell lines analysed	Imprinting stability
Paternally expressed gene	*KCNQ1OT1*	12			12	Stable
	NDN	7			7	
	NDNL1	1			1	
	SNRPN	12			12	
	IPW	11	1		12	
	PEG3	5			5	
	WT1			6	6	
	PEG10	3		1	4	Unstable
	PEG1 isoform1	10	1	1	12	
	PEG1 isoform2	1	1	10	12	
	MESTIT1	9	2	1	12	
	IGF2		1	9	10	
	DLK1				-	-
Maternally expressed gene	*KCNQ1*	8			8	Stable
	CDKN1C		3		3	
	TP73			8	8	
	IGF2R			14	14	
	SLC22A18			7	7	
	H19	11		2	13	Unstable
	GTL2	8	1	1	10	
	NESP55	8		1	9	
	PHLDA2		4	6	10	
	ATP10C	2	2	7	11	
Non-imprinted gene	*NAPIL4*			9	9	Stable
	TSSC4			3	3	
	SLC22A1	5	2	2	9	Variable

3.3.1 Genes that are stably imprinted

3.3.1.1 Genes that are monoallelically expressed

8 imprinted genes, *NDN*, *NDNL1*, *SNRPN*, *IPW*, *PEG3*, *KCNQ1*, *KCNQ1OT1* and *CDKN1C*, were identified to be monoallelically expressed in all informative hESC lines, indicating that the genes are stably imprinted and maintained upon *in vitro* culture. This concurred with the imprinting stability previously observed for *SNRPN*, *IPW*, *NDNL1*, *KCNQ1* and *KCNQ1OT1* imprinting in a range of studies which examined between 1 and 24 informative cell lines (Adewumi et al., 2007; Mitalipov, 2006; Rugg-Gunn et al., 2005; Sun et al., 2006).

Interestingly, *NDN*, *NDNL1*, *SNRPN* and *IPW* genes are known to be clustered on human chromosome 15q11 ~ q13. (El-Maarri et al., 2001; MacDonald and Wevrick, 1997; Sutcliffe et al., 1994; Wevrick et al., 1994). Furthermore, *KCNQ1*, *KCNQ1OT1* and *CDK1NC* genes are also clustered on human chromosome 11p15 (Lee et al., 1999; Lee et al., 1997; Mitsuya et al., 1999; Smilinich et al., 1999). In mouse and monkey ESC lines, the imprinting stability has been reported in their orthologous regions (Dean et al., 1998; Fujimoto et al., 2006; Schumacher and Doerfler, 2004). These evidences indicate that imprinting stability can be regionalised in mammalian ESC lines. The reason for such a regionalised stability is not clear, but one possibility is that stably established methylation imprints at imprinting control regions (ICRs) in blastocyst stage embryos can be inherited into mammalian ESCs and this can be maintained with monoallelic expression of their corresponding genes upon *in vitro* culture. Indeed, *KvDMR1* and *SNRPN* DMR are known as ICRs in the human and mouse, and their maternal methylation imprints are stably established during oogenesis (Geuns et al., 2003; Geuns et al., 2007b; Lucifero et al., 2002; Sato et al., 2007). These stable imprints are maintained throughout preimplantation stage embryo development with monoallelic expression of their relative genes (Geuns et al., 2003; Geuns et al., 2007b; Huntriss et al., 1998; Lewis et al., 2004; Salpekar et al., 2001). Therefore, these imprints can be stably inherited into ESCs and this may be not susceptible to DNA methylation changes upon *in vitro* culture.

3.3.1.2 Genes that are biallelically expressed

Unexpectedly, 4 imprinted genes, *TP73*, *IGF2R*, *WT1*, and *SLC22A18*, were biallelically expressed in all informative hESC lines (Table 3-4). There are two possibilities to explain this. Firstly, their imprints have not been established in blastocyst stage embryos and thus their derived hESC lines are still biallelically expressed. Currently, the allele-specific expression of *TP73*, *IGF2R*, *WT1*, and *SLC22A18* has not been examined in human gametes and preimplantation embryos to confirm this possibility. Secondly, it can be also explained by tissue-specific imprinting. *TP73*, *IGF2R*, *WT1*, and *SLC22A18* are imprinted in a tissue-specific manner (Chen et al., 2000b; Cooper et al., 1998; Dong et al., 2002; Jinno et al., 1994; Mitsuya et al., 1997; Monk et al., 2006a; Xu et al., 1993). For example, *WT1* and *IGF2R* are biallelically expressed in normal placentas and kidneys, although other tissues show monoallelic expression (Jinno et al., 1994; Mitsuya et al., 1997; Monk et al., 2006a; Xu et al., 1993). Moreover, *TP73* is biallelically expressed in normal brain, ovary and cervix tissues (Chen et al., 2000b; Dong et al., 2002), although it monoallelically expressed in normal gastric, pancreatic and thymus tissues (Kang et al., 2000; Mai et al., 1998a). Thus, the biallelic expression of *IGF2R*, *WT1*, *SLC22A18* and *TP73* could be normal in hESC lines.

In this Chapter, 3 non-imprinted genes (*TSSC4*, *NAPIL4* and *SLC22A1*) were used as control for biallelic expression. *TSSC4* and *NAPIL4* were biallelically expressed in all informative lines. This was consistent with previous observations in hESCs and fetal tissues (Monk et al., 2006a; Rugg-Gunn et al., 2005). However, *SLC22A1*, which was previously identified to be not imprinted in human and mouse tissues (Monk et al., 2006a), showed variable imprinting in hESC lines. *SLC22A1* was monoallelically or predominant monoallelically expressed 7 of 9 informative cell lines. Only 2 cell lines (HUES7 and HESC-NL1) showed biallelic expression. Thus, *SLC22A1* may be potentially imprinted or polymorphically imprinted in early embryonic cells.

3.3.2 Genes that are unstably expressed

9 imprinted genes (*H19*, *GTL2*, *PEG1* isoform 1 and 2, *PEG10*, *MESTIT1*, *NESP55*, *ATP10C*, *PHLDA2* and *IGF2*) showed unstable imprinting status in some informative cell lines (see Table 3-3 and 3-4). This concurred with the imprinting instability previously observed for *H19*, *IGF2*, *GTL2*, *PEG1* and *NESP55* imprinting in 7 to 20 informative cell lines examined (Adewumi et al., 2007).

3.3.2.1 Loss of imprinting

Of 9 genes, 6 imprinted genes (*PEG10*, *PEG1 isoform 1*, *MESTIT1*, *H19*, *GTL2* and *NESP55*) were identified to have loss of imprinting in at least one hESC lines. In detail, *PEG10* was monoallelically expressed in 3/4 informative cell lines, but it was biallelically expressed in HUES5, indicating loss of imprinting. *NESP55* was monoallelically expressed in 8/9 informative cell lines. Only one cell line, HUES5 showed biallelic expression, indicating loss of imprinting. *PEG1 isoform 1* was monoallelically expressed in 11/12 cell lines, but NOTT2 showed biallelic expression, indicating loss of imprinting. *H19* was monoallelically expressed in almost all informative cell lines, but HES-2 and NOTT2 showed biallelic expression. *MESTIT1* was monoallelically expressed in 11/12 informative cell lines. HUES15 showed biallelic expression of *MESTIT1*, indicating loss of imprinting. *GTL2* was monoallelically expressed in 9/10, but HUES15 showed biallelic expression, indicating loss of imprinting.

Loss of imprinting of *PEG10*, *PEG1 isoform 1*, *MESTIT1*, *H19*, *GTL2* and *NESP55* is known to be associated with various cancers and congenital disorders (Bastepe et al., 2005; Gicquel et al., 2005; Nakanishi et al., 2004; Okabe et al., 2003; Pedersen et al., 2002; Tsou et al., 2003; Weksberg et al., 1993). For example, loss of imprinting of *PEG1 isoform 1* is associated with human breast and lung carcinomas (Nakanishi et al., 2004; Pedersen et al., 2002). Moreover, loss of imprinting of *H19*, *GTL2*, *NESP55* and *MESTIT1* is associated with human cancers, BWS patients and SRS patients (Bliek et al., 2001; Chen et al., 2000a; Gicquel et al., 2005; Reik et al., 1995). In this Chapter, NOTT2 have loss of imprinting of *PEG1 isoform 1* and *H19*. HUES5 have loss of imprinting of *PEG10* and *NESP55*. HUES15 have loss of imprinting of *MESTIOT1* and *GTL2*. HES-2 has loss of imprinting of *H19*. Although developmental consequences have not examined in the Chapter, these cell lines need to be carefully considered to be excluded for human therapeutic applications.

3.3.2.2 Gain of imprinting

4 imprinted genes, *IGF2*, *PEG1 isoform 2*, *PHLDA2* and *ATP10C*, appeared to have gain of imprinting in at least one informative line. In detail, *IGF2* was biallelically expressed in almost all informative hESC lines (9/10). Only one cell line, HUES9,

showed predominantly monoallelic expression, indicating gain of imprinting. Moreover, *PEG1 isoform 2* is normally biallelically expressed in human tissues (Kosaki et al., 2000; McMinn et al., 2006; Nakabayashi et al., 2002). Consistently, biallelic expression of *PEG1 isoform 2* was detected in 10/12 cell lines. However, HUES16 and NOTT1 showed monoallelic or predominantly monoallelic expression, indicating gain of imprinting. In addition, of 10 informative cell lines examined, *PHLDA2* was biallelically expressed in almost informative cell lines. However, HUES1, HUES2, HUES7 and HESC-NL1 showed predominantly monoallelic expression, indicating gain of imprinting. Finally, *ATP10C* was biallelically expressed in 7/11 informative cell lines. However, HUES5, HUES6, HUES7 and HUES16 showed monoallelic or predominantly monoallelic expression, indicating gain of imprinting.

The imprinting disruption of *IGF2*, *PEG1*, *PHLDA2* and *ATP10C* is known to be associated with congenital disorders and cancers (Gicquel et al., 2005; Meguro et al., 2001; Muller et al., 2000; Nakanishi et al., 2004; Sparago et al., 2004; Weksberg et al., 1993). Thus, HUES1, HUES2, HUES6, HUES7, HUES9, HUES16, HESC-NL1 and NOTT1 cell lines, identified to have gain of imprinting of at least one imprinted locus, also need to be considered to be excluded for human therapeutic applications.

Interestingly, *IGF2*, which was previously known to be monoallelically expressed in most human and mouse tissues (Giannoukakis et al., 1993; Ohlsson et al., 1993), was biallelically expressed in hESC lines. There are three scenarios that could explain biallelic expression of *IGF2* in hESC lines. One is that the *in vitro* culture conditions lead to loss of imprinting of *IGF2*. In monkey ESC lines, of 7 informative cell lines examined, loss of imprinting of *IGF2* was detected in all informative lines, as a consequence of *in vitro* culture conditions (Fujimoto et al., 2006). Another explanation is that the *IGF2* imprint was not established yet in the ICMs of blastocyst stage embryos. Indeed, *IGF2* was reported to be biallelically expressed in mouse and human blastocyst stage embryos, but it became monoallelically expressed after postimplantation (Murrell, 2006; Oswald et al., 2000). Finally, the *IGF2* expression in hESCs could be in a dosage-dependent manner. A recent study has demonstrated that *IGF2* is one of key factors to regulate for stem cell survival (Bendall et al., 2007).

Thus, biallelic expression of *IGF2* may be required to grow hESCs and maintain them in an undifferentiated state.

3.3.3 Imprinting errors associated with *in vitro* culture

Available data from mouse preimplantation stage embryos and their-derived stem cell lines have suggested that imprinting errors can be accumulated during *in vitro* prolonged culture (Dean et al., 1998; Humpherys et al., 2001; Khosla et al., 2001a; Li et al., 2005b). Similarly, altered *IGF2* and *H19* imprinting has been detected in hESC lines during *in vitro* long-term culture (Adewumi et al., 2007; Rugg-Gunn et al., 2005). Adewumi et al., (2007) have found that *IGF2* is monoallelically expressed at earlier passages of the CCTL-9 cell line, but it become biallelically expressed at later passages. Moreover, Rugg-Gunn et al., (2005) has found *H19* is biallelically expressed in H9 at later passages, although it was monoallelic at earlier passages. In this study, HESC-NL1 (passages 22 and 58) and HES-2 (passages 56, 65 and 96) were used to confirm this possibility. However, no imprinting changes were detected at *H19* and *IGF2* loci. Furthermore, of other imprinted genes examined, none showed imprinting changes upon *in vitro* prolonged culture. Instead, in this Chapter, imprinting errors were observed at earlier passages of hESC lines. The passage numbers of cell lines, which are identified to have imprinting errors, are 22 to 35 (see Table 2-1), suggesting that short period in *in vitro* culture may be sufficient to cause imprinting errors in hESC lines.

3.3.4 Imprinting errors derived from donor embryos

In this Chapter, 16 HUES-lines were included to examine the imprinting stability. Interestingly, 8 cell lines (HUES1, HUES2, HUES5, HUES6, HUES7, HUES9, HUES15 and HUES16) appeared to be unstable, but the other 8 cell lines (HUES3, HUES4, HUES8, HUES10, HUES12, HUES13, HUES14 and HUES17) appeared to be stable, although they were derived and cultured in same methods and materials (Cowan et al., 2004). The passage numbers are also similar (from 26 to 37). Only known variations between cell lines are donor embryos.

Previous reports have demonstrated that oocytes and preimplantation stage embryos can have imprinting errors, when ART procedures (e.g. IVF and IVC) are applied (Horsthemke and Ludwig, 2005; Khosla et al., 2001b; Lucifero et al., 2004a; Maher,

2005; Young and Fairburn, 2000). These imprinting errors in mouse embryos are stably inherited into ESCs (Li et al., 2005). All 16 HUES-lines are derived from embryos *in vitro* fertilised and cultured up to blastocyst stage (Cowan et al., 2004). Thus, it is possible that some blastocyst stage embryos used for derivation of 16 HUES-lines can have imprinting errors, while they are *in vitro* fertilised and cultured. These errors can be stably inherited into some HUES-lines (Allegrucci et al., 2004).

Another possibility is that 16 HUES-lines are derived from slightly different stage of blastocyst stage embryos (Cowan et al., 2004), implicating that some imprints were not fully established in some blastocyst stage embryos. Moreover, 16 HUES-lines have derived from frozen and thawed low-grade embryos having different blastocysts grade scores (3AA to 4CB), as classified by Gardner et al., (2000). These factors can also influence that some cell lines appear to be stable but some cell lines are not.

3.3.5 Imprinting errors and other factors

It has been suggested that, imprinting of maternally expressed genes (e.g. *H19* and *NESP55*) can be easily disrupted in *in vitro* long-term culture of hESC lines (Rugg-Gunn et al., 2005). In this Chapter, of 11 paternally expressed genes examined, 4 genes (*PEG10*, *PEG1*, *MESTIT1* and *IGF2*) showed unstable imprinting in hESC lines. Of 10 maternally expressed genes examined, 5 genes (*H19*, *GTL2*, *NESP55*, *PHLDA2* and *ATP10C*) showed unstable imprinting in hESC lines. This indicates no relationship between imprinting disruption and typical parental expression status (i.e. maternal or paternal). Moreover, the imprinting disruption between hESC lines showed no relationship with karyotypic aberrations, chromosomal locations, genders, and culture conditions (see Table 2-1).

3.3.6 Further works needed

Previously, it has been reported that mice derived from mESCs having imprinting errors, have widespread cancer formation (Holm et al., 2005). In this Chapter, it was not examined whether imprinting errors in hESC lines can be associated with developmental consequences during lineage-specific differentiation and post-transplantation. To investigate this, *in vivo* and *in vitro* differetnation studies need to be examined with hESC lines having imprinting defects. The allele-specific expression of imprinted genes is guided by differential epigenetic marks (e.g DNA

methylation and histone modifications) at their imprinting regulatory regions. This needs to be examined to understand mechanistic insight into imprinting instability of some hESC lines.

4 DNA METHYLATION AT IMPRINTING REGULATORY REGIONS IN HUMAN EMBRYONIC STEM CELL LINES

4.1 Introduction

The allele-specific expression of imprinted genes can be regulated by allele-specific differential DNA methylation at their regulatory regions (reviewed by Constancia et al., 2004; Ferguson-Smith and Surani, 2001; Reik and Walter, 2001; Surani, 2001). Thus, this chapter aimed to determine whether overall DNA methylation in selected 12 imprinting regulatory regions is associated with the allele-specific expression status of imprinted genes in hESC lines examined in Chapter 3.

4.1.1 DNA methylation associated with imprinted gene expression

DNA methylation is responsible for regulating the allele-specific expression of imprinted genes, although histone lysine methylation and H3 and H4 acetylation have been reported to be involved in this (Carr et al., 2007; Fournier et al., 2002; Lau et al., 2004; Lewis et al., 2004; Umlauf et al., 2004; Vu et al., 2004). DNA methylation at imprinted loci occurs in a specific region named as a differentially methylated region (DMR) (Fitzpatrick et al., 2002; Lin et al., 2003; Sparago et al., 2004). Often DMRs contain more than one CpG island (Fitzpatrick et al., 2002; Lin et al., 2003; Sparago et al., 2004). The DMR is differentially methylated between parental alleles to direct the allele-specific expression of its relative imprinted genes (reviewed by Reik and Walter, 2001; Surani, 2001). For example, *PEG1* (*paternally expressed gene 1*) is expressed from the paternally allele mediated by paternal unmethylation at the *PEG1* DMR (Kosaki et al., 2000; Nakabayashi et al., 2002; Pedersen et al., 2002; Riesewijk et al., 1997). On the other hand, maternal methylation at the *PEG1* DMR directs transcriptional silencing of *PEG1* from the maternal allele.

So far, ~ 15 DMRs have been identified in the human and mouse (see Table 1-2). Most DMRs are frequently found in the promoter region of imprinted genes, but some DMRs are located in the intronic region of imprinted genes that is associated with the expression of antisense transcripts (Mancini-Dinardo et al., 2006; Sleutels et al., 2002; Smilinich et al., 1999; Wutz et al., 1997; Zwart et al., 2001). The imprinting control region (ICR), which is also differentially methylated on both parental alleles, act as a regional imprinting controller that can direct allele-specific expression of its

surrounding genes (Gicquel et al., 2005; Lin et al., 2003; Schoenherr et al., 2003; Sparago et al., 2004). For example, on human chromosome 11p15.5 (mouse distal chromosome 7), two ICRs (ICR1 also known as *H19* DMR and ICR2 also known as *KvDMR1*) have been identified to direct the allele-specific expression of more than 13 imprinted genes (see Figure 1-4).

4.1.2 Imprinting regulatory regions

4.1.2.1 *KvDMR1* (ICR2)

The *KvDMR1* (*potassium voltage differentially methylated region 1*), a ~2kb CpG island, is located in intron 10 of *KCNQ1* (*potassium voltage-gated channel, KQT-like subfamily, member 1*) on human chromosome 11p15.5 (mouse distal chromosome 7) (Lee et al., 1999; Smilinich et al., 1999; Umlauf et al., 2004). In the human and mouse, *KvDMR1* is known to be a germ-line DMR which is methylated in oocytes but is unmethylated in sperm (Geuns et al., 2007b; Khoureiry et al., 2008; Lewis et al., 2004), indicating that the maternal allele-specific methylation at *KvDMR1* is established during gametogenesis. This germ-line specific methylation at *KvDMR1* is maintained throughout mammalian development (Geuns et al., 2007b; Khoureiry et al., 2008; Lewis et al., 2004).

Deletion studies in the mouse and human have revealed that the paternal allele of *KvDMR1* is essential for regulating the allele-specific expression of 9 imprinted genes in the centromeric region of a cluster (Fitzpatrick et al., 2002; Horike et al., 2000; Lewis et al., 2004; Mancini-Dinardo et al., 2006). In mice, for example, the deletion of unmethylated paternal allele of *KvDMR1* leads to transcriptional silencing of *Kcnq1ot1* and biallelic expression of *Tssc3*/*Ipl*, *Slc22a18*/*Tssc5*, *Cdkn1c*/*p57*^{Kip2}, *Kcnq1*, *Tssc4*, *Osbpl5*, *Cd81* and *Ascl2*/*Mash2* (Fitzpatrick et al., 2002; Lewis et al., 2004; Mancini-Dinardo et al., 2006). However, the deletion of methylated maternal allele of *KvDMR1* shows no changes in allele-specific expression of these imprinted genes. Similar results have been reported in the human (Horike et al., 2000). The deletion of *KvDMR1* on the paternally inherited chromosome in chicken DT40 cells leads to transcriptional silencing of *KCNQ1OT1* and increased expression of both *CDKN1C* and *KCNQ1* genes, implicating loss of imprinting of *CDKN1C* and *KCNQ1* (Horike et al., 2000). Importantly, Fitzpatrick et al., (2002) and Horike et al., (2000)

have demonstrated that the deletion of *KvDMR1* show no perturbation of the imprinting status of the *IGF2-H19* domain located in the more telomeric region of a cluster, indicating that *KvDMR1* is associated with allele-specific expression of imprinted genes within the centromeric region of a cluster (see Figure 4-1).

Loss of maternal methylation at *KvDMR1* leads to loss of imprinting of *KCNQ1OT1* that has been frequently found in BWS patients and Wilms' tumours (Bliek et al., 2001; Lee et al., 1999; Smilinich et al., 1999). Moreover, gain of imprinting of *CDKN1C* has been reported as a consequence of loss of methylation at *KvDMR1* that is frequently found in hepatocarcinomas (Schwienbacher et al., 2000).

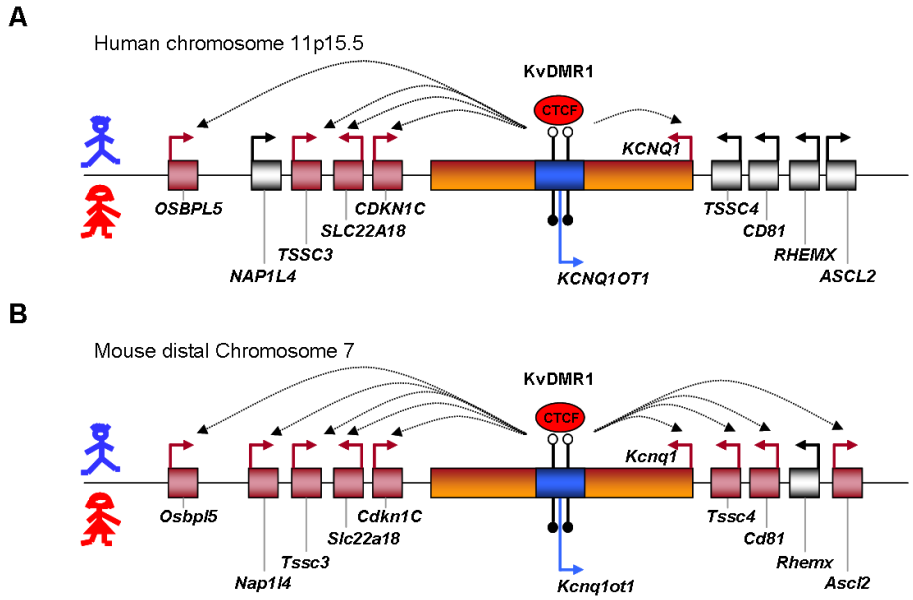

Figure 4-1. *KvDMR1* in the human and mouse
(A) Human *KvDMR1* in chromosome 11p15.5. (B) Mouse *KvDMR1* in distal chromosome 7. *KvDMR1* know as ICR2 which is paternally unmethylated (maternally methylated) that directs the allele-specific expression of imprinted genes (*OSBPL5*, *NAP1L4*, *SLC22A18*, *CDK1NC*, *KCNQ1*, *KCNQ1OT1*, *TSSC4*, *CD81* and *ASCL2*) in a cluster. Maternally expressed genes shown in red. A gene (*KCNQ1OT1*) is paternally expressed shown in blue. Genes are biallelically expressed shown in black. The CTCF protein binds to the unmethylated paternal allele of *KvDMR1*. Vertical bars indicate CpG dinucleotides. Filled circles represent methylated CpG dinucleotides. Unfilled circles represent unmethylated CpG dinucleotides.

4.1.2.2 *H19* DMR (ICR1)

The *H19 DMR* (ICR1), a ~2kb CpG island, is located in the more telomeric region of a cluster on human chromosome 11p15.5 and in the orthologous region on mouse distal chromosome 7 (Olek and Walter, 1997; Pant et al., 2004; Thorvaldsen et al., 1998). The *H19* DMR lies between ~ 2 kb upstream of the *H19* promoter and ~ 90kb

downstream of the *IGF2* gene (Thorvaldsen et al., 1998). In the human and mouse, the *H19* DMR is known to be a germ-line DMR which is methylated in matured spermatogonia but unmethylated in oocytes (Borghol et al., 2006; Kerjean et al., 2000; Olek and Walter, 1997; Ueda et al., 2000), indicating that paternal allele-specific methylation at the *H19* DMR is established during gametogenesis. This germline-specific methylation at the *H19* DMR is maintained throughout mammalian development (Fedoriw et al., 2004; Kerjean et al., 2000; Li et al., 2004; Szabo et al., 2002).

Deletion studies in the mouse and human have revealed that the *H19* DMR is responsible for regulating the allele-specific expression of both *H19* and *IGF2* genes (Schoenherr et al., 2003; Sparago et al., 2004; Thorvaldsen et al., 1998). The deletion of the *H19* DMR on the paternally inherited allele leads to loss of imprinting of *H19* and reduced expression of *Igf2* (Thorvaldsen et al., 1998). Furthermore, the deletion of the *H19* DMR on the maternally inherited allele leads to loss of imprinting of *Igf2* and reduced expressed of *H19* (Schoenherr et al., 2003; Thorvaldsen et al., 1998). Thus, both parental alleles at *H19* DMR are required for regulating the allele-specific expression of *IGF2* and *H19* genes in the human and mouse.

The CTCF (CCCTC-binding factor) proteins and enhancer elements are also required for regulating the monoallelic expression of both *IGF2* and *H19* genes (Figure 4-2 A). Seven CTCF biding sites have been identified in the human *H19* DMR (four CTCF biding sites in the mouse *H19* DMR) (Hark et al., 2000). Two enhancer elements are identified which lie between 7 and 9 kb downstream of the *H19* promoter and ~100 kb downstream of the *Igf2* promoter (Figure 4-2 A). The CTCF proteins bind to the unmethylated maternal allele of their biding sites in the *H19* DMR and acts as an insulator that blocks interaction between the *Igf2* promoter and enhancer elements on the maternal allele (Hark et al., 2000; Schoenherr et al., 2003; Sparago et al., 2004). Thus, *IGF2* is transcriptionally silenced from the maternal allele, whereas *H19* is transcriptionally active. On the other hand, the methylated paternal allele of the *H19* DMR suppresses the accessibility of CTCF proteins that allows enhance elements to bind to the *IGF2* promoter, resulting in paternal expression of *IGF2* and transcriptional silencing of *H19* (Hark et al., 2000; Schoenherr et al., 2003; Sparago et al., 2004). Deletion and mutation studies have revealed that the CTCF proteins have

an important role for maintaining DNA methylation patterns at the *H19* DMR (Fedoriw et al., 2004; Pant et al., 2004; Pant et al., 2003; Schoenherr et al., 2003). The inactivation of CTCF proteins and point mutation of their biding sites lead to *de novo* methylation at the unmethylated maternal allele of the *H19* DMR that is associated with loss of imprinting of *H19* and *IGF2* genes (Fedoriw et al., 2004; Pant et al., 2004; Pant et al., 2003; Schoenherr et al., 2003).

Aberrant DNA methylation patterns at the *H19* DMR can be found in patients who are suffering from Silver-Russell syndrome (SRS), BWS and various cancers (Bliek et al., 2001; Gicquel et al., 2005; Reik et al., 1995; Weksberg et al., 2003). For example, in SRS patients, loss of paternal methylation at the *H19* DMR has been detected in association with reduced expression of *IGF2* and biallelic expression of *H19* (Gicquel et al., 2005). Moreover, gain of methylation at the *H19* DMR has been detected in some BWS patients and Wilms' tumours that is associated with reduced expression of *H19* and biallelic expression of *IGF2* (Bliek et al., 2001; Prawitt et al., 2005; Reik et al., 1995; Weksberg et al., 1993).

The *H19* DMR in preimplantation stage embryos and their derived ESCs is known to be highly susceptible to DNA methylation changes upon *in vitro* culture that leads to phenotypic abnormalities during prenatal and postnatal development (Dean et al., 1998; Doherty et al., 2000; Fernandez-Gonzalez et al., 2004; Khosla et al., 2001a; Li et al., 2005b; Mitalipov et al., 2007; Rugg-Gunn et al., 2005). For instance, hypermethylation at the *H19* DMR (associated with transcriptional silencing of *H19* and biallelic expression of *IGF2*) has been detected in mouse blastocyst stage embryos and mESCs as a consequence of *in vitro* culture conditions (Dean et al., 1998; Doherty et al., 2000; Khosla et al., 2001a; Mann et al., 2004). Their derived foetuses have phenotypic abnormities including polyhydramnios, poor mandible development, interstitial bleeding and increased fetal mass (Dean et al., 1998 and Khosla et al., 2001a).

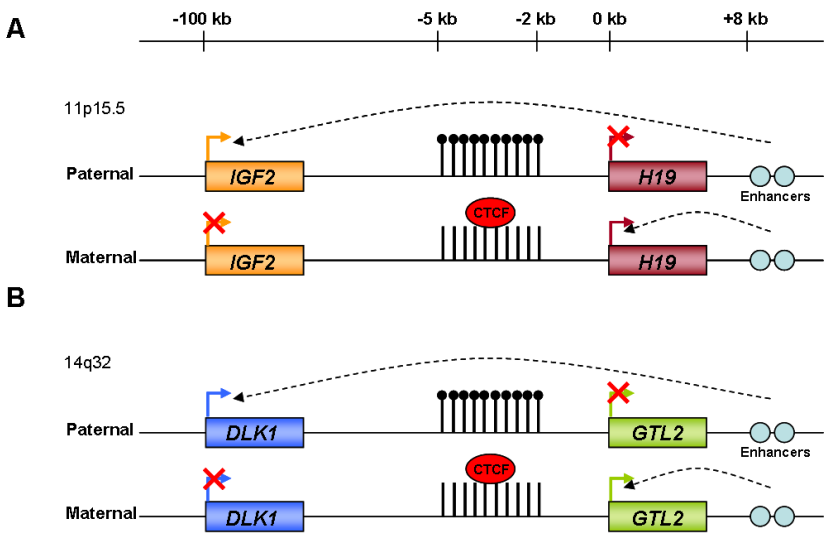

Figure 4-2. *IGF2-H19* and *DLK1-GTL2* DMRs
(A) *IGF2-H19* domain on human chromosome 11p15.5. (B) *DLK1-GTL2* domain on human chromosome 14q32. *IGF2* and *DLK2* are paternally expressed, whereas *H19* and *GTL2* are maternally expressed. *IGF2* and *DLK1* are protein encoding genes, whereas *H19* and *GTL2* are non-coding genes. The monoallelic expression of these genes is mediated by allele-specific differential methylation at DMRs, CTCF proteins and enhancer elements. Vertical bars indicate CpG dinucleotides. Filled circles represent methylated CpG dinucleotides. Arrows on rectangular boxes indicate gene transcription.

4.1.2.3 *GTL2* DMR (IG-DMR)

The *GTL2* (*gene trap locus 2*) DMR (also known as IG-DMR), a ~4kb CpG island, is located in human chromosome 14q32 (mouse distal chromosome 12) (Astuti et al., 2005; Kawakami et al., 2006; Lin et al., 2003; Takada et al., 2002). In the human and mouse, the *GTL2* DMR is known to be a germ-line DMR which is methylated in sperm but unmethylated in GV, MI and MII stage oocytes (Geuns et al., 2007a; Lin et al., 2003), indicating that paternal allele-specific methylation at the *GTL2* DMR is established during gametogenesis. This germ-line specific methylation at the *GTL2* DMR is maintained throughout mammalian development (Geuns et al., 2007a; Lin et al., 2003; Takada et al., 2002; Wylie et al., 2000).

A deletion study in mice has suggested that the maternal allele of the *Gtl2* DMR is essential for regulating the allele-specific expression of its surrounding 4 imprinted genes within a cluster on mouse distal chromosome 12 (Lin et al., 2003). The deletion of the *Gtl2* DMR from the maternally inherited allele leads to biallelic expression of *Dlk1* (*delta, drosophila, homolog-like 1*), *Dio3* (*deiodinase iodothyronine type 3*) and *Rtl1* (*retrotransposon-like 1*), and transcriptional silencing of *Gtl2* (Lin et al., 2003).

However, the deletion of the *Gtl2* DMR from the paternally inherited allele shows no changes in allele-specific expression of these genes (Lin et al., 2003). Interestingly, additional two CpG islands (CpG1 and CpG2) have been identified in the *DLK1-GTL2* domain (Astuti et al., 2005; Carr et al., 2007; Kawakami et al., 2006; Takada et al., 2002; Wylie et al., 2000). However, it has not been examined yet whether they can direct allele-specific expression of imprinted genes within a cluster.

Spatial, structural, epigenetic characteristics of the *DLK1-GTL2* domain are similar to those of the *IGF2-H19* domain (Figure 4-2). *IGF2* and *DLK2* are expressed on the paternally inherited allele, whereas *H19* and *GTL2* are maternally expressed (Bartolomei et al., 1991; DeChiara et al., 1991; Kobayashi et al., 2000; Miyoshi et al., 2000). *IGF2* and *DLK1* are protein encoding genes, whereas *H19* and *GTL2* encode for non-coding RNA (ncRNA) (Bartolomei et al., 1991; Kalscheuer et al., 1993; Wylie et al., 2000). The allele-specific expression of these genes is mediated by differential allele-specific methylation at *H19* and *GTL2* DMRs (Lin et al., 2003; Sparago et al., 2004; Thorvaldsen et al., 1998; Wylie et al., 2000). Moreover, similar to the *H19* DMR, there are CTCF binding sites (located 1131 bp and 840 bp, respectively, upstream of a *GTL2* transcription start site) and enhancer elements (located 8.9 kb and 10.7 kb, respectively, downstream of a *GTL2* transcription start site) within the *GTL2* DMR (Figure 4-2) (Takada et al., 2002; Wylie et al., 2000), implicating that allele-specific expression of *DLK1* and *GTL2* genes may be guided by CTCF proteins and enhancer elements.

Aberrant DNA methylation patterns at the *GTL2* DMR have been reported in human cancers and oligospermia patients (Astuti et al., 2005; Kawakami et al., 2006; Kobayashi et al., 2007). Gain of methylation at the unmethylated maternal allele of the *GTL2* DMR has been found in neuroblastomas, phaeochromocytoma, renal cell carcinomas and Wilms' tumours (Astuti et al., 2005; Kawakami et al., 2006). Moreover, loss of paternal methylation at the *GTL2* DMR has been detected in oligospermia patients, as a consequence of impaired spermatogenesis (Kobayashi et al., 2007).

4.1.2.4 *PEG1* DMR

The *PEG1* (*paternally expressed gene 1*) DMR, a ~600 bp CpG island, is located in the promoter and exon 1 of *PEG1* on human chromosome 7q32 (mouse chromosome 6) (Riesewijk et al., 1997). In the human and mouse, the *PEG1* DMR is known to be a germ-line DMR which is methylated in oocytes but unmethylated in sperm (Kerjean et al., 2003; Kerjean et al., 2000; Lucifero et al., 2004b; Obata and Kono, 2002; Sato et al., 2007). This indicates maternal allele-specific methylation at the *PEG1* DMR is established in the germ line. This germ-line specific methylation at the *PEG1* DMR is maintained throughout mammalian development (McMinn et al., 2006; Nakabayashi et al., 2002; Pedersen et al., 2002).

MESTIOT1 (*MEST intronic transcript 1*)/*PEG1-AS*, which is maternally imprinted, has been identified to be transcribed in the opposite direction to *PEG1* and shares the promoter region of *PEG1 isoform 1* (Li et al., 2002; Nakabayashi et al., 2002). Thus, it has been suggested that maternal allele-specific methylation at the *PEG1* DMR can also direct the paternal expression of *MESTIOT1* (Li et al., 2002; Nakabayashi et al., 2002). However, clear evidences about this have not been reported yet.

Aberrant DNA methylation at the *PEG1* DMR can be found in oligospermia patients (Kobayashi et al., 2007; Marques et al., 2004) and superovulated oocytes (Kerjean et al., 2003; Sato et al., 2007). This may be due to impaired spermatogenesis and oogenesis. Moreover, loss of imprinting of *PEG1* has been detected in breast and lung carcinomas that is associated with loss of maternal methylation at the *PEG1* DMR (Nakanishi et al., 2004; Pedersen et al., 2002).

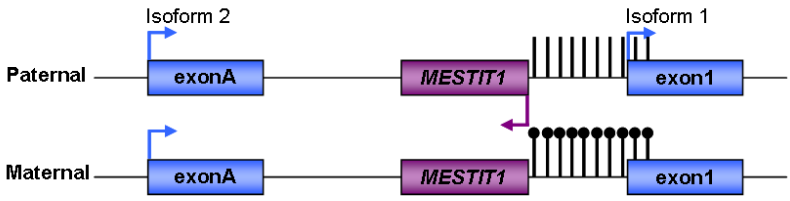

Figure 4-3. *PEG1 DMR* in the human
The *PEG1* DMR is maternally methylated, but it is paternally unmethylated. *PEG1 isoform 1* transcribed from exon 1 is paternally expressed, whereas *PEG1 isoform 2* transcribed from exon A is expressed from both parental alleles. Paternal-specific unmethylation at the*PEG1* DMR is responsible for expression of *PEG1 isoform 1* and *MESTIT1* from the paternal chromosome. *MESTIT1* is located on an intron of *PEG1* isoform 2, shares the promoter region of *PEG1* isoform 1 and is transcribed in the opposite direction to *PEG1*. Vertical bars indicate CpG dinucleotides. Filled circles represent methylated CpG dinucleotides. Arrows indicate gene transcription.

4.1.2.5 *IGF2R* DMR1 and DMR2

The *Igf2r* (*insulin-like growth factor2 receptor*) gene contains two DMRs (DMR1 and DMR2) in mouse proximal chromosome 17 (Barlow et al., 1991; Kalscheuer et al., 1993; Stoger et al., 1993) (Figure 4-4). DMR1 is located in the promoter region of the *Igf2r* gene which is methylated on the paternal chromosome but unmethylated on the maternal chromosome (Stoger et al., 1993). DMR2, a ~ 2kb CpG island, is located in intron 2 of *Igf2r*, which is methylated on the maternal allele but unmethylated on the paternal allele (Stoger et al., 1993). In the mouse, paternal allele-specific methylation at the *Igf2r* DMR1 is acquired after fertilization, indicating that it is a somatic DMR (Stoger et al., 1993). However, maternal allele-specific methylation at the *Igf2r* DMR2 is acquired during gametogenesis, indicating that it is a germ-line DMR (Lucifero et al., 2002; Stoger et al., 1993). This has not been examined in human gametes and preimplantation embryos.

Deletion studies in mice have revealed that differential methylation at the *Igf2r* DMR2 and the presence of the *Air* transcript are essential for regulating allele-specific expression of *Igf2r*, *Air*, and two placental-specific imprinted genes (*Slc22a2* and *Slc22a3*) in a cluster (Sleutels et al., 2003; Sleutels et al., 2002; Wutz et al., 1997; Zwart et al., 2001). For example, the deletion of the *Igf2r* DMR2 in mice leads to loss of imprinting of *Igf2r*, *Slc22a2* and *Slc22a3* and transcriptional silencing of *Air* (Wutz et al., 1997; Zwart et al., 2001). Moreover, the deletion of the *Air* transcript leads to loss of imprinting of *Igf2r*, *Slc22a2* and *Slc22a3* (Sleutels et al., 2003; Sleutels et al., 2002).

In the human, only *IGF2R* DMR2 has been reported to be differentially methylated on human chromosome 6q26, whereas *IGF2R* DMR1 is completely unmethylated on both parental alleles (Smrzka et al., 1995), implicating that *IGF2R* DMR2 may direct monoallelic expression of *IGF2R*. However, biallelic expression of *IGF2R* has been mostly detected in lymphoblastoid cells and fetal and adult tissues including placentae, heart and liver, although preferential expression of the maternal allele of *IGF2R* has been reported in some tissues (Kalscheuer et al., 1993; Monk et al., 2006a; Xu et al., 1993). This indicates no correlation between *IGF2R* imprinting and differential methylation at *IGF2R* DMR2. Thus, recent studies have suggested that other epigenetic marks at histones may be involved in *IGF2R* imprinting (Monk et al.,

2006a; Vu et al., 2004). Alternatively, the lack of methylation at *IGF2* DMR1 may be associated with the biallelic expression of *IGF2R* (Hu et al., 1998).

In the mouse, aberrant DNA methylation at *Igf2r* DMR2 has been detected in superovulated oocytes, and *in vitro* cultured embryos and mESCs (Dean et al., 1998; Kerjean et al., 2003). This may be due to impaired oogenesis and *in vitro* culture conditions. Moreover, loss of methylation at the *IGF2R* DMR2 has been reported in sheep, as a consequence of *in vitro* culture of ovine embryos that is associated with Large Offspring syndrome (LOS) (Young et al., 2001).

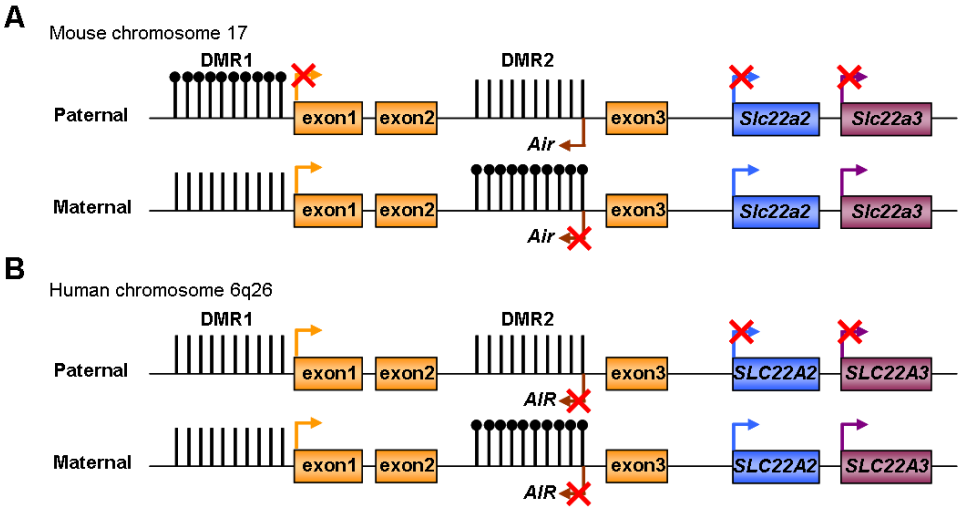

Figure 4-4. *IGF2R* DMR1 and DMR2 in the mouse and human
(A) In the mouse, DMR1 is paternally methylated but maternally unmethylated. DMR2 is maternally methylated but paternally unmethylated. (B) In the human, DMR1 is completely unmethylated, whereas DMR2 is differentially methylated. No AIR transcript is detected in the human. Vertical bars indicate CpG dinucleotides. Filled circles represent methylated CpG dinucleotides. Arrows indicate gene transcription.

4.1.2.6 *PEG3* DMRs

The *PEG3* (*paternally expressed gene 3*) DMR, a 364bp CpG island, is located in the promoter and exon1 of *PEG3* on human chromosome 19q13.4 (mouse proximal chromosome 7) (Dowdy et al., 2005; Kim et al., 2003; Li et al., 1999; Maegawa et al., 2001). In the mouse, the *Peg3* DMR is know to be a germ-line DMR which is methylated in oocytes but unmethylated in sperm (Arnaud et al., 2006; Lucifero et al., 2002), indicating that maternal specific methylation at *Peg3* DMR is acquired in the germ line. This has not been determined in human gametes and preimplantation stage embryos.

In the mouse, 5 additional imprinted genes (*Usp29*, *Zf264*, *Zim1*, *Zim2* and *Zim3*) have been indentified within the surrounding *Peg3* DMR (Kim et al., 2000a; Kim et al., 2001; Kim et al., 2003; Kim et al., 2000b), implicating that the *Peg3* DMR may act as a ICR in a cluster on chromosome 7 to direct allele-specific expression of these genes. To examine this possibility, deletion and mutation studies are required. In the human, *ZIM2* has been reported to be imprinted, whereas the imprinting status of other genes has not been identified (Kim et al., 2000a; Kim et al., 2001).

Interestingly, the Gli-type transcription factor, YY1, has been reported to bind to the unmethylated allele of the *Peg3* DMR (Kim and Kim, 2008; Kim et al., 2003; Kim et al., 2006). Similar to the CTCF protein, YY1 acts as a methylation sensitive insulator that can regulate allele-specific expression of *Peg3* and its neighbouring genes (Kim and Kim, 2008; Kim et al., 2003; Kim et al., 2006). The inactivation of the YY1 protein in mice leads to down-regulation of *Peg3* expression mediated by gain of methylation at the *Peg3* DMR (Kim and Kim, 2008), indicating that YY1 is essential for maintaining an unmethylated state at the paternal allele of the *Peg3* DMR.

Loss of methylation at the *PEG3* DMR has been detected in various cancer cell lines including JEG3 and BeWo, HTB-16, HTB-17, and CRL-1620, RL-95, C33A, ME180, Ovcar-3 and Ovcar-5 that is associated with loss of imprinting of *PEG3* (Dowdy et al., 2005; Maegawa et al., 2001).

4.1.2.7 *NDN* and *SNRPN* DMRs

The *NDN* DMR, a 880bp CpG island, is located in the promoter region of *NDN* (Boccaccio et al., 1999; El-Maarri et al., 2001; Lau et al., 2004). The *SNRPN* DMR, a ~4.3kb CpG island, is located in the promoter and exon1 of *SNRPN* (El-Maarri et al., 2001; Sutcliffe et al., 1994). Both *NDN* and *SNRPN* DMRs are maternally methylated but paternally unmethylated in normal tissues on human chromosome 15q11 (mouse chromosome 7) (MacDonald and Wevrick, 1997; Tsai et al., 1999). In the human and mouse, both DMRs are known as germ-line DMRs which are methylated in oocytes but unmethylated in sperm (El-Maarri et al., 2001; Geuns et al., 2003; Hanel and Wevrick, 2001; Lucifero et al., 2002), indicating that maternal allele-specific methylation at *NDN* and *SNRPN* DMRs is acquired during gametogenesis. This germ-

line specific DNA methylation is maintained during mammalian development (El-Maarri et al., 2001; Geuns et al., 2003; Huntriss et al., 1998; Salpekar et al., 2001).

Aberrant DNA methylation at *NDN* and *SNRPN* DMRs has been reported in PWS, AS and oligospermia patients (Cox et al., 2002; Kobayashi et al., 2007; Orstavik et al., 2003; Sutcliffe et al., 1994). For example, loss of methylation at *NDN* and *SNRPN* DMRs has been found in some PWS patients that is associated with loss of imprinting of *SNRPN* (El-Maarri et al., 2001; Reis et al., 1994; Sutcliffe et al., 1994). Moreover, loss of methylation at the *SNRPN* DMR is frequently found in ART-conceived AS children (Cox et al., 2002; Orstavik et al., 2003). Gain of methylation at the *SNRPN* DMR has been reported in oligospermia patients, as a consequence of impaired spermatogenesis (Kobayashi et al., 2007).

4.1.3 DNA methylation at DMRs in ESCs

In vitro derived and cultured mouse and rhesus monkey ESCs have been identified to have imprinting errors associated with aberrant DNA methylation at imprinting regulatory regions (Dean et al., 1998; Feil et al., 1997; Fujimoto et al., 2006; Humpherys et al., 2001). In contrast to mouse and rhesus monkey ESCs, 5 hESC lines exhibit a substantial degree of imprinting stability in association with normal monoallelic DNA methylation patterns at *SNRPN*, *H19*, *GTL2*, *NESP55* and *KvDMR1* DMRs (Plaia et al., 2006; Rugg-Gunn et al., 2005). Only one cell line, H9, shows gain of methylation at the *H19* DMR at later passages (p66 ~ p101) that is not associated with biallelic expression of *H19* (Rugg-Gunn et al., 2005).

4.1.4 Chapter aims

Unstable and variable imprinting has been detected by increasing the number of hESC lines and imprinted genes examined in Chapter 3. Thus, the aim of this Chapter is to determine whether imprinting instability in hESC lines are correlated to DNA methylation changes at potential imprinting regulatory regions.

4.2 Results

Direct bisulphite sequencing was performed to give an overview of the mean methylation status at *TP73*, *KCNQ1*, *CDKN1C* and *SLC22A18* promoters, and *KvDMR1*, *PEG1*, *PEG10*, *IGF2*, *GTL2*, *NDN* and *NESP55* DMRs in all informative cell lines characterised in Chapter 3. Clonal bisulphite sequencing and combined bisulphite restriction analysis (COBRA) were performed to confirm DNA methylation at the *NESP55*, *PEG1*, *PEG10*, *GTL2* and *NESP55* DMRs.

4.2.1 Direct bisulphite sequencing electrophoretograms

Figure 4-5 shows direct bisulphite sequencing electrophoretograms at the *PEG1* DMR in HUES7, HUES12, HUES17, BG01 and NOTT2. The degree of DNA methylation in each CpG dinucleotide is determined by the relative peak height of C (cytosine) and T (thymine) as follows: 1) If a C peak is higher than a T peak in a CpG dinucleotide, the CpG dinucleotide is defined to be predominantly methylated (yellow rectangle). 2) If a T peak is higher than a C peak in a CpG dinucleotide, the CpG dinucleotide is defined to be predominantly unmethylated (blue rectangle). 3) If both C and T peaks are present at the equal height in a CpG dinucleotide, the CpG dinucleotide is defined to be monoallelically methylated (grey rectangle). 4) If a C peak alone is present in a CpG dinucleotide, the CpG dinucleotide is defined to be methylated (black rectangle). 5) If a T peak alone is present in a CpG dinucleotide, the CpG dinucleotide is defined to be unmethylated (white rectangle). 6) A red rectangle indicates the mutation of CpG dinucleotides. Six criteria were previously defined by Frigola *et al*., (2006). On the basis of these criteria, direct bisulphite sequencing was performed in selected 12 imprinting regulatory regions.

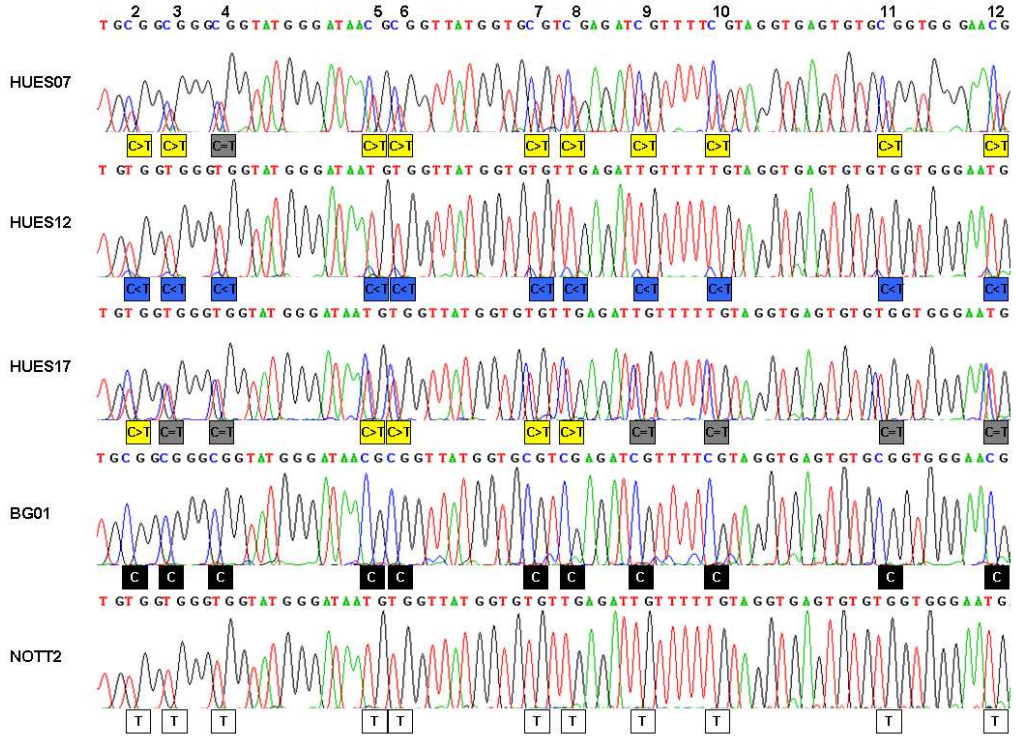

Figure 4-5. Direct bisulphite sequencing electrophoretograms
PCR with bisulphite modified DNA of HUES7, HUES12, HUES17, BG01 and NOTT2 and direct sequencing were performed to give an overview of the mean DNA methylation status of the *PEG1* DMR. Sequencing data were analysed by Chromas Lite v2.01. The CpG dinucleotides are numbered as 2 to 12. The degree of methylation in each CpG dinucleotide is determined by the relative peak height of C and T. C>T indicates predominant methylation (yellow rectangles). C<T indicates predominant unmethylation (blue rectangles). C=T indicates hemimethylation (grey rectangles). C alone indicates complete methylation (black rectangles). T alone indicates complete unmethylation (white rectangles). Three types (C>T, C<T and C=T) are defined to be differentially methylated at CpG dinucleotides.

4.2.2 *TP73* promoter

DNA methylation at 50 CpG dinucleotides within the *TP73* promoter was analysed by direct bisulphite sequencing (Dong et al., 2002). PCR with bisulphite modified genomic DNA of 8 informative cell lines (see section 3.2.1, HUES1, HUES6, HUES7, HUES8, HUES10, HUES16, HES-2 and NOTT2), HESC-NL1 (passages 22, 58) and NTERA2, and direct sequencing were performed. The degree of methylation was determined by the relative peak height of C and T. 50 CpG dinucleotides in the promoter region of *TP73* were completely unmethylated in all hESC lines (Figure 4-6 A). However, NTERA2 showed predominant methylation at 27/50 CpG dinucleotides. No methylation changes were detected in *in vitro* prolonged culture of HES-2 (passages 56, 65, 96) and HESC-NL1 (passages 22, 58) (Figure 4-6 A and B).

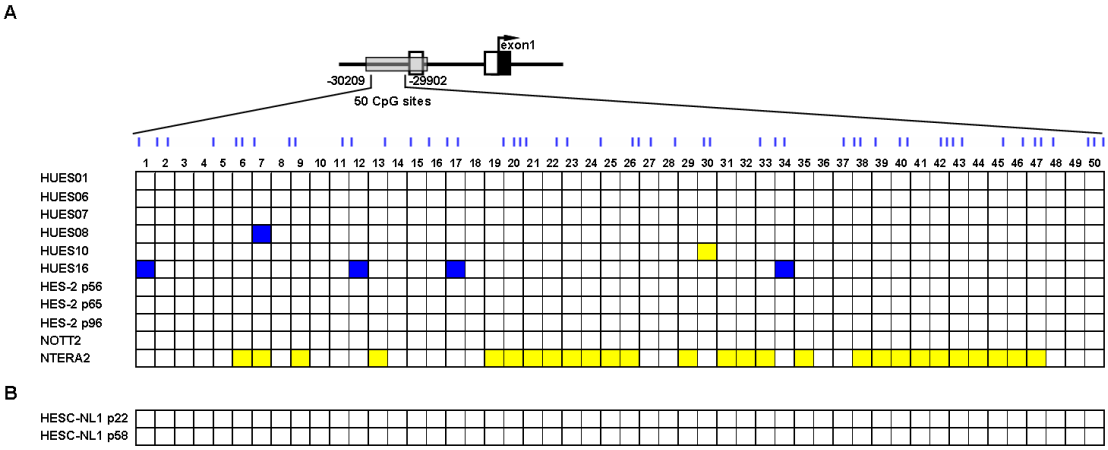

Figure 4-6. DNA methylation at the *TP73* promoter
(A) DNA methylation at the *TP73* promoter region was analysed in 8 informative cell lines determined in Chapter 3. (B) DNA methylation at the *TP73* promoter was analysed in HESC-NL1 (passages 22, 58). In the schematic diagram, a block box represents exon 1, two white boxes represent untranslated regions (URTs), and a gray box indicates a CpG island. An arrow indicates a transcriptional start site. Numbers (-30209 to -29902) indicate the sequence position analysed within a CpG island. The first and last CpG dinucleotides are numbered relative to a transcription start site. Blue vertical bars indicate CpG dinucleotides within the region analysed. Yellow rectangles indicate predominant methylation at CpG dinucleotides. Blue rectangles indicate predominant unmethylation at CpG dinucleotides. White rectangles indicate unmethylation at CpG dinucleotides.

4.2.3 PEG10 DMR

DNA methylation at 15 CpG dinucleotides at the *PEG10* DMR was analysed by direct bisulphite sequencing (Suzuki et al., 2007). PCR with bisulphite modified genomic DNA of 4 informative hESC lines (see section 3.2.3, HUES5, HUES7, HUES10 and HUES12) and direct sequencing were performed. The degree of methylation was determined by the relative peak height of C and T. Differential methylation at the *PEG10* DMR was detected in HUES7, HUES10 and HUES12 (Figure 4-7 A). However, *PEG10* DMR was completely unmethylated in HUES5. These methylation patterns were confirmed by COBRA (Figure 4-7 B and C). Two *Bst*UI restriction enzyme sites were analysed to determine methylation-dependent sequence differences in PCR products of bisulphite modified genomic DNA (Figure 4-7 B). Three digested bands and one undigested band were detected in HUES7, HUES10 and HUES12 cell lines, indicating differential methylation at the *PEG10* DMR (Figure 4-7 C). However, only one undigested band was detected in HUES5, indicating unmethylation at *PEG10* DMR.

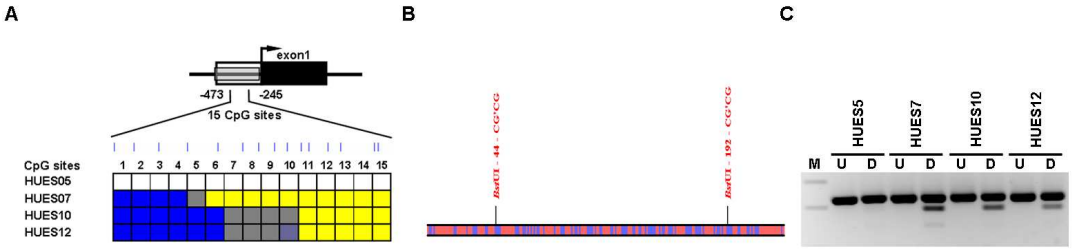

Figure 4-7. DNA methylation at the *PEG10* DMR
(A) DNA methylation at the *PEG10* DMR was analysed in 4 informative cell lines determined in Chapter 3. In the schematic diagram, a block box represents exon 1, a white box represents an untranslated region (URT), and a gray box indicates a CpG island. An arrow indicates a transcriptional start site. Numbers (-473 to -245) indicate the sequence position analysed within a CpG island. The first and last CpG dinucleotides are numbered relative to a transcription start site. Blue vertical bars indicate CpG dinucleotides within the region analysed. Yellow rectangles indicate predominant methylation at CpG dinucleotides. Blue rectangles indicate predominant unmethylation at CpG dinucleotides. Grey rectangles indicate hemimethylation at CpG dinucleotides. White rectangles indicate unmethylation at CpG dinucleotides. (B) A schematic diagram shows two *Bst*UI enzyme sites at the *PEG10* DMR. (C) The COBRA analysis of the *PEG10* DMR. M, 100 bp DNA Ladder; U, *Bst*UI-undigested; D: *Bst*UI-digested.

4.2.4 *PEG1* DMR

25 CpG sites within the *PEG1* DMR were subjected to DNA methylation analyses by direct bisulphite sequencing (Kerjean et al., 2000). PCR with bisulphite modified genomic DNA of 13 informative cell lines (see section 3.2.4, HUES1, HUES2, HUES7, HUES10, HUES12, HUES15, HUES16, HUES17, BG01, HES-2, NOTT1, NOTT2 and NTERA2) and direct sequencing were performed. The degree of methylation was determined by the relative peak height of C and T. Differential DNA methylation of the *PEG1* DMR was detected in HUES1, HUES2, HUES7, HUES10, HUES12, HUES15, HUES16, HUES17, HES-2 and NOTT1 (Figure 4-8 A). However, the *PEG1* DMR was completely unmethylated in NOTT2 and NTERA2 and completely methylated in BG01. These methylation patterns at the *PEG1* DMR were confirmed by clonal bisulphite sequencing (Figure 4-8 B). Of 10 clones examined in HES-2, 5 clones were methylated at the *PEG1* DMR (filled circles), but other 5 clones were unmethylated (unfilled circles), indicating differential methylation on both parental alleles. Moreover, NOTT1 showed differential methylation at the *PEG1* DMR (6 clones unmethylated, 4 clones methylated). However, all 10 clones were completely unmethylated in both NOTT2 and NTERA2. DNA methylation changes were detected during *in vitro* prolonged culture of HES-2 (passages 56, 65, 96),

although no DNA methylation changes were detected in NL-HESC1 (passages 22, 58). HES-2 (p56) showed predominant methylation or hemimethylation at 25 CpG dinucleotides. However, they became predominantly unmethylated in HES-2 (p65 and p96).

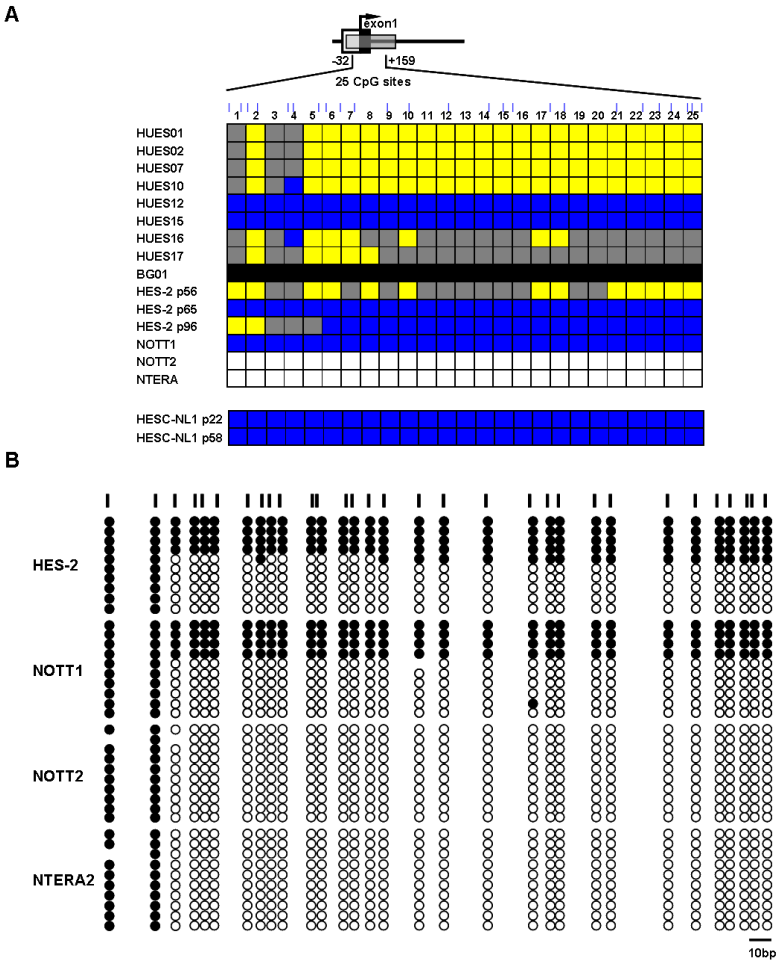

Figure 4-8. DNA methylation at the *PEG1* DMR
(A) DNA methylation at the *PEG1* DMR was analysed in13 informative cell lines determined in Chapter 3. In the schematic diagram, a block box represents exon 1, a white box represents an untranslated region (URT), and a gray box indicates a CpG island. An arrow indicates a transcriptional start site. Numbers (-32 to +159) indicate the sequence position analysed within a CpG island. The first and last CpG dinucleotides are numbered relative to a transcription start site. Yellow rectangles indicate predominant methylation at CpG dinucleotides. Blue rectangles indicate predominant unmethylation at CpG dinucleotides. Grey rectangles indicated hemimethylation at CpG dinucleotides. White rectangles indicate unmethylation at CpG dinucleotides. (B) Clonal bisulphite sequencing at the *PEG1* DMR in HES-2, NOTT1, NOTT2 and NTERA2. Black vertical bars indicate CpG dinucleotides within the region analysed. A scale bar corresponds to 10 bp. Open and filled circles represent unmethylated and methylated CpG sites respectively.

4.2.5 IGF2 DMR0

DNA methylation at 5 CpG sites in the P0 promoter region of *IGF2* was analysed by direct bisulphite sequencing (Monk et al., 2006b). PCR with bisulphite modified genomic DNA of 10 informative cell lines (see section 3.2.8, HUES1, HUES5, HUES6, HUES8, HUES9, HUES16, HUES17, HESC-NL1, HES-2 and NOTT2) and direct sequencing were performed. The degree of methylation was determined by the relative peak height of C and T. Differential DNA methylation of the *IGF2* DMR0 was detected in all cell lines (Figure 4-9). No methylation changes at the *IGF2* DMR0 were detected during *in vitro* prolonged culture of HESC-NL1 (passages 22 to 58) and HES-2 (passages 56 and 96).

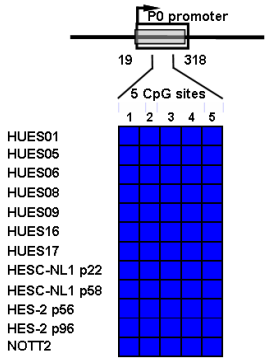

Figure 4-9. DNA methylation at the *IGF2* DMR0
DNA methylation at the *IGF2R* DMR0 was analysed in 10 informative cell lines determined in Chapter 3. In the schematic diagram, a white box represents an untranslated region (URT), and a gray box indicates a CpG island. An arrow indicates a transcriptional start site. Numbers (19 to 318) indicate the sequence position analysed within a CpG island. Numbering refers to accession no. NM_001007139. Blue rectangles indicate predominant unmethylation at CpG dinucleotides. Blue vertical bars indicate 5 CpG dinucleotides within the region analysed.

4.2.6 *KCNQ1* promoter

DNA methylation at 19 CpG dinucleotides in the promoter region of *KCNQ1* was analysed by direct bisulphite sequencing (Monk et al., 2006a). PCR with bisulphite modified genomic DNA of 8 informative cell lines (see section 3.2.9, HUES1, HUES2, HUES6, HUES8, HUES9, HUES12, HUES13 and NOTT1), and direct sequencing were performed. The degree of methylation was determined by the relative peak height of C and T. The *KCNQ1* promoter was completely unmethylated in all cell lines examined (Figure 4-10).

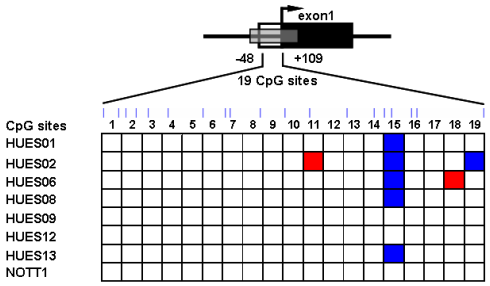

Figure 4-10. DNA methylation at the *KCNQ1* promoter
DNA methylation at the promoter region of *KCNQ1* was analysed in 8 informative cell lines determined in Chapter 3. In the schematic diagram, a block box represents exon 1, a white box represents an untranslated region (URT), and a gray box indicates a CpG island. An arrow indicates a transcriptional start site. Numbers (-48 to +109) indicate the sequence position analysed within a CpG island (accession number: AJ006345). The first and last CpG dinucleotides are numbered relative to a transcription start site. Blue rectangles indicate predominant unmethylation at CpG dinucleotides. White rectangles indicate unmethylation at CpG dinucleotides. Red rectangles indicate the mutation of CpG dinucleotides. Blue vertical bars indicate CpG dinucleotides within the region analysed.

4.2.7 KvDMR1

DNA methylation at 17 CpG sites within the *KvDMR1* was analysed by direct bisulphite sequencing (Monk et al., 2006a). PCR with bisulphite modified genomic DNA of 18 cell lines and direct sequencing were performed. The degree of methylation was determined by the relative peak height of C and T. *KvDMR1* was differentially methylated in all cell lines (Figure 4-11). The differential methylation pattern at *KvDMR1* was not changed during *in vitro* prolonged culture of HESC-NL1 (passages 22 to 58) and HES-1 (passages 56, 65 and 96) (Figure 4-11).

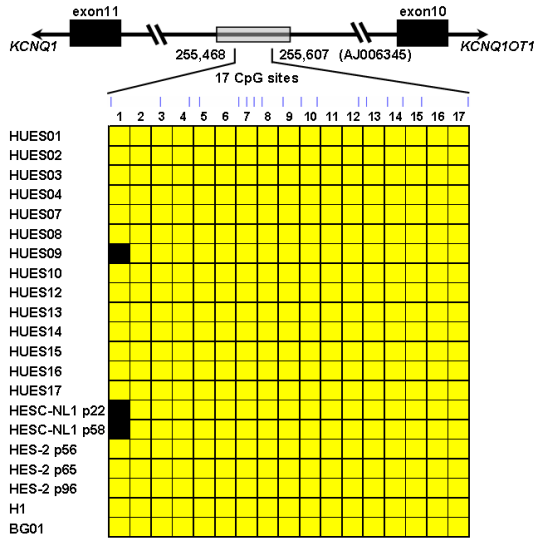

Figure 4-11. DNA methylation at the *KvDMR1*

DNA methylation at the *KvDMR1* was analysed in 18 cell lines (*KCNQ1OT1*, *KCNQ1*, *CDK1NC* and *TSSC5* informative cell lines) characterised in Chapter 3. In the schematic diagram, block boxes represent exon11 and exon10 respectively and a gray box indicates a CpG island. Numbers (255,468 to 255.607) indicate the sequence position analysed within a CpG island. Numbering refers to accession no. AJ006345. Yellow rectangles indicate predominant methylation at CpG dinucleotides. Black rectangles indicate methylation at CpG dinucleotides. Blue vertical bars indicate CpG dinucleotides within the region analysed.

4.2.8 *CDKN1C* promoter

DNA methylation at 26 CpG sites in the promoter region of *CDKN1C* was analysed by direct bisulphite sequencing (Monk et al., 2006a). PCR with bisulphite modified genomic DNA of 3 informative cell lines (see section 3.2.11, HUES4, HUES14 and HUES16) and direct sequencing were performed. The degree of methylation was determined by the relative peak height of C and T. Half of the promoter region was completely unmethylated (CpG sites from 2 to 13), but the other half was predominantly unmethylated in these cell lines (CpG sites from 14 to 25) (Figure 4-12).

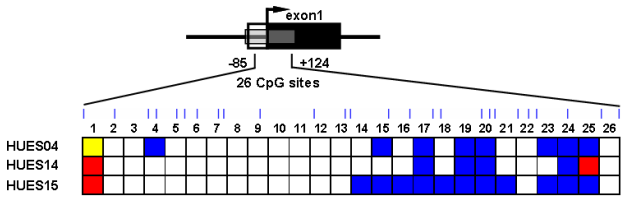

Figure 4-12. DNA methylation at the *CDKN1C* promoter
DNA methylation at the promoter region of *CDKN1C* was analysed in 3 informative cell lines determined in Chapter 3. In the schematic diagram, a block box represents exon 1, a white box represents an untranslated region (URT), and a gray box indicates a CpG island. An arrow indicates a transcriptional start site. Numbers (-85 to +124) indicate the sequence position analysed within a CpG island (accession number: AC005950). The first and last CpG dinucleotides are numbered relative to a transcription start site. A yellow rectangle indicates predominant methylation at a CpG dinucleotide. Blue rectangles indicate predominant unmethylation in CpG dinucleotides. White rectangles indicate unmethylation at CpG dinucleotides. Red rectangles indicate the mutation of CpG dinucleotides. Blue vertical bars indicate CpG dinucleotides within the region analysed.

4.2.9 *SLC22A18* promoter

DNA methylation at 32 CpG sites in the promoter region of *SLC22A18* was analysed by direct bisulphite sequencing (Monk et al., 2006a). PCR with bisulphite modified genomic DNA of 6 informative cell lines (see section 3.2.13, HUES5, HUES12, HUES13, HUES15, HESC-NL1 and NOTT2) and direct sequencing were performed.

The degree of methylation was determined by the relative peak height of C and T. *SLC22A18* promoter was unmethylated in all cell lines (Figure 4-13). No methylation changes at the *SLC22A18* promoter were detected during *in vitro* prolonged culture of HESC-NL1 (passages 22, 58) and HES-2 (passages 56, 65, 96).

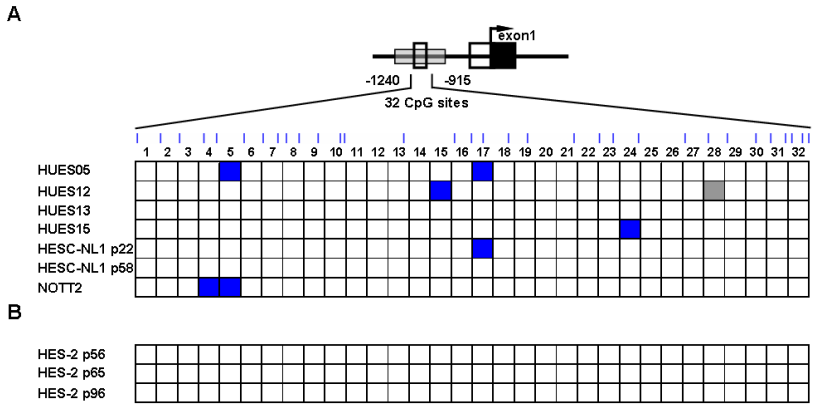

Figure 4-13. DNA methylation at the *SLC22A18* promoter
(A) DNA methylation at the promoter region of *SLC22A18* was analysed in 6 informative cell lines determined in Chapter 3 and (B) in the HES-2 cell line (passages 56, 65, 96). In the schematic diagram, a block box represents exon 1, two white boxes represent untranslated regions (URTs), and a gray box indicates a CpG island. An arrow indicates a transcriptional start site. Numbers (-1240 to -915) indicate the sequence position analysed within a CpG island (accession number: AC013791). The first and last CpG dinucleotides are numbered relative to a transcription start site. Blue rectangles indicate predominant unmethylation at CpG dinucleotides. A Grey rectangle indicates hemimethylation at a CpG dinucleotide. White rectangles indicate unmethylation at CpG dinucleotides. Blue vertical bars indicate CpG dinucleotides within the region analysed.

4.2.10 *GTL2* CpG2 and DMR

The *GTL2* CpG2 (10 CpG dinucleotides) and *GTL2* DMR (32 CpG dinucleotides) were subjected to analyse the DNA methylation status by direct bisulphite sequencing (Kawakami et al., 2006; Wylie et al., 2000). PCR with bisulphite modified genomic DNA of 11 informative cell lines (see section 3.2.15, HUES3, HUES7, HUES10, HUES12, HUES13, HUES14, HUES15, HUES17, HESC-NL1, NOTT2 and H1) and direct sequencing were performed. The degree of methylation was determined by the relative peak height of C and T. *GTL2* CpG2 was completely methylated in all cell lines (Figure 4-14 A). Differential methylation of the *GTL2* DMR was observed in HUES3, HUES7, HUES10, HUES12, HESC-NL1 (passage 22) and NOTT1. However, the *GTL2* DMR was methylated in HUES13, HUES14, HUES15, HUES17 and H1. These DNA methylation patterns at *GTL2* DMR were confirmed by COBRA (Figure

4-14 C and D). Two *Hpy*CH4IV restriction enzyme sites were analysed to determine methylation-dependent sequences differences in PCR products of bisulphite modified genomic DNA (Figure 4-14 C). The COBRA analysis showed that two *Hpy*CH4IV sites were methylated in HUES10, HUES13, HUES14, HUES15, HUES17 and H1 (only two digested bands detected). However, HUES3, HUES7, HUES12, HESC-NL1 (p22) and NOTT1 showed differential methylation on both parental alleles (one undigested band and two digested bands detected). DNA methylation changes at the *GTL2* DMR were detected during *in vitro* prolonged culture of HESC-NL1 (passages 22, 58) and HES-2 (passages 56, 65, 96). The *GTL2* DMR was differentially methylated in HESC-NL1 (p22) and HES-2 (p56), but it became hypermethylated in HESC-NL1 (p58) and HES-2 (p65 and 96) in all CpG dinucleotides. DNA methylation patterns at the *GTL2* CpG2 were maintained during *in vitro* prolonged culture of HESC-NL1 (passages 22 and 58) and HES-2 (passages 56, 65 and 96).

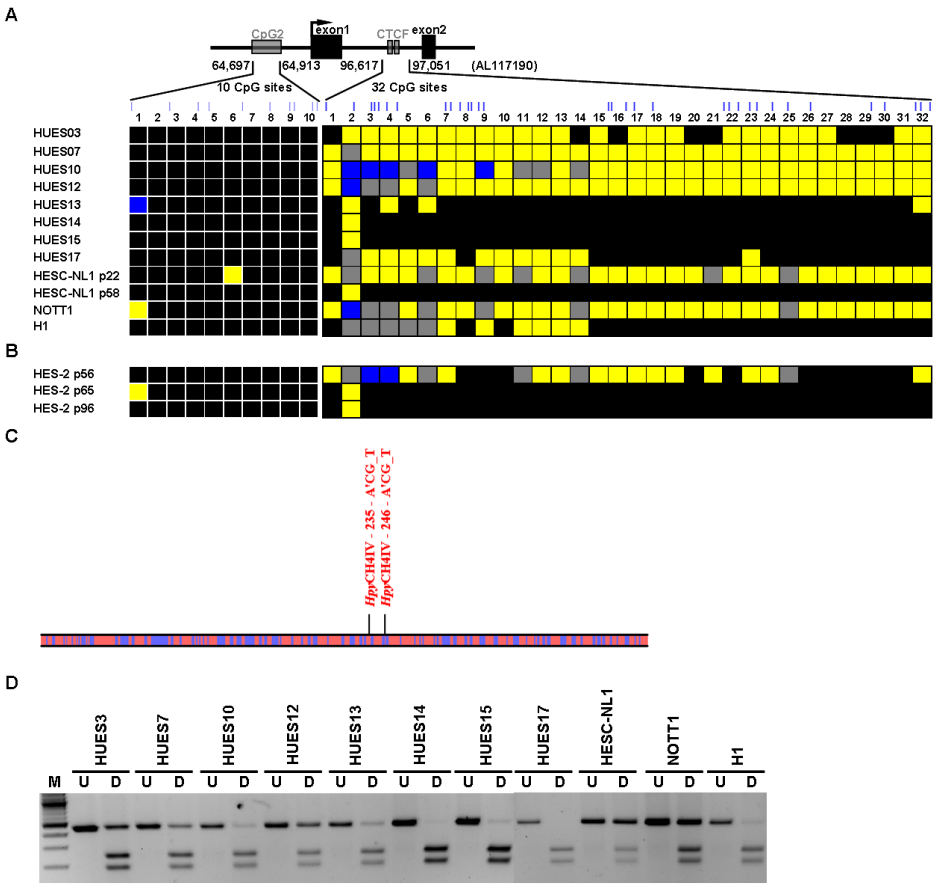

Figure 4-14. DNA methylation at the *GTL2* CpG2 and DMR
(A) DNA methylation at the *GTL2* CpG2 and *GTL2* DMR was analysed in 11 informative cell lines determined in Chapter 3. In the schematic diagram, two block boxes represent exon1 and exon2 respectively, and two gray boxes indicate CpG2 (64,697 to 64,913) and DMR (96,617 to 97,051) respectively. An arrow indicates a transcriptional start site. Numbers indicate the sequence position analysed within a

CpG island. Numbering refers to accession no. AL117190. Blue vertical bars indicate CpG dinucleotides within the region analysed. (B) DNA methylation at the *GTL2* CpG2 and DMR was analysed in HES-2 (passages 56, 65, 96). Yellow rectangles indicate predominant methylation at CpG dinucleotides. Blue rectangles indicate predominant unmethylation at CpG dinucleotides. Grey rectangles indicate hemimethylation at CpG dinucleotides. (C) A schematic diagram shows two *Hpy*CH4IV restriction enzyme sites at the *GTL2* DMR. (D) The COBRA analysis of the *GTL2* DMR. M, 100 bp DNA Ladder; U, *Hpy*CH4IV-undigested; D: *Hpy*CH4IV-digested.

4.2.11 *NDN* DMR

DNA methylation at 26 CpG sites within the *NDN* DMR was analysed by direct bisulphite sequencing (El-Maarri et al., 2001). PCR with bisulphite modified genomic DNA of 7 informative cell lines (see section 3.2.16, HUES4, HUES8, HUES15, HUES17, BG01, H1 and NOTT2), and direct sequencing were performed. The degree of methylation was determined by the relative peak height of C and T. Differential methylation of *NDN* DMR was detected in HUES4, HUES8, HUES17, BG01 and H1. However, the *NDN* DMR was completely unmethylated in both HUES15 and NOTT2 cell lines (Figure 4-15).

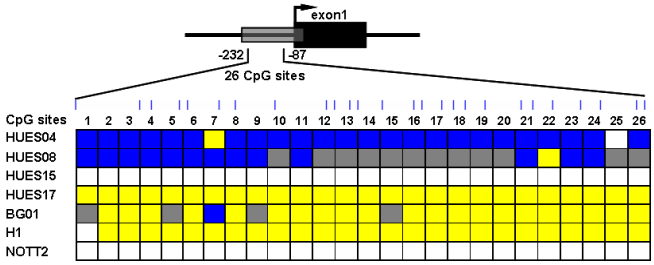

Figure 4-15. DNA methylation at the *NDN* DMR
DNA methylation at the *NDN* DMR was analysed in 7 informative cell lines determined in Chapter 3. In the schematic diagram, a block box represents exon 1 and a gray box indicates a CpG island. An arrow indicates a transcriptional start site. Numbers (-232 to -87) indicate the sequence position analysed within a CpG island. The first and last CpG dinucleotides are numbered relative to a transcription start site. Blue vertical bars indicate CpG dinucleotides within the region analysed. Yellow rectangles indicate predominant methylation at CpG dinucleotides. Blue rectangles indicate predominant unmethylation at CpG dinucleotides. Grey rectangles indicate hemimethylation at CpG dinucleotides. White rectangles indicate unmethylation at CpG dinucleotides.

4.2.12 NESP55 DMR

DNA methylation at 28 CpG sites within the *NESP55* DMR was analysed by direct bisulphite sequencing (Judson et al., 2002). PCR with bisulphite modified genomic DNA of 9 informative cell lines (see section 3.2.22, HUES1, HUES4, HUES5,

HUES9, HUES12, HUES14, HUES15, HESC-NL1 and BG01) and direct sequencing were performed. The degree of methylation was determined by the relative peak height of C and T. Differential methylation at the *NESP55* DMR was detected in all hESC lines, except for HUES5. HUES5 showed complete unmethylation at the *NESP55* DMR. No methylation changes of *NESP55* DMR were detected during *in vitro* culture of HESC-NL1 (passages 22, 58) and HES-2 (passages 56, 65, 96) (Figure 4-16 A and B). These methylation patterns were confirmed by clonal bisulphite sequencing (Figure 4-16 C) and COBRA (Figure 4-16 D and E). Clonal bisulphite sequencing revealed that all cell lines have differential methylation at the *NESP55* DMR, except for HUES5 (Figure 4-16 C). Consistently, the COBRA analysis showed that only one undigested band was detected in HUES5 indicating unmethylation (Figure 4-16 E). However, other cell lines showed that three digested bands and one undigested band together, indicating differential methylation.

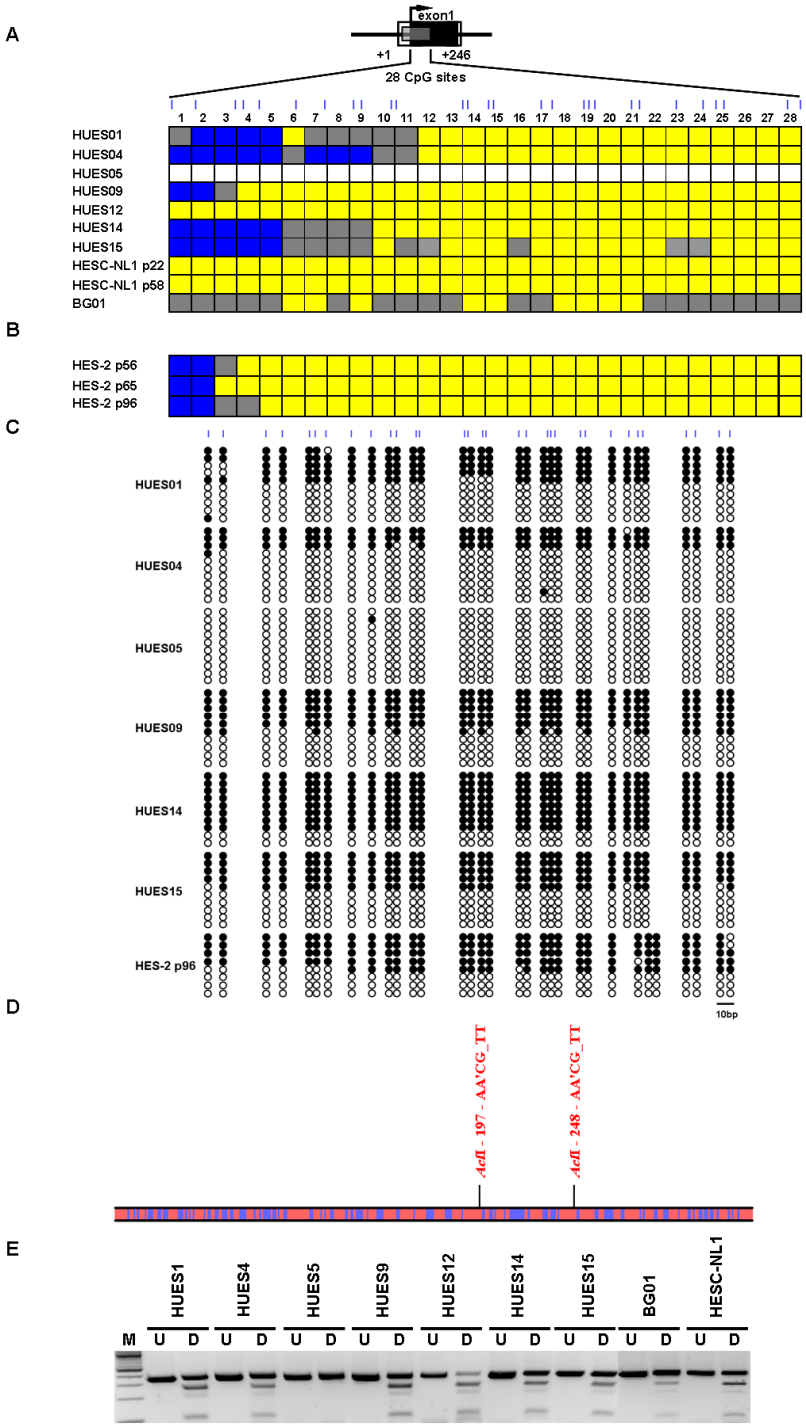

Figure 4-16. DNA methylation at the *NESP55* DMR

(A) DNA methylation at the *NESP55* DMR was analysed in 9 informative cell lines determined in Chapter 3 and (B) HES-2 (passages 56, 65, 96). In the schematic diagram, a block box represents exon 1, a white box represents an untranslated region (URT), and a gray box indicates a CpG island. An arrow indicates a transcriptional start site. Numbers (+1 to +246) indicate the sequence position analysed within a CpG island. The first and last CpG dinucleotides are numbered relative to a transcription start site. Yellow rectangles indicate predominant methylation at CpG dinucleotides. Blue rectangles indicate predominant unmethylation at CpG dinucleotides. Grey rectangles indicate hemimethylation at CpG dinucleotides. White rectangles indicate unmethylation at CpG dinucleotides. (C) Clonal bisulphite sequencing at the *NESP55*

DMR in HUES1, HUES4, HUES5, HUES9, HUES14, HUES15 and HES-2 (p96). Blue vertical bars indicate CpG dinucleotides within the region analysed. A scale bar corresponds to 10 bp. Open and filled circles represent unmethylated and methylated CpG dinucleotides respectively. (D) A schematic diagram shows two *Acl*I enzyme sites at the *NESP55* DMR. (E) The COBRA analysis of the *NESP55* DMR. M, 100 bp DNA Ladder; U, *Acl*I-undigested; D: *Acl*I-digested.

Table 4-1. Summary of DNA methylation status of 12 potential imprinting regulatory regions in hESC lines

Locus	Gene	region	HUES1	HUES2	HUES3	HUES4	HUES5	HUES6	HUES7	HUES8	HUES9	HUES10	HUES12	HUES13	HUES14	HUES15	HUES16	HUES17	BG01	H1	HESC-NL1	HES-2	NOTT1	NOTT2	NTERA2
1p36.33	*TP73*	Promoter	U					U	U	U		U					U				U	U		U	PM
7q21	*PEG10*	DMR					U		D			D	D												
7q32	*PEG1*	DMR	D	D					D			D	D			D	D	D	M		D	D/PU[a]	D	U	U
11p15.5	*SLC22A18*	Promoter					U						U	U	U	U					U	U		U	
	CDKN1C	Promoter				PU									PU	PU									
	KCNQIOTI	KvDMR1	D	D	D	D	D	D	D	D	D	D	D	D	D	D	D	D	D	D	D	D	D	D	
	KCNQ1	Promoter	U	U				U		U	U		U	U									U		
	IGF2	DMR0	D				D	D		D	D						D	D			D	D		D	
14q32	*GTL2*	DMR			D				D			D	D	M	M	M		PM		PM	D/M[b]	D/M[b]	D		
		CpG2			M				M			M	M	M	M	M		M		M	M		M		
15q11	*NDN*	DMR				D				D						U		D	D	D				U	
20q13.2	*NESP55*	DMR	D			D	U				D		D		D	D			D		D	D			

U, unmethylated; M, methylated; D, differentially methylated; PM, predominantly methylated; PU, predominantly unmethylated

[a], *in vitro* culture induced loss of methylation

[b], *in vitro* culture induced gain of methylation

4.3 Discussion

The purpose of this study was to investigate whether overall DNA methylation at 12 potential imprinting regulatory regions was associated with the typical expression status of their relevant imprinted genes in hESC lines as determined in Chapter 3. Of 12 regions examined by bisulphite sequencing and COBRA, 6 regions (*TP73* promoter, *PEG10* DMR, *PEG1* DMR, *SLC22A18* promoter, *KvDMR1* and *NESP55* DMR) showed the association between DNA methylation and allele-specific expression of 8 imprinted genes (*TP73*, *PEG10*, *PEG1 isoform 1*, *SLC22A18*, *KCNQ1*, *KCNQ1OT1*, *CDK1NC* and *NESP55*) in hESC lines (Table 4-3), indicating a regulatory role for DNA methylation at these imprinted loci. However, DNA methylation at *IGF2* DMR, *GTL2* CpG2, *GTL2* DMR and *NDN* DMR was not associated with allele-specific expression of *IGF2*, *GTL2* and *NDN* (Table 4-3). This indicates that DNA methylation does not regulate allele-specific expression of at least some imprinted genes in hESC lines.

Table 4-2. The association between DNA methylation and imprinting in hESC lines

Locus	Gene	Imprinting status	Methylation		Association
			Region	Status	
1p36.33	*TP73*	B	Promoter	U	Associated
7q21	*PEG10*	M	DMR	D	Associated
		B		U	
7q32	*PEG1* isoform1	M	DMR	D	Associated, *PEG1* isoform 2 not associated
		B		U	
	MESTIOT1	M		D	Not associated
		D		D	
11p15.5	*SLC22A18*	B	Promoter	U	Associated, but not associated with KvDMR1
	CDKN1C	PM	Promoter	U	Associated with KvDMR1
	KCNQIOTI	M	KvDMR1	D	
	KCNQ1	M	Promoter	U	
	IGF2	B	H19 DMR *	D	Not associated
			DMR2 *	D	
			DMR0	D	
14q32	*GTL2*	M	DMR	D/M	Not associated
		B		M	
		M	CpG2	D/M	
		B		M	
		M	CpG1	-	-
		B		-	
15q11	*NDN*	M	DMR	D/U	Not associated, but associated with SNRPN-SNURF DMR *
20q13.2	*NESP55*	M	DMR	D	Associated

		B		U	

M, monoallelic expression; PM, predominant monoallelic expression; B, biallelic expression; U, unmethylated; M, methylated; D, differentially methylated; DMR, differentially methylated region; * indicates Data from Alexandra Thurston Ph.D. thesis (2006). The allele-specific expression of each gene was previously described in Chapter3.

4.3.1 DNA methylation associated imprinting in hESCs

4.3.1.1 PEG10, PEG1 and NESP55 DMRs

The differential methylation at the *PEG10* DMR is associated with the monoallelic expression of *PEG10* in HUES7, HUES10 and HUES12 (see section 3.2.3). Moreover, loss of methylation at the *PEG10* DMR was correlated to the biallelic expression of *PEG10* in HUES5. The *PEG1* DMR was differentially methylated in 10 of *PEG1 isoform 1* monoallelic cell lines, whereas it was unmethylated in NOTT2 and NETRA2, exhibiting biallelic expression of *PEG1 isoform1* (see section 3.2.4). Finally, differential methylation at the *NESP55* DMR was associated with monoallelic expression of *NESP55* in HUES1, HUES4, HUES9, HUES12, HUES14, HUES15, BG01 and HESC-NL1 (see section 3.2.22). Only one cell line, HUES5, showed loss of methylation at the *NESP55* DMR that was associated with the biallelic expression of *NESP55*. These evidences indicate that *PEG10*, *PEG1* and *NESP55* imprinting in hESC lines mediated by differential methylation at their DMRs. This association has been reported in other human fetal and adult tissues including brain, kidney, placenta and testis (Bastepe et al., 2005; Kerjean et al., 2000; McMinn et al., 2006; Riesewijk et al., 1997; Suzuki et al., 2007).

MESTIOT1 is previously identified as an antisense transcript of *PEG1* which is transcribed in the opposite direction of *PEG1* (Li et al., 2002; Nakabayashi et al., 2002). Because *MESTIOT1* shares the promoter region of *PEG1 isoform 1*, and both *MESTIOT1* and *PEG1 isoform 1* are expressed on the paternally inherited allele, it has been suggested that paternal allele-specific unmethylation at the *PEG1* DMR can also direct the paternal expression of *MESTIOT1* (Li et al., 2002; Nakabayashi et al., 2002). In this Chapter, however, no obvious relationship between DNA methylation at the *PEG1* DMR and *MESTIOT1* imprinting was detected. For instance, although the *PEG1* DMR was differentially methylated in HUES15, *MESTIOT1* was biallelically expressed (see section 3.2.5). Moreover, NOTT2 showed monoallelic expression of

MESTIOT1, although the *PEG1* DMR was completely unmethylated. Thus, other epigenetic modifications, rather than DNA methylation, may be involved in *MESTIOT1* imprinting. Alternatively, other undiscovered differentially methylated regions could direct *MESTIOT1* imprinting.

4.3.1.2 KvDMR1

KCNQ1, *KCNQ1OT1*, *CDK1NC* and *SLC22A18* have been identified to be clustered in the centromeric region on human chromosome 11p15.5 (mouse distal chromosome 7) (Morison et al., 2005; Reik and Walter, 2001; Robertson, 2005). *KvDMR1* located in intron 10 of *KCNQ1* is differentially methylated on both parental alleles, although *KCNQ1*, *CDK1NC* and *SLC22A18* promoters are predominantly unmethylated in human and mouse tissues (Fitzpatrick et al., 2007; Fitzpatrick et al., 2002; Lewis et al., 2004; Mancini-Dinardo et al., 2006; Monk et al., 2006a; Smilinich et al., 1999). Thus, it has been suggested that allele-specific expression of *KCNQ1*, *KCNQ1OT1*, *CDK1NC* and *SLC22A18* is guided by monoallelic methylation at the *KvDMR1* (Fitzpatrick et al., 2007; Fitzpatrick et al., 2002; Lewis et al., 2004; Mancini-Dinardo et al., 2006; Monk et al., 2006a; Smilinich et al., 1999). In this Chapter, *KCNQ1*, *CDK1NC* and *SLC22A18* promoters were predominantly unmethylated or unmethylated in hESC lines, whereas both methylated and unmethylated alleles at the *KvDMR1* were present across the 16 CpG dinucleotides examined, correlating with the monoallelic or predominant monoallelic expression of *KCNQ1*, *KCNQ1OT1*, and *CDK1NC*, but not the biallelic expression of *SLC22A18*. This indicates that differential methylation at *KvDMR1* can direct *KCNQ1*, *KCNQ1OT1*, and *CDK1NC*, (but not *SLC22A18*) imprinting in hESC lines.

Interestingly, although *KvDMR1* was differentially methylated in hESC lines, *SLC22A18* was biallelically expressed (see section 3.2.13). There are two possibilities to explain this. One possibility is that other epigenetic marks at histones may direct *SLC22A18* imprinting in hESC lines. Recently, Monk et al., (2006) has demonstrated that, in human tissues including placentae, liver, muscle and lymphocyte, active histone marks (H3K4me2 and H3K9Ac) appear at the maternal allele of *SLC22A18*, whereas repressive histone marks (H3K9me2 and H3K27me3) appear at paternal allele, suggesting that differential histone marks lead to maternal expression of

SLC22A18. Another possibility is that unmethylation at the *SLC22A18* promoter directs the biallelic specific expression of *SLC22A18* in hESC lines.

4.3.1.3 *TP73* Promoter

Previously, unmethylation at the *TP73* promoter in normal human tissues including brain, ovary and cervix was reported to be associated with the biallelic expression of *TP73* (Chen et al., 2000b; Dong et al., 2002). In this Chapter, 50 CpG dinucleotides in the *TP73* promoter were completely unmethylated in all hESC lines examined, consistent with the biallelic expression of *TP73* (see section 3.2.1). Importantly, however, no reports are currently available about the monoallelic expression of *TP73* mediated by differential methylation at the *TP73* promoter. Thus, it is still unclear how *TP73* imprinting is regulated in the human.

TP73 is known to be a tumour-suppressor gene which is transcriptionally inactive in human brain and ovarian cancers mediated by hypermethylation at its promoter (Chen et al., 2000b; Dong et al., 2002). In this Chapter, similarly, hypermethylation at the *TP73* promoter was detected in NTERA2, a testicular germ cell tumour. The mRNA level of *TP73* in NTERA2 now needs to be examined to determine association between DNA methylation and gene expression.

4.3.2 DNA methylation not associated imprinting in hESCs

4.3.2.1 *GTL2* CpG2 and DMR

Human fetal tissues (heart, kidney, liver, lung and brain) show differential methylation at the *GTL2* DMR that is associated with monoallelic expression of *GTL2* (Kawakami et al., 2006; Wylie et al., 2000). In this Chapter, however, no obvious relationship between DNA methylation at the *GTL2* DMR and its imprinting was detected. For example, of 32 CpG dinucleotides surrounding the *GTL2* DMR, most CpG dinucleotides were completely methylated in HUES13, HUES14, HUES17 and H1 that was not associated with monoallelic expression of *GTL2* (see section 3.2.15). Furthermore, *GTL2* was biallelically expressed in HUES15, inconsistent with complete methylation at 31 CpG dinucleotides within the *GTL2* DMR. Thus, these evidences indicate that DNA methylation at the *GTL2* DMR may be not able to direct allele-specific expression of *GTL2* in hESC lines. There are two possibilities to

explain *GTL2* imprinting in hESC lines. One possibility is that other regulatory regions can be involved in allele-specific expression of *GTL2*. Previous studies have been identified that there are two additional CpG islands (CpG1 and CpG2) in a cluster on human chromosome 14q32, which are also differentially methylated in peripheral blood lymphocytes (Astuti et al., 2005; Kawakami et al., 2006; Wylie et al., 2000). In this Chapter, however, all 10 CpG dinucleotides examined at the *GTL2* CpG2, all CpG dinucleotides were fully methylated in all informative cell lines, indicating no association between DNA methylation at the *GTL2* CpG2 and its imprinting. DNA methylation at *GTL2* CpG1 now needs to be examined. Another possibility is that other epigenetic marks at histones can be involved in *GTL2* imprinting in hESC lines. A recent study in mice has suggested that maternal specific histone acetylation at the *Gtl2* DMR is necessary for regulating *Gtl2* imprinting (Carr et al., 2007). This has not been reported in human tissues.

4.3.2.2 NDN DMR

A similar discrepancy was observed in the *NDN* DMR, with HUES15 and NOTT2 exhibiting unmethylated CpG dinucleotides that did not correlate with monoallelic expression of *NDN* (see section 3.2.16). This may be explained by two ways. One is that other epigenetic modifications can direct *NDN* imprinting in hESC lines. Previous studies in the mouse and human have suggested that differential histone acetylation and methylation marks on parental alleles are involved in the allele-specific expression of *NDN* (Forsberg et al., 2000; Fulmer-Smentek and Francke, 2001; Lau et al., 2004; Xin et al., 2003). Another explanation is that other imprinting regulatory regions can be involved in regulating *NDN* imprinting in the human. Previously, two ICRs (PWS ICR and AS ICR) have been indentified which can direct the allele-specific expression of their surrounding imprinted genes including *NDN*, *NDNL1*, *MKRN3*, *SNRPN*, *UBE3A* and *ATP10C* in the PWS/AS imprinting cluster on human chromosome 15q11 (MacDonald and Wevrick, 1997; Sutcliffe et al., 1994; Tsai et al., 1999). Alexandra Thurston (University of Nottingham) examined the DNA methylation status at the PWS ICR in hESC lines. The region was differentially methylated in all *NDN* informative cell lines (Alexandra Thurston Ph.D thesis 2006). Thus, this indicates that the PWS ICR can direct allele-specific expression of *NDN* in hESC lines.

4.3.2.3 IGF2 DMR0

Although biallelic expression of *IGF2* was detected in almost all hESC lines (see section 3.2.8), *IGF2* DMR0 and DMR2 were differentially methylated. This indicates no association between DNA methylation at *IGF2* DMRs and its imprinting. Previous studies have suggested that gain of methylation at the maternal allele of the *H19* DMR is associated with biallelic expression of *IGF2* in both human and mouse tissues (Pant et al., 2004; Pant et al., 2003; Thorvaldsen et al., 1998). Of 23 CpG dinucleotides surrounding the *H19* DMR, most CpG dinucleotides were differentially methylated in hESC lines (Alexandra Thurston Ph.D. thesis 2006), indicating no association between DNA methylation at the *H19* DMR and *IGF2* imprinting. A recent study in mice has been suggested that paternal H3K27me3 and macroH2A1 at the *H19* promoter and paternal H3K9 acetylation and H3K4me at *IGF2* DMRs are associated with the allele-specific expression of *Igf2* (Han et al., 2008; Li et al., 2008). Furthermore, human *IGF2* can be imprinted in a promoter-specific manner, independent of epigenetic modifications (Ekstrom et al., 1995; Vu and Hoffman, 1994). Thus, these potential factors can be involved in biallelic expression of *IGF2* in hESC lines.

4.3.3 *In vitro* culture induced DNA methylation changes

Recently, DNA methylation changes (gain or loss of methylation) at non-imprinted loci have been reported in *in vitro* long-term cultured hESC lines (Allegrucci et al., 2007; Bibikova et al., 2006; Calvanese et al., 2008; Maitra et al., 2005). Maitra et al. (2005) has found that gain of methylation at the promoter region of two tumour-suppressor genes (*RASSF1* and *PTPN6*) in BG01, BG02, BG03, hES2, hES3, H7, H9 and SA002 at later passages from 41 to 147, indicating *in vitro* culture induced hypermethylation. Allegrucci et al., (2007) and Bibikova et al., (2006) have demonstrated that DNA methylation changes can accumulate in hESC lines upon *in vitro* prolonged culture, although most changes have been detected from them at earlier passages from 23 to32. In this Chapter, of 8 imprinting regulatory regions examined, two regions (*GTL2* DMR and *PEG1* DMR) showed DNA methylation changes in *in vitro* long-term cultured HES-2 (passages 56, 65 and 96 examined) and HESC-NL1 (passages 22 and 58 examined). *GTL2* DMR and *PEG1* DMR were differentially methylated in HESC-NL1 (p22) and HES-2 (p56). However, the *GTL2*

DMR became hypermethylated in HESC-NL1 (p58) and HES-2 (p65 and p96). Moreover, the *PEG1* DMR became hypomethylated in HES-2 (p65 and p96). Other 6 regions (*TP73* promoter, *SLC22A18* promoter, *KvDMR1*, *IGF2 DMR0*, *GTL2* CpG2 and *NESP55* DMR) showed no DNA methylation changes, indicating DNA methylation can be altered in a locus-specific manner upon *in vitro* culture. The reasons why particular imprinted loci are more or less prone to epigenetic disruptions than others during *in vitro* culture are not yet understood. Similar results have been detected in *in vitro* cultured mouse and monkey ESCs and preimplantation stage embryos (Dean et al., 1998; Doherty et al., 2000; Khosla et al., 2001a; Mann et al., 2004; Mitalipov et al., 2007), demonstrating that *KvDMR1* and *Snrpn* DMR are more likely stable loci and thus appear insensitive to DNA methylation changes upon *in vitro* culture (Kerjean et al., 2003; Kobayashi et al., 2007; Marques et al., 2004; Sato et al., 2007). However, others including *Igf2*, *H19*, *Gtl2* and *Peg1* DMRs appear to be more variable and unstably in DNA methylation changes (Kerjean et al., 2003; Kobayashi et al., 2007; Marques et al., 2004; Sato et al., 2007). Possibly, this may be due to a regionalised stability associated with the establishment of imprints that was previously described in section 3.3.1.

4.3.4 Further works needed

In this chapter, it was not examined whether other epigenetic factors such as histone methylation and acetylation can be associated with allele-specific expression of imprinted genes. This needs to be examined to explain the lack of detected association between the allele-specific expression of some imprinted genes and DNA methylation at their regulatory regions. DNA methylation alternations (especially, loss of methylation) at several imprinted regulatory regions were detected in some hESC lines during *in vitro* culture that may be overcame by overexpression of maintenance *methyltransferase* 1, DNMT1. This possibility needs to be examined.

5 HUMAN EMBRYONIC STEM CELL LINES OVEREXPRESSING DNA Methyltransferase 1 (DNMT1)

5.1 Introduction

DNA methylation changes at tumour suppressor gene promoters, imprinting regulatory regions and certain CpG islands have been reported in *in vitro* cultured human embryonic stem cell (hESC) lines (Allegrucci et al., 2007; Bibikova et al., 2006; Calvanese et al., 2008; Maitra et al., 2005; Rugg-Gunn et al., 2005). Bibikova et al., (2006) used a microarray-based assay of bisulphite treated DNA to compare the DNA methylation status at different passages of 14 independently derived hESC lines. Of 1,536 CpG loci investigated, ~ 30 CpG loci including *RASSF1* (*ras association domain family 1*) *EPO* (*Erythropoietin*) and *PEG10* (*paternally expressed gene 10*) underwent loss of methylation upon *in vitro* prolonged culture (Bibikova et al., 2006). Moreover, Allegrucci et al., (2007) used a restriction landmark genomic scanning (RLGS) technique to compare the DNA methylation status at different passages of 6 hESC lines (NCL1, H7, HES-2, BG01, NOTT1 and HUES-7). Of ~ 2,200 CpG loci examined, ~ 30 CpG loci including *ZC3HAV1L*, *SPRN* and *AFG3L1* became demethylated or hypomethylated during *in vitro* culture (Allegrucci et al., 2007). Thus, current *in vitro* culture conditions for hESCs may lead to loss of methylation at certain CpG islands. The reasons for this are not known but one possibility is that relatively low expression of DNMT1 in hESCs fails to maintain DNA methylation at some CpG islands (Emma Lucas Ph.D. thesis 2008). In this Chapter, DNMT1 overexpression is used to test this hypothesis.

The expression level of DNMT1 (DNA methyltransferase 1) has been reported to be associated with the degree of DNA methylation in mammalian cells (Biniszkiewicz et al., 2002; Chen et al., 2007; Feltus et al., 2003; Hattori et al., 2004). For instance, loss of methylation at repetitive sequences and imprinting regulatory regions has been detected in mESCs, mouse embryonic fibroblast (MEF) cells and human cancer cells, when DNMT1 is not or little expressed (Chen et al., 2007; Hattori et al., 2004; Jackson-Grusby et al., 2001; Lei et al., 1996; Li et al., 1992). On the other hand, gain of methylation at pericentromeric regions, tumour-suppressor gene promoters and imprinting regulatory regions has been detected in mESCs, human fibroblast cells and cancer cells, when DNMT1 is overexpressed (Biniszkiewicz et al., 2002; Etoh et al.,

2004; Feltus et al., 2003; Sawada et al., 2007; Vertino et al., 1996). In hESC lines, Emma Lucas (University of Nottingham) has used immunofluorescence and real-time PCR techniques to assess the relative expression level of DNMT1 associated with global DNA methylation (5-methylcytosine) patterns in a BJ fibroblast cell line (derived from human foreskin), 2 hESC lines (HUES7 and NOTT1) and a mESC line. The expression of DNMT1 is readily detected in the human BJ fibroblast cell line and mESC line, but not hESC lines (Emma Lucas Ph.D. thesis 2008). Furthermore, 5-methylcytosine staining shows that hESC lines are 20% less methylated than the human BJ fibroblast cell line (Emma Lucas Ph.D. thesis 2008). Thus, relatively undermethylation in hESCs could be due to the low expression of DNMT1, although *de novo* methyltransferases, DNMT3A and DNMT3B, are highly expressed in hESC lines. Additionally, this may be one of reasons why some CpG sties in hESCs become demethylated during *in vitro* culture.

Thus, this chapter aimed to determine 1) whether the overexpression of exogenous *DNMT1* in hESCs can prevent region-specific loss of methylation upon *in vitro* prolonged culture and 2) whether an increase in the expression level of DNMT1 in hESCs can be associated with gain of methylation at imprinting regulatory regions, repetitive sequences, tumour-suppressor gene promoters and certain CpG islands.

5.1.1 DNMT1

DNMT1 is known as a maintenance methyltransferase that is responsible for the stable inheritance of DNA methylation patterns from the parental strand to the daughter stand, when DNA is replicated during S phase (Bestor et al., 1988; Leonhardt et al., 1992; Li et al., 1992). DNMT1 is ubiquitously expressed in proliferating cells and localised in replication foci via proliferating cell nuclear antigen (PCNA) and ubiquitin-like, containing PHD and RING finger domains 1 (UHRF1; also known as NP95 and ICBP90) (Bostick et al., 2007; Chuang et al., 1997; Leonhardt et al., 1992; Sharif et al., 2007). So far, three DNMT1 isoforms derived from three different sex-specific promoters have been indentified in the mouse and human; a somatic form (DNMT1s), a pachytene spermatocyte-specific form (DNMT1p) and an oocyte-specific form (DNMT1o) (Hayward et al., 2003; Mertineit et al., 1998). Their distinct behaviours and roles have been previously described in section 1.2.3.1.1.

Mouse *Dnmt1* spans 56 kb of genomic DNA, is organised into 39 exons and encodes a protein of 1,620 amino acids with a molecular mass of 190 kDa (Bestor et al., 1988). Human *DNMT1* is similarly organised, except for the presence of an additional intron (Bestor, 2000; Cheng and Blumenthal, 2008). The DNMT1 protein is composed of two domains, a regulatory N-terminal domain (~ 1,100 amino acids) and a catalytic C-terminal domain (~ 550 amino acids) (see Figure 1-3). The N-terminal domain of DNMT1 contains several domains including a proliferating cell nuclear antigen (PCNA) binding domain (PBD), a nuclear localisation signal (NLS), a DNA replication foci targeting sequence (RFT or TS), a cysteine-rich Zn^{2+} binding motif (ATRX), and a polybromo homology domain (PBHD) (Bestor, 2000; Cheng and Blumenthal, 2008). The functions of these domains have been characterised by various truncation mutation studies (Chuang et al., 1997; Kim et al., 2002; Leonhardt et al., 1992; Margot et al., 2003; Schermelleh et al., 2007). For example, RFT and NLS domains are responsible for targeting to sites of newly synthesised hemi-methylated DNA in nuclei at S phase (Chuang et al., 1997; Leonhardt et al., 1992; Rountree et al., 2000). Moreover, an ATRX domain is responsible for binding to DNA sequences containing CpG dinucleotides (Cheng and Blumenthal, 2008). The C-terminal domain of DNMT1 contains six conserved motifs (I, IV, VI, VIII, IX and X). These motifs are responsible for transferring methyl groups (CH_3) from S-adenosyl-L-methionine (AdoMet) to cytosines in CpG dinucleotides (Bestor et al., 1988; Lauster et al., 1989; Posfai et al., 1989). The distinct roles of each motif have been previously described in section 1.2.3.4.1.

5.1.2 The loss- and gain-of-function of *DNMT1* in mammalian cells

The studies of loss- and gain-of-function of *DNMT1* in mammalian cells have suggested that appropriate *DNMT1* expression is essential for normal embryonic development and tissue-specific differentiation (Biniszkiewicz et al., 2002; Jackson et al., 2004; Lei et al., 1996; Li et al., 1992; Li et al., 2007). For example, the inactivation of endogenous *DNMT1* in mouse and human cells leads to the extensive perturbation of embryonic development, cellular growth, telomere length and lineage-specific differentiation that may be due to genome-wide demethylation at repetitive sequences, imprinting regulatory regions and sub-telomeric domains (Chen et al., 2007; Gonzalo et al., 2006; Hattori et al., 2004; Jackson-Grusby et al., 2001; Jackson et al., 2004; Lei et al., 1996; Li et al., 1993; Li et al., 1992). Furthermore, the

overexpression of exogenous *DNMT1* leads to the embryonic lethality in mice and growth retardation in human fibroblast cells that may be due to genome-wide hypermethylation at repetitive sequences, imprinting regulatory regions and tumour-suppressor gene promoters (Biniszkiewicz et al., 2002; Feltus et al., 2003; Vertino et al., 1996).

5.1.2.1 Loss-of-function of *DNMT1*

5.1.2.1.1 Mouse embryonic stem cells

The first *Dnmt1*$^{n/n}$ J1 ES cell line has been generated by homologous recombination of the N-terminal domain (the *Nae*I site 20bp upstream of the transcriptional start site) (Li et al., 1992). In addition, Lei et al., (1996) has established the *Dnmt1*$^{c/c}$ J1 ES cell line by homologous recombination of the C-terminal domain (the PC motif 4 and ENV motif 6). Although both *Dnmt1*$^{n/n}$ and *Dnmt1*$^{c/c}$ J1 ES cell lines exhibit normal ES cell morphology, growth rate and prolonged survival in culture, reduced maintenance DNMT activity, DNMT1 protein level and 5-methylcytosine content are detected (Jackson-Grusby et al., 2001; Jackson et al., 2004; Lei et al., 1996; Li et al., 1992). Moreover, genome-wide and gene-specific demethylation have been detected in both *Dnmt1*$^{n/n}$ and *Dnmt1*$^{c/c}$ J1 ES cell lines (Hattori et al., 2004; Jackson-Grusby et al., 2001; Jackson et al., 2004; Lei et al., 1996; Li et al., 1992). Specifically, the multiple endogenous retrovirus (Mo-MuLV), pericentromeric minor satellite repeat (pMR150), long interspersed nuclear element-1 (LINE1) and intracisternal A particle (IAP) are demethylated in both cell lines (Jackson-Grusby et al., 2001; Jackson et al., 2004; Lei et al., 1996; Li et al., 1992). Furthermore, of 1300 CpG loci examined by RLGS, an additional 236 spots were detected in the *Dnmt1*$^{c/c}$ J1 ES cell line, indicating demethylation (Hattori et al., 2004). Finally, loss of methylation at the *H19* DMR and *Igf2r* (*insulin-like growth factor 2 receptor*) DMR2 is detected in the *Dnmt1*$^{n/n}$ J1 ES cell line (Li et al., 1993). This is associated with the biallelic expression of *H19* and transcriptional silencing of *Igf2* (*insulin-like growth factor 2*) and *Igf2r* (Li et al., 1993).

Importantly, *Dnmt1*$^{c/c}$ J1 ES cells show a reduced ability to differentiate into embryoid bodies (EBs) and specific lineages including hematopoietic (erythroid and myeloid colonies) and cardiac lineages, compared to heterozygous- and wide-type ES cells

(Jackson et al., 2004). Furthermore, *Oct3/4* and *Nanog* transcripts (pluripotent markers) are still detected in differentiated *Dnmt1*$^{c/c}$ J1 ES cells and remain unmethylated at their promoters (Jackson et al., 2004; Li et al., 2007). Immunocytochemistry analysis has revealed that trophoblast-specific (Pl-1 and Tpbp), mesodermal (Brachyury, β h1-globin and α- globin) and endodermal (Hnf4a and albumin) markers are abnormally expressed in differentiated *Dnmt1*$^{c/c}$ J1 ES cells (Jackson et al., 2004). Finally, the injection of *Dnmt1*$^{n/n}$ and *Dnmt1*$^{c/c}$ J1 ES cells into diploid and tetraploid blastocyst stage mouse embryos resulted in embryonic lethality during postimplantation development (Lei et al., 1996; Li et al., 1992). Thus, *Dnmt1* is essential for maintaining DNA methylation in the mammalian genome that requires normal embryonic development and lineage-specific differentiation.

5.1.2.1.2 Mouse embryonic fibroblasts

The *Dnmt1*$^{1lox/1lox}$ MEF cell line has been generated by Cre/lox mediated deletion of the N-terminal domain (exon 3 to exon 6) (Jackson-Grusby et al., 2001). This cell line exhibits no endogenous *Dnmt1* expression, as confirmed by Western blot. Extensive demethylation at the IAP, centromeric satellite and moloney murine leukemia virus loci has been demonstrated by Southern blot (Jackson-Grusby et al., 2001). Importantly, TUNEL assay has revealed that ~ 20% of *Dnmt1*$^{1lox/1lox}$ MEF cells undergo apoptosis (Jackson-Grusby et al., 2001). Moreover, oligonucleotide microarray analysis has revealed that ~ 10% of genes are abnormally expressed in *Dnmt1*$^{1lox/1lox}$ MEF cells, including DNA repair genes (*Tdg*, *Rad52*, *Mre11a* and *Pold1*), indicating that *Dnmt1* is also involved in regulating genomic stability (Jackson-Grusby et al., 2001; Mortusewicz et al., 2005).

5.1.2.1.3 Human colon cancer cells

Two *DNMT1*$^{2loxP/KO}$ cell lines (designated as 201 and 202) have been generated by Cre/lox mediated deletion of the catalytic domain (PC and ENV motifs) in the human colon cancer cell line, HCT116 (Chen et al., 2007). In addition, one *DNMT1*$^{-/-}$ cell line has been established by homologous recombination of the regulatory domain (exon 3 to exon 5) in HCT116 (Rhee et al., 2002; Rhee et al., 2000). 201 and 202 cells show morphology changes (more enlarged and flattened) during *in vitro* culture, compared to heterozygous- and wide-type HCT116 cells (Chen et al., 2007). However, the

DNMT1$^{-/-}$ cell line shows no morphology changes (Rhee et al., 2002; Rhee et al., 2000). This discrepancy may be due to functional differences in the different domains deleted. Moreover, 201 and 202 cells undergo various mitotic defects including broken chromosomes and anaphase bridges and they die either at the metaphase or at the metaphase-to-anaphase transition (Chen et al., 2007). This have not been reported in *DNMT1*$^{-/-}$ cells

Interestingly, although significantly reduced maintenance DNMT activity (~ 90% reduced) and DNMT1 protein level (rarely or not detected) are observed in 201, 202 and *DNMT1*$^{-/-}$ cells, only ~ 20% of the 5-methylcytosine content is reduced (Chen et al., 2007; Rhee et al., 2002; Rhee et al., 2000). Furthermore, in these cells, the analysis of specific genomic regions by Southern blot has revealed that genome-wide demethylation occurs at only classical Satellite 2 and 3 sequences, but not α-Satellite and Alu repeats (Chen et al., 2007; Rhee et al., 2002; Rhee et al., 2000). In addition, no methylation changes are detected in the number of CpG islands including *MLH1*, *CDKN2A*, *p16*^{INK4A} and *TIMP-3* promoters (Chen et al., 2007; Rhee et al., 2002; Rhee et al., 2000). There are three ways to explain lack of extensive perturbation of DNA methylation. Firstly, Egger et al., (2006) has demonstrated that a truncated DNMT1 protein is present in cells. This truncated DNMT1 protein retains the catalytic domain so that is able to methylate hemimethylated CpG dinucleotides (Egger et al., 2006). Secondly, Chen et al., (2007) has suggested that trace amounts of DNMT1 are still present in cells that functionally work to maintain DNA methylation. Finally, Rhee et al., (2002) has suggested that DNMT3A and DNMT3B compensate loss of DNMT1 to maintain DNA methylation patterns in *DNMT1*$^{-/-}$ cells. Indeed, *DNMT1* and *DNMT3B* DKO (double knockout) in HCT116 shows significantly loss of genomic DNA methylation (~ 95%) at α-Satellite and Alu repeats (Rhee et al., 2002). Moreover, the promoter regions of *p16*^{INK4a} (*a prototypic INK4 protein*), *TIMP-3* (*tissue inhibitor of metalloproteinase 3*) and *IGF2* are completely demethylated in DKO cells (Rhee et al., 2002).

5.1.2.2 Gain-of-function of *DNMT1*

5.1.2.2.1 Human lung fibroblasts

8 human fetal lung fibroblast (IMR90/SV40) cell lines overexpressing *DNMT1* (HMT.S41, HMT.S36, HMT.L36, HMT.S33, HMT.L41, HMT.17, HMT.19 and HMT.1E1) have been established by chemical transfection of the pCMVneoBam vector containing a full-length *DNMT1* cDNA (Vertino et al., 1996). These cell lines have both endogenous and exogenous DNMT1, as confirmed by Western blot on a 6.5% sodium dodecyl sulphate-polyacrylamide gel electrophoresis (SDS-PAGE) gel. Interestingly, the expression levels of exogenous DNMT1 between cell lines are variable, although endogenous DNMT1 was equally expressed (Vertino et al., 1996). Exogenous DNMT1 was relatively highly expressed in HMT.17, HMT.19 and HMT.1E1 than other cell lines (HMT.S41, HMT.S36, HMT.L36, HMT.S33 and HMT.L41). This may to due to variations either 1) the number of exogenous *DNMT1* copies integrates in the genome of each cell line or 2) where they integrate into the genome.

By digesting DNA with methylation sensitive restriction enzymes (e.g. *Not*I, *Sac*II and *Eag*I), followed by Southern blot, hypermethylation at tumour suppressor gene promoters and certain CpG islands has been detected in HMT.17, HMT.19 and HMT.1E1 (Feltus et al., 2003; Vertino et al., 1996). Of 12 tumour suppressor gene promoters examined, 5 genes (*Estrogen receptor*, *Alpha Globin*, *E-cadherin*, *Somatostatin* and *HIC-1*) show gain of methylation at their promoters (Vertino et al., 1996). Moreover, Feltus et al., (2003) has examined the global DNA methylation status in HMT.17, HMT.19 and HMT.1E1 cell lines by RLGS. Of 1749 CpG loci examined, 373 spots (~ 21%) disappeared, indicating gain of methylation (Feltus et al., 2003). Thus, the overexpression of *DNMT1* is associated with genome-wide and gene-specific hypermethylation (or *de novo* methylation) in human fibroblast cells.

5.1.2.2.2 Mouse embryonic stem cells

A Mouse J1 ES cell line overexpressing *Dnmt1* (*Dnmt1*$^{+/+;BAC}$) has been generated by chemical transfection of a 150 kb bacterial artificial chromosome (BAC) containing the *Dnmt1* gene (Biniszkiewicz et al., 2002). Increased Dnmt1 protein level, 5-methylcytosine content and maintenance Dnmt activity are detected in the *Dnmt1*$^{+/+;BAC}$ cells by Western blot, reverse-phase HPLC (high-performance liquid chromatography) and Dnmt activity assays (Biniszkiewicz et al., 2002). Furthermore, hypermethylation at repetitive sequences (including minor centromeric repeats and

retroviral IAP elements) is detected in the *Dnmt1*$^{+/+;BAC}$ cells by Southern blot (Biniszkiewicz et al., 2002). Hypermethylation at IAP in the *Dnmt1*$^{+/+;BAC}$ cells is correlated with transcriptional silencing of IAP. Of 6 imprinted genes (*Igf2r*, *Peg3*, *Grf1*, *Snrpn*, *Igf2* and *H19*) and 3 non-imprinted genes (*p21*, *p16* and *telomerase*) examined in *Dnmt1*$^{+/+;BAC}$ cells, hypermethylation is detected at the *H19* DMR that is associated with biallelic expression of *Igf2* and transcriptional repression of *H19* (Biniszkiewicz et al., 2002). Furthermore, the injection of *Dnmt1*$^{+/+;BAC}$ cells into diploid and tetraploid blastocyst stage embryos results in embryonic lethality at 14.5 dpc. Thus, overexpression of *Dnmt1* is associated with hypermethylation at imprinting regulatory regions and repetitive sequences that interferes with normal embryonic development.

5.2 Results

5.2.1 Construction of plasmids

5.2.1.1 pCAG-hDNMT1-IRES-PAC

The pDsRed2-C1-hDNMT1 plasmid was produced during a previous project in the laboratory of Prof. Yong-Mahn Han (KAIST). This plasmid contains a 5.2kb full-length human DNMT1 cDNA, *Discosoma sp*. Human codon-optimised Red Fluorecent protein (DsRed2) coding sequences, a human cytomegalovirus (CMV) immediate early promoter and kanamycin/neomycin resistant genes. To obtain 5.2 kb *DNMT1* cDNA, pDsRed2-C1-hDNMT1 was digested by *Eco*RI (Figure 5-1). Two bands, 5,262bp (*DNMT1* cDNA) and 4,686bp (pDsRed2-C1) were expected to be digested by *Eco*RI (Figure 5-1 A). However, it was difficult to discriminate between two bands, because they are closely located on the 8% gel (Figure 5-1 B). Thus, another enzyme, *Rsr*II, was selected to digest the middle part of the pDsRed2 C1 (Figure 5-1 C). Then, three bands (5,262bp, 2,768bp and 1,918bp) were identified on the 8% gel, following *Rsr*II and *EcoR*I double digestion of pDsRed2 C1-hDNMT1 (Figure 5-1 D). A 5.2kb band was cut from the gel, and *DNMT1* cDNA was purified.

The p336 (pCAG-eGFP-IRES-PAC) plasmid was provided by Prof. Chris Denning (University of Nottingham). Several transgenic approaches with this plasmid have been reported in hESCs and mESCs (Anderson et al., 2007; Liew et al., 2007; Ren et al., 2006; Vallier et al., 2004b; Ying et al., 2003b; Zaragosi et al., 2007). This plasmid contains a enhanced green fluorescent protein (eGFP), a chicken β-actin/cytomegalovirus (CMV) hybrid promoter (pCAG), an internal ribosome entry site (IRES) and a puromycin resistant gene (Denning et al., 2006; Ying et al., 2003b). The p336 plasmid was digested by *Eco*RI (Figure 5-1 E and F). Three bands (6,383bp, 795bp and 117bp) were identified by gel electrophoresis (Figure 5-1 F). A 6,383bp band was cut from the gel. The linearised p336 plasmid was purified from the gel. Shrimp Alkaline Phosphatase (SAP) was used to treat into the *Eco*RI digested p336 plasmid to prevent self-ligation by removing 5' phosphates groups of both *EcoR*I sites.

Ligation between 5.2 kb of *DNMT1* cDNA (*EcoR*I digested) and 6.3kb of p336 (*EcoR*I digested and SAP treated) and transformation were performed. Individual 20

colonies were inoculated and cultured. From 20 colonies, 20 plasmids were extracted by Miniprep. Four restriction enzymes (*EcoR*I, *Pci*I, *Xcm*I and *Sac*I) were selected to confirm the correct insertion of *DNMT1* cDNA into p336 (Figure 5-2). 17 colonies (*EcoR*I), 9 colonies (*Sac*I), 9 colonies (*Pci*I) and 14 colonies (*Xcm*I) were identified to be correctly inserted. Of those, two colonies (10-1 and 11-5) were selected and Midiprep was performed. Finally, two plasmids derived from 10-1 and 11-5 colonies were named as pCAG-hDNMT1-IRES-PAC #10-1 and pCAG-hDNMT1-IRES-PAC #11-5 for use within this Chapter.

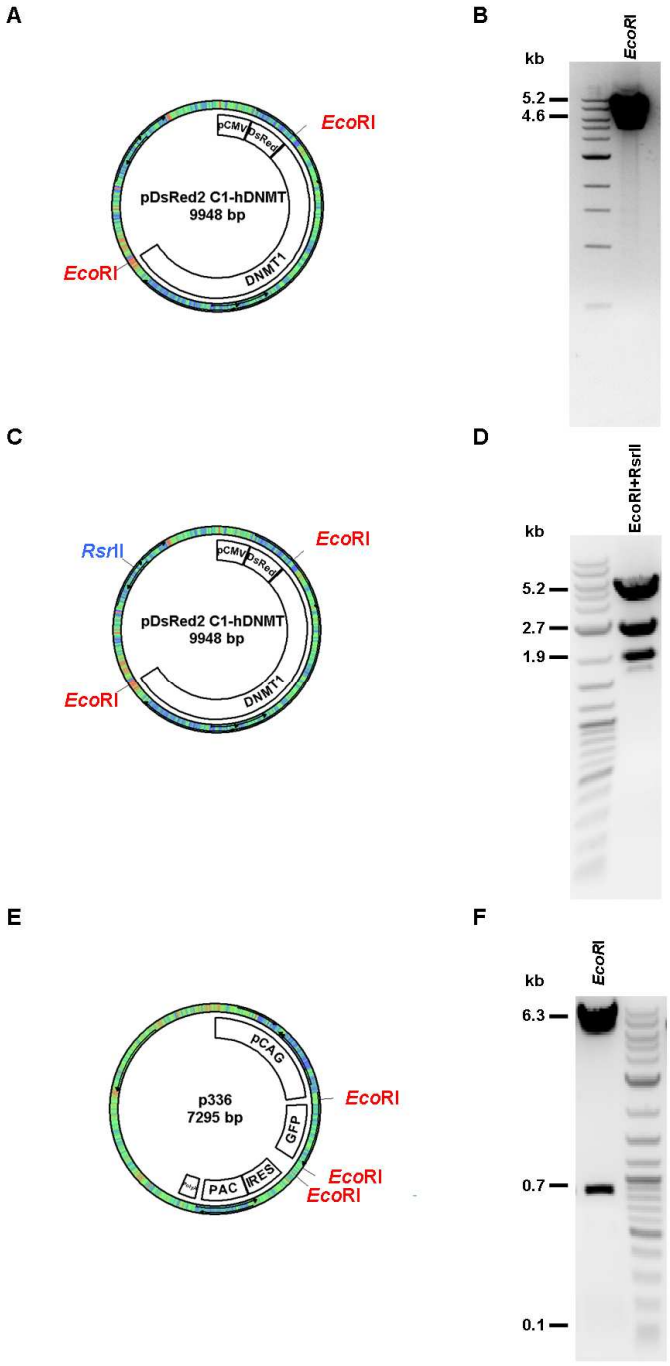

Figure 5-1. The construction of the pCAG-hDNMT1-IRES-PAC plasmid (part 1)

(A) The schematic diagram of pDsRed2-C1-DNMT1. Two *Eco*RI sites are shown in red. (B) Gel electrophoresis of pDsRed2-C1-DNMT1 after the *Eco*RI digestion. (C) The schematic diagram of pDsRed2-C1-DNMT1. Two *Eco*RI sites are shown in red and a *Rsr*II site is shown in blue. (D) Gel electrophoresis of pDsRed2-C1-DNMT1 after the *Eco*RI and *Rsr*II double digestion. (E) The schematic diagram of p336. Three *Eco*RI sites are shown in green (F) Gel electrophoresis of p336 after the *Eco*RI digestion. 0.8% agarose gels were used for gel electrophoresis. The 2-Log DNA ladder (NEB) was used as a molecular maker. Restriction enzymes used for the digestion shown on the top of gel images. The molecular size of digested bands is shown on the left of gel images. The schematic diagrams were generated by pDRAW32 (A, C and E).

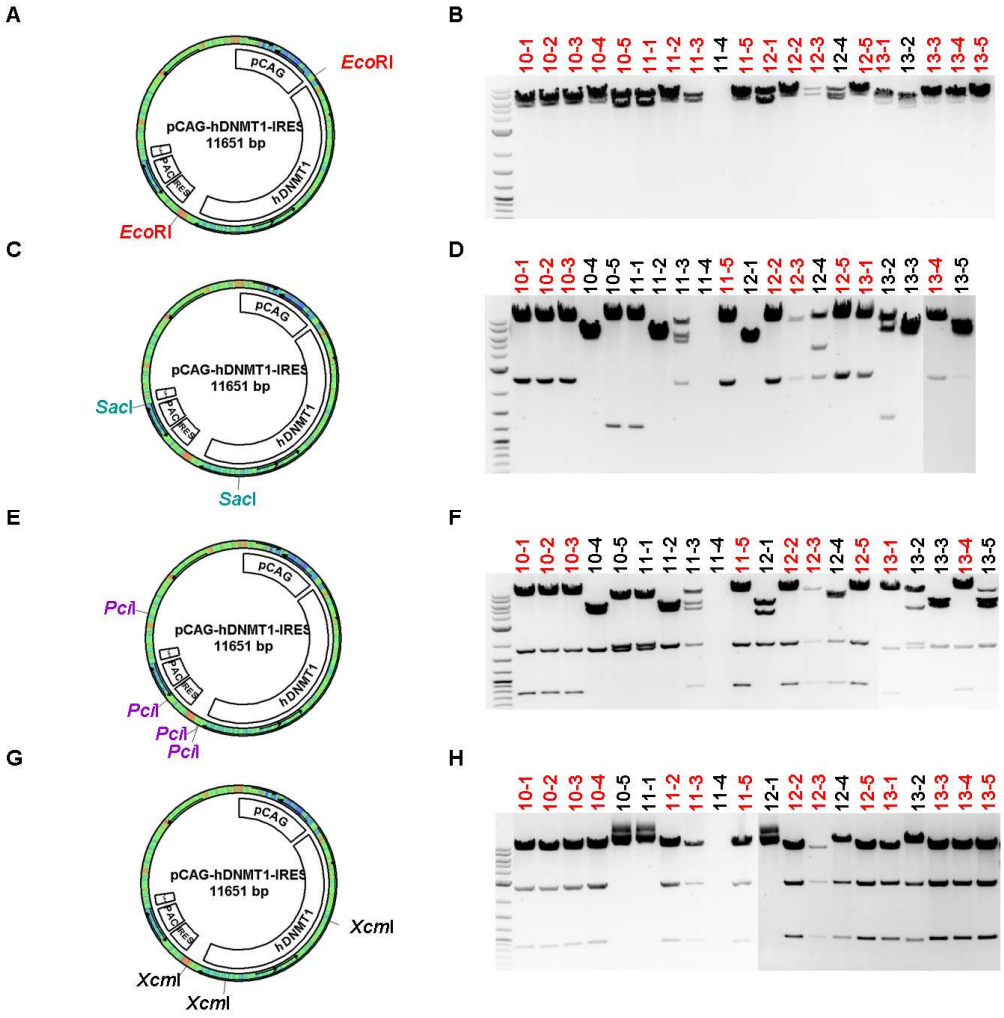

Figure 5-2. The construction of the pCAG-hDNMT1-IRES-PAC plasmid (part 2)

(A) The schematic diagram of two *Eco*RI sites in pCAG-DNMT1-IRES-PAC. (B) Gel electrophoresis of pCAG-DNMT1-IRES-PAC after the *Eco*RI digestion. (C) The schematic diagram of two *Sac*I sites in pCAG-DNMT1-IRES-PAC. (D) Gel electrophoresis of pCAG-DNMT1-IRES-PAC after the *Sac*I digestion. (E) The schematic diagram of four *Pci*I sites in pCAG-DNMT1-IRES-PAC. (F) Gel electrophoresis of pCAG-DNMT1-IRES-PAC after the *Pci*I digestion. (G) The schematic diagram of three *Xcm*I sites in pCAG-DNMT1-IRES-PAC. (H) Gel electrophoresis of pCAG-DNMT1-IRES-PAC after the *Xcm*I digestion. 0.8% agarose gels were used for gel electrophoresis. The 2-Log DNA ladder (NEB) was used as a molecular maker. Colonies were numbered as shown on the top of gel images. Red coloured numbers indicate the correct insertion of DNMT1 cDNA into p336. The schematic diagrams were generated by pDRAW32 (A, C, E and G).

5.2.1.2 pCAG-DsRed2-C1-hDNMT1-IRES-PAC

The pDsRed2-C1-hDNMT1 plasmid was digested with *Sal*I (Figure 5-3 A and B) and Klenow was filled in the *Sal*I site to make a blunt end. This blunt end will ligate into the *Pme*I site of p388. Subsequently, *Age*I digestion was performed in *Sal*I

digested/Klenow-filled pDsRed2-C1-hDNMT1 to obtain DsRed2-*DNMT1* cDNA. Following gel electrophoresis, two bands, 5,983bp and 3,965bp were identified (Figure 5-3 B). A 5,983bp band was cut from the gel and DsRed2-*DNMT1* cDNA was purified.

The p388 (p336+linker) plasmid was also provided by Prof. Chris Denning (University of Nottingham). p388 was double digested with *Pme*I and *Age*I (Figure 5-3 C and D). Two bands, 6469 bp and 21bp, were identified by gel electrophoresis (Figure 5-3 D). A 6469bp band was cut from the gel. The linearised p388 plasmid was purified from the gel.

Ligation between 5.9 kb DsRed2-*DNMT1* (*Sal*I digested-Klenow filled-*Age*I digested) and 6.4 kb p388 (*Pme*I and *Age*I digested) and transformation were performed. From 12 colonies were inoculated and cultured, 12 plasmids were extracted by Mini prep. Three restriction enzymes (*Bam*HI, *Sac*I and *Eco*RI) were selected and use to digest the 12 plasmids to confirm the correct insertion of DsRed2-*DNMT1* cDNA into p388 (Figure 5-4). 9 colonies were identified to be correctly inserted. Of those, two colonies (#7 and #12) were selected and cultured, and Midiprep was performed. Finally, two plasmids were derived from (#7 and #12) and named as pCAG-DsRed2 C1-hDNMT1-IRES-PAC #7 and pCAG-DsRed2 C1-hDNMT1-IRES-PAC #12 for use within this Chapter.

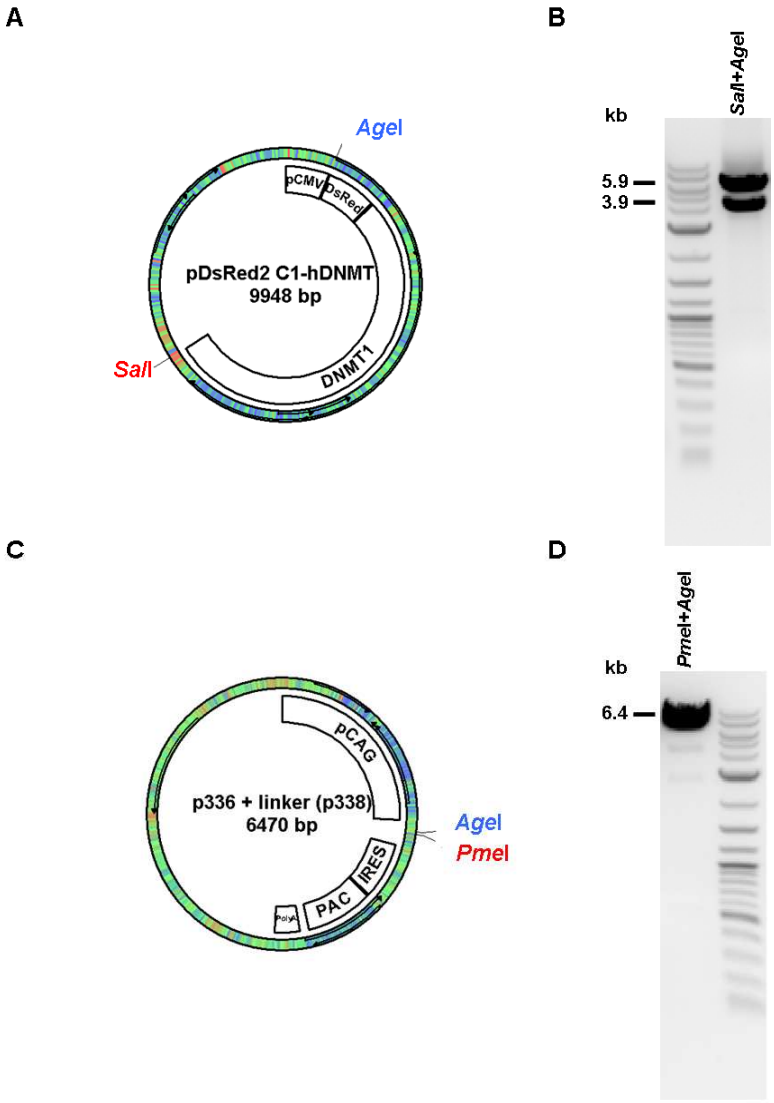

Figure 5-3. The construction of the pCAG-DsRed2-C1-hDNMT1-IRES-PAC plasmid (part 1)

(A) The schematic diagram of pDsRed2-C1-DNMT1. *Age*I and *Sal*I sites are shown. (B) Gel electrophoresis of pDsRed2-C1-DNMT1 after the *Age*I and *Sal*I digestion. (C) The schematic diagram of p388. *Age*I and *Pme*I sites are shown. (D) Gel electrophoresis of p388after the *Age*I and *Pme*I double digestion. 0.8% agarose gels were used for gel electrophoresis. The 2-Log DNA ladder was used as a molecular maker. Restriction enzymes used for the digestion shown on the top of gel images. The molecular size of digested bands is shown on the left of gel images. The schematic diagrams were generated by pDRAW32 (A and C).

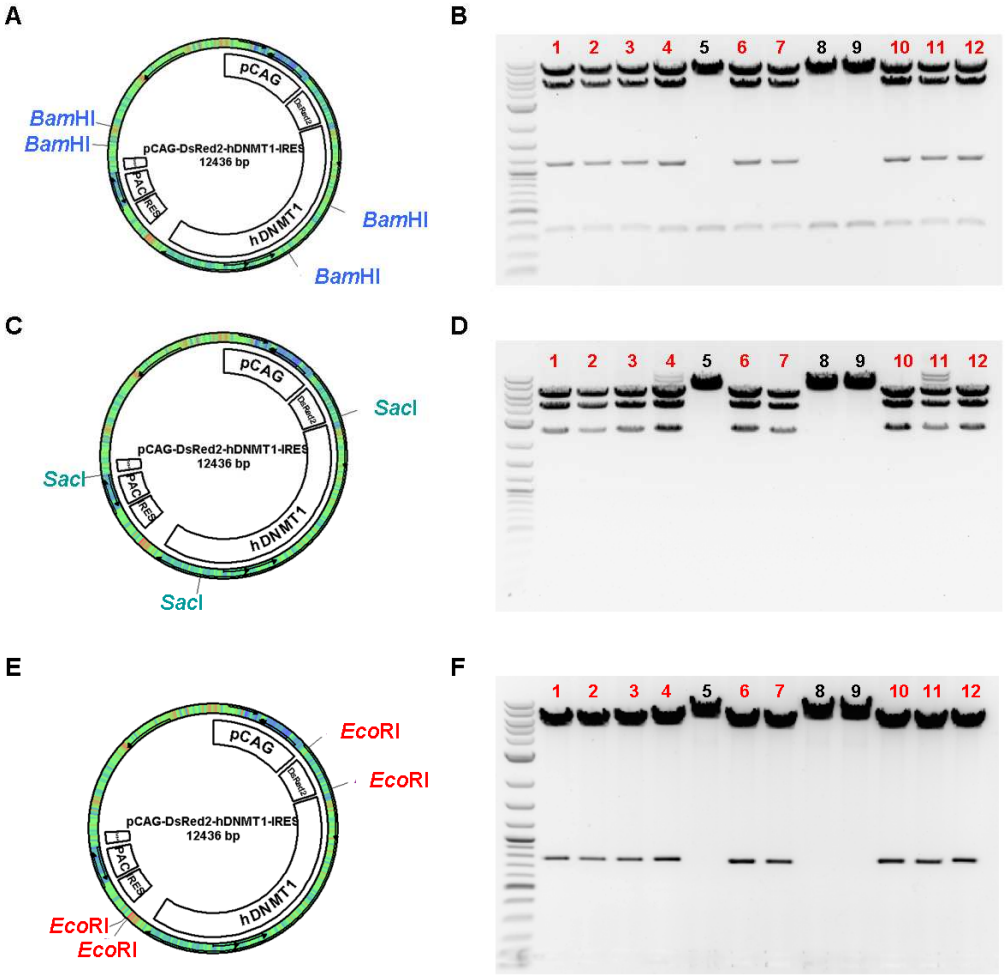

Figure 5-4. The construction of the pCAG-DsRed2-C1-hDNMT1-IRES-PAC plasmid (part 2)

(A) The schematic diagram of four *Bam*HI sites in pCAG-DsRed2-DNMT1-IRES-PAC. (B) Gel electrophoresis of pCAG-DsRed2-DNMT1-IRES-PAC after the *Bam*HI digestion. (C) The schematic diagram of three *Sac*I sites in pCAG-DsRed2-DNMT1-IRES-PAC. (D) Gel electrophoresis of pCAG-DsRed2-DNMT1-IRES-PAC after the *Sac*I digestion. (E) The schematic diagram of four *Eco*RI sites in pCAG-DsRed2-DNMT1-IRES-PAC. (F) Gel electrophoresis of pCAG-DsRed2-DNMT1-IRES-PAC after the *Eco*RI digestion. 0.8% agarose gels were used for gel electrophoresis. The 2-Log DNA ladder (NEB) was used as a molecular maker. Colonies were numbered as shown on the top of gel images. Red coloured numbers indicate the correct insertion of DsRed-*DNMT1* cDNA into p388. The schematic diagrams were generated by pDRAW32 (A, C and E).

5.2.2 Transient transfection

To examine whether reconstructed plasmids functionally worked into human embryonic stem cells (hESCs), circular p336, p388, pCAG-DsRed2-C1-hDNMT1-IRES-PAC #7 and pCAG-hDNMT1-IRES-PAC #10-1 plasmids were transiently transfected in HUES7 (passage 22) using GeneJammer (Stratagene). After 48 hours, the expression of exogenous eGFP and DsRed2 was determined by fluorescence

microscope (Figure 5-5). In cells transfected by p336, green signals were detected in both the cytoplasm and nucleus (see an enlarged image). Furthermore, in cells transfected by pCAG-DsRed2-C1-hDNMT1-IRES-PAC #7, red signals were detected in the nucleus only (see an enlarged image), because the N-terminal domain of DNMT1 contained a nuclear localisation signal (NLS) domain (Bestor, 2000; Cheng and Blumenthal, 2008). Cells transfected by other plasmids showed no green and red signals, indicating that these plasmids did not contain fluorescence genes (Figure 5-5).

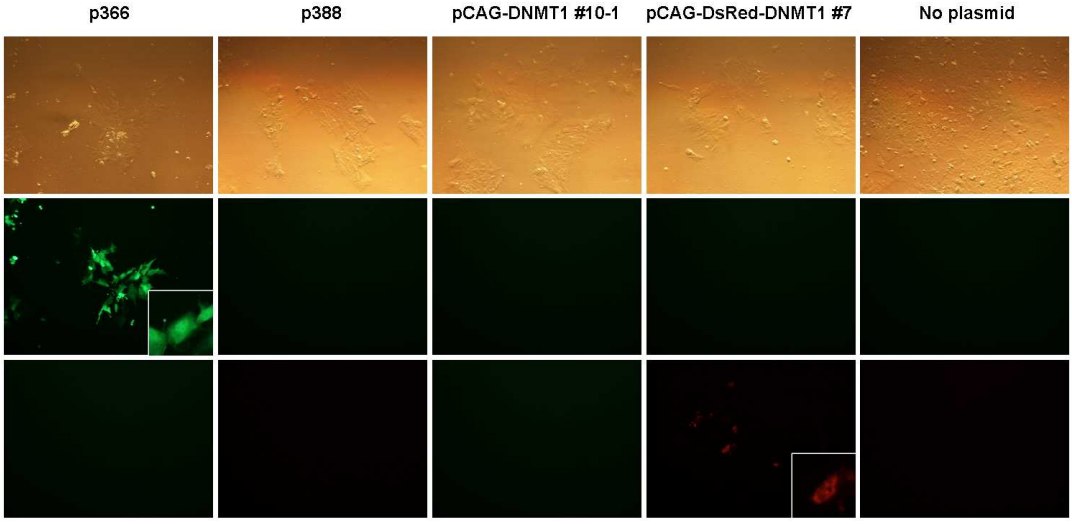

Figure 5-5. Immunofluorescence analysis in transiently transfected HUES7 p22
Circular p336, p388, pCAG-DsRed2-C1-hDNMT1-IRES-PAC #7 and pCAG-hDNMT1-IRES-PAC #10-1 plasmids were transiently transfected in HUES7 (p22) by GeneJammer. Green signals were detected in cells transfected by p336. Red signals were detected in cells transfected by pCAG-DsRed2-C1-hDNMT1-IRES-PAC #7. No fluorescence signals were detected in cells transfected by p388, pCAG-hDNMT1-IRES-PAC #10-1 and no plasmid. Top panels show brightfield images. Middle panels show eGFP filter images. Bottom panels show DsRed2 filter images.

5.2.3 Stable transfection

5.2.3.1 Preparation of plasmids

Plasmids were linearised by *Ahd*I and *Pvu*I restriction enzymes. An *Ahd*I enzyme was used for linearisating p336 and p388 plasmids. A *Pvu*I enzyme was used for linearisating pCAG-DNMT1-IRES-PAC #10-1 and pCAG-DsRed2-C1-DNMT1-IRES-PAC #7 plasmids (Figure 5-6). Linearised plasmids were purified by phenol-chloroform extraction.

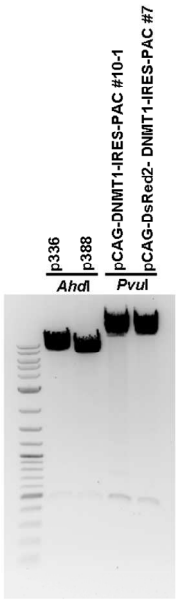

Figure 5-6. Linearisation of plasmids for stable transfection
An *Ahd*I enzyme was used for linearising p336 and p388 plasmids. A *Pvu*I enzyme was used for linearising pCAG-hDNMT1-IRES-PAC #10-1 and pCAG-DsRed2-C1-hDNMT1-IRES-PAC #7. Restriction enzymes used and plasmids are shown on the top of a gel image. A 0.8% agarose gel was used for gel electrophoresis. The 2-Log DNA ladder (NEB) was used as a molecular maker.

5.2.3.2 Electroporation and puromycin selection

Electroporation methods for establishing stable transfected hESC lines have been optimised by Prof. Chris Denning and Dr. David Anderson (University of Nottingham). Electroporation was performed with 1×10^6 HUES7 (p22) cells and 50 µg of each linearised plasmid using previously optimised setting of 600 V/30 µs (Anderson et al., 2007; Denning et al., 2006). After 24 hours, these cells were subject to puromycin selection. Puromycin resistant colonies appeared after 10 days in culture (Figure 5-7). Interestingly, although 58 colonies were found in dishes containing cells transfected by p336 and p388, only 27 colonies were found in dishes containing cells transfected by pCAG-hDNMT1-IRES-PAC #10-1 and pCAG-DsRed2-C1-hDNMT1-IRES-PAC #7. Furthermore, the size of colonies was comparable between control plasmids transfected and plasmids containing *DNMT1* cDNA transfected. Colonies of p336 and p388 were relatively bigger than those of pCAG-hDNMT1-IRES-PAC #10-1 and pCAG-DsRed2-C1-hDNMT1-IRES-PAC #7 (Figure 5-7). These colonies were handpicked by pipette, transferred into one well of a 12-well plate, and expanded until they were confluent in one well of a 6-well plate. Finally, 14 of p366 cell lines, 17 of p388 cell lines, 8 of hESOD1 (human embryonic stem cell lines overexpressing

DNMT1) cell lines (derived from pCAG-hDNMT1-IRES-PAC #10-1) and 11 of hESOrD1 (human embryonic stem cells overexpressing DsRed-DNMT1) cell lines (derived from pCAG-DsRed2-C1-hDNMT1-IRES-PAC #7) were established after ~ 4 weeks of puromycin selection (Table 5-1). Once cell lines were established, they were named and numbered; p336 (p336 #1, -#3, -#4, -#6, -#7, -#9, -#12, -#13, -#14, -#15, -#16, -#17, -#19, -#23), p388 (p388 #1, -#2,--#3, -#4, -#5, -#7, -#8, -#9, -#10, -#11, -#12, -#13, -#14, -#15, -#16, -#18, -#23), pCAG-DNMT1-IRES-PAC #10-1 (hESOD1 #1, -#2, -#3, -#4, -#5, -#6, -#7, -#9), pCAG-DsRed2-C1-DNMT1-IRES-PAC #7 (hESOrD1 #1, -#2, -#3, -#5, -#6, -#8, -#9, -#10, -#11, -#12, -#13).

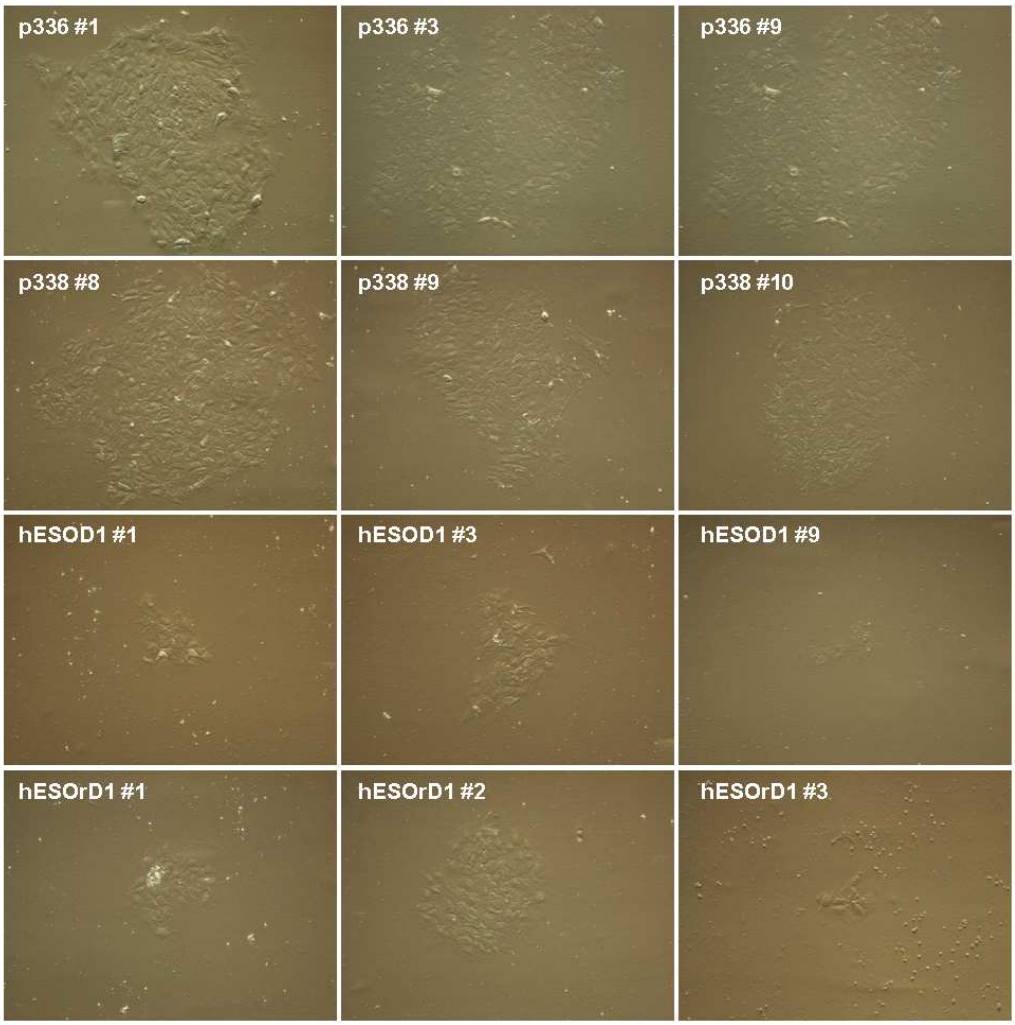

Figure 5-7. The formation of puromycin resistant colonies
Linearised plasmids were transfected into HUES7 (p22) by electoroporation. Cells were subject to puromycin selection. After 10 days, 27 colonies (p336), 31 colonies (p388), 13 colonies (pCAG-DNMT1-IRES-PAC #10-1) and 14 (pCAG-DsRed2-C1-DNMT1-IRES-PAC #7) colonies were found. The size of p336 #1, p336 #3, p336 #9, p388 #8, p388 #9 and p388 #10 colonies are relatively bigger than that of hESOD #1, hESOD #3, hESOD #9, hESOrD #1, hESOrD #2 and hESOrD #3 colonies. All images were captured in brightfield microscopy.

Table 5-1. The number of puromycin resistant colonies and established cell lines

Plasmid	No. of colonies found	No. of colonies picked	No. of cell lines established
p336	27	23	14
pCAG-DNMT1-IRES-PAC #10-1	13	13	8
p388	31	23	17
pCAG-DsRed2-c1-DNMT1-IRES-PAC#7	14	14	11
Without plasmid[a]	0	0	0

[a] Transfection was performed without the plasmid. During puromycin selection, all cells died so that no cell lines were established.

5.2.3.3 Characterisation of cell lines overexpressing *DNMT1*

To indentify cell lines having both endogenous and exogenous DNMT1 expression, Western blot was performed on the 6% SDS-PAGE gel (Figure 5-8). Then, the blot was probed with a polyclonal DNMT1 antibody (NEB) raised against the N-terminal region. Consistent with previous reports (Chen et al., 2007; Esteve et al., 2005; Esteve et al., 2006; Kim et al., 2002; Pradhan and Kim, 2002), one DNMT1 specific band of 190kDa was detected in all cell lines (Figure 5-8). The expression level of DNMT1 protein was variable between cell lines, although α-Tubulin as a loading control was similarly expressed. Moreover, Ponceau S staining showed that equal amounts of proteins were loaded in each lane. DNMT1 is highly expressed in hESOD1 #1, hESOD1 #3, hESOD1 #4, hESOD1 #5, hESOD1 #6, hESOD1 #9, hESOrD1 #3, hESOrD1 #5 and hESOrD1 #8 in comparison to control cell lines, p366 #1, p366 #9, p388 #8, p388 #9, p388 #10, p388 #12, transfection control (TC) and HUES7 (p25).

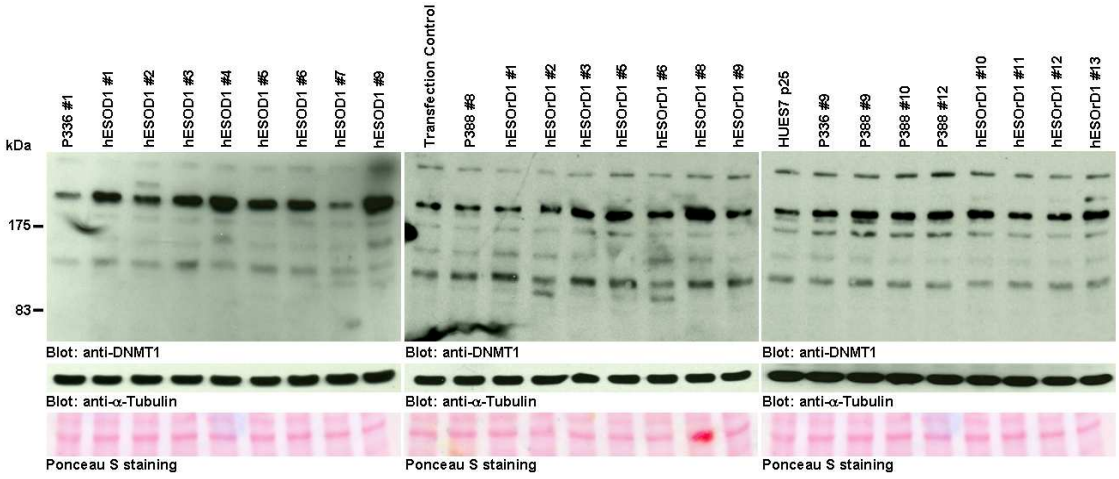

Figure 5-8. Western blot analysis of established cell lines on the 6% SDS-PAGE gel

30 µg protein extracts from each cell line were loaded onto each lane of the 6% SDS-PAGE gel, electroblotted into the nitrocellulose membrane, and probed with DNMT1

and α-Tubulin antibodies. The cell lines examined are shown on the top of gel images. Molecular masses are shown on the left of a gel image. α-Tubulin blot and Ponceau S staining were used as loading controls.

Although cell lines overexpressing DNMT1 were identified on the 6% SDS-PAGE gel (Figure 5-8), this failed to discriminate between endogenous and exogenous DNMT1 expression. Thus, Western blot was performed on the 4% SDS-PAGE gel (Figure 5-9). However, this also failed to discriminate between endogenous and exogenous DNMT1 expression. Similar to the 6% SDS-PAGE gel, one DNMT1 specific band was detected around 190kDa on the 4% SDS-PAGE gel (Figure 5-9 A). The expression levels of DNMT1 were quantified by the Aida image analyser and normalised to expression levels of α-Tubulin (Figure 5-9 B). Over 3 fold increased DNMT1 expression was detected in hESOD1 #3 (3.0 fold), hESOD1 #4 (3.7 fold) and hESOD1 #9 (3.5 fold), against control cell lines (p336 #1, p336 #9, p388 #8 and p388 #9). In addition, hESOD1 #1 (2.4 fold), hESOD1 #5 (2.5 fold) and hESOD1 #6 (2.0 fold) showed over 2 fold increased DNMT1 expression, compared to control cell lines. hESOD1 #7 had a similar expression level to control cell lines. Following Western blot analysis, 4 control cell lines (p366#1, p336#9, p388 #8, p388 #9) and 4 hESOD1 cell lines (hESOD1 #1, hESOD1 #3, hESOD1 #4 and hESOD1 #9) were selected for further studies.

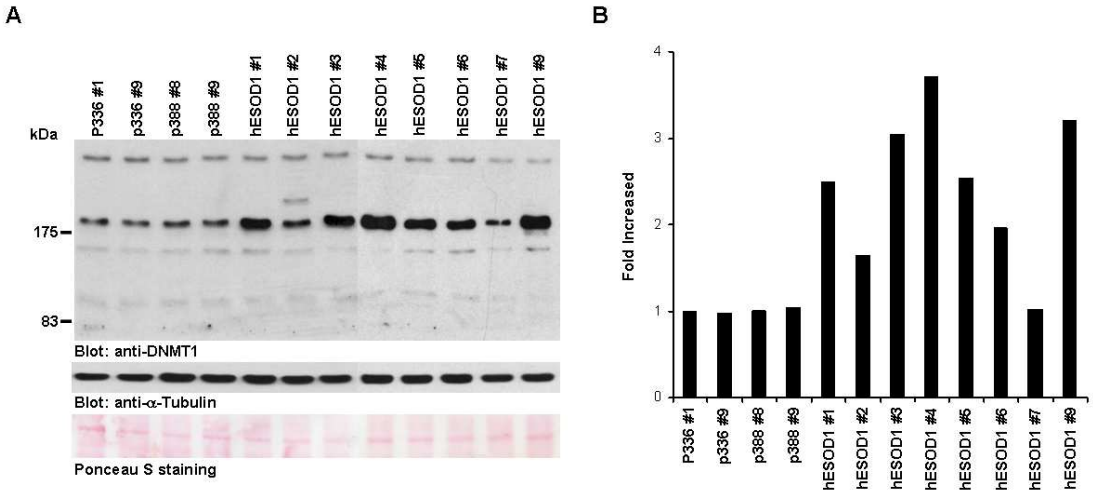

Figure 5-9. Western blot analysis of established cell lines on the 4% SDS-PAGE gel

(A) Total 30 µg protein extracts from each cell line were loaded onto each lane of the 4% SDS-PAGE gel, electroblotted into the nitrocellulose membrane, and probed with DNMT1 and α-Tubulin antibodies. The cell lines studied are shown on the top of a gel image. Molecular masses are shown on the left of a gel image. α-Tubulin blot and Ponceau S staining were used as loading controls. (B) The expression level of

DNMT1 was quantified by the Aida image analyser and normalised by the expression level of α-Tubulin.

5.2.3.4 Maintenance DNMT activity assay

In mammalian cells, the increased expression of DNMT1 protein has been reported to be associated with increased maintenance DNMT activity (Biniszkiewicz et al., 2002; Vertino et al., 1996). Thus, the *in vitro* maintenance DNMT activity assay was performed, as previously described by Butler et al., (2006). This assay was performed by Dr. Jeong-Heon Lee and Prof. David G. Skalnik (Indiana University). Nuclear extracts were extracted from each cell line, incubated with [^{3}H]SAM (*S*-adenosyl-L-methionine) and oligonucleotides as substrates (Figure 5-10 C) and loaded into each lane of a 10.5% native PAGE gel. The gel was dried, exposed to the X-ray film and developed (Figure 5-10 A). The maintenance DNMT activities were illustrated by the bands coreesponding hemi-methylated oligonuclotides (Figure 5-10 A). The intensty of bands was quantifed by the Aida image analyser (Figure 5-10 B). Over 2 fold increased maintenance DNMT activities were detected in hESOD1 #3, hESOD1 #4 and hESOD1 #9, against control cell lines (p336#1, p336#9, p388#8 and p388#9) (Figure 5-10 B). Moreover, over 1.5 fold increased maintenance DNMT activities were detected in hESOD1 #2, hESOD1 #5, hESOD1 #6 and hESOD1 #7. Thus, exogenously expressed *DNMT1* in hESC lines functionally worked as a maintenance methyltransferase.

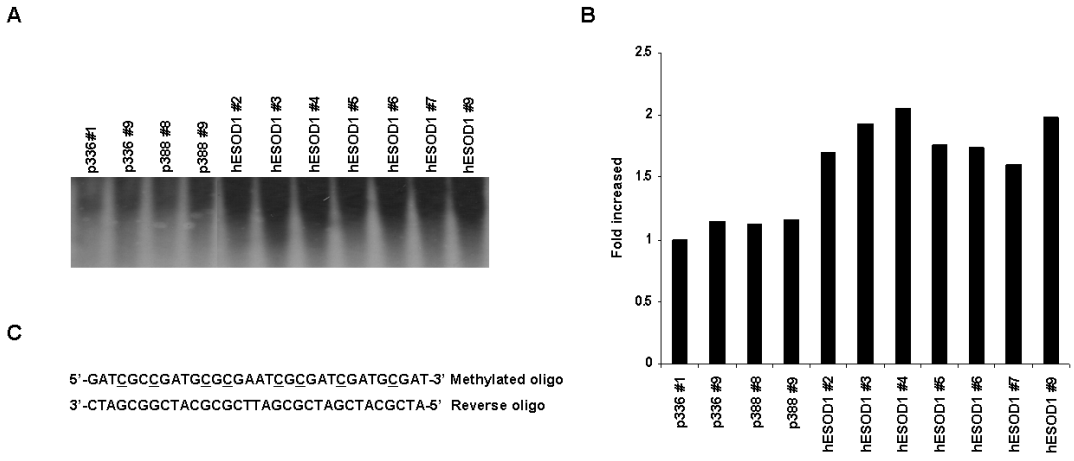

Figure 5-10. *In vitro* maintenance DNMT activity assay in established cell lines

(A) Maintenance DNMT activity assay was performed on the 10.5% native PAGE gel. *In vitro* DNMT activity was measured by the incorporation of methyl groups (CH_3) from [^{3}H]SAM (*S*-adenosyl-L-methionine) into double-strand oligonucleotides used

as substrates (C). (B) The activity level of each cell line was quantified by the Aida image analyser.

5.2.4 Stem cell characteristics

5.2.4.1 Morphology

Brightfield microscopy analysis was performed in 8 cell lines to identify potential morphology changes induced by exogenous *DNMT1* expression. This revealed no morphological changes in cell lines, although exogenous *DNMT1* was expressed in hESOD1 cell lines (Figure 5-11).

Figure 5-11. The morphology analysis of established cell lines
All cell lines were examined at passage 30. All images captured under the microscopy of the brightfield filter showed no morphology changes of hESOD1 lines, compared to control lines (p366#1, p336#9, p388 #8 and p388 #9).

5.2.4.2 OCT4, NANOG and SSEA4 expression

Immunostaining and Western blot for pluripotency markers were performed to identify whether hESOD1 cell lines (p30 and p45) were maintained in an undifferentiated state. Immunostaining revealed that OCT3/4 and NANOG were expressed in the nucleus of all cell lines (Figure 5-12 A). Furthermore, SSEA4 was expressed in the surface of all cell lines (Figure 5-12 A). By Western blot, similar expression levels of OCT3/4 and NANOG were detected in all cell lines at passages 30 and 45 (Figure 5-12 B and C). Thus, the overexpression of exogenous DNMT1 did not interfere with the maintenance of an undifferentiated state of hESCs.

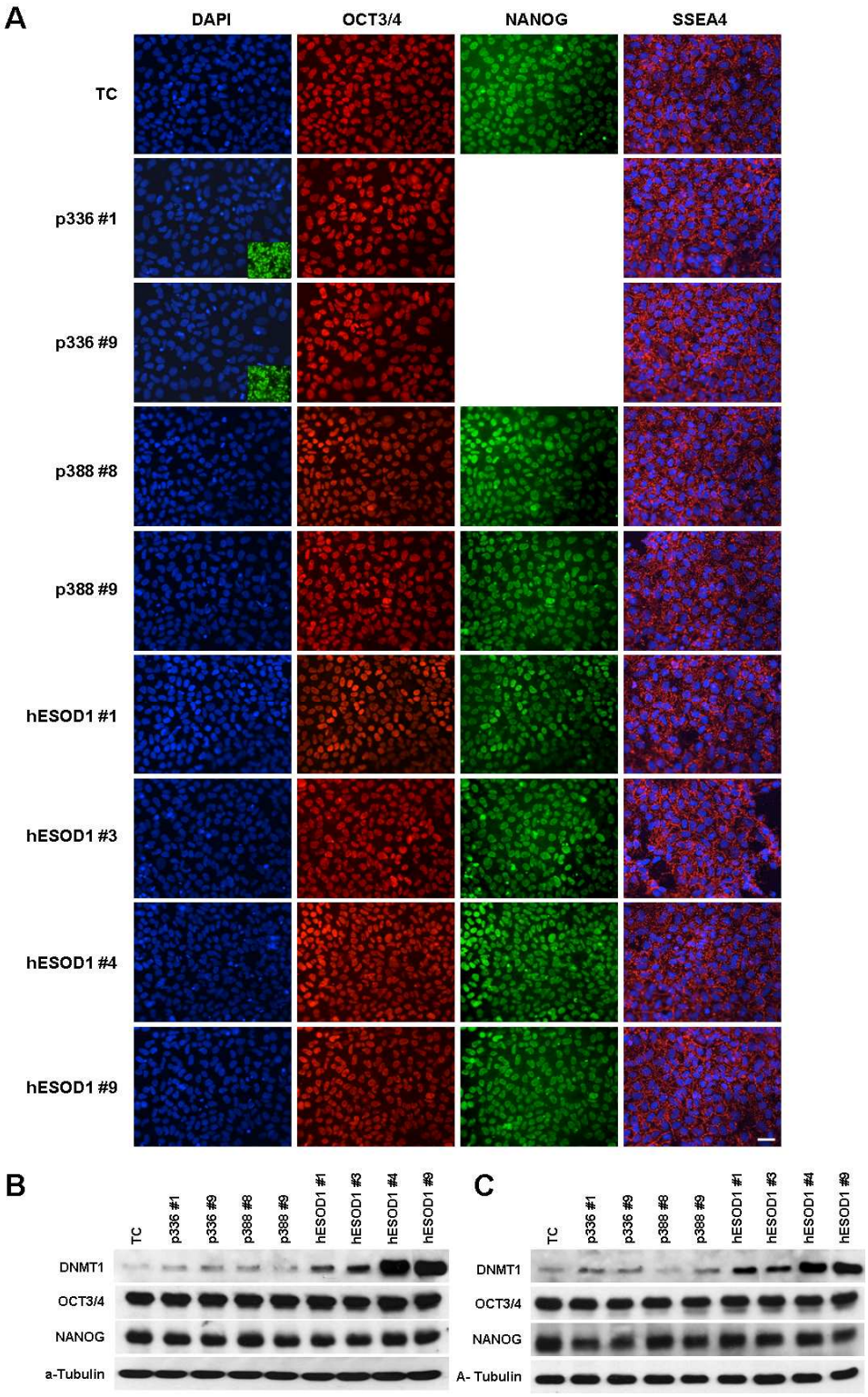

Figure 5-12. OCT3/4, NANOG and SSEA4 expression in established cell lines

(A) Immunostaining of OCT3/4, NANOG and SEEA4 with respective antibodies (see section 2.2). The nucleus is visualised by DAPI (blue) staining. (B) Western analysis of cell lines at passages 30 and (C) p45. Western blot was performed on 4% ~ 8% SDS-PAGE gels. Total 30 µg protein extracts from each cell line were loaded onto each lane of the gel, electroblotted into the nitrocellulose membrane, and probed with respective antibodies (see section 2.2). α-Tubulin blots were used as loading controls.

5.2.4.3 Population double time and cell cycle

The population doubling (PD) time was measured during 12 days (4 passages) in culture to identify whether hESOD1 cell lines had normal growth rates. The number of cells was counted by the hemocytometer. PD times were calculated using the formula: log (the number of subcultures established at the each passage)/log2 (assuming 100% cell survival at each passage) (Allegrucci et al., 2007; Denning et al., 2006) (Figure 5-13). In control cell lines, TC, p336 #1, p336 #9, p388 #8 and p399 #9, PD times were 59.2h, 60.2h, 61.3h, 60h and 61.4h, respectively. However, PD times of hESOD1 cell lines, hESOD1 #1, hESOD1 #3, hESOD1 #4 and hESOD1 #9 were 70.5h, 64.8h, 68.5h and 71.7h, respectively. Thus, there are ~ 10h differences between control cell lines and hESOD1 cell lines ($p<0.05$), indicating that hESOD1 cell lines are slow growing, compared to control cell lines.

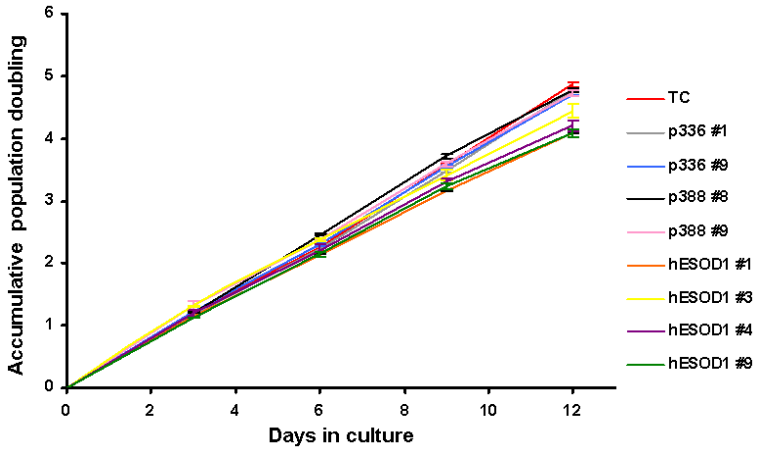

Figure 5-13. The population doubling (PD) time of established cell lines
The number of cells was calculated by hemocytometer during 12 days. PD times were calculated using the log scale. The statistical analysis was performed by Post Hoc, Mann-Whitney and Kruskal-Wallis tests that showed there are significant differences between control cell lines and hESOD1 cell lines ($p<0.05$) (see appendix 2).

Cell cycle analysis was performed by flow cytometry, following PI (propidium iodide) staining. Data were analysed by WinMDI and Cylchred programmes (see section 2.3.23). Control cell lines (HUES7 p22, p336 #1, p336#9, p388 #8 and p388 #9) showed similar proportions of G1, S and G2-M phase cells (Figure 5-14 A and B). However, the proportion of S phase cells significantly decreased in hESOD1 #1, hESOD1 #4 and hESOD1 #9, compared to control cell lines ($p<0.05$). Moreover, the proportion of G2-M phase cells significantly increased in hESOD1 #1, hESOD1 #4 and hESOD1 #9 ($p<0.05$), compared to control cell lines. Interestingly, hESOD1 #3

showed similar proportions of G1, S and G2-M cells of control cell lines (Figure 5-14 B).

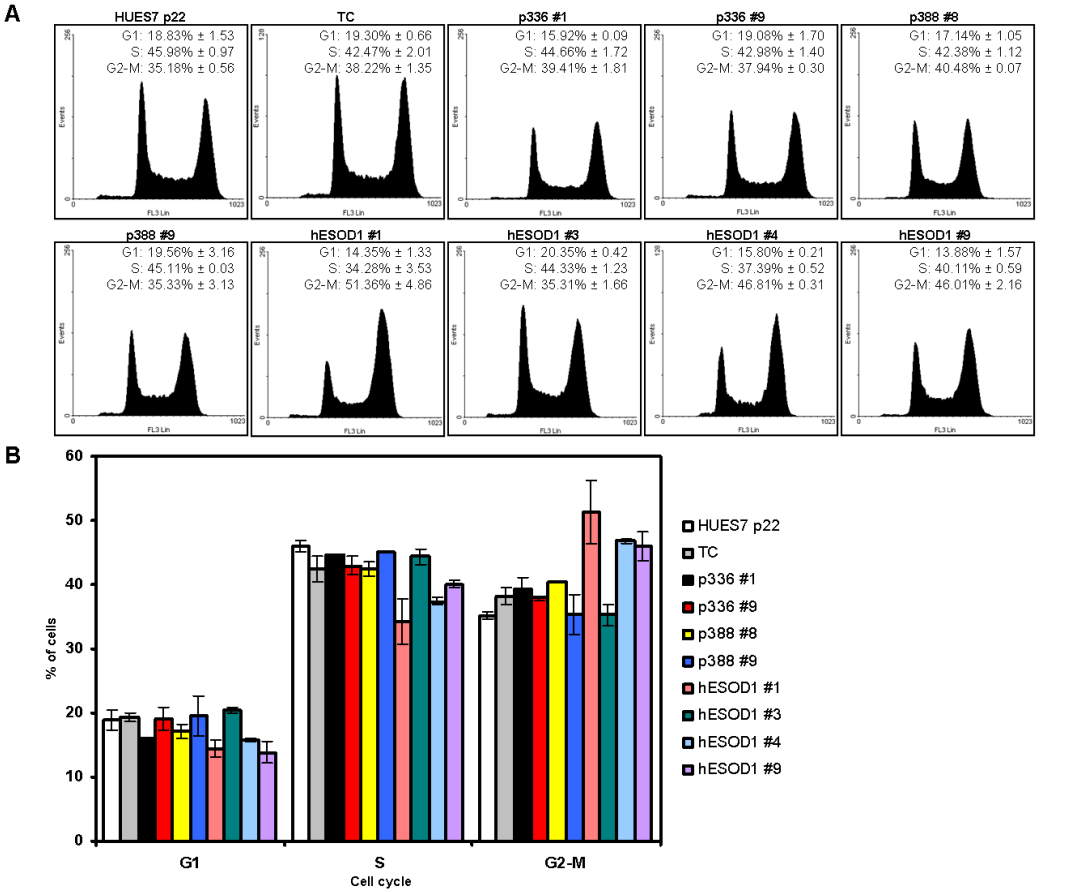

Figure 5-14. Cell cycle analysis of established cell lines
(A) The total cell population was examined by flow cytometry. Data were analysed by WinMDI and Cylchred programmes and (B) the bar chart was generated based on the data. Statistical analysis was performed by Post Hoc, Mann-Whitney and Kruskal-Wallis tests that showed there are significant differences between control cell lines and hESOD1 cell lines (P<0.05).

5.2.5 DNA methylation

5.2.5.1 DNA methylation at 14 imprinting regulatory regions

DNA methylation at 14 imprinting regulatory regions was analysed in hESOD1 cell lines (passages 30 and 45) by combined bisulphite restriction analysis (COBRA). In Chapter 4, overall DNA methylation levels at 14 imprinted regulatory regions were characterised in 22 hESC cell lines, when imprinted loci are informative. PCR was performed with bisulphite modified genomic DNA. PCR products were digested by appropriate restriction enzymes (Figure 5-15 and 5-16). Of 14 imprinted loci examined, none showed DNA methylation changes in both hESOD1 and control cell

lines. In detail, the promoter region of *TP73, SLC22A18* and *CDK1NC* was unmethylated in both control (HUES7 p22, p336 #1, p336 #9, p388 #8 and p388 #9) and hESOD1 cell lines (hESOD1 #1, hESOD1 #3, hESOD1 #4 and hESOD1 #9). *IGF2R* DMR2 was methylated in all cell lines. Of other 10 imprinting regulatory regions (*PEG10, PEG1, KvDMR1, IGF2, H19, GLT2, SNRPN, PEG3, NESP55* and *GNAS1 XLαs* DMRs) examined, all showed differential methylation on both parental alleles in all cell lines, except for the *H19* CTCF6 *Aci*I site.

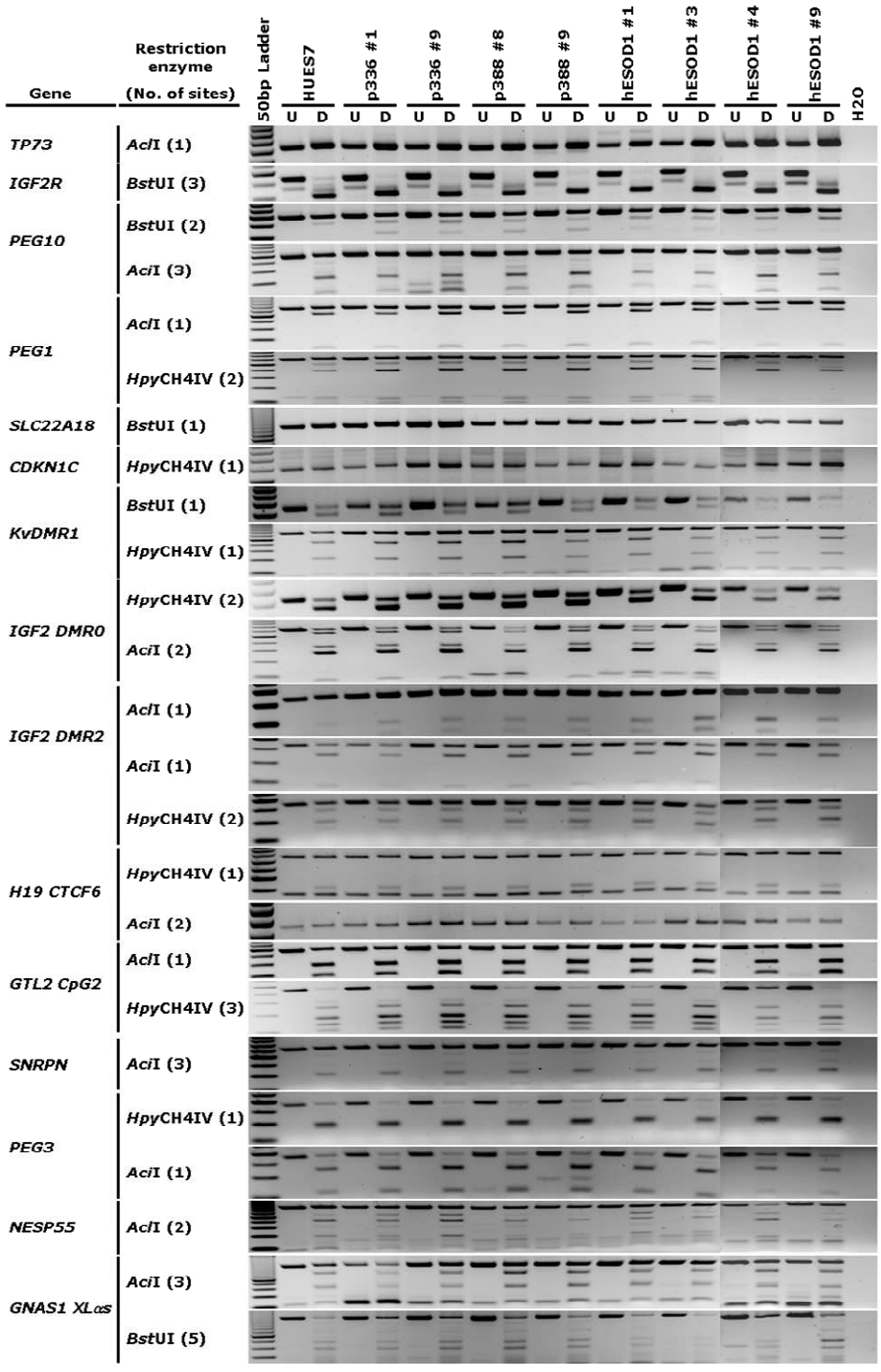

Figure 5-15. DNA methylation at 14 imprinting regulatory regions in established cell lines (p30)

The COBRA analysis was performed with appropriate restriction enzymes to determine methylation-dependent sequence differences in PCR products of bisulphite modified genomic DNA. 14 imprinted genes studied, appropriate restriction enzymes and the number of restriction enzyme sites are shown on the left side of gel images. The name of each cell line is shown on the top of the gel image. 3% agarose gels were used for gel electrophoresis. H_2O was used as a negative control for PCR. The 50 bp DNA Ladder (NEB) was used for a molecular maker. U indicates digested and D indicates undigested.

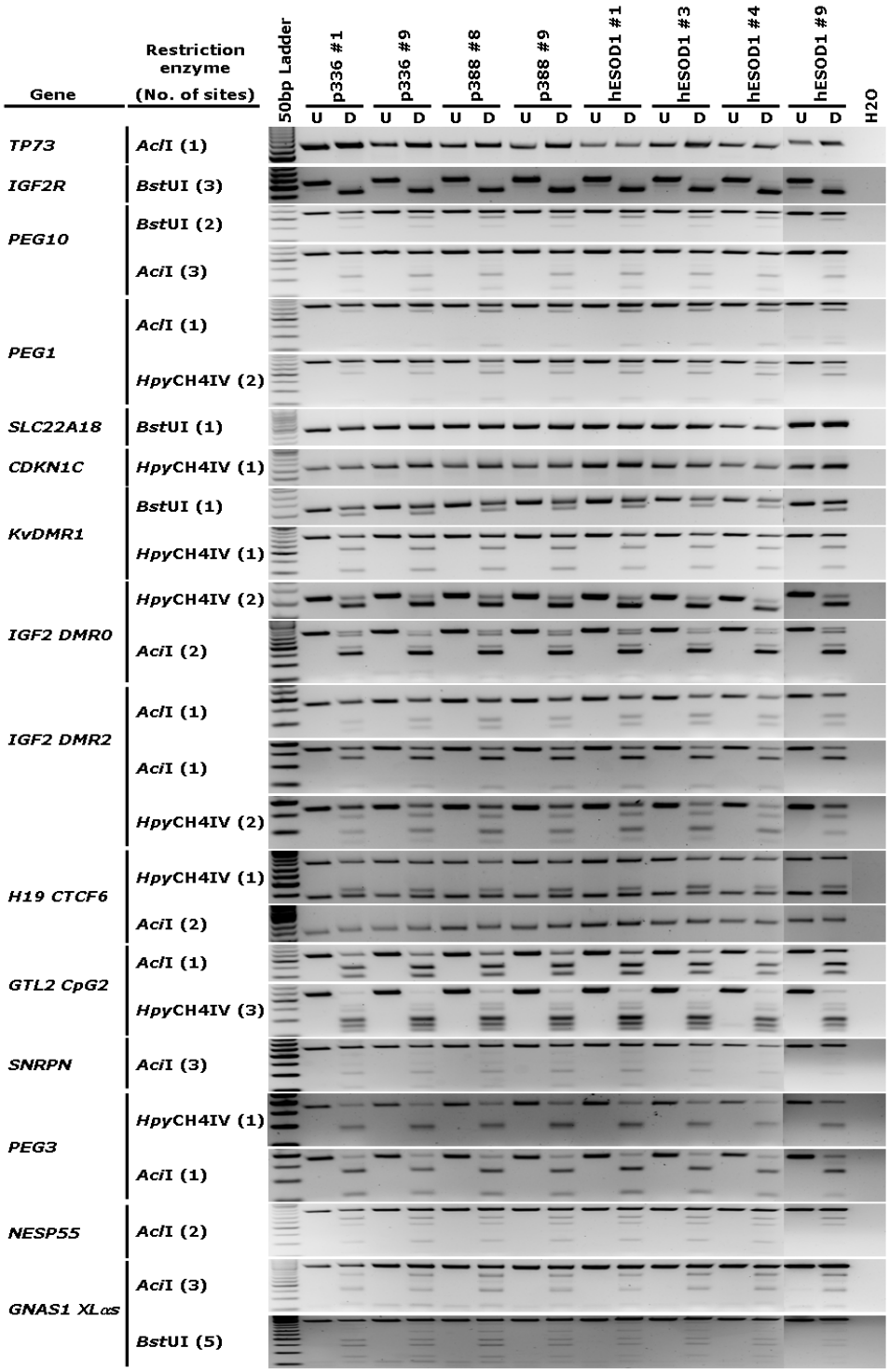

Figure 5-16. DNA methylation at 14 imprinting regulatory regions in established cell lines (p45)

The COBRA analysis was performed with appropriate restriction enzymes to determine methylation-dependent sequence differences in PCR products of bisulphite modified genomic DNA. 14 imprinted genes studied, appropriate restriction enzymes and the number of restriction enzyme sites are shown on the left side of gel images. The name of each cell line is shown on the top of the gel image. 3% agarose gels were used for gel electrophoresis. H_2O was used as a negative control for PCR. The 50 bp DNA Ladder (NEB) was used for a molecular maker. U indicates digested and D indicates undigested.

5.2.5.2 DNA methylation at 9 tumour-suppressor gene promoters

The overexpression of endogenous *DNMT1* is associated with hypermethylation at the promoter regions of tumour-suppressor genes in human cancers (Etoh et al., 2004; Peng et al., 2006; Sawada et al., 2007). Furthermore, human fibroblast cell lines overexpressing exogenous *DNMT1* show hypermethylation at the promoter regions of 5 tumour-suppressor genes (Vertino et al., 1996). Thus, DNA methylation at 9 previously reported tumour-suppressor gene promoters was analysed in hESOD1 and control cell lines by methylation-specific PCR (MSP). These genes were selected, since they are functionally known to be important for metastasis, angiogenesis, apoptosis, cell cycle and DNA repair (Akiyama et al., 2003; Dong et al., 2001; Evron et al., 2001; Herman et al., 1996; Imura et al., 2006; Zochbauer-Muller et al., 2001). Furthermore, some of genes (e.g. GATA4 and GATA5) are critically involved in embryonic development and differentiation of hESCs (Akiyama et al., 2003; Ohm et al., 2007). These gene promoters are previously shown to be unmethylated in the hESC line (WA01 also know as H1), whereas HCT116 exhibits hypermethylation (Ohm et al., 2007). Thus, HCT116 was used for a control for methylation. In addition, *in vitro* methylated HUES7 p21 and human liver DNA by the *Sss*I methylase were used as controls for positive methylation.

Of 10 gene promoters examined, most promoters were unmethylated in HUES7 p21, except for *p16* and *TIMP-3* promoters (Figure 5-17). However, 6 promoters (*CCND1*, *ESR1*, *MGMT*, *GATA4*, *HIC-1* and *p16* promoters) were methylated in HCT116. Interestingly, gain of methylation at *MGMT*, *HIC-1* and *GATA5* promoters was detected in differentiated HUES7 (EBs d27), although other promoters showed similar methylation patterns between undifferentiated and differentiated cells (Figure 5-17). In *in vitro* methylated HUES7 p21 and human liver DNA, either methylation or predominate methylation was detected at all promoters (Figure 5-17). In *in vitro* methylated HUES7 p21 DNA, *TIMP-3*, *CCND1*, *ESR1*, *GATA5* promoters were completely methylated, whereas *CDH1*, *DAPK1*, *MGMT*, *HIC-1*, *GATA4* and *p16* promoters were predominantly methylated. In *in vitro* methylated human live DNA, the *CCND1* promoter was completely methylated and other promoters were predominantly methylated. Based on these observations, DNA methylation patterns at 10 gene promoters were analysed in hESOD1 cell lines at passage 30 (Figure 5-17). Gain of methylation at the *TIMP-3* promoter was detected in all hESOD1 cell lines.

Moreover, gain of methylation at *MGMT* was detected in hESOD1#1. However, other promoters showed no methylation changes in hESOD1 cell lines.

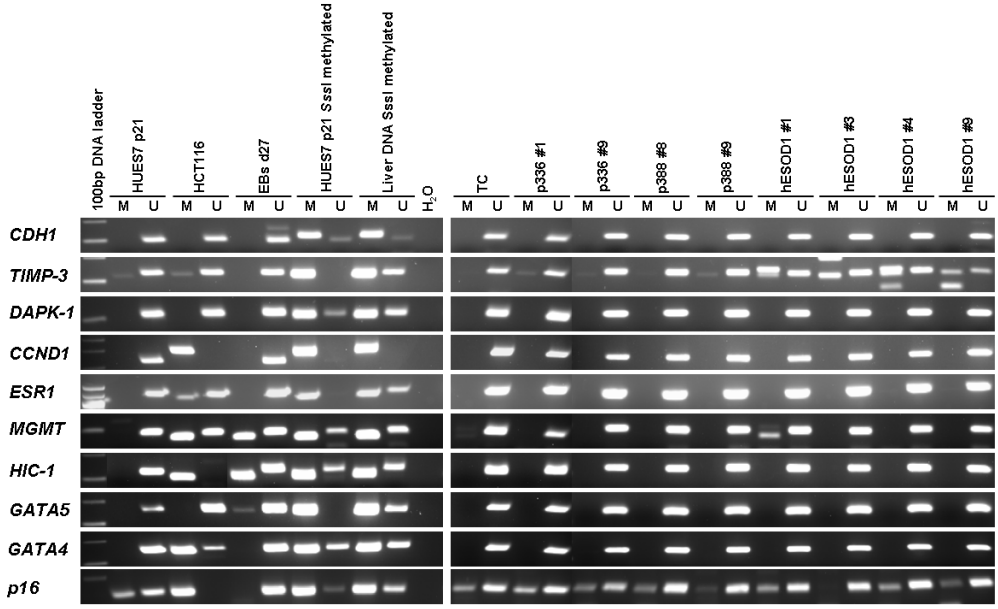

Figure 5-17. MSP DNA methylation analysis at 10 tumour-suppressor gene promoters in established cell lines (p30)
Genes studied are shown on the left of each panel. Cell lines studied as shown on the top of the panel. M indicates amplified PCR products recognising methylated CpGs. U indicates amplified PCR products recognising unmethylated CpGs. HUES7 p21 was used as a control for unmethylation. HCT116, *in vitro* methylated HUES7 p21 and human liver DNA were used as controls for methylation. H_2O used as a negative control for PCR. The 100bp DNA Ladder (NEB) was used as a molecular maker.

It has been reported that DNA methylation changes accumulate in human fibroblast cell lines overexpressing *DNMT1* during *in vitro* prolonged culture (Vertino et al., 1996). Thus, the DNA methylation status at 10 tumour-suppressor gene promoter was analysed in hESOD1 cell lines at passage 45 (Figure 5-18). Gain of methylation at the *TIMP-3* promoter was still retained in all hESOD1 lines (p45). Also, gain of methylation at *MGMT* promoter persisted during *in vitro* culture of hESOD1 #1. Interestingly, gain of methylation at *DAPK-1* was detected in hESOD1 #9 p45 (Figure 5-18). Furthermore, gain of methylation at the *MGMT* promoter was detected in hESOD1 #3 p45, hESOD1 #9 p45 and p388#8 p45. Thus, DNA methylation changes accumulated at some promoters during *in vitro* culture.

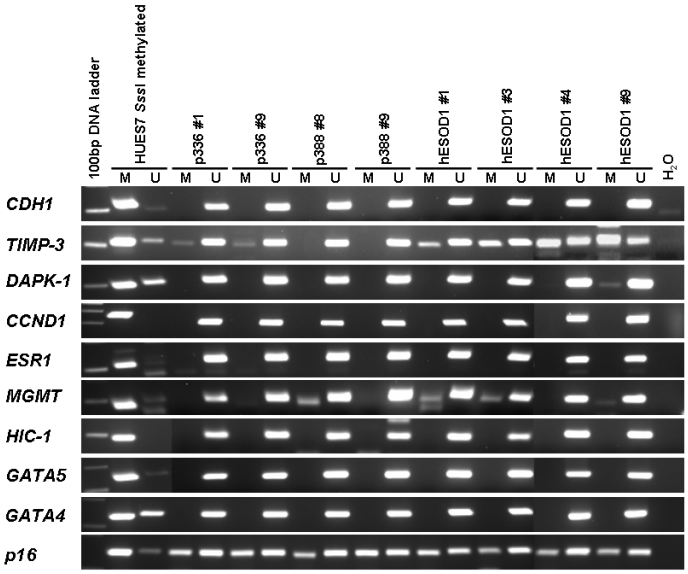

Figure 5-18. MSP DNA methylation analysis at 10 tumour-suppressor gene promoters in established cell lines (p45)
Genes studied are shown on the left of each panel. Cell lines studied as shown on the top of the panel. M indicates amplified PCR products recognising methylated CpGs. U indicates amplified PCR products recognising unmethylated CpGs. HUES7 p21 was used as a control for unmethylation. *In vitro* methylated HUES7 p21 was used as a control for methylation. H_2O used as a negative control for PCR. The 100bp DNA Ladder (NEB) is used as a molecular maker.

5.2.5.2.1 Association between DNA methylation and gene expression

Hypermethylation at promoter regions of tumour suppressor genes can be associated with transcriptional silencing of the genes (Esteller, 2007; Feinberg, 2007). Thus, RT-PCR was performed to identify association between gain of methylation at *MGMT* and *TIMP-3* promoters and transcriptional repression of the genes. *TIPM-3* was expressed in HUES7 p22, HCT116 and EBs d27 in a similar level that was associated with unmethylation at its promoter (Figure 5-17 and 5-19). *GATA4* and *GATA5* were highly expressed in EBs (compared to HUES7 p22 and HCT116) that was also associated with unmethylation at their promoters (Figure 5-17 and 5-19). However, even if the *GATA5* promoter was unmethylated in HCT116, its expression was not detected, indicating no association between DNA methylation at the region examined and gene expression. Furthermore, no association was detected in *MGMT* and *HIC-1* genes. *MGMT* was expressed in HUES7 p22, HCT116 and EBs d27 in a similar level that was not associated with predominant methylation at its promoter in HCT116 and EBs d27 (Figure 5-17 and 5-19). *HIC-1* is expressed in HUES7 p22, HCT116 and EBs d27 that was not associated with predominant methylation at its promoter in HCT116 and

EBs d27. In a similar scenario, no associations were detected in hESOD1 cell lines. Although gain of methylation at *MGMT* and *TIMP-3* promoters in hESOD1 cell lines, their expression levels were similar to control cell lines (Figure 5-17 and 5-19).

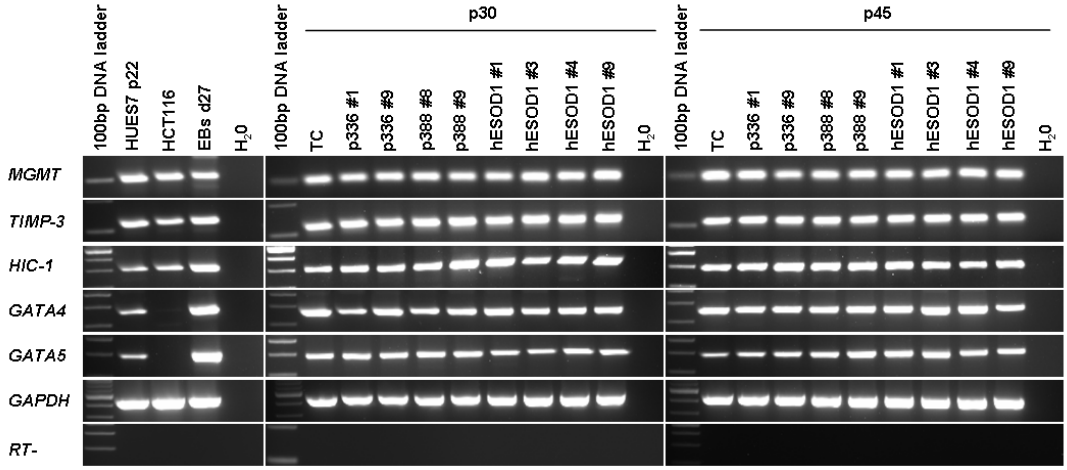

Figure 5-19. The RT-PCR analysis of 5 tumour-suppressor genes in established cell lines

PCR amplification was performed with cDNA of cell lines. 2% agarose gels were used for gel electrophoresis. The 100bp DNA ladder (NEB) was used as a molecular maker. Cell lines studied are shown on the top of the panel. Genes studied are shown on the left of panels. H_2O was used as a negative control for PCR. RT- indicates no reverse transcription reaction.

5.2.5.3 DNA methylation at repetitive sequences

DNA methylation analysis was performed for LINE1, Satellite 2 and Satellite 3 by Southern blot. DNA was digested with either *Msp*I which cut at the sequence CCGG or *Hpa*II which dose not cut when the cytosine is methylated (Lei et al., 1996; Rhee et al., 2002; Rhee et al., 2000). Southern blot analysis revealed that DNA methylation did not vary between control and hESOD1 cell lines (Figure 5-20). In all cell lines examined, larger DNA fragments were detected in *Hpa*II digests compared to *Msp*I digests at LINE1, Satellite 2 and Satellite 3, indicating that these regions were heavily methylated in all cell lines. Interestingly, small fragments at LINE1, Satellite 2 and Satellite 3 were detected in *Hpa*II digests of EBs day 27, indicating that these regions were less methylated in differentiated hESCs (Figure 5-20).

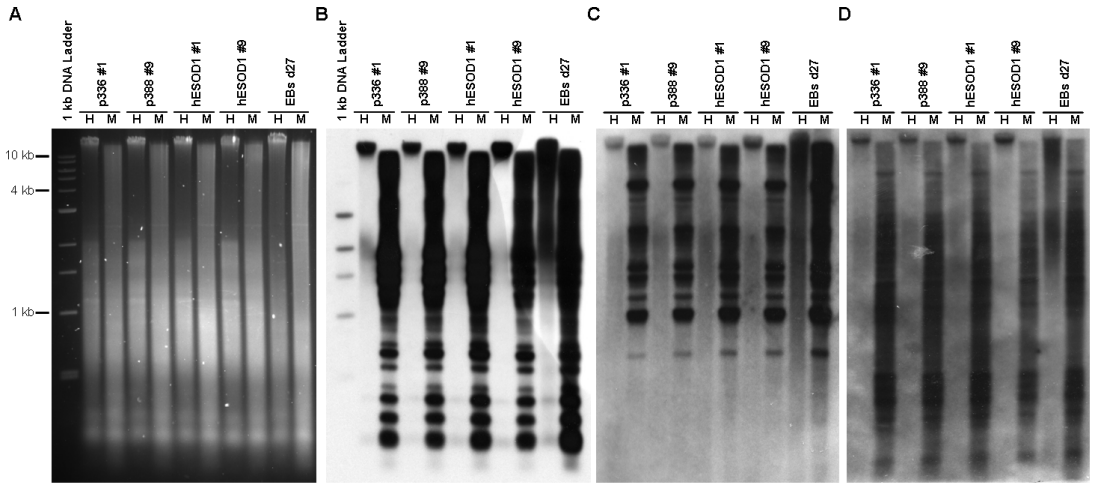

Figure 5-20. The methylation analysis at LINE1, Satellite 2 and Satellite 3 in established cell lines

Gel electrophoresis followed by ethidium bromide staining, (B) LINE1 blot, (C) Satellite 2 blot and (D) Satellite 3 blot. The methylation status was determined by digesting DNA with *Msp*I (M) and *Hpa*II (H). Digested DNA fragments were separated by gel electrophoresis, transferred into nitrocellulose membranes, and hybridised with ^{32}P-labeled DNA probes. Cell lines studied and restriction enzymes are shown on the top of images. The 2-Log DNA ladder (NEB) was used as a molecular maker.

5.2.5.4 DNA methylation at ~ 2,200 CpG islands

RLGS analysis was performed by Jayson Bispham (University of Nottingham). All procedures were described in a previous report (Allegrucci et al., 2007). Of ~ 2,200 CpG loci examined, 6 loci showed DNA methylation changes (2 loci were hypermethylated and 4 loci were demethylated) in p388#9 p46, against HUES7 p22 (Table 5-2). However, only 1 or 2 loci showed DNA methylation changes (1 locus was hypermethylated and l locus was demethylated) in hESOD1#1 p45 and hESOD1#4 p45, against HUES7 p22.

Table 5-2. The methylation analysis at ~ 2,200 CpG islands

p388#9 p45			hESOD#1 p45			hESOD#4 p45		
Loci	**Methylation**	**Gene name**	**Loci**	**Methylation**	**Gene name**	**Loci**	**Methylation**	**Gene name**
2CA	Hypermethylated	-	2E14	Hypermethylated	TM7SF2	3D18	Demethylated	SNIP
2D1	Demethylated	-	3D18	Demethylated	SNIP			
2EJ	Demethylated	-						
2FC	Demethylated	-						
2G41	Hypermethylated	-						
3E57	Demethylated	Mouse AK047384 cDNA						

5.3 Discussion

Recent studies have reported that some CpG islands within imprinted and non-imprinted loci in hESCs undergo loss of DNA methylation during *in vitro* long-term culture (Allegrucci et al., 2007; Bibikova et al., 2006). A potential reason for loss of methylation may be due to relatively low expression level of endogenous DNMT1 in hESCs (Emma Lucas and Lorraine Young unpublished), although other potential factors (e.g. non-physiological culture conditions and *in vitro* environmental factors) might be involved in this (Allegrucci et al., 2004; Allegrucci et al., 2007; Steele et al., 2005). Thus, the aim of this Chapter was to determine whether increasing DNMT1 expression and its functional activity could prevent loss of methylation from spreading in the genome of hESCs during *in vitro* prolonged culture. In order to test this hypothesis, hESC lines overexpressing *DNMT1* cDNA (hESOD1 lines) were established.

5.3.1 The establishment of hESC lines overexpressing *DNMT1*

To establish cell lines stably expressing a specific transgene, the optimal choice of the promoter and backbone plasmid (or expression cassette) is critically required (Liew et al., 2007; Smith et al., 2008). Previous studies have demonstrated that the generation of long-term stably transfected mammalian ESC lines is difficult due to transcriptional silencing of transgene promoters mediated by DNA methylation-dependent or -independent mechanisms (Liew et al., 2007; Ren et al., 2006; Smith et al., 2008; Vallier et al., 2004a; Ying et al., 2003b). For example, enhanced green fluorescent protein (eGFP) expression mediated by the cytomegalovirus (CMV) immediate early promoter (pCMV) becomes silenced during the generation of stably transfected hESC lines (Liew et al., 2007). Furthermore, eGFP expression derived by other mammalian promoters including pUbiC (human UbiquitinC), pR26 (ROSA26) and pCAGG (chicken β-actin/rabbit β-globin gene hybrid promoter) in hESC and human embryonal carcinoma (EC) lines is substantially lost during *in vitro* culture (Liew et al., 2007). DNA methylation-dependent promoter silencing of exogenously expressed retroviral vectors has been reported in mESCs, mouse EC cells and hESCs (Jahner et al., 1982; Kameda et al., 2006; Stewart et al., 1982).

However, hESC lines stably expressing eGFP have been successfully established using the pCAG-eGFP-IRES-PAC plasmid containing a chicken β-actin/cytomegalovirus (CMV) hybrid promoter (pGAG) linked to a polyma virus mutant enhancer (PyF101), an internal ribosome entry site (IRES) and a puromycin N-acetyltranferease (PAC) resistant gene (Denning et al., 2006; Liew et al., 2007; Vallier et al., 2004b). Liew et al., (2007) has pointed out that PyF101 acts as an enhancer that is essential for maintaining stable transgene expression in hESC lines. Thus, in this Chapter, the pCAG-eGFP-IRES-PAC plasmid was selected as a vehicle to carry 5.2 kb of a full-length *DNMT1* cDNA into the genome of HUES7. pCAG-hDNMT1-IRES-PAC and pCAG-DsRed2-C1-hDNMT1-IRES-PAC plasmids were generated and transfected into HUES7. Following puromycin selection, 9 cell lines overexpressing exogenous *DNMT1* (hESOD1 lines) were indentified by Western blot, indicating that an exogenously expressed *DNMT1* cDNA was stably integrated into the genome of HUES7, transcribed and translated. Moreover, these cell lines showed increased maintenance DNMT activities as measured *in vitro* with a hemimethylated oligonucleotide as substrate, indicating that the translated protein targeted to hemimethylated CpG dinucleotides in nuclei and functionally worked as a maintenance methyltransferase. Furthermore, Western blot analysis revealed that hESOD1 cell lines were propagated with exogenous *DNMT1* expression during further 30 passages, indicating that no transcriptional silencing of pCAG promoter. Thus, the pCAG-eGFP-IRES-PAC plasmid was suitable for the generation of hESC lines stably expressing a specific transgene.

In mESCs and human fibroblast cells, previously, cell lines overexpressing exogenous *DNMT1* have been established, showing both increased DNMT1 protein levels and DNMT activities (Biniszkiewicz et al., 2002; Vertino et al., 1996). Interestingly, human fetal lung fibroblast (IMR90/SV40) cell lines overexpressing *DNMT1* (HMT lines) show ~ 50 fold increased DNMT1 protein level and DNMT activity (Vertino et al., 1996). However, the mESC line overexpressing *Dnmt1* (*Dnmt1*$^{+/+;BAC}$) shows only ~ 4 fold increased Dnmt1 protein level and ~ 2.5 fold increased Dnmt activity (Biniszkiewicz et al., 2002). In this Chapter, similar to a mouse study, hESOD1 cell lines produced ~ 3.5 fold increased amounts of DNMT1 protein and they had ~ 2.5 fold increase in maintenance DNMT activity. The underlying mechanisms of differences in DNMT1 protein levels and enzymatic activities between embryonic

stem cells and fibroblast cells are not known. However, it can be suggested that embryonic stem cells have a more limited ability to express a transgene than fibroblast cells. This could be associated with developmental stage- or tissue-specific chromatin condensation (Bernstein et al., 2005; Bibikova et al., 2008; Frigola et al., 2006; Ohm et al., 2007).

Two plasmids were generated in this Chapter. 1) The pCAG-hDNMT1-IRES-PAC plasmid contains a 5.2 kb full-length cDNA of human *DNMT1* which is inserted into *EcoR*I restriction sites in the place of eGFP of p336, and 2) the pCAG-DsRed2-C1-hDNMT1-IRES-PAC plasmid contains a 5.9kb DsRed2 conjugated *DNMT1* cDNA which is inserted into *Pme*I and *Age*I restriction sites of p388. Interestingly, cells transiently transfected by pCAG-DsRed2-C1-hDNMT1-IRES-PAC had DsRed2 signals detected in nuclei using fluorescence microscopy. However, following the puromycin selection for ~ 4 weeks, established cell lines (hESOrD1 cell lines) showed no DsRed2 signals, although exogenous *DNMT1* was still expressed, as determined by Western blot. In the pCAG-DsRed2-C1-hDNMT1-IRES-PAC plasmid, DsRed2 coding sequences lie downstream of pCAG promoter and upstream of DNMT1 cDNA (see Figure 5-3 and 5-4). Thus, it was expected that both DsRed2 and exogenous DNMT1 were simultaneously expressed in nuclei. If the pCAG promoter is transcriptionally silenced by either DNA methylation-dependent or -independent mechanism, neither protein can be produced. However, in hESOrD cell lines, only exogenous *DNMT1* expression was detected, implying that other mechanisms may be involved in the transcriptional silencing of DsRed2. Thus, hESOrD cell lines were excluded from further studies.

5.3.2 Stem cell characteristics and proliferation

The inactivation or overexpression of *Dnmt1* in mESCs did not interfere with the maintenance of an undifferentiated state of the cells (Biniszkiewicz et al., 2002; Chen et al., 2003; Jackson et al., 2004; Li et al., 2007). For example, transcription factors such as *Oct3/4* and *Nanog* were stably expressed in *Dnmt1* deficient mESCs ($Dnmt1^{n/n}$ and $Dnmt1^{c/c}$ J1 ES cells) and mESCs overexpressing *Dnmt1* ($Dnmt1^{+/+;BAC}$) and remained unmethylated at their promoters (Biniszkiewicz et al., 2002; Chen et al., 2003; Jackson et al., 2004; Li et al., 2007). Moreover, they have no morphology changes and can be *in vitro* propagated as wild-type ESCs. In this chapter, Western

blot and immunostaining analyses revealed that normal expression patterns of OCT3/4, NANOG and SSEA4 upon *in vitro* culture (up to 30 passages). Furthermore, no phenotypic changes were detected in hESOD1 cell lines, showing prominent nucleoli and a high ratio of nucleus to cytoplasm, as expected. Thus, consistent with a previous finding in mESCs (Biniszkiewicz et al., 2002), exogenously expressed *DNMT1* in hESCs did not interfere with stem cell characteristics and their phenotypic changes upon *in vitro* culture.

It has been reported that *Dnmt1* is critically involved in cellular differentiation of mESCs (Biniszkiewicz et al., 2002; Jackson et al., 2004; Li et al., 2007). The deletion of *Dnmt1* in mESCs leads to the failure of the formation of embryoid bodies (EBs) and differentiation into hematopoietic and cardiac lineages (Jackson et al., 2004). *Oct3/4* and *Nanog* were still expressed in differentiated *Dnmt1*$^{c/c}$ J1 ES cells, and they were unmethylated at their promoters (Li et al., 2007). In addition, differentiation-specific (trophoblast, mesodermal and endodermal) markers were abnormally expressed in differentiated *Dnmt1*$^{c/c}$ J1 ES cells (Jackson et al., 2004). Moreover, embryonic lethality has been reported as a consequence of overexpression of exogenous *Dnmt1* in mESCs (Biniszkiewicz et al., 2002). This indicates that appropriate *DNMT1* expression is essential lineage-specific differentiation of mESCs (Biniszkiewicz et al., 2002; Jackson et al., 2004; Li et al., 2007). In this Chapter, all studies were performed with undifferentiated hESOD1 cell lines. Now, differentiation studies are required to examine whether *DNMT1* dosage plays an important role for tissue-specific differentiation in hESCs.

Even with no detectable morphology changes and embryonic stem cell characteristics, growth rates were affected in hESOD1 cell lines. hESOD1 cell lines took longer to expand *in vitro*, compared to control cell lines. Control cell lines took for ~ 3 days to be confluent into T25 flasks, whereas hESOD1 cell lines took for ~ 3.5 to 4 days. Thus, in this Chapter, population doubling (PD) time was analysed between cell lines over 12 days in culture. Consistent with previous reports (Allegrucci et al., 2007; Cowan et al., 2004; Denning et al., 2006), the PD time of HUES7 p22 and control cell lines was ~ 60 h. However, the PD time of hESOD1 cell lines was ~ 70 h so that there are ~ 10 h differences between control and hESOD1 lines. Similar results have been reported in human fibroblast cell lines overexprsesing *DNMT1* (HMT cell lines)

(Vertino et al., 1996). The PD time of control cell lines (NEO cell lines) were ~ 28 h, whereas that of HMT cell lines were ~ 40 h (Vertino et al., 1996). One possibility to explain prolonged PD times in hESOD1 and HMT cell lines is that exogenous *DNMT1* cDNA may integrate into some loci related to cellular growth and cell cycle that interferes with normal gene expression within these loci. This, in turn, may lead to the perturbation of normal cell cycle and cell proliferation. Indeed, flow cytometry analysis of DNA content, in this Chapter, revealed that hESOD1 cells showed ~ 20% increased proportion of cells in G2-M phases, compared to control cell lines, and ~ 8% decreased proportion of cells in S phase, suggesting that prolonged PD times in hESOD1 cell lines may be associated with impaired cell cycle. The alteration of cell cycle has been reported to be associated with the abnormal expression of cell cycle related genes such as Cyclin B1, Cyclin E and PCNA (proliferating cell nuclear antigen) (Chen et al., 2007). Thus, it is now required to determine how cell cycle regulators are expressed in hESOD1 cell lines.

5.3.3 DNA methylation changes

The inactivation and overexpression of *Dnmt1* in mESCs lead to the perturbation of DNA methylation patterns at imprinting regulatory regions that is associated with loss of imprinting of their relative genes (Biniszkiewicz et al., 2002; Jackson-Grusby et al., 2001; Li et al., 1993). Thus, in this Chapter, the DNA methylation status at 14 imprinting regulatory regions was analysed in hESOD1 cell lines by combined bisulphite restriction analysis (COBRA). Inconsistent with a previous study (Biniszkiewicz et al., 2002), of 14 regions examined, none showed DNA methylation changes in hESOD1 cell lines. There are three possible ways to explain this. One is that ~ 3 fold increased expression of exogenous *DNMT1* and ~ 2 fold increased maintenance DNMT activity could not be enough to induce DNA methylation changes at imprinting regulatory regions. Secondly, stably established imprints during gametogenesis and embryogenesis may not be susceptible to DNA methylation changes caused by overexpression of exogenous *DNMT1* (Murrell, 2006; Reik and Walter, 2001; Surani, 2001). Thirdly, methylation-sensitive biding factors (e.g. CTCF, YY1, MBDs), which tightly bind to either the unmethylated or methylated allele of imprinting regulatory regions (Donohoe et al., 2007; Fitzpatrick et al., 2007; Hark et al., 2000; Kim et al., 2006; Schoenherr et al., 2003), may inhibit exogenous DNMT1 from accessing into imprinting regulatory regions.

Vertino et al., (1996) and Feltus et al., (2003) have demonstrated that the overexpression of exogenous *DNMT1* in human fibroblast cells is associated with tumour progression though transcriptional silencing of some tumour-suppressor genes guided by hypermethylation at their promoters. Moreover, the overexpression of endogenous *DNMT1* is frequently found in human cancers including gastric, cervix and pancreatic cancers (Etoh et al., 2004; Peng et al., 2006; Sawada et al., 2007). This is associated with transcriptional silencing of some tumour-suppressor genes mediated by hyperemthylation at their promoters (Etoh et al., 2004; Peng et al., 2006; Sawada et al., 2007). Thus, in this Chapter, DNA methylation at 10 previously reported tumour-suppressor gene promoters was analysed by methylation-specific PCR (MSP). Consistent with a previous study (Vertino et al., 1996), gain of methylation was detected at three gene promoters (*TIMP-3*, *MGMT* and *DAPK-1*) in hESOD1 cell lines, but others showed no DNA methylation changes, indicating locus-specific DNA methylation changes caused by overexpression of exogenous *DNMT1*. Moreover, DNA methylation changes accumulated at *MGMT* and *DAPK-1* promoters during *in vitro* culture from p30 to p45, suggesting that overexpression of *DNMT1* in hESCs can promote time-dependent accumulation of DNA methylation at some gene promoters.

Interestingly, RT-PCR analysis revealed that *TIMP*-3 and *MGMT* genes in hESOD1 were similarly expressed to control cell lines, although their promoters were methylated, indicating no association DNA methylation and their gene expression. There are two possibilities to explain this. One is that DNA methylation alone induced by exogenous *DNMT1* is not sufficient to mediate transcriptional silencing of TSGs. Other factors or co-repressors may be required for this. Indeed, previous reports have suggested that both histone H3 methylated Lys27 (H3K27) and Lys9 (H3K9) need to be co-operated with DNA hypermethylation to mediate transcriptional silencing of TSGs (Calvanese et al., 2008; Ohm et al., 2007). Another possibility is that DNA methylation has not been expanded into transcriptional regulatory regions of *TIMP*-3, *MGMT* and *DAPK1* genes. Thus, this allows their expression in hESOD1 cell lines. Indeed, the MSP analysis employed in this thesis allows to examine about 100 bp (few CpG dinucleotides) of TSG promoters (Table 2-6). Therefore, more upstream or downstream regions need to be examined to identify this possibility.

The overexpression of *Dnmt1* in mESC gives rise to genome-wide hypermethylation at minor centromeric repeats, endogenous C-type retrovirus repeats (pMO), minor and major satellite repeats and IAP elements, as confirmed by Southern blot (Biniszkiewicz et al., 2002; Chen et al., 2003). Thus, in this Chapter, the DNA methylation status at LINE1, Satellite 2 and Satellite 3 was analysed. Southern blot analysis revealed that three regions showed no particular DNA methylation changes in both control and hESOD1 cell lines. All cell lines including control cell lines were hypermethylated at these repetitive sequences. Because, in the human genome, ~ 80% CpG dinucleotides are normally hypermethylated (Lander et al., 2001; Venter et al., 2001), it was difficult to discriminate DNA methylation changes by Southern blot. Thus, more sensitive approaches such as bisulphite sequencing and Hairpin-bisulphite PCR are required to determine DNA methylation changes in a genome-wide level. Alternatively, the RLGS technique and epigenome-sequencing might be useful to determine this.

In this Chapter, the restriction landmark genome scanning (RLGS) technique was performed to examine an overview of DNA methylation changes between control and hESOD1 cell lines upon *in vitro* culture. Of ~2,200 CpG loci examined, 6 CpG loci were identified to be hypermethylated or demethylated in p388#9 p45 (compared to HUES7 p22), indicating *in vitro* culture induced DNA methylation changes over 23 passages. This was consistent with previous finding in hESCs (Allegrucci et al., 2007). However, only 2 loci appeared to be hypermethylated or demethylated in hESOD1 cell lines p45 (against HUES7 p22), indicating that overexpression of exogenous *DNMT1* in hESCs resulted in increased epigenetic stability. However, only one cell line (HUES7), which is previously characterised to be epigenetically stable relative to other cell lines, as described in Chapter 3 and 4, and Allegrucci et al., (2007), was employed and more studies are required for conclusive proof.

5.3.4 Further works needed

In this Chapter, all studies were performed with undifferentiated control and hESOD1 cell lines. Thus, *in vitro* differentiation studies are required to examine how the *DNMT1* dosage is involved in tissue-specific differentiation of hESCs. The karyotype

analysis was not performed in this Chapter. This is also required to identify karyotypic stability of hESOD1 upon *in vitro* culture.

6 SUMMARY AND DISCUSSION

6.1 Imprinting instability in Human embryonic stem cell lines

This thesis has demonstrated that human embryonic stem cell (hESC) lines have altered imprinted gene expression that can be mediated by aberrant DNA methylation at their imprinting regulatory regions (Chapter 3 and 4). Preliminary studies of 10 imprinted genes in 1 to 6 informative cell lines (in total 9 individually established cell lines examined) have suggested that hESC lines possess a substantial degree of imprinting stability in both the differentiated and undifferentiated state (Mitalipov, 2006; Plaia et al., 2006; Rugg-Gunn et al., 2005; Sun et al., 2006). In this thesis, however, imprinting instability can be readily detected by increasing the number of cell lines and imprinted genes analysed (Chapter 3). Of 22 potential imprinted genes examined in 1 to 12 informative cell lines (in total 22 hESC lines examined), 9 genes (*PEG10*, *PEG1*, *MESTIT1*, *IGF2*, *H19*, *GTL2*, *NESP55*, *PHLDA2* and *ATP10C*) showed variable allele-specific expression between cell lines, but other 12 genes (*KCNQ1OT1*, *NDN*, *NDNL1*, *SNRPN*, *IPW*, *PEG3*, *KCNQ1*, *CDKN1C*, *TP73*, *IGF2R*, *WT1* and *SLC22A18*) showed consistent allele-specific expression in hESC lines, indicating that genomic imprinting can be disrupted in a gene-specific manner. This was consistent with a recent report of 10 imprinted genes in 3 to 24 informative cell lines (total 49 individually established cell lines examined), 6 genes (*IGF2*, *PEG1*, *H19*, *NESP55*, *GTL2* and *SLC22A18*) showed imprinting disruptions and variations between cell lines (Adewumi et al., 2007). Furthermore, in this thesis, DNA methylation was examined at 12 potential imprinting regulatory regions to indentify an association between the variability observed in interline allele-specific expression status and DNA methylation (Chapter 4). The allele-specific expression of 8 imprinted genes (*TP73*, *PEG10*, *PEG1 isoform1*, *SLC22118*, *CDKN1C*, *KCNQ1OT1*, *KCNQ1* and *NESP55*) was associated with DNA methylation patterns at 6 regions (*TP73* promoter, *PEG10* DMR, *PEG1* DMR, *SLC22A18* promoter, *KvDMR1* and *NESP55* DMR). However, DNA methylation patterns at *IGF2*, *GLT2* and *NDN* DMRs were not associated with the allele-specific expression of their corresponding genes. This indicates that DNA methylation does not regulate the allele-specific expression of some imprinted genes.

6.2 How imprinting is variable and unstable in hESC lines?

Currently, the underlying mechanism how genomic imprinting can be disrupted in hESC lines is not clear. However, there are at least two possible ways to explain this, based on a larger number of studies in various animal species. (1) Genomic imprinting in hESC lines can be disrupted due to *in vitro* culture conditions. (2) Imprinting errors in hESC lines can be originated from donor embryos fertilised and cultured *in vitro*.

6.2.1 Imprinting errors caused by *in vitro* culture conditions

Once hESC lines are derived from human blastocyst stage embryos, they need to be *in vitro* propagated in medium to obtain sufficient cells for freezing, characterising, and further expanding (reviewed by Allegrucci and Young, 2007; Fenno et al., 2008; Hoffman and Carpenter, 2005; Laslett et al., 2003). Sometimes, they need to be long-term cultured in medium for the purpose of scientific research. According to previous studies observed in preimplantation stage mouse embryos, mESCs and monkey ESCs, detrimental effects on the stability of imprinting caused by *in vitro* culture medium containing fetal bovine serum (FBS) and insufficient amino acids have been reported (Dean et al., 1998; Feil et al., 1997; Fujimoto et al., 2006; Humpherys et al., 2001; Mitalipov et al., 2007). For instance, imprinted gene expression and DNA methylation appear to be variable and unstable upon derivation and subsequent propagation of mouse and monkey ESC lines, as a consequence of culture medium containing fetal bovine serum (FBS) (Dean et al., 1998; Feil et al., 1997; Fujimoto et al., 2006; Mitalipov et al., 2007). Moreover, the lack of methionine and other amino acids supplements supplied in culture medium causes altered imprinted gene expression and DNA methylation in preimplantation stage mouse embryos (Doherty et al., 2000; Mann et al., 2004; Rinaudo and Schultz, 2004). These evidences implicates that hESC lines can have imprinting instability, when they are cultured in media containing non-physiological levels of amino acids and FBS (or serum replacement, KSR) (reviewed by Allegrucci et al., 2005).

Currently, hESC lines are cultured in media containing 15 ~ 20% of FBS or 5 ~ 20% of KSR (reviewed by Allegrucci et al., 2005). Moreover, current media, DMEM (Dulbecco's modified Eagle medium), KO-DMEM and DMEM-F12, for culturing hESC lines contain non-physiological levels of amino acids and vitamins (Allegrucci

et al., 2005; Steele et al., 2005). Specifically, these media contain 500 ~ 1500 fold physiological concentration of methionine/folate cycle components (including methionine, folate, vitamin B_6, B_{12}, selenium, betaine and polyamines) (Allegrucci et al., 2005; Steele et al., 2005). Thus, these components may influence DNA methylation alterations of hESC lines cultured in it (Allegrucci et al., 2005; Steele et al., 2005). Previously, Alexandra Thurston (University of Nottingham) and Cinzia Allegrucci (University of Nottingham) have examined the effect of methyl cycle components on the DNA methylation status at imprinting regulatory regions in HUES7 and BG01. They are cultured up to 5 passages (~ 20 days) in either medium containing supra-physiological levels of methionine/folate cycle components (named as HMG) or custom-made KO-DMEM medium containing physiological levels of these components (named as PMG). Interestingly, most CpG dinucleotides within the *PEG3* DMR retained basic methylation levels and few CpG dinucleotides became hypomethylated in cell lines cultured in PMG, whereas some CpG dinucleotides within the region became hypermethylated in cell lines cultured in HMG, (Alexandra Thurston Ph.D. thesis 2006). This indicates that supra-physiological levels of methionine/folate cycle components in culture may lead to hypermethylation at some CpG dinucleotides within imprinting regulatory regions (Allegrucci et al., 2007; Steele et al., 2005). In this thesis, gain of methylation was detected at the *GTL2* DMR in both HES-2 and HESC-NL1 cell lines cultured up to ~ 40 passages in the HMG medium. In addition, hypermethylation at certain CpG islands, tumour-suppressor gene promoters and one imprinted locus (*H19* DMR) has been reproted in additional 21 hESC lines (including H1, HES-3 and Shef-1) cultured in DMEM based media across a range of studies (Allegrucci et al., 2007; Bibikova et al., 2006; Calvanese et al., 2008; Maitra et al., 2005; Rugg-Gunn et al., 2005). Thus, the current culture system is not able to maintain normal DNA methylation patterns in the genome of hESCs. Thus, optimal culture systems need to be developed possibly to reflect the *in vivo* environment of blastocyst cells.

6.2.2 Imprinting errors inherited from donor embryos.

hESC lines, derived from the inner cell masses (ICMs) of human embryos fertilised and cultured *in vitro* up to the blastocyst stage, can have imprinting errors originated from the donor embryos (Allegrucci et al., 2004; Pannetier and Feil, 2007; Rugg-Gunn et al., 2007). According to previous studies, imprinting can be disrupted in

oocytes and preimplantation stage embryos, when assistant reproductive technology (ART) procedures (including superovulation, *in vitro* maturation, *in vitro* culture, *in vitro* fertilisation) are applied (Doherty et al., 2000; Fortier et al., 2008; Kerjean et al., 2003; Khosla et al., 2001a; Li et al., 2005b; Mann et al., 2004; Sato et al., 2007; Young et al., 2001). For example, preimplantation stage mouse embryos fertilised and cultured *in vitro* result in biallelic expression of imprinted genes mediated by loss of methylation at their imprinting regulatory regions, whereas *in vivo* derived embryos show monoallelic expression of imprinted genes mediated by monoallelic methylation at their imprinting regulatory regions (Doherty et al., 2000; Khosla et al., 2001a; Li et al., 2005b; Mann et al., 2004). Moreover, human and mouse oocytes show that aberrant DNA methylation patterns at some imprinting regulatory regions have been detected, as a consequence of superovulation (Fortier et al., 2008; Sato et al., 2007). These studies have suggested that ART procedures can accelerate oocyte and embryo growth that may interfere with establishment and maintenance of imprints during oogenesis and embryogenesis (reviewed by Horsthemke and Ludwig, 2005; Lucifero et al., 2004a; Maher, 2005). In this manner, human oocytes and embryos can have epigenetic errors at imprinted loci, when they are superovulated, and *in vitro* fertilised and cultured (Allegrucci et al., 2004). Subsequently, these errors could be stably inherited in hESC lines during the progression of derivation and propagation. To test this possibility, the comparative analysis of allele-specific expression of imprinted genes and DNA methylation at imprinting regulatory regions is required between *in vitro* and *in vivo* derived human blastocyst stage embryos that may be limited by the availability of embryos due to practical and ethical issues.

Other factors (e.g. embryo quality and cryopreservation) related to donor embryos can be suggested to be involved in epigenetic errors at imprinted loci in hESC lines. Currently, most hESC lines have been derived from supernumerary, low-grade fresh and/or frozen blastocyst stage embryos donated from infertile couples who underwent IVF treatment (reviewed by Allegrucci and Young, 2007; Hoffman and Carpenter, 2005). In fact, almost all cell lines used in this thesis are generated from low-grade fresh and/or frozen embryos. Specifically, Reubinoff et al., (2002) has used 4 of low-grade (3CC to 5CB classified by Gardner et al., (2000)) and frozen blastocyst stage embryos to establish HES-1 and HES-2 cell lines. Moreover, Cowan et al., (2004) has used 344 of frozen low-grade (3AA to 4CB) blastocyst stage embryos to derive 17

HUES-cell lines. The BG01 cell line is derived from a fresh 3CC blastocyst stage embryo (Mitalipova et al., 2003). So far, a direct evidence has not been reported whether the embryo quality and cryopreservation are more likely susceptible to epigenetic alterations at imprinted loci, than high-quality and fresh embryos. However, studies observed in mouse sperm and mESCs demonstrate that epigenetic alterations can occur at both imprinted and non-imprinted loci, as a consequence of cryopreservation and its related chemical, dimethyl sulfoxide (DMSO; an amphipathic molecule) (Fernandez-Gonzalez et al., 2008; Iwatani et al., 2006). Moreover, a recent study in mice has demonstrated that aged oocytes in the ovary are more likely associated with loss of methylation at imprinting regulatory regions, than young oocytes (Liang et al., 2008). Thus, the quality of oocytes and embryos and cryopreservation procedures could be one of factors to give a rise to epigenetic errors at imprinted loci in donor embryos that can be inherited into hESC lines.

During derivation of hESC lines, possibly they can acquire epigenetic errors at imprinted loci, because of the procedures used during derivation that may be physically and chemically detrimental to the donor embryos (Solter and Knowles, 1975). In addition, the procedures are also progressed on medium containing either KSR or FBS (Cowan et al., 2004; Inzunza et al., 2005; Mitalipova et al., 2003; Reubinoff et al., 2000; Richards et al., 2002; Simon et al., 2005), that may be also involved in epigenetic errors at imprinted loci. For instance, in order to derive 17 HUES-lines, 97 inner cell masses (ICMs) were isolated from 344 blastocyst stage embryos in medium containing 8 ~ 10% KSR, 8 ~ 10% plasmate, 5% FBS, LIF and bFGF (Cowan et al., 2004). Reubinoff et al., (2000) has used medium containing 20% FBS and LIF for isolating 4 ICMs from 4 blastocyst stage embryos to establish HES-1 and HES-2 cell lines. VAL-1 and VAL-2 cell lines have been established from 14 ICMs isolated from 16 blastocyst stage embryos in medium containing 20% KSR and bFGF (Simon et al., 2005). Furthermore, to remove zona pellucidae (ZP) and to isolate ICMs from blastocyst stage embryos, Reubinoff et al. (2000), Richards et al. (2002), Mitalipova et al. (2003) and Inzunza et al. (2005) have used pronase and immunosurgery and Cowan et al. (2004) has used Tyrode's acid and immunosurgery. Currently, a direct evidence has not been reported whether these procedures and their related chemicals (including antibodies) can cause epigenetic errors at imprinted loci in human embryos. However, mouse studies have demonstrated that ZP-free mouse

embryos removed by pronase show a significant reduction in DNA methylation (5-methylcytosine) level, compared to mechanical isolated ZP-free embryos (Ribas et al., 2006). Moreover, the methylation analysis of immunosurgically isolated mouse ICMs shows the loss of methylation at imprinting regulatory regions (Mann et al., 2004). Thus, these factors may be also associated with epigenetic errors at imprinted loci in donor embryos that may be inherited into hESC lines.

6.3 Is it important to have epigenetic stability in hESC lines?

Most imprinted genes are expressed in a dosage-dependent manner (reviewed by Constancia et al., 2004; Ferguson-Smith and Surani, 2001; Reik and Walter, 2001). Thus, loss or gain of stable imprinting, resulting in biallelic expression or monoallelic expression, changes the dosage of corresponding gene products and their relevant enzymatic activities that may interfere with the expression of their downstream or upstream genes in mammalian cells (reviewed by Feinberg, 2007; Jaenisch and Bird, 2003; Rugg-Gunn et al., 2007). Eventually, this may lead to abnormal cell proliferation and differentiation, and various diseases including cancers and congenital disorders (e.g. BWS, PWS and AS) during mammalian development (reviewed by Jelinic and Shaw, 2007; Murrell, 2006; Robertson, 2005). For example, overexpression of certain imprinted genes in mESCs results in myogenic differentiation (Prelle et al., 2000). Moreover, inappropriate expression of imprinted genes in preimplantation mouse embryos and mESCs causes phenotypic abnormalities (including polyhydramnios and interstitial bleeding), embryonic lethality and tumourigenesis in their derived foetuses (Dean et al., 1998; Fernandez-Gonzalez et al., 2004; Khosla et al., 2001a; Mann et al., 2004; Okano et al., 1999). In this thesis, the analysis of allele-specific expression revealed that 9 genes (*PEG10*, *PEG1*, *MESTIT1*, *IGF2*, *H19*, *GTL2*, *NESP55*, *PHLDA2* and *ATP10C*) appeared to be unstable or variable between cell lines (Table 3-3 and 3-4). Importantly, these genes are previously identified to have an important role in embryonic development, congenital disorders, tumorigensis and lineage-specific differentiation (Table 1-3 and section 1.3.5). Although developmental consequences of altered imprinted gene expression and DNA methylation in hESC lines were not examined in this thesis, it can be suggested that some cell lines having imprinting errors may readily be more spontaneously differentiated or tumorigenic, when they are *in vitro* long-term cultured or transplanted. Thus, 12 cell lines (HUES1, HUES2, HUES5, HUES6, HUES7,

HUES9, HUES15, HUES16, HESC-NL1, HES-2, NOTT1 and NOTT2), which exhibit imprinting errors at more than one locus (Chapter 3 and 4), might be excluded for human therapeutic applications. Alternatively, however, these cell lines can be a model for understanding mechanisms of certain human diseases and a material for pharmaceutical screening.

Currently, over 400 hESC lines are presumed to have been established over 20 countries (reviewed by Allegrucci and Young, 2007; Fenno et al., 2008; Hoffman and Carpenter, 2005). Under appropriate conditions, they can have the potential to differentiate into all cell types of the human body that may use for treating a wide range of human diseases (reviewed by Pera, 2001; Thomson and Odorico, 2000; Unger et al., 2008). However, before they are considered to use for human therapeutic purpose, genetically, karyotypically and epigenetically unstable cell lines should be excluded. In order to screen this, established hESC lines need to be fully characterised using previously reported 6 criteria, including hESC-specific markers (e.g. SSEA-3 and SSEA-4), transcription factors (e.g. OCT3/4 and NANOG), karyotyping, telomerase activity, teratoma formation and *in vitro* differentiation into three germ layers (endoderm, mesoderm and ectoderm) (reviewed by Allegrucci and Young, 2007; Hoffman and Carpenter, 2005; Laslett et al., 2003). This may allow to determine which hESC lines have proliferative, pluripotency, differentiative capacities and karyotypic stability. In addition, genetic alterations and variations need to be identified by analysing in nuclear DNA copy numbers and mitochondrial DNA sequences (Maitra et al., 2005; Wu et al., 2008). Finally, it is very important to know the occurrence of epigenetic instability in hESC lines upon *in vitro* culture. This can be determined by additional 6 criteria; (1) variations and alterations in allele-specific expression of imprinted genes, (2) aberrant DNA methylation at imprinting regulatory regions, (3) aberrant DNA methylation and transcriptional silencing of tumour-suppressor genes, (4) altered DNA methylation at repetitive sequences, (5) perturbation of X-chromosome inactivation and (6) altered expression of epigenetic regulators (e.g. *DNMTs*, *G9A* and *HDACs*) (Adewumi et al., 2007; Bibikova et al., 2006; Calvanese et al., 2008; Maitra et al., 2005; Rugg-Gunn et al., 2005; Shen et al., 2008).

hESC lines and their derivatives are limited by the problem of immune rejection (reviewed by Allegrucci and Young, 2007; Hoffman and Carpenter, 2005; Unger et al., 2008). The rejection can be inhibited or prevented by immunosuppressive medications (Chidgey et al., 2008). However, these medications can have serious side effects and are so expensive (Chidgey et al., 2008). Thus, recently, patient-specific pluripotent stem cell lines have been established using various reprogramming approaches (e.g. parthenogenesis and cell fusion) in the human (Cowan et al., 2005; Revazova et al., 2007) that may avoid the problem of immuno rejection. However, there are at least three limitations to utilise these cell lines as therapeutic materials; (1) the low efficiency of reprogramming somatic cells, (2) chromosomal duplication (tetraploid) and (3) epigenetic instability at imprinted loci (Humpherys et al., 2001; Lee et al., 2002) that are not acceptable for safe human transplantation. Very recently, moreover, induced pluripotent stem (iPS) cell lines have been derived from somatic cells (e.g. lung and dermal fibroblasts) by viral introduction of transcriptional factors including *OCT3/4* and *SOX2* with either *NANOG* and *LIN28* (Yu et al., 2007), or *c-MYC* and *KLF4* (Park et al., 2008; Takahashi et al., 2007). However, these cell lines also have several limitations; (1) the low efficiency, (2) the integration of viral transgenes and (3) the use of oncogenes (e.g. *c-MYC*). Furthermore, it has not been defined yet whether iPS cell lines epigenetically stable upon *in vitro* derivation and propagation. Thus, this is urgently required.

6.4 Can epigenetic stability be repaired by overexpression of exogenous DNMT1?

In addition to the imprinting instability uncovered in this thesis, previous works in our laboratory (Allegrucci et al., 2007; Emmas Lucas and Alexandra Thurston Ph.D. theses) and this thesis (Chapter 4) have shown epigenetic instability in various genomic regions. To test whether this was due to insufficient expression of the maintenance methyltransferase, DNMT1, overexpression was used to examine whether epigenetic stability can be repaired at imprinting regulatory regions, tumour-suppressor gene promoters, repetitive sequences and certain CpG islands (Chapter 5).

Previously, DNA methylation changes (particularly loss of methylation) at certain CpG loci related to developmental genes, cancer-related genes, ribosomal DNA and cell cycle regulators are readily detected in *in vitro* cultured hESC lines (Allegrucci et

al., 2007; Bibikova et al., 2006). Some of these changes accumulate over extended culture, but most of them are already detected at early passages (Allegrucci et al., 2007; Bibikova et al., 2006; Calvanese et al., 2008). This indicates that even short period in *in vitro* culture is sufficient to cause DNA methylation at some CpG loci in hESC lines. Currently, the underlying mechanisms for this are not clear, but one possibility is that relatively low expression of endogenous *DNMT1* in hESCs (compared to mESCs and human BJ fibroblast cells) may fail to maintain DNA methylation patterns at some CpG islands during *in vitro* culture (Emmas Lucas Ph.D. thesis 2008), although *de novo* methyltransferases, *DNMT3A* and *DNMT3B*, are highly expressed (Adewumi et al., 2007; Sperger et al., 2003 and Emmas Lucas Ph.D. thesis 2008). Thus, in this thesis, 8 hESOD1 (human embryonic stem cells overexpressing DNMT1) cell lines were generated by utilising a transgenic approach, in order to test this possibility (Chapter 5).

The restriction landmark genome scanning (RLGS) technique was performed to examine an overview of DNA methylation changes between control (only endogenous DNMT1 expressed) and hESOD1 cell lines (both endogenous and exogenous DNMT1 expressed) upon *in vitro* culture. Of ~2,200 CpG loci examined, 6 CpG loci were identified to be hypermethylated or demethylated in p388#9 p45 (against HUES7 p22), indicating *in vitro* culture induced DNA methylation changes over 23 passages. However, only 2 loci appeared to be hypermethylated or demethylated in hESOD1 cell lines p45 (against HUES7 p22). These evidences indicate that overexpression of exogenous *DNMT1* in hESCs results in increased epigenetic stability. Unfortunately, however, of other imprinting regulatory regions, tumour-suppressor gene promoters and repetitive sequences examined by combined bisulphite restriction analysis (COBRA), methylation-specific PCR (MSP) and Southern blot, no supporting evidences of this were detected. Moreover, only one cell line (HUES7), which is previously known to be epigenetically stable upon *in vitro* culture, was employed in Chapter 5 that is too limited to be able to conclude this (Allegrucci et al., 2007). Thus, more cell lines are needed to be examined for conclusive proof. HUES5, HUES15 and BG01, which are characterised to be epigenetically unstable upon *in vitro* culture (see Chapter 3, 4 and Allegrucci et al., 2007), may be the best cell lines to follow up this possibility and conclusion.

6.5 Hypermethylation caused by overexpression of DNMT1

Previously, HMT cell lines have been generated in human lung fibroblast cells by overexpressing *DNMT1* cDNA (Vertino et al., 1996). In HMT cell lines, hypermethylation caused by overexpression of exogenous *DNMT1* is defined by Southern blot and RLGS analyses (Feltus et al., 2003; Vertino et al., 1996). Of 12 tumour-suppressor gene (TSG) promoters examined by Sothern blot, 5 TSG (*ER*, *HIC-1*, *a-globin*, *CDH1* and *Somatostatin*) promoters are hypermethylated or *de novo* methylated in HMT cell lines (Vertino et al., 1996). Moreover, of 1,749 CpG islands examined by RLGS, 373 CpG islands (21%) are identified to be hypermethylated or *de novo* methylated in HMT cell lines (Feltus et al., 2003). In the thesis, however, of 14 imprinting regulatory regions examined by COBRA, none showed DNA methylation changes in hESOD1 cell lines (Figure 5-15 and 5-16). Moreover, of 10 TSG promoters examined by MSP (Figure 5-17 and 5-18), only 3 TSG (*TIMP-3*, *MGMT* and *DAPK-1*) promoters were identified to be hypermethylated (or *de novo* methylated) in hESOD1 cell lines. Finally, of ~ 2,000 CpG islands examined by RLGS, only 1 locus (*TM7SF2*) was identified to be hypermethylated in hESOD1 cell lines. These evidences indicate most CpG loci examined in hESOD1 cell lines are resistant to hypermethylation or *de novo* methylation caused by overexpression of exogenous *DNMT1*. The underlying mechanism is not clear, but one possibility is that relatively low expression of exogenous *DNMT1* in hESOD1 cell lines, compared to HMT cell lines. Indeed, hESOD1 cell lines showed about 3.5-fold increased DNMT1 expression and its activity (Figure 5-9), whereas HMT cell lines showed over 50-fold increased DNMT1 expression and its activity (Vertino et al., 1996). This was consistent with a previous study of 6 imprinting regulatory regions and 3 non-imprinted loci examined in the *Dnmt1*$^{+/+;BAC}$ cell line (mouse J1 ES cell line overexpressing *Dnmt1*), exhibiting about 4-fold increased Dnmt1 protein level and over 2.5-fold increased Dnmt activity, only one imprinted locus is identified to be hypermethylated (Biniszkiewicz et al., 2002). Alternatively, HUES7 is epigenetically stable so that it may be not susceptible to DNA methylation alterations caused by overexpression of exogenous *DNMT1*. This possibility can also be confirmed by examining other cell lines (e.g. HUES5, HUES15 and BG01).

The overexpression of endogenous *DNMT1* is frequently found in various cancers associated with transcriptional silencing of some TSGs (e.g. *E-cadherin*, *MGMT* and

p16) mediated by hypermethylation at their promoters (Etoh et al., 2004; Peng et al., 2006; Sawada et al., 2007). Moreover, overexpression of exogenous *DNMT1* in human fibroblast cells is also associated with transcriptional silencing of some TGSs (e.g. *E-cadherin*, *HIC-1* and *Estrogen receptor*) mediated by hypermethylation at their corresponding promoters (Vertino et al., 1996). In this thesis, of 10 TSG promoters examined, almost all (except for *p16*) were unmethylated in HUES7. This was consistent with a previous report of 29 TSG promoters examined in H1 cell line, all were unmethylated (Ohm et al., 2007). However, when exogenous *DNMT1* was expressed in HUES7, particular three genes (*TIMP*-3, *MGMT* and *DAPK1*) promoters became hypermethylated or *de novo* methylated. Previously, these genes promoters are shown to be hypermethylated in various cancer cell lines and tumours (including brain, breast, colon, gastric and liver) (Ohm et al., 2007). Moreover, these genes are known to be associated with metastasis, invasion, angiogenesis, apoptosis and DNA repair in tumours (Akiyama et al., 2003; Dong et al., 2001; Evron et al., 2001; Herman et al., 1996; Imura et al., 2006; Zochbauer-Muller et al., 2001). Thus, hESOD1 cell lines could be a model for understanding mechanisms of tumour progression and a material for discovering and developing an anti-cancer medicine.

7 References

The American Association for Cancer Research Human Epigenome Task Force & European Union, Network of Excellence, Scientific Advisory Board (2008). Moving AHEAD with an international human epigenome project. Nature *454*, 711-715.

Aapola, U., Kawasaki, K., Scott, H.S., Ollila, J., Vihinen, M., Heino, M., Shintani, A., Minoshima, S., Krohn, K., Antonarakis, S.E., *et al.* (2000). Isolation and initial characterization of a novel zinc finger gene, DNMT3L, on 21q22.3, related to the cytosine-5-methyltransferase 3 gene family. Genomics *65*, 293-298.

Aapola, U., Liiv, I., and Peterson, P. (2002). Imprinting regulator DNMT3L is a transcriptional repressor associated with histone deacetylase activity. Nucleic Acids Res *30*, 3602-3608.

Aapola, U., Lyle, R., Krohn, K., Antonarakis, S.E., and Peterson, P. (2001). Isolation and initial characterization of the mouse Dnmt3l gene. Cytogenet Cell Genet *92*, 122-126.

Adewumi, O., Aflatoonian, B., Ahrlund-Richter, L., Amit, M., Andrews, P.W., Beighton, G., Bello, P.A., Benvenisty, N., Berry, L.S., Bevan, S., *et al.* (2007). Characterization of human embryonic stem cell lines by the International Stem Cell Initiative. Nat Biotechnol *25*, 803-816.

Akiyama, Y., Watkins, N., Suzuki, H., Jair, K.W., van Engeland, M., Esteller, M., Sakai, H., Ren, C.Y., Yuasa, Y., Herman, J.G., *et al.* (2003). GATA-4 and GATA-5 transcription factor genes and potential downstream antitumor target genes are epigenetically silenced in colorectal and gastric cancer. Mol Cell Biol *23*, 8429-8439.

Allegrucci, C., Denning, C., Priddle, H., and Young, L. (2004). Stem-cell consequences of embryo epigenetic defects. Lancet *364*, 206-208.

Allegrucci, C., Denning, C.N., Burridge, P., Steele, W., Sinclair, K.D., and Young, L.E. (2005). Human embryonic stem cells as a model for nutritional programming: an evaluation. Reprod Toxicol *20*, 353-367.

Allegrucci, C., Wu, Y.Z., Thurston, A., Denning, C.N., Priddle, H., Mummery, C.L., Ward-van Oostwaard, D., Andrews, P.W., Stojkovic, M., Smith, N., *et al.* (2007). Restriction landmark genome scanning identifies culture-induced DNA methylation instability in the human embryonic stem cell epigenome. Hum Mol Genet *16*, 1253-1268.

Allegrucci, C., and Young, L.E. (2007). Differences between human embryonic stem cell lines. Hum Reprod Update *13*, 103-120.

Amit, M., Carpenter, M.K., Inokuma, M.S., Chiu, C.P., Harris, C.P., Waknitz, M.A., Itskovitz-Eldor, J., and Thomson, J.A. (2000). Clonally derived human embryonic stem cell lines maintain pluripotency and proliferative potential for prolonged periods of culture. Dev Biol *227*, 271-278.

Amit, M., Shariki, C., Margulets, V., and Itskovitz-Eldor, J. (2004). Feeder layer- and serum-free culture of human embryonic stem cells. Biol Reprod *70*, 837-845.

Anderson, D., Self, T., Mellor, I.R., Goh, G., Hill, S.J., and Denning, C. (2007). Transgenic enrichment of cardiomyocytes from human embryonic stem cells. Mol Ther *15*, 2027-2036.

Andrews, P.W., Damjanov, I., Simon, D., Banting, G.S., Carlin, C., Dracopoli, N.C., and Fogh, J. (1984). Pluripotent embryonal carcinoma clones derived from the human teratocarcinoma cell line Tera-2. Differentiation in vivo and in vitro. Lab Invest *50*, 147-162.

Aoki, A., Suetake, I., Miyagawa, J., Fujio, T., Chijiwa, T., Sasaki, H., and Tajima, S. (2001). Enzymatic properties of de novo-type mouse DNA (cytosine-5) methyltransferases. Nucleic Acids Res *29*, 3506-3512.

Arnaud, P., Hata, K., Kaneda, M., Li, E., Sasaki, H., Feil, R., and Kelsey, G. (2006). Stochastic imprinting in the progeny of Dnmt3L-/- females. Hum Mol Genet *15*, 589-598.

Astuti, D., Latif, F., Wagner, K., Gentle, D., Cooper, W.N., Catchpoole, D., Grundy, R., Ferguson-Smith, A.C., and Maher, E.R. (2005). Epigenetic alteration at the DLK1-GTL2 imprinted domain in human neoplasia: analysis of neuroblastoma, phaeochromocytoma and Wilms' tumour. Br J Cancer *92*, 1574-1580.

Avner, P., and Heard, E. (2001). X-chromosome inactivation: counting, choice and initiation. Nat Rev Genet *2*, 59-67.

Bachman, K.E., Rountree, M.R., and Baylin, S.B. (2001). Dnmt3a and Dnmt3b are transcriptional repressors that exhibit unique localization properties to heterochromatin. J Biol Chem *276*, 32282-32287.

Bacolla, A., Pradhan, S., Roberts, R.J., and Wells, R.D. (1999). Recombinant human DNA (cytosine-5) methyltransferase. II. Steady-state kinetics reveal allosteric activation by methylated dna. J Biol Chem *274*, 33011-33019.

Bai, Y., Akiyama, Y., Nagasaki, H., Yagi, O.K., Kikuchi, Y., Saito, N., Takeshita, K., Iwai, T., and Yuasa, Y. (2000). Distinct expression of CDX2 and GATA4/5, development-related genes, in human gastric cancer cell lines. Mol Carcinog *28*, 184-188.

Baker, D.E., Harrison, N.J., Maltby, E., Smith, K., Moore, H.D., Shaw, P.J., Heath, P.R., Holden, H., and Andrews, P.W. (2007). Adaptation to culture of human embryonic stem cells and oncogenesis in vivo. Nat Biotechnol *25*, 207-215.

Barlow, D.P., Stoger, R., Herrmann, B.G., Saito, K., and Schweifer, N. (1991). The mouse insulin-like growth factor type-2 receptor is imprinted and closely linked to the Tme locus. Nature *349*, 84-87.

Bartolomei, M.S., Zemel, S., and Tilghman, S.M. (1991). Parental imprinting of the mouse H19 gene. Nature *351*, 153-155.

Bastepe, M., Frohlich, L.F., Linglart, A., Abu-Zahra, H.S., Tojo, K., Ward, L.M., and Juppner, H. (2005). Deletion of the NESP55 differentially methylated region causes loss of maternal GNAS imprints and pseudohypoparathyroidism type Ib. Nat Genet *37*, 25-27.

Beattie, G.M., Lopez, A.D., Bucay, N., Hinton, A., Firpo, M.T., King, C.C., and Hayek, A. (2005). Activin A maintains pluripotency of human embryonic stem cells in the absence of feeder layers. Stem Cells *23*, 489-495.

Bendall, S.C., Stewart, M.H., Menendez, P., George, D., Vijayaragavan, K., Werbowetski-Ogilvie, T., Ramos-Mejia, V., Rouleau, A., Yang, J., Bosse, M., *et al.* (2007). IGF and FGF cooperatively establish the regulatory stem cell niche of pluripotent human cells in vitro. Nature *448*, 1015-1021.

Bernstein, B.E., Kamal, M., Lindblad-Toh, K., Bekiranov, S., Bailey, D.K., Huebert, D.J., McMahon, S., Karlsson, E.K., Kulbokas, E.J., 3rd, Gingeras, T.R., *et al.* (2005). Genomic maps and comparative analysis of histone modifications in human and mouse. Cell *120*, 169-181.

Bestor, T., Laudano, A., Mattaliano, R., and Ingram, V. (1988). Cloning and sequencing of a cDNA encoding DNA methyltransferase of mouse cells. The carboxyl-terminal domain of the mammalian enzymes is related to bacterial restriction methyltransferases. J Mol Biol *203*, 971-983.

Bestor, T.H. (2000). The DNA methyltransferases of mammals. Hum Mol Genet *9*, 2395-2402.

Bibikova, M., Chudin, E., Wu, B., Zhou, L., Garcia, E.W., Liu, Y., Shin, S., Plaia, T.W., Auerbach, J.M., Arking, D.E., *et al.* (2006). Human embryonic stem cells have a unique epigenetic signature. Genome Res *16*, 1075-1083.

Bibikova, M., Laurent, L.C., Ren, B., Loring, J.F., and Fan, J.B. (2008). Unraveling epigenetic regulation in embryonic stem cells. Cell Stem Cell *2*, 123-134.

Biniszkiewicz, D., Gribnau, J., Ramsahoye, B., Gaudet, F., Eggan, K., Humpherys, D., Mastrangelo, M.A., Jun, Z., Walter, J., and Jaenisch, R. (2002). Dnmt1 overexpression causes genomic hypermethylation, loss of imprinting, and embryonic lethality. Mol Cell Biol *22*, 2124-2135.

Bird, A. (2002). DNA methylation patterns and epigenetic memory. Genes Dev *16*, 6-21.

Blagitko, N., Mergenthaler, S., Schulz, U., Wollmann, H.A., Craigen, W., Eggermann, T., Ropers, H.H., and Kalscheuer, V.M. (2000). Human GRB10 is imprinted and expressed from the paternal and maternal allele in a highly tissue- and isoform-specific fashion. Hum Mol Genet *9*, 1587-1595.

Bliek, J., Maas, S.M., Ruijter, J.M., Hennekam, R.C., Alders, M., Westerveld, A., and Mannens, M.M. (2001). Increased tumour risk for BWS patients correlates with aberrant H19 and not KCNQ1OT1 methylation: occurrence of KCNQ1OT1 hypomethylation in familial cases of BWS. Hum Mol Genet *10*, 467-476.

Boccaccio, I., Glatt-Deeley, H., Watrin, F., Roeckel, N., Lalande, M., and Muscatelli, F. (1999). The human MAGEL2 gene and its mouse homologue are paternally expressed and mapped to the Prader-Willi region. Hum Mol Genet *8*, 2497-2505.

Borghol, N., Lornage, J., Blachere, T., Sophie Garret, A., and Lefevre, A. (2006). Epigenetic status of the H19 locus in human oocytes following in vitro maturation. Genomics *87*, 417-426.

Bostick, M., Kim, J.K., Esteve, P.O., Clark, A., Pradhan, S., and Jacobsen, S.E. (2007). UHRF1 plays a role in maintaining DNA methylation in mammalian cells. Science *317*, 1760-1764.

Bourc'his, D., Xu, G.L., Lin, C.S., Bollman, B., and Bestor, T.H. (2001). Dnmt3L and the establishment of maternal genomic imprints. Science *294*, 2536-2539.
Brena, R.M., Huang, T.H., and Plass, C. (2006). Toward a human epigenome. Nat Genet *38*, 1359-1360.

Brons, I.G., Smithers, L.E., Trotter, M.W., Rugg-Gunn, P., Sun, B., Chuva de Sousa Lopes, S.M., Howlett, S.K., Clarkson, A., Ahrlund-Richter, L., Pedersen, R.A., *et al.* (2007). Derivation of pluripotent epiblast stem cells from mammalian embryos. Nature *448*, 191-195.

Burridge, P.W., Anderson, D., Priddle, H., Barbadillo Munoz, M.D., Chamberlain, S., Allegrucci, C., Young, L.E., and Denning, C. (2007). Improved human embryonic stem cell embryoid body homogeneity and cardiomyocyte differentiation from a novel V-96 plate aggregation system highlights interline variability. Stem Cells *25*, 929-938.

Calvanese, V., Horrillo, A., Hmadcha, A., Suarez-Alvarez, B., Fernandez, A.F., Lara, E., Casado, S., Menendez, P., Bueno, C., Garcia-Castro, J., *et al.* (2008). Cancer genes hypermethylated in human embryonic stem cells. PLoS ONE *3*, e3294.

Cardoso, M.C., and Leonhardt, H. (1999). DNA methyltransferase is actively retained in the cytoplasm during early development. J Cell Biol *147*, 25-32.

Carr, M.S., Yevtodiyenko, A., Schmidt, C.L., and Schmidt, J.V. (2007). Allele-specific histone modifications regulate expression of the Dlk1-Gtl2 imprinted domain. Genomics *89*, 280-290.

Charlier, C., Singh, N.A., Ryan, S.G., Lewis, T.B., Reus, B.E., Leach, R.J., and Leppert, M. (1998). A pore mutation in a novel KQT-like potassium channel gene in an idiopathic epilepsy family. Nat Genet *18*, 53-55.

Chen, C.L., Ip, S.M., Cheng, D., Wong, L.C., and Ngan, H.Y. (2000a). Loss of imprinting of the IGF-II and H19 genes in epithelial ovarian cancer. Clin Cancer Res *6*, 474-479.

Chen, C.L., Ip, S.M., Cheng, D., Wong, L.C., and Ngan, H.Y. (2000b). P73 gene expression in ovarian cancer tissues and cell lines. Clin Cancer Res *6*, 3910-3915.

Chen, T., Hevi, S., Gay, F., Tsujimoto, N., He, T., Zhang, B., Ueda, Y., and Li, E. (2007). Complete inactivation of DNMT1 leads to mitotic catastrophe in human cancer cells. Nat Genet *39*, 391-396.

Chen, T., Tsujimoto, N., and Li, E. (2004). The PWWP domain of Dnmt3a and Dnmt3b is required for directing DNA methylation to the major satellite repeats at pericentric heterochromatin. Mol Cell Biol *24*, 9048-9058.

Chen, T., Ueda, Y., Dodge, J.E., Wang, Z., and Li, E. (2003). Establishment and maintenance of genomic methylation patterns in mouse embryonic stem cells by Dnmt3a and Dnmt3b. Mol Cell Biol *23*, 5594-5605.

Chen, T., Ueda, Y., Xie, S., and Li, E. (2002). A novel Dnmt3a isoform produced from an alternative promoter localizes to euchromatin and its expression correlates with active de novo methylation. J Biol Chem *277*, 38746-38754.

Cheng, X., and Blumenthal, R.M. (2008). Mammalian DNA methyltransferases: a structural perspective. Structure *16*, 341-350.

Chi, S.G., Chang, S.G., Lee, S.J., Lee, C.H., Kim, J.I., and Park, J.H. (1999). Elevated and biallelic expression of p73 is associated withprogression of human bladder cancer. Cancer Res *59*, 2791-2793.

Chidgey, A.P., Layton, D., Trounson, A., and Boyd, R.L. (2008). Tolerance strategies for stem-cell-based therapies. Nature *453*, 330-337.

Chuang, L.S., Ian, H.I., Koh, T.W., Ng, H.H., Xu, G., and Li, B.F. (1997). Human DNA-(cytosine-5) methyltransferase-PCNA complex as a target for p21WAF1. Science *277*, 1996-2000.

Chung, Y., Klimanskaya, I., Becker, S., Li, T., Maserati, M., Lu, S.J., Zdravkovic, T., Ilic, D., Genbacev, O., Fisher, S., *et al.* (2008). Human embryonic stem cell lines generated without embryo destruction. Cell Stem Cell *2*, 113-117.

Coffigny, H., Bourgeois, C., Ricoul, M., Bernardino, J., Vilain, A., Niveleau, A., Malfoy, B., and Dutrillaux, B. (1999). Alterations of DNA methylation patterns in germ cells and Sertoli cells from developing mouse testis. Cytogenet Cell Genet *87*, 175-181.

Constancia, M., Kelsey, G., and Reik, W. (2004). Resourceful imprinting. Nature *432*, 53-57.

Cooper, P.R., Smilinich, N.J., Day, C.D., Nowak, N.J., Reid, L.H., Pearsall, R.S., Reece, M., Prawitt, D., Landers, J., Housman, D.E., *et al.* (1998). Divergently transcribed overlapping genes expressed in liver and kidney and located in the 11p15.5 imprinted domain. Genomics *49*, 38-51.

Cowan, C.A., Atienza, J., Melton, D.A., and Eggan, K. (2005). Nuclear reprogramming of somatic cells after fusion with human embryonic stem cells. Science *309*, 1369-1373.

Cowan, C.A., Klimanskaya, I., McMahon, J., Atienza, J., Witmyer, J., Zucker, J.P., Wang, S., Morton, C.C., McMahon, A.P., Powers, D., *et al.* (2004). Derivation of embryonic stem-cell lines from human blastocysts. N Engl J Med *350*, 1353-1356.

Cox, G.F., Burger, J., Lip, V., Mau, U.A., Sperling, K., Wu, B.L., and Horsthemke, B. (2002). Intracytoplasmic sperm injection may increase the risk of imprinting defects. Am J Hum Genet *71*, 162-164.

Cui, H., Horon, I.L., Ohlsson, R., Hamilton, S.R., and Feinberg, A.P. (1998). Loss of imprinting in normal tissue of colorectal cancer patients with microsatellite instability. Nat Med *4*, 1276-1280.

Daniels, R., Zuccotti, M., Kinis, T., Serhal, P., and Monk, M. (1997). XIST expression in human oocytes and preimplantation embryos. Am J Hum Genet *61*, 33-39.

Dao, D., Frank, D., Qian, N., O'Keefe, D., Vosatka, R.J., Walsh, C.P., and Tycko, B. (1998). IMPT1, an imprinted gene similar to polyspecific transporter and multi-drug resistance genes. Hum Mol Genet *7*, 597-608.

Davis, T.L., Yang, G.J., McCarrey, J.R., and Bartolomei, M.S. (2000). The H19 methylation imprint is erased and re-established differentially on the parental alleles during male germ cell development. Hum Mol Genet *9*, 2885-2894.

Dean, W., Bowden, L., Aitchison, A., Klose, J., Moore, T., Meneses, J.J., Reik, W., and Feil, R. (1998). Altered imprinted gene methylation and expression in completely ES cell-derived mouse fetuses: association with aberrant phenotypes. Development *125*, 2273-2282.

DeBaun, M.R., Niemitz, E.L., and Feinberg, A.P. (2003). Association of in vitro fertilization with Beckwith-Wiedemann syndrome and epigenetic alterations of LIT1 and H19. Am J Hum Genet *72*, 156-160.

DeChiara, T.M., Robertson, E.J., and Efstratiadis, A. (1991). Parental imprinting of the mouse insulin-like growth factor II gene. Cell *64*, 849-859.

Deng, Y., and Wu, X. (2000). Peg3/Pw1 promotes p53-mediated apoptosis by inducing Bax translocation from cytosol to mitochondria. Proc Natl Acad Sci U S A *97*, 12050-12055.

Denning, C., Allegrucci, C., Priddle, H., Barbadillo-Munoz, M.D., Anderson, D., Self, T., Smith, N.M., Parkin, C.T., and Young, L.E. (2006). Common culture conditions for maintenance and cardiomyocyte differentiation of the human embryonic stem cell lines, BG01 and HUES-7. Int J Dev Biol *50*, 27-37.

Dennis, K., Fan, T., Geiman, T., Yan, Q., and Muegge, K. (2001). Lsh, a member of the SNF2 family, is required for genome-wide methylation. Genes Dev *15*, 2940-2944.

Diaz-Meyer, N., Yang, Y., Sait, S.N., Maher, E.R., and Higgins, M.J. (2005). Alternative mechanisms associated with silencing of CDKN1C in Beckwith-Wiedemann syndrome. J Med Genet *42*, 648-655.

Dodge, J.E., Kang, Y.K., Beppu, H., Lei, H., and Li, E. (2004). Histone H3-K9 methyltransferase ESET is essential for early development. Mol Cell Biol *24*, 2478-2486.

Dodge, J.E., Okano, M., Dick, F., Tsujimoto, N., Chen, T., Wang, S., Ueda, Y., Dyson, N., and Li, E. (2005). Inactivation of Dnmt3b in mouse embryonic fibroblasts results in DNA hypomethylation, chromosomal instability, and spontaneous immortalization. J Biol Chem *280*, 17986-17991.

Doherty, A.S., Mann, M.R., Tremblay, K.D., Bartolomei, M.S., and Schultz, R.M. (2000). Differential effects of culture on imprinted H19 expression in the preimplantation mouse embryo. Biol Reprod *62*, 1526-1535.

Dong, S., Pang, J.C., Hu, J., Zhou, L.F., and Ng, H.K. (2002). Transcriptional inactivation of TP73 expression in oligodendroglial tumors. Int J Cancer *98*, 370-375.

Dong, S.M., Kim, H.S., Rha, S.H., and Sidransky, D. (2001). Promoter hypermethylation of multiple genes in carcinoma of the uterine cervix. Clin Cancer Res *7*, 1982-1986.

Donohoe, M.E., Zhang, L.F., Xu, N., Shi, Y., and Lee, J.T. (2007). Identification of a Ctcf cofactor, Yy1, for the X chromosome binary switch. Mol Cell *25*, 43-56.

Dowdy, S.C., Gostout, B.S., Shridhar, V., Wu, X., Smith, D.I., Podratz, K.C., and Jiang, S.W. (2005). Biallelic methylation and silencing of paternally expressed gene 3 (PEG3) in gynecologic cancer cell lines. Gynecol Oncol *99*, 126-134.

Draper, J.S., Pigott, C., Thomson, J.A., and Andrews, P.W. (2002). Surface antigens of human embryonic stem cells: changes upon differentiation in culture. J Anat *200*, 249-258.

Draper, J.S., Smith, K., Gokhale, P., Moore, H.D., Maltby, E., Johnson, J., Meisner, L., Zwaka, T.P., Thomson, J.A., and Andrews, P.W. (2004). Recurrent gain of chromosomes 17q and 12 in cultured human embryonic stem cells. Nat Biotechnol *22*, 53-54.

Egger, G., Jeong, S., Escobar, S.G., Cortez, C.C., Li, T.W., Saito, Y., Yoo, C.B., Jones, P.A., and Liang, G. (2006). Identification of DNMT1 (DNA methyltransferase 1) hypomorphs in somatic knockouts suggests an essential role for DNMT1 in cell survival. Proc Natl Acad Sci U S A *103*, 14080-14085.

Ekstrom, T.J., Cui, H., Li, X., and Ohlsson, R. (1995). Promoter-specific IGF2 imprinting status and its plasticity during human liver development. Development *121*, 309-316.

El-Maarri, O., Buiting, K., Peery, E.G., Kroisel, P.M., Balaban, B., Wagner, K., Urman, B., Heyd, J., Lich, C., Brannan, C.I., *et al.* (2001). Maternal methylation imprints on human chromosome 15 are established during or after fertilization. Nat Genet *27*, 341-344.

Esteller, M. (2007). Cancer epigenomics: DNA methylomes and histone-modification maps. Nat Rev Genet *8*, 286-298.

Esteve, P.O., Chin, H.G., and Pradhan, S. (2005). Human maintenance DNA (cytosine-5)-methyltransferase and p53 modulate expression of p53-repressed promoters. Proc Natl Acad Sci U S A *102*, 1000-1005.

Esteve, P.O., Chin, H.G., Smallwood, A., Feehery, G.R., Gangisetty, O., Karpf, A.R., Carey, M.F., and Pradhan, S. (2006). Direct interaction between DNMT1 and G9a coordinates DNA and histone methylation during replication. Genes Dev *20*, 3089-3103.

Etoh, T., Kanai, Y., Ushijima, S., Nakagawa, T., Nakanishi, Y., Sasako, M., Kitano, S., and Hirohashi, S. (2004). Increased DNA methyltransferase 1 (DNMT1) protein expression correlates significantly with poorer tumor differentiation and frequent DNA hypermethylation of multiple CpG islands in gastric cancers. Am J Pathol *164*, 689-699.

Evron, E., Umbricht, C.B., Korz, D., Raman, V., Loeb, D.M., Niranjan, B., Buluwela, L., Weitzman, S.A., Marks, J., and Sukumar, S. (2001). Loss of cyclin D2 expression in the majority of breast cancers is associated with promoter hypermethylation. Cancer Res *61*, 2782-2787.

Fedoriw, A.M., Stein, P., Svoboda, P., Schultz, R.M., and Bartolomei, M.S. (2004). Transgenic RNAi reveals essential function for CTCF in H19 gene imprinting. Science *303*, 238-240.

Feil, R., Boyano, M.D., Allen, N.D., and Kelsey, G. (1997). Parental chromosome-specific chromatin conformation in the imprinted U2af1-rs1 gene in the mouse. J Biol Chem *272*, 20893-20900.

Feinberg, A.P. (2007). Phenotypic plasticity and the epigenetics of human disease. Nature *447*, 433-440.

Feltus, F.A., Lee, E.K., Costello, J.F., Plass, C., and Vertino, P.M. (2003). Predicting aberrant CpG island methylation. Proc Natl Acad Sci U S A *100*, 12253-12258.
Fenno, L.E., Ptaszek, L.M., and Cowan, C.A. (2008). Human embryonic stem cells: emerging technologies and practical applications. Curr Opin Genet Dev.

Ferguson-Smith, A.C., and Surani, M.A. (2001). Imprinting and the epigenetic asymmetry between parental genomes. Science *293*, 1086-1089.

Fernandez-Gonzalez, R., Moreira, P., Bilbao, A., Jimenez, A., Perez-Crespo, M., Ramirez, M.A., Rodriguez De Fonseca, F., Pintado, B., and Gutierrez-Adan, A. (2004). Long-term effect of in vitro culture of mouse embryos with serum on mRNA expression of imprinting genes, development, and behavior. Proc Natl Acad Sci U S A *101*, 5880-5885.

Fernandez-Gonzalez, R., Moreira, P.N., Perez-Crespo, M., Sanchez-Martin, M., Ramirez, M.A., Pericuesta, E., Bilbao, A., Bermejo-Alvarez, P., de Dios Hourcade, J., de Fonseca, F.R.,

et al. (2008). Long-term effects of mouse intracytoplasmic sperm injection with DNA-fragmented sperm on health and behavior of adult offspring. Biol Reprod *78*, 761-772.

Fitzpatrick, G.V., Pugacheva, E.M., Shin, J.Y., Abdullaev, Z., Yang, Y., Khatod, K., Lobanenkov, V.V., and Higgins, M.J. (2007). Allele-specific binding of CTCF to the multipartite imprinting control region KvDMR1. Mol Cell Biol *27*, 2636-2647.

Fitzpatrick, G.V., Soloway, P.D., and Higgins, M.J. (2002). Regional loss of imprinting and growth deficiency in mice with a targeted deletion of KvDMR1. Nat Genet *32*, 426-431.

Forsberg, E.C., Downs, K.M., Christensen, H.M., Im, H., Nuzzi, P.A., and Bresnick, E.H. (2000). Developmentally dynamic histone acetylation pattern of a tissue-specific chromatin domain. Proc Natl Acad Sci U S A *97*, 14494-14499.

Fortier, A.L., Lopes, F.L., Darricarrere, N., Martel, J., and Trasler, J.M. (2008). Superovulation alters the expression of imprinted genes in the midgestation mouse placenta. Hum Mol Genet *17*, 1653-1665.

Fournier, C., Goto, Y., Ballestar, E., Delaval, K., Hever, A.M., Esteller, M., and Feil, R. (2002). Allele-specific histone lysine methylation marks regulatory regions at imprinted mouse genes. EMBO J *21*, 6560-6570.

Frigola, J., Song, J., Stirzaker, C., Hinshelwood, R.A., Peinado, M.A., and Clark, S.J. (2006). Epigenetic remodeling in colorectal cancer results in coordinate gene suppression across an entire chromosome band. Nat Genet *38*, 540-549.

Fujimoto, A., Mitalipov, S.M., Kuo, H.C., and Wolf, D.P. (2006). Aberrant genomic imprinting in rhesus monkey embryonic stem cells. Stem Cells *24*, 595-603.

Fujita, N., Watanabe, S., Ichimura, T., Tsuruzoe, S., Shinkai, Y., Tachibana, M., Chiba, T., and Nakao, M. (2003). Methyl-CpG binding domain 1 (MBD1) interacts with the Suv39h1-HP1 heterochromatic complex for DNA methylation-based transcriptional repression. J Biol Chem *278*, 24132-24138.

Fuks, F., Burgers, W.A., Brehm, A., Hughes-Davies, L., and Kouzarides, T. (2000). DNA methyltransferase Dnmt1 associates with histone deacetylase activity. Nat Genet *24*, 88-91.

Fuks, F., Burgers, W.A., Godin, N., Kasai, M., and Kouzarides, T. (2001). Dnmt3a binds deacetylases and is recruited by a sequence-specific repressor to silence transcription. Embo J *20*, 2536-2544.

Fuks, F., Hurd, P.J., Deplus, R., and Kouzarides, T. (2003). The DNA methyltransferases associate with HP1 and the SUV39H1 histone methyltransferase. Nucleic Acids Res *31*, 2305-2312.

Fulmer-Smentek, S.B., and Francke, U. (2001). Association of acetylated histones with paternally expressed genes in the Prader--Willi deletion region. Hum Mol Genet *10*, 645-652.

Gaudet, F., Rideout, W.M., 3rd, Meissner, A., Dausman, J., Leonhardt, H., and Jaenisch, R. (2004). Dnmt1 expression in pre- and postimplantation embryogenesis and the maintenance of IAP silencing. Mol Cell Biol *24*, 1640-1648.

Ge, Y.Z., Pu, M.T., Gowher, H., Wu, H.P., Ding, J.P., Jeltsch, A., and Xu, G.L. (2004). Chromatin targeting of de novo DNA methyltransferases by the PWWP domain. J Biol Chem *279*, 25447-25454.

Geiman, T.M., Sankpal, U.T., Robertson, A.K., Zhao, Y., and Robertson, K.D. (2004). DNMT3B interacts with hSNF2H chromatin remodeling enzyme, HDACs 1 and 2, and components of the histone methylation system. Biochem Biophys Res Commun *318*, 544-555.

Geuns, E., De Rycke, M., Van Steirteghem, A., and Liebaers, I. (2003). Methylation imprints of the imprint control region of the SNRPN-gene in human gametes and preimplantation embryos. Hum Mol Genet *12*, 2873-2879.

Geuns, E., De Temmerman, N., Hilven, P., Van Steirteghem, A., Liebaers, I., and De Rycke, M. (2007a). Methylation analysis of the intergenic differentially methylated region of DLK1-GTL2 in human. Eur J Hum Genet *15*, 352-361.

Geuns, E., Hilven, P., Van Steirteghem, A., Liebaers, I., and De Rycke, M. (2007b). Methylation analysis of KvDMR1 in human oocytes. J Med Genet *44*, 144-147.

Giannoukakis, N., Deal, C., Paquette, J., Goodyer, C.G., and Polychronakos, C. (1993). Parental genomic imprinting of the human IGF2 gene. Nat Genet *4*, 98-101.

Gicquel, C., Gaston, V., Mandelbaum, J., Siffroi, J.P., Flahault, A., and Le Bouc, Y. (2003). In vitro fertilization may increase the risk of Beckwith-Wiedemann syndrome related to the abnormal imprinting of the KCN1OT gene. Am J Hum Genet *72*, 1338-1341.

Gicquel, C., Rossignol, S., Cabrol, S., Houang, M., Steunou, V., Barbu, V., Danton, F., Thibaud, N., Le Merrer, M., Burglen, L., *et al.* (2005). Epimutation of the telomeric imprinting center region on chromosome 11p15 in Silver-Russell syndrome. Nat Genet *37*, 1003-1007.

Ginis, I., Luo, Y., Miura, T., Thies, S., Brandenberger, R., Gerecht-Nir, S., Amit, M., Hoke, A., Carpenter, M.K., Itskovitz-Eldor, J., *et al.* (2004). Differences between human and mouse embryonic stem cells. Dev Biol *269*, 360-380.

Goll, M.G., Kirpekar, F., Maggert, K.A., Yoder, J.A., Hsieh, C.L., Zhang, X., Golic, K.G., Jacobsen, S.E., and Bestor, T.H. (2006). Methylation of tRNAAsp by the DNA methyltransferase homolog Dnmt2. Science *311*, 395-398.

Gonzalo, S., Jaco, I., Fraga, M.F., Chen, T., Li, E., Esteller, M., and Blasco, M.A. (2006). DNA methyltransferases control telomere length and telomere recombination in mammalian cells. Nat Cell Biol *8*, 416-424.

Gould, T.D., and Pfeifer, K. (1998). Imprinting of mouse Kvlqt1 is developmentally regulated. Hum Mol Genet *7*, 483-487.

Gowher, H., and Jeltsch, A. (2002). Molecular enzymology of the catalytic domains of the Dnmt3a and Dnmt3b DNA methyltransferases. J Biol Chem *277*, 20409-20414.

Grandjean, V., O'Neill, L., Sado, T., Turner, B., and Ferguson-Smith, A. (2001). Relationship between DNA methylation, histone H4 acetylation and gene expression in the mouse imprinted Igf2-H19 domain. FEBS Lett *488*, 165-169.

Gregory, R.I., Randall, T.E., Johnson, C.A., Khosla, S., Hatada, I., O'Neill, L.P., Turner, B.M., and Feil, R. (2001). DNA methylation is linked to deacetylation of histone H3, but not H4, on the imprinted genes Snrpn and U2af1-rs1. Mol Cell Biol *21*, 5426-5436.

Hajkova, P., Erhardt, S., Lane, N., Haaf, T., El-Maarri, O., Reik, W., Walter, J., and Surani, M.A. (2002). Epigenetic reprogramming in mouse primordial germ cells. Mech Dev *117*, 15-23.

Han, L., Lee, D.H., and Szabo, P.E. (2008). CTCF is the master organizer of domain-wide allele-specific chromatin at the H19/Igf2 imprinted region. Mol Cell Biol *28*, 1124-1135.

Hanel, M.L., and Wevrick, R. (2001). Establishment and maintenance of DNA methylation patterns in mouse Ndn: implications for maintenance of imprinting in target genes of the imprinting center. Mol Cell Biol *21*, 2384-2392.

Hark, A.T., Schoenherr, C.J., Katz, D.J., Ingram, R.S., Levorse, J.M., and Tilghman, S.M. (2000). CTCF mediates methylation-sensitive enhancer-blocking activity at the H19/Igf2 locus. Nature *405*, 486-489.

Hartmann, S., Bergmann, M., Bohle, R.M., Weidner, W., and Steger, K. (2006). Genetic imprinting during impaired spermatogenesis. Mol Hum Reprod *12*, 407-411.

Hashimoto, K., Azuma, C., Koyama, M., Ohashi, K., Kamiura, S., Nobunaga, T., Kimura, T., Tokugawa, Y., Kanai, T., and Saji, F. (1995). Loss of imprinting in choriocarcinoma. Nat Genet *9*, 109-110.

Hata, K., Okano, M., Lei, H., and Li, E. (2002). Dnmt3L cooperates with the Dnmt3 family of de novo DNA methyltransferases to establish maternal imprints in mice. Development *129*, 1983-1993.

Hatada, I., and Mukai, T. (1995). Genomic imprinting of p57KIP2, a cyclin-dependent kinase inhibitor, in mouse. Nat Genet *11*, 204-206.

Hatada, I., Ohashi, H., Fukushima, Y., Kaneko, Y., Inoue, M., Komoto, Y., Okada, A., Ohishi, S., Nabetani, A., Morisaki, H., *et al.* (1996). An imprinted gene p57KIP2 is mutated in Beckwith-Wiedemann syndrome. Nat Genet *14*, 171-173.

Hattori, N., Abe, T., Suzuki, M., Matsuyama, T., Yoshida, S., Li, E., and Shiota, K. (2004). Preference of DNA methyltransferases for CpG islands in mouse embryonic stem cells. Genome Res *14*, 1733-1740.

Hwang W.S., Pyu Y.J., Park J.H., Park E.S., Lee E.G., Koo J.M., Jeon H.Y., Lee B.C., Kang S.K., Kim S.J., Ahn C., Hwang J.H., Park K.Y., Cibelli J.B., and Moon S.Y. (2004). Evidende of a pluripotent human embryhonic stem cell line derived from a cloned blastocyst. *Science* 303, 1669-1974. Retracted by Kennedy D. (2006). *Science* 311, 335.

Hayward, B.E., Barlier, A., Korbonits, M., Grossman, A.B., Jacquet, P., Enjalbert, A., and Bonthron, D.T. (2001). Imprinting of the G(s)alpha gene GNAS1 in the pathogenesis of acromegaly. J Clin Invest *107*, R31-36.

Hayward, B.E., De Vos, M., Judson, H., Hodge, D., Huntriss, J., Picton, H.M., Sheridan, E., and Bonthron, D.T. (2003). Lack of involvement of known DNA methyltransferases in familial hydatidiform mole implies the involvement of other factors in establishment of imprinting in the human female germline. BMC Genet *4*, 2.

Henderson, J.K., Draper, J.S., Baillie, H.S., Fishel, S., Thomson, J.A., Moore, H., and Andrews, P.W. (2002). Preimplantation human embryos and embryonic stem cells show comparable expression of stage-specific embryonic antigens. Stem Cells *20*, 329-337.

Herman, J.G., Graff, J.R., Myohanen, S., Nelkin, B.D., and Baylin, S.B. (1996). Methylation-specific PCR: a novel PCR assay for methylation status of CpG islands. Proc Natl Acad Sci U S A *93*, 9821-9826.

Hikichi, T., Kohda, T., Kaneko-Ishino, T., and Ishino, F. (2003). Imprinting regulation of the murine Meg1/Grb10 and human GRB10 genes; roles of brain-specific promoters and mouse-specific CTCF-binding sites. Nucleic Acids Res *31*, 1398-1406.

Hoffman, L.M., and Carpenter, M.K. (2005). Characterization and culture of human embryonic stem cells. Nat Biotechnol *23*, 699-708.

Holm, T.M., Jackson-Grusby, L., Brambrink, T., Yamada, Y., Rideout, W.M., 3rd, and Jaenisch, R. (2005). Global loss of imprinting leads to widespread tumorigenesis in adult mice. Cancer Cell *8*, 275-285.

Horike, S., Mitsuya, K., Meguro, M., Kotobuki, N., Kashiwagi, A., Notsu, T., Schulz, T.C., Shirayoshi, Y., and Oshimura, M. (2000). Targeted disruption of the human LIT1 locus defines a putative imprinting control element playing an essential role in Beckwith-Wiedemann syndrome. Hum Mol Genet *9*, 2075-2083.

Horsthemke, B., and Ludwig, M. (2005). Assisted reproduction: the epigenetic perspective. Hum Reprod Update *11*, 473-482.

Howell, C.Y., Bestor, T.H., Ding, F., Latham, K.E., Mertineit, C., Trasler, J.M., and Chaillet, J.R. (2001). Genomic imprinting disrupted by a maternal effect mutation in the Dnmt1 gene. Cell *104*, 829-838.

Hu, J.F., Oruganti, H., Vu, T.H., and Hoffman, A.R. (1998). Tissue-specific imprinting of the mouse insulin-like growth factor II receptor gene correlates with differential allele-specific DNA methylation. Mol Endocrinol *12*, 220-232.

Hu, J.F., Pham, J., Dey, I., Li, T., Vu, T.H., and Hoffman, A.R. (2000). Allele-specific histone acetylation accompanies genomic imprinting of the insulin-like growth factor II receptor gene. Endocrinology *141*, 4428-4435.

Humpherys, D., Eggan, K., Akutsu, H., Hochedlinger, K., Rideout, W.M., 3rd, Biniszkiewicz, D., Yanagimachi, R., and Jaenisch, R. (2001). Epigenetic instability in ES cells and cloned mice. Science *293*, 95-97.

Huntriss, J., Daniels, R., Bolton, V., and Monk, M. (1998). Imprinted expression of SNRPN in human preimplantation embryos. Am J Hum Genet *63*, 1009-1014.

Imura, M., Yamashita, S., Cai, L.Y., Furuta, J., Wakabayashi, M., Yasugi, T., and Ushijima, T. (2006). Methylation and expression analysis of 15 genes and three normally-methylated genes in 13 Ovarian cancer cell lines. Cancer Lett *241*, 213-220.

Inzunza, J., Gertow, K., Stromberg, M.A., Matilainen, E., Blennow, E., Skottman, H., Wolbank, S., Ahrlund-Richter, L., and Hovatta, O. (2005). Derivation of human embryonic stem cell lines in serum replacement medium using postnatal human fibroblasts as feeder cells. Stem Cells *23*, 544-549.

Iwatani, M., Ikegami, K., Kremenska, Y., Hattori, N., Tanaka, S., Yagi, S., and Shiota, K. (2006). Dimethyl sulfoxide has an impact on epigenetic profile in mouse embryoid body. Stem Cells *24*, 2549-2556.

Jackson-Grusby, L., Beard, C., Possemato, R., Tudor, M., Fambrough, D., Csankovszki, G., Dausman, J., Lee, P., Wilson, C., Lander, E., *et al.* (2001). Loss of genomic methylation causes p53-dependent apoptosis and epigenetic deregulation. Nat Genet *27*, 31-39.

Jackson, J.P., Lindroth, A.M., Cao, X., and Jacobsen, S.E. (2002). Control of CpNpG DNA methylation by the KRYPTONITE histone H3 methyltransferase. Nature *416*, 556-560.

Jackson, M., Krassowska, A., Gilbert, N., Chevassut, T., Forrester, L., Ansell, J., and Ramsahoye, B. (2004). Severe global DNA hypomethylation blocks differentiation and induces histone hyperacetylation in embryonic stem cells. Mol Cell Biol *24*, 8862-8871.

Jaenisch, R., and Bird, A. (2003). Epigenetic regulation of gene expression: how the genome integrates intrinsic and environmental signals. Nat Genet *33 Suppl*, 245-254.

Jahner, D., Stuhlmann, H., Stewart, C.L., Harbers, K., Lohler, J., Simon, I., and Jaenisch, R. (1982). De novo methylation and expression of retroviral genomes during mouse embryogenesis. Nature *298*, 623-628.

James, D., Levine, A.J., Besser, D., and Hemmati-Brivanlou, A. (2005). TGFbeta/activin/nodal signaling is necessary for the maintenance of pluripotency in human embryonic stem cells. Development *132*, 1273-1282.

Jeddeloh, J.A., Stokes, T.L., and Richards, E.J. (1999). Maintenance of genomic methylation requires a SWI2/SNF2-like protein. Nat Genet *22*, 94-97.
Jelinic, P., and Shaw, P. (2007). Loss of imprinting and cancer. J Pathol *211*, 261-268.

Jinno, Y., Yun, K., Nishiwaki, K., Kubota, T., Ogawa, O., Reeve, A.E., and Niikawa, N. (1994). Mosaic and polymorphic imprinting of the WT1 gene in humans. Nat Genet *6*, 305-309.

Judson, H., Hayward, B.E., Sheridan, E., and Bonthron, D.T. (2002). A global disorder of imprinting in the human female germ line. Nature *416*, 539-542.

Jurkowski, T.P., Meusburger, M., Phalke, S., Helm, M., Nellen, W., Reuter, G., and Jeltsch, A. (2008). Human DNMT2 methylates tRNA(Asp) molecules using a DNA methyltransferase-like catalytic mechanism. RNA *14*, 1663-1670.

Kafri, T., Ariel, M., Brandeis, M., Shemer, R., Urven, L., McCarrey, J., Cedar, H., and Razin, A. (1992). Developmental pattern of gene-specific DNA methylation in the mouse embryo and germ line. Genes Dev *6*, 705-714.

Kaghad, M., Bonnet, H., Yang, A., Creancier, L., Biscan, J.C., Valent, A., Minty, A., Chalon, P., Lelias, J.M., Dumont, X., *et al.* (1997). Monoallelically expressed gene related to p53 at 1p36, a region frequently deleted in neuroblastoma and other human cancers. Cell *90*, 809-819.

Kalscheuer, V.M., Mariman, E.C., Schepens, M.T., Rehder, H., and Ropers, H.H. (1993). The insulin-like growth factor type-2 receptor gene is imprinted in the mouse but not in humans. Nat Genet *5*, 74-78.

Kameda, T., Smuga-Otto, K., and Thomson, J.A. (2006). A severe de novo methylation of episomal vectors by human ES cells. Biochem Biophys Res Commun *349*, 1269-1277.

Kanai, Y., Hui, A.M., Sun, L., Ushijima, S., Sakamoto, M., Tsuda, H., and Hirohashi, S. (1999). DNA hypermethylation at the D17S5 locus and reduced HIC-1 mRNA expression are associated with hepatocarcinogenesis. Hepatology *29*, 703-709.

Kaneda, M., Okano, M., Hata, K., Sado, T., Tsujimoto, N., Li, E., and Sasaki, H. (2004). Essential role for de novo DNA methyltransferase Dnmt3a in paternal and maternal imprinting. Nature *429*, 900-903.

Kang, M.J., Park, B.J., Byun, D.S., Park, J.I., Kim, H.J., Park, J.H., and Chi, S.G. (2000). Loss of imprinting and elevated expression of wild-type p73 in human gastric adenocarcinoma. Clin Cancer Res *6*, 1767-1771.

Kawakami, T., Chano, T., Minami, K., Okabe, H., Okada, Y., and Okamoto, K. (2006). Imprinted DLK1 is a putative tumor suppressor gene and inactivated by epimutation at the region upstream of GTL2 in human renal cell carcinoma. Hum Mol Genet *15*, 821-830.

Kerjean, A., Couvert, P., Heams, T., Chalas, C., Poirier, K., Chelly, J., Jouannet, P., Paldi, A., and Poirot, C. (2003). In vitro follicular growth affects oocyte imprinting establishment in mice. Eur J Hum Genet *11*, 493-496.

Kerjean, A., Dupont, J.M., Vasseur, C., Le Tessier, D., Cuisset, L., Paldi, A., Jouannet, P., and Jeanpierre, M. (2000). Establishment of the paternal methylation imprint of the human H19 and MEST/PEG1 genes during spermatogenesis. Hum Mol Genet *9*, 2183-2187.

Khosla, S., Dean, W., Brown, D., Reik, W., and Feil, R. (2001a). Culture of preimplantation mouse embryos affects fetal development and the expression of imprinted genes. Biol Reprod *64*, 918-926.

Khosla, S., Dean, W., Reik, W., and Feil, R. (2001b). Culture of preimplantation embryos and its long-term effects on gene expression and phenotype. Hum Reprod Update *7*, 419-427.

Khoureiry, R., Ibala-Rhomdane, S., Mery, L., Blachere, T., Guerin, J.F., Lornage, J., and Lefevre, A. (2008). Dynamic CpG methylation of the KCNQ1OT1 gene during maturation of human oocytes. J Med Genet *45*, 583-588.

Kim, G.D., Ni, J., Kelesoglu, N., Roberts, R.J., and Pradhan, S. (2002). Co-operation and communication between the human maintenance and de novo DNA (cytosine-5) methyltransferases. EMBO J *21*, 4183-4195.

Kim, J., Bergmann, A., and Stubbs, L. (2000a). Exon sharing of a novel human zinc-finger gene, ZIM2, and paternally expressed gene 3 (PEG3). Genomics *64*, 114-118.

Kim, J., Bergmann, A., Wehri, E., Lu, X., and Stubbs, L. (2001). Imprinting and evolution of two Kruppel-type zinc-finger genes, ZIM3 and ZNF264, located in the PEG3/USP29 imprinted domain. Genomics *77*, 91-98.

Kim, J., and Kim, J.D. (2008). In vivo YY1 knockdown effects on genomic imprinting. Hum Mol Genet *17*, 391-401.

Kim, J., Kollhoff, A., Bergmann, A., and Stubbs, L. (2003). Methylation-sensitive binding of transcription factor YY1 to an insulator sequence within the paternally expressed imprinted gene, Peg3. Hum Mol Genet *12*, 233-245.

Kim, J., Noskov, V.N., Lu, X., Bergmann, A., Ren, X., Warth, T., Richardson, P., Kouprina, N., and Stubbs, L. (2000b). Discovery of a novel, paternally expressed ubiquitin-specific

processing protease gene through comparative analysis of an imprinted region of mouse chromosome 7 and human chromosome 19q13.4. Genome Res *10*, 1138-1147.

Kim, J.D., Hinz, A.K., Bergmann, A., Huang, J.M., Ovcharenko, I., Stubbs, L., and Kim, J. (2006). Identification of clustered YY1 binding sites in imprinting control regions. Genome Res *16*, 901-911.

Kim, K., Ng, K., Rugg-Gunn, P.J., Shieh, J.H., Kirak, O., Jaenisch, R., Wakayama, T., Moore, M.A., Pedersen, R.A., and Daley, G.Q. (2007a). Recombination signatures distinguish embryonic stem cells derived by parthenogenesis and somatic cell nuclear transfer. Cell Stem Cell *1*, 346-352.

Kleinman, H.K., and Martin, G.R. (2005). Matrigel: basement membrane matrix with biological activity. Semin Cancer Biol *15*, 378-386.

Klimanskaya, I., Chung, Y., Becker, S., Lu, S.J., and Lanza, R. (2006). Human embryonic stem cell lines derived from single blastomeres. Nature *444*, 481-485.

Kobayashi, H., Sato, A., Otsu, E., Hiura, H., Tomatsu, C., Utsunomiya, T., Sasaki, H., Yaegashi, N., and Arima, T. (2007). Aberrant DNA methylation of imprinted loci in sperm from oligospermic patients. Hum Mol Genet *16*, 2542-2551.

Kobayashi, M., Taniura, H., and Yoshikawa, K. (2002). Ectopic expression of necdin induces differentiation of mouse neuroblastoma cells. J Biol Chem *277*, 42128-42135.

Kobayashi, S., Wagatsuma, H., Ono, R., Ichikawa, H., Yamazaki, M., Tashiro, H., Aisaka, K., Miyoshi, N., Kohda, T., Ogura, A., *et al.* (2000). Mouse Peg9/Dlk1 and human PEG9/DLK1 are paternally expressed imprinted genes closely located to the maternally expressed imprinted genes: mouse Meg3/Gtl2 and human MEG3. Genes Cells *5*, 1029-1037.

Kosaki, K., Kosaki, R., Craigen, W.J., and Matsuo, N. (2000). Isoform-specific imprinting of the human PEG1/MEST gene. Am J Hum Genet *66*, 309-312.

Kreidberg, J.A., Sariola, H., Loring, J.M., Maeda, M., Pelletier, J., Housman, D., and Jaenisch, R. (1993). WT-1 is required for early kidney development. Cell *74*, 679-691.

Kurihara, Y., Kawamura, Y., Uchijima, Y., Amamo, T., Kobayashi, H., Asano, T., and Kurihara, H. (2008). Maintenance of genomic methylation patterns during preimplantation development requires the somatic form of DNA methyltransferase 1. Dev Biol *313*, 335-346.

La Salle, S., Mertineit, C., Taketo, T., Moens, P.B., Bestor, T.H., and Trasler, J.M. (2004). Windows for sex-specific methylation marked by DNA methyltransferase expression profiles in mouse germ cells. Dev Biol *268*, 403-415.

Lachner, M., O'Sullivan, R.J., and Jenuwein, T. (2003). An epigenetic road map for histone lysine methylation. J Cell Sci *116*, 2117-2124.

Lander, E.S., Linton, L.M., Birren, B., Nusbaum, C., Zody, M.C., Baldwin, J., Devon, K., Dewar, K., Doyle, M., FitzHugh, W., *et al.* (2001). Initial sequencing and analysis of the human genome. Nature *409*, 860-921.

Lane, N., Dean, W., Erhardt, S., Hajkova, P., Surani, A., Walter, J., and Reik, W. (2003). Resistance of IAPs to methylation reprogramming may provide a mechanism for epigenetic inheritance in the mouse. Genesis *35*, 88-93.

Laslett, A.L., Filipczyk, A.A., and Pera, M.F. (2003). Characterization and culture of human embryonic stem cells. Trends Cardiovasc Med *13*, 295-301.

Lau, J.C., Hanel, M.L., and Wevrick, R. (2004). Tissue-specific and imprinted epigenetic modifications of the human NDN gene. Nucleic Acids Res *32*, 3376-3382.

Lauster, R., Trautner, T.A., and Noyer-Weidner, M. (1989). Cytosine-specific type II DNA methyltransferases. A conserved enzyme core with variable target-recognizing domains. J Mol Biol *206*, 305-312.

Lee, J., Inoue, K., Ono, R., Ogonuki, N., Kohda, T., Kaneko-Ishino, T., Ogura, A., and Ishino, F. (2002). Erasing genomic imprinting memory in mouse clone embryos produced from day 11.5 primordial germ cells. Development *129*, 1807-1817.

Lee, M.P., DeBaun, M.R., Mitsuya, K., Galonek, H.L., Brandenburg, S., Oshimura, M., and Feinberg, A.P. (1999). Loss of imprinting of a paternally expressed transcript, with antisense orientation to KVLQT1, occurs frequently in Beckwith-Wiedemann syndrome and is independent of insulin-like growth factor II imprinting. Proc Natl Acad Sci U S A *96*, 5203-5208.

Lee, M.P., Hu, R.J., Johnson, L.A., and Feinberg, A.P. (1997). Human KVLQT1 gene shows tissue-specific imprinting and encompasses Beckwith-Wiedemann syndrome chromosomal rearrangements. Nat Genet *15*, 181-185.

Lee, M.P., Reeves, C., Schmitt, A., Su, K., Connors, T.D., Hu, R.J., Brandenburg, S., Lee, M.J., Miller, G., and Feinberg, A.P. (1998). Somatic mutation of TSSC5, a novel imprinted gene from human chromosome 11p15.5. Cancer Res *58*, 4155-4159.

Lehmann, U., Hasemeier, B., Christgen, M., Muller, M., Romermann, D., Langer, F., and Kreipe, H. (2008). Epigenetic inactivation of microRNA gene hsa-mir-9-1 in human breast cancer. J Pathol *214*, 17-24.

Lehnertz, B., Ueda, Y., Derijck, A.A., Braunschweig, U., Perez-Burgos, L., Kubicek, S., Chen, T., Li, E., Jenuwein, T., and Peters, A.H. (2003). Suv39h-mediated histone H3 lysine 9 methylation directs DNA methylation to major satellite repeats at pericentric heterochromatin. Curr Biol *13*, 1192-1200.

Lei, H., Oh, S.P., Okano, M., Juttermann, R., Goss, K.A., Jaenisch, R., and Li, E. (1996). De novo DNA cytosine methyltransferase activities in mouse embryonic stem cells. Development *122*, 3195-3205.

Leonhardt, H., Page, A.W., Weier, H.U., and Bestor, T.H. (1992). A targeting sequence directs DNA methyltransferase to sites of DNA replication in mammalian nuclei. Cell *71*, 865-873.

Lewis, A., Mitsuya, K., Umlauf, D., Smith, P., Dean, W., Walter, J., Higgins, M., Feil, R., and Reik, W. (2004). Imprinting on distal chromosome 7 in the placenta involves repressive histone methylation independent of DNA methylation. Nat Genet *36*, 1291-1295.

Li, E. (2002). Chromatin modification and epigenetic reprogramming in mammalian development. Nat Rev Genet *3*, 662-673.

Li, E., Beard, C., and Jaenisch, R. (1993). Role for DNA methylation in genomic imprinting. Nature *366*, 362-365.

Li, E., Bestor, T.H., and Jaenisch, R. (1992). Targeted mutation of the DNA methyltransferase gene results in embryonic lethality. Cell *69*, 915-926.

Li, J.Y., Lees-Murdock, D.J., Xu, G.L., and Walsh, C.P. (2004). Timing of establishment of paternal methylation imprints in the mouse. Genomics *84*, 952-960.

Li, J.Y., Pu, M.T., Hirasawa, R., Li, B.Z., Huang, Y.N., Zeng, R., Jing, N.H., Chen, T., Li, E., Sasaki, H., *et al.* (2007). Synergistic function of DNA methyltransferases Dnmt3a and Dnmt3b in the methylation of Oct4 and Nanog. Mol Cell Biol *27*, 8748-8759.

Li, L., Forman, S.J., and Bhatia, R. (2005a). Expression of DLK1 in hematopoietic cells results in inhibition of differentiation and proliferation. Oncogene *24*, 4472-4476.

Li, L., Keverne, E.B., Aparicio, S.A., Ishino, F., Barton, S.C., and Surani, M.A. (1999). Regulation of maternal behavior and offspring growth by paternally expressed Peg3. Science *284*, 330-333.

Li, T., Hu, J.F., Qiu, X., Ling, J., Chen, H., Wang, S., Hou, A., Vu, T.H., and Hoffman, A.R. (2008). CTCF regulates allelic expression of Igf2 by orchestrating a promoter-polycomb repressive complex-2 intrachromosomal loop. Mol Cell Biol.

Li, T., Vu, T.H., Lee, K.O., Yang, Y., Nguyen, C.V., Bui, H.Q., Zeng, Z.L., Nguyen, B.T., Hu, J.F., Murphy, S.K., *et al.* (2002). An imprinted PEG1/MEST antisense expressed predominantly in human testis and in mature spermatozoa. J Biol Chem *277*, 13518-13527.

Li, T., Vu, T.H., Ulaner, G.A., Littman, E., Ling, J.Q., Chen, H.L., Hu, J.F., Behr, B., Giudice, L., and Hoffman, A.R. (2005b). IVF results in de novo DNA methylation and histone methylation at an Igf2-H19 imprinting epigenetic switch. Mol Hum Reprod *11*, 631-640.

Liang, X.W., Zhu, J.Q., Miao, Y.L., Liu, J.H., Wei, L., Lu, S.S., Hou, Y., Schatten, H., Lu, K.H., and Sun, Q.Y. (2008). Loss of methylation imprint of Snrpn in postovulatory aging mouse oocyte. Biochem Biophys Res Commun *371*, 16-21.

Liew, C.G., Draper, J.S., Walsh, J., Moore, H., and Andrews, P.W. (2007). Transient and stable transgene expression in human embryonic stem cells. Stem Cells *25*, 1521-1528.

Lighten, A.D., Hardy, K., Winston, R.M., and Moore, G.E. (1997). IGF2 is parentally imprinted in human preimplantation embryos. Nat Genet *15*, 122-123.

Lin, S.P., Youngson, N., Takada, S., Seitz, H., Reik, W., Paulsen, M., Cavaille, J., and Ferguson-Smith, A.C. (2003). Asymmetric regulation of imprinting on the maternal and paternal chromosomes at the Dlk1-Gtl2 imprinted cluster on mouse chromosome 12. Nat Genet *35*, 97-102.

Liu, H.S., Jan, M.S., Chou, C.K., Chen, P.H., and Ke, N.J. (1999). Is green fluorescent protein toxic to the living cells? Biochem Biophys Res Commun *260*, 712-717.

Liu, J., Yu, S., Litman, D., Chen, W., and Weinstein, L.S. (2000). Identification of a methylation imprint mark within the mouse Gnas locus. Mol Cell Biol *20*, 5808-5817.

Liu, Z., and Fisher, R.A. (2004). RGS6 interacts with DMAP1 and DNMT1 and inhibits DMAP1 transcriptional repressor activity. J Biol Chem *279*, 14120-14128.

Lucifero, D., Chaillet, J.R., and Trasler, J.M. (2004a). Potential significance of genomic imprinting defects for reproduction and assisted reproductive technology. Hum Reprod Update *10*, 3-18.

Lucifero, D., La Salle, S., Bourc'his, D., Martel, J., Bestor, T.H., and Trasler, J.M. (2007). Coordinate regulation of DNA methyltransferase expression during oogenesis. BMC Dev Biol *7*, 36.

Lucifero, D., Mann, M.R., Bartolomei, M.S., and Trasler, J.M. (2004b). Gene-specific timing and epigenetic memory in oocyte imprinting. Hum Mol Genet *13*, 839-849.

Lucifero, D., Mertineit, C., Clarke, H.J., Bestor, T.H., and Trasler, J.M. (2002). Methylation dynamics of imprinted genes in mouse germ cells. Genomics *79*, 530-538.

Ludwig, T.E., Bergendahl, V., Levenstein, M.E., Yu, J., Probasco, M.D., and Thomson, J.A. (2006a). Feeder-independent culture of human embryonic stem cells. Nat Methods *3*, 637-646.

Ludwig, T.E., Levenstein, M.E., Jones, J.M., Berggren, W.T., Mitchen, E.R., Frane, J.L., Crandall, L.J., Daigh, C.A., Conard, K.R., Piekarczyk, M.S., *et al.* (2006b). Derivation of human embryonic stem cells in defined conditions. Nat Biotechnol *24*, 185-187.

MacDonald, H.R., and Wevrick, R. (1997). The necdin gene is deleted in Prader-Willi syndrome and is imprinted in human and mouse. Hum Mol Genet *6*, 1873-1878.

Maegawa, S., Yoshioka, H., Itaba, N., Kubota, N., Nishihara, S., Shirayoshi, Y., Nanba, E., and Oshimura, M. (2001). Epigenetic silencing of PEG3 gene expression in human glioma cell lines. Mol Carcinog *31*, 1-9.

Mager, J., Montgomery, N.D., de Villena, F.P., and Magnuson, T. (2003). Genome imprinting regulated by the mouse Polycomb group protein Eed. Nat Genet *33*, 502-507.

Maher, E.R. (2005). Imprinting and assisted reproductive technology. Hum Mol Genet *14 Spec No 1*, R133-138.

Maher, E.R., Afnan, M., and Barratt, C.L. (2003). Epigenetic risks related to assisted reproductive technologies: epigenetics, imprinting, ART and icebergs? Hum Reprod *18*, 2508-2511.

Mai, M., Qian, C., Yokomizo, A., Tindall, D.J., Bostwick, D., Polychronakos, C., Smith, D.I., and Liu, W. (1998a). Loss of imprinting and allele switching of p73 in renal cell carcinoma. Oncogene *17*, 1739-1741.

Mai, M., Yokomizo, A., Qian, C., Yang, P., Tindall, D.J., Smith, D.I., and Liu, W. (1998b). Activation of p73 silent allele in lung cancer. Cancer Res *58*, 2347-2349.

Maitra, A., Arking, D.E., Shivapurkar, N., Ikeda, M., Stastny, V., Kassauei, K., Sui, G., Cutler, D.J., Liu, Y., Brimble, S.N., *et al.* (2005). Genomic alterations in cultured human embryonic stem cells. Nat Genet *37*, 1099-1103.

Mancini-Dinardo, D., Steele, S.J., Levorse, J.M., Ingram, R.S., and Tilghman, S.M. (2006). Elongation of the Kcnq1ot1 transcript is required for genomic imprinting of neighboring genes. Genes Dev *20*, 1268-1282.

Mann, M.R., Lee, S.S., Doherty, A.S., Verona, R.I., Nolen, L.D., Schultz, R.M., and Bartolomei, M.S. (2004). Selective loss of imprinting in the placenta following preimplantation development in culture. Development *131*, 3727-3735.

Manning, M., Lissens, W., Bonduelle, M., Camus, M., De Rijcke, M., Liebaers, I., and Van Steirteghem, A. (2000). Study of DNA-methylation patterns at chromosome 15q11-q13 in children born after ICSI reveals no imprinting defects. Mol Hum Reprod *6*, 1049-1053.

Margot, J.B., Ehrenhofer-Murray, A.E., and Leonhardt, H. (2003). Interactions within the mammalian DNA methyltransferase family. BMC Mol Biol *4*, 7.

Marino-Ramirez, L., Spouge, J.L., Kanga, G.C., and Landsman, D. (2004). Statistical analysis of over-represented words in human promoter sequences. Nucleic Acids Res *32*, 949-958.

Marques, C.J., Carvalho, F., Sousa, M., and Barros, A. (2004). Genomic imprinting in disruptive spermatogenesis. Lancet *363*, 1700-1702.

Matsuoka, S., Edwards, M.C., Bai, C., Parker, S., Zhang, P., Baldini, A., Harper, J.W., and Elledge, S.J. (1995). p57KIP2, a structurally distinct member of the p21CIP1 Cdk inhibitor family, is a candidate tumor suppressor gene. Genes Dev *9*, 650-662.

Mayer, W., Niveleau, A., Walter, J., Fundele, R., and Haaf, T. (2000). Demethylation of the zygotic paternal genome. Nature *403*, 501-502.

McMinn, J., Wei, M., Sadovsky, Y., Thaker, H.M., and Tycko, B. (2006). Imprinting of PEG1/MEST isoform 2 in human placenta. Placenta *27*, 119-126.

Meguro, M., Kashiwagi, A., Mitsuya, K., Nakao, M., Kondo, I., Saitoh, S., and Oshimura, M. (2001). A novel maternally expressed gene, ATP10C, encodes a putative aminophospholipid translocase associated with Angelman syndrome. Nat Genet *28*, 19-20.

Mertineit, C., Yoder, J.A., Taketo, T., Laird, D.W., Trasler, J.M., and Bestor, T.H. (1998). Sex-specific exons control DNA methyltransferase in mammalian germ cells. Development *125*, 889-897.

Mitalipov, S., Clepper, L., Sritanaudomchai, H., Fujimoto, A., and Wolf, D. (2007). Methylation status of imprinting centers for H19/IGF2 and SNURF/SNRPN in primate embryonic stem cells. Stem Cells *25*, 581-588.

Mitalipov, S.M. (2006). Genomic imprinting in primate embryos and embryonic stem cells. Reprod Fertil Dev *18*, 817-821.

Mitalipova, M., Calhoun, J., Shin, S., Wininger, D., Schulz, T., Noggle, S., Venable, A., Lyons, I., Robins, A., and Stice, S. (2003). Human embryonic stem cell lines derived from discarded embryos. Stem Cells *21*, 521-526.

Mitsuya, K., Meguro, M., Lee, M.P., Katoh, M., Schulz, T.C., Kugoh, H., Yoshida, M.A., Niikawa, N., Feinberg, A.P., and Oshimura, M. (1999). LIT1, an imprinted antisense RNA in the human KvLQT1 locus identified by screening for differentially expressed transcripts using monochromosomal hybrids. Hum Mol Genet *8*, 1209-1217.

Mitsuya, K., Sui, H., Meguro, M., Kugoh, H., Jinno, Y., Niikawa, N., and Oshimura, M. (1997). Paternal expression of WT1 in human fibroblasts and lymphocytes. Hum Mol Genet *6*, 2243-2246.

Miyoshi, N., Wagatsuma, H., Wakana, S., Shiroishi, T., Nomura, M., Aisaka, K., Kohda, T., Surani, M.A., Kaneko-Ishino, T., and Ishino, F. (2000). Identification of an imprinted gene, Meg3/Gtl2 and its human homologue MEG3, first mapped on mouse distal chromosome 12 and human chromosome 14q. Genes Cells *5*, 211-220.

Monk, D., Arnaud, P., Apostolidou, S., Hills, F.A., Kelsey, G., Stanier, P., Feil, R., and Moore, G.E. (2006a). Limited evolutionary conservation of imprinting in the human placenta. Proc Natl Acad Sci U S A *103*, 6623-6628.

Monk, D., Sanches, R., Arnaud, P., Apostolidou, S., Hills, F.A., Abu-Amero, S., Murrell, A., Friess, H., Reik, W., Stanier, P., *et al.* (2006b). Imprinting of IGF2 P0 transcript and novel alternatively spliced INS-IGF2 isoforms show differences between mouse and human. Hum Mol Genet *15*, 1259-1269.

Monk, M., and Salpekar, A. (2001). Expression of imprinted genes in human preimplantation development. Mol Cell Endocrinol *183 Suppl 1*, S35-40.

Morison, I.M., Eccles, M.R., and Reeve, A.E. (2000). Imprinting of insulin-like growth factor 2 is modulated during hematopoiesis. Blood *96*, 3023-3028.

Morison, I.M., Ramsay, J.P., and Spencer, H.G. (2005). A census of mammalian imprinting. Trends Genet *21*, 457-465.

Mortusewicz, O., Schermelleh, L., Walter, J., Cardoso, M.C., and Leonhardt, H. (2005). Recruitment of DNA methyltransferase I to DNA repair sites. Proc Natl Acad Sci U S A *102*, 8905-8909.

Muller, S., van den Boom, D., Zirkel, D., Koster, H., Berthold, F., Schwab, M., Westphal, M., and Zumkeller, W. (2000). Retention of imprinting of the human apoptosis-related gene TSSC3 in human brain tumors. Hum Mol Genet *9*, 757-763.

Murrell, A. (2006). Genomic imprinting and cancer: from primordial germ cells to somatic cells. ScientificWorldJournal *6*, 1888-1910.

Nakabayashi, K., Bentley, L., Hitchins, M.P., Mitsuya, K., Meguro, M., Minagawa, S., Bamforth, J.S., Stanier, P., Preece, M., Weksberg, R., *et al.* (2002). Identification and characterization of an imprinted antisense RNA (MESTIT1) in the human MEST locus on chromosome 7q32. Hum Mol Genet *11*, 1743-1756.

Nakanishi, H., Suda, T., Katoh, M., Watanabe, A., Igishi, T., Kodani, M., Matsumoto, S., Nakamoto, M., Shigeoka, Y., Okabe, T., *et al.* (2004). Loss of imprinting of PEG1/MEST in lung cancer cell lines. Oncol Rep *12*, 1273-1278.

Narsa Reddy, M., Tang, L.Y., Lee, T.L., and James Shen, C.K. (2003). A candidate gene for Drosophila genome methylation. Oncogene *22*, 6301-6303.

Neyroud, N., Tesson, F., Denjoy, I., Leibovici, M., Donger, C., Barhanin, J., Faure, S., Gary, F., Coumel, P., Petit, C., *et al.* (1997). A novel mutation in the potassium channel gene KVLQT1 causes the Jervell and Lange-Nielsen cardioauditory syndrome. Nat Genet *15*, 186-189.

Nikaido, I., Saito, C., Mizuno, Y., Meguro, M., Bono, H., Kadomura, M., Kono, T., Morris, G.A., Lyons, P.A., Oshimura, M., *et al.* (2003). Discovery of imprinted transcripts in the mouse transcriptome using large-scale expression profiling. Genome Res *13*, 1402-1409.

Nishikawa, S., Goldstein, R.A., and Nierras, C.R. (2008). The promise of human induced pluripotent stem cells for research and therapy. Nat Rev Mol Cell Biol *9*, 725-729.

Oakes, C.C., La Salle, S., Smiraglia, D.J., Robaire, B., and Trasler, J.M. (2007). Developmental acquisition of genome-wide DNA methylation occurs prior to meiosis in male germ cells. Dev Biol *307*, 368-379.

Obata, Y., and Kono, T. (2002). Maternal primary imprinting is established at a specific time for each gene throughout oocyte growth. J Biol Chem *277*, 5285-5289.

Ohlsson, R., Nystrom, A., Pfeifer-Ohlsson, S., Tohonen, V., Hedborg, F., Schofield, P., Flam, F., and Ekstrom, T.J. (1993). IGF2 is parentally imprinted during human embryogenesis and in the Beckwith-Wiedemann syndrome. Nat Genet *4*, 94-97.

Ohm, J.E., McGarvey, K.M., Yu, X., Cheng, L., Schuebel, K.E., Cope, L., Mohammad, H.P., Chen, W., Daniel, V.C., Yu, W., *et al.* (2007). A stem cell-like chromatin pattern may predispose tumor suppressor genes to DNA hypermethylation and heritable silencing. Nat Genet *39*, 237-242.

Okabe, H., Satoh, S., Furukawa, Y., Kato, T., Hasegawa, S., Nakajima, Y., Yamaoka, Y., and Nakamura, Y. (2003). Involvement of PEG10 in human hepatocellular carcinogenesis through interaction with SIAH1. Cancer Res *63*, 3043-3048.

Okano, M., Bell, D.W., Haber, D.A., and Li, E. (1999). DNA methyltransferases Dnmt3a and Dnmt3b are essential for de novo methylation and mammalian development. Cell *99*, 247-257.

Okano, M., Xie, S., and Li, E. (1998a). Cloning and characterization of a family of novel mammalian DNA (cytosine-5) methyltransferases. Nat Genet *19*, 219-220.

Okano, M., Xie, S., and Li, E. (1998b). Dnmt2 is not required for de novo and maintenance methylation of viral DNA in embryonic stem cells. Nucleic Acids Res *26*, 2536-2540.

Olek, A., and Walter, J. (1997). The pre-implantation ontogeny of the H19 methylation imprint. Nat Genet *17*, 275-276.

Onyango, P., Jiang, S., Uejima, H., Shamblott, M.J., Gearhart, J.D., Cui, H., and Feinberg, A.P. (2002). Monoallelic expression and methylation of imprinted genes in human and mouse embryonic germ cell lineages. Proc Natl Acad Sci U S A *99*, 10599-10604.

Orstavik, K.H., Eiklid, K., van der Hagen, C.B., Spetalen, S., Kierulf, K., Skjeldal, O., and Buiting, K. (2003). Another case of imprinting defect in a girl with Angelman syndrome who was conceived by intracytoplasmic semen injection. Am J Hum Genet *72*, 218-219.

Oswald, J., Engemann, S., Lane, N., Mayer, W., Olek, A., Fundele, R., Dean, W., Reik, W., and Walter, J. (2000). Active demethylation of the paternal genome in the mouse zygote. Curr Biol *10*, 475-478.

Pal, R., and Ravindran, G. (2006). Assessment of pluripotency and multilineage differentiation potential of NTERA-2 cells as a model for studying human embryonic stem cells. Cell Prolif *39*, 585-598.

Pannetier, M., and Feil, R. (2007). Epigenetic stability of embryonic stem cells and developmental potential. Trends Biotechnol *25*, 556-562.

Pant, V., Kurukuti, S., Pugacheva, E., Shamsuddin, S., Mariano, P., Renkawitz, R., Klenova, E., Lobanenkov, V., and Ohlsson, R. (2004). Mutation of a single CTCF target site within the H19 imprinting control region leads to loss of Igf2 imprinting and complex patterns of de novo methylation upon maternal inheritance. Mol Cell Biol *24*, 3497-3504.

Pant, V., Mariano, P., Kanduri, C., Mattsson, A., Lobanenkov, V., Heuchel, R., and Ohlsson, R. (2003). The nucleotides responsible for the direct physical contact between the chromatin insulator protein CTCF and the H19 imprinting control region manifest parent of origin-specific long-distance insulation and methylation-free domains. Genes Dev *17*, 586-590.

Park, I.H., Zhao, R., West, J.A., Yabuuchi, A., Huo, H., Ince, T.A., Lerou, P.H., Lensch, M.W., and Daley, G.Q. (2008). Reprogramming of human somatic cells to pluripotency with defined factors. Nature *451*, 141-146.

Park, S., Schalling, M., Bernard, A., Maheswaran, S., Shipley, G.C., Roberts, D., Fletcher, J., Shipman, R., Rheinwald, J., Demetri, G., *et al.* (1993). The Wilms tumour gene WT1 is expressed in murine mesoderm-derived tissues and mutated in a human mesothelioma. Nat Genet *4*, 415-420.

Patten, J.L., Johns, D.R., Valle, D., Eil, C., Gruppuso, P.A., Steele, G., Smallwood, P.M., and Levine, M.A. (1990). Mutation in the gene encoding the stimulatory G protein of adenylate cyclase in Albright's hereditary osteodystrophy. N Engl J Med *322*, 1412-1419.

Pedersen, I.S., Dervan, P., McGoldrick, A., Harrison, M., Ponchel, F., Speirs, V., Isaacs, J.D., Gorey, T., and McCann, A. (2002). Promoter switch: a novel mechanism causing biallelic PEG1/MEST expression in invasive breast cancer. Hum Mol Genet *11*, 1449-1453.

Peng, D.F., Kanai, Y., Sawada, M., Ushijima, S., Hiraoka, N., Kitazawa, S., and Hirohashi, S. (2006). DNA methylation of multiple tumor-related genes in association with overexpression of DNA methyltransferase 1 (DNMT1) during multistage carcinogenesis of the pancreas. Carcinogenesis *27*, 1160-1168.

Pera, M.F. (2001). Human pluripotent stem cells: a progress report. Curr Opin Genet Dev *11*, 595-599.

Pera, M.F., Andrade, J., Houssami, S., Reubinoff, B., Trounson, A., Stanley, E.G., Ward-van Oostwaard, D., and Mummery, C. (2004). Regulation of human embryonic stem cell differentiation by BMP-2 and its antagonist noggin. J Cell Sci *117*, 1269-1280.

Peters, A.H., Kubicek, S., Mechtler, K., O'Sullivan, R.J., Derijck, A.A., Perez-Burgos, L., Kohlmaier, A., Opravil, S., Tachibana, M., Shinkai, Y., *et al.* (2003). Partitioning and plasticity of repressive histone methylation states in mammalian chromatin. Mol Cell *12*, 1577-1589.

Peters, A.H., O'Carroll, D., Scherthan, H., Mechtler, K., Sauer, S., Schofer, C., Weipoltshammer, K., Pagani, M., Lachner, M., Kohlmaier, A., *et al.* (2001). Loss of the Suv39h histone methyltransferases impairs mammalian heterochromatin and genome stability. Cell *107*, 323-337.

Plaia, T.W., Josephson, R., Liu, Y., Zeng, X., Ording, C., Toumadje, A., Brimble, S.N., Sherrer, E.S., Uhl, E.W., Freed, W.J., *et al.* (2006). Characterization of a new NIH-registered variant human embryonic stem cell line, BG01V: a tool for human embryonic stem cell research. Stem Cells *24*, 531-546.

Posfai, J., Bhagwat, A.S., Posfai, G., and Roberts, R.J. (1989). Predictive motifs derived from cytosine methyltransferases. Nucleic Acids Res *17*, 2421-2435.

Pradhan, S., Bacolla, A., Wells, R.D., and Roberts, R.J. (1999). Recombinant human DNA (cytosine-5) methyltransferase. I. Expression, purification, and comparison of de novo and maintenance methylation. J Biol Chem *274*, 33002-33010.

Pradhan, S., and Kim, G.D. (2002). The retinoblastoma gene product interacts with maintenance human DNA (cytosine-5) methyltransferase and modulates its activity. EMBO J *21*, 779-788.

Prawitt, D., Enklaar, T., Gartner-Rupprecht, B., Spangenberg, C., Oswald, M., Lausch, E., Schmidtke, P., Reutzel, D., Fees, S., Lucito, R., *et al.* (2005). Microdeletion of target sites for insulator protein CTCF in a chromosome 11p15 imprinting center in Beckwith-Wiedemann syndrome and Wilms' tumor. Proc Natl Acad Sci U S A *102*, 4085-4090.

Prelle, K., Wobus, A.M., Krebs, O., Blum, W.F., and Wolf, E. (2000). Overexpression of insulin-like growth factor-II in mouse embryonic stem cells promotes myogenic differentiation. Biochem Biophys Res Commun *277*, 631-638.

Pritchard-Jones, K., Fleming, S., Davidson, D., Bickmore, W., Porteous, D., Gosden, C., Bard, J., Buckler, A., Pelletier, J., Housman, D., *et al.* (1990). The candidate Wilms' tumour gene is involved in genitourinary development. Nature *346*, 194-197.

Przyborski, S.A., Morton, I.E., Wood, A., and Andrews, P.W. (2000). Developmental regulation of neurogenesis in the pluripotent human embryonal carcinoma cell line NTERA-2. Eur J Neurosci *12*, 3521-3528.

Qian, N., Frank, D., O'Keefe, D., Dao, D., Zhao, L., Yuan, L., Wang, Q., Keating, M., Walsh, C., and Tycko, B. (1997). The IPL gene on chromosome 11p15.5 is imprinted in humans and mice and is similar to TDAG51, implicated in Fas expression and apoptosis. Hum Mol Genet *6*, 2021-2029.

Ramsahoye, B.H., Biniszkiewicz, D., Lyko, F., Clark, V., Bird, A.P., and Jaenisch, R. (2000). Non-CpG methylation is prevalent in embryonic stem cells and may be mediated by DNA methyltransferase 3a. Proc Natl Acad Sci U S A *97*, 5237-5242.

Ray, P.F., Winston, R.M., and Handyside, A.H. (1997). XIST expression from the maternal X chromosome in human male preimplantation embryos at the blastocyst stage. Hum Mol Genet *6*, 1323-1327.

Reik, W. (2007). Stability and flexibility of epigenetic gene regulation in mammalian development. Nature *447*, 425-432.

Reik, W., Brown, K.W., Schneid, H., Le Bouc, Y., Bickmore, W., and Maher, E.R. (1995). Imprinting mutations in the Beckwith-Wiedemann syndrome suggested by altered imprinting pattern in the IGF2-H19 domain. Hum Mol Genet *4*, 2379-2385.

Reik, W., Dean, W., and Walter, J. (2001). Epigenetic reprogramming in mammalian development. Science *293*, 1089-1093.

Reik, W., and Walter, J. (2001). Genomic imprinting: parental influence on the genome. Nat Rev Genet *2*, 21-32.

Reis, A., Dittrich, B., Greger, V., Buiting, K., Lalande, M., Gillessen-Kaesbach, G., Anvret, M., and Horsthemke, B. (1994). Imprinting mutations suggested by abnormal DNA methylation patterns in familial Angelman and Prader-Willi syndromes. Am J Hum Genet *54*, 741-747.

Ren, C., Zhao, M., Yang, X., Li, D., Jiang, X., Wang, L., Shan, W., Yang, H., Zhou, L., Zhou, W., *et al.* (2006). Establishment and applications of epstein-barr virus-based episomal vectors in human embryonic stem cells. Stem Cells *24*, 1338-1347.

Reubinoff, B.E., Pera, M.F., Fong, C.Y., Trounson, A., and Bongso, A. (2000). Embryonic stem cell lines from human blastocysts: somatic differentiation in vitro. Nat Biotechnol *18*, 399-404.

Revazova, E.S., Turovets, N.A., Kochetkova, O.D., Kindarova, L.B., Kuzmichev, L.N., Janus, J.D., and Pryzhkova, M.V. (2007). Patient-Specific Stem Cell Lines Derived from Human Parthenogenetic Blastocysts. Cloning Stem Cells.

Rhee, I., Bachman, K.E., Park, B.H., Jair, K.W., Yen, R.W., Schuebel, K.E., Cui, H., Feinberg, A.P., Lengauer, C., Kinzler, K.W., *et al.* (2002). DNMT1 and DNMT3b cooperate to silence genes in human cancer cells. Nature *416*, 552-556.

Rhee, I., Jair, K.W., Yen, R.W., Lengauer, C., Herman, J.G., Kinzler, K.W., Vogelstein, B., Baylin, S.B., and Schuebel, K.E. (2000). CpG methylation is maintained in human cancer cells lacking DNMT1. Nature *404*, 1003-1007.

Ribas, R.C., Taylor, J.E., McCorquodale, C., Mauricio, A.C., Sousa, M., and Wilmut, I. (2006). Effect of zona pellucida removal on DNA methylation in early mouse embryos. Biol Reprod *74*, 307-313.

Rice, J.C., Briggs, S.D., Ueberheide, B., Barber, C.M., Shabanowitz, J., Hunt, D.F., Shinkai, Y., and Allis, C.D. (2003). Histone methyltransferases direct different degrees of methylation to define distinct chromatin domains. Mol Cell *12*, 1591-1598.

Richards, M., Fong, C.Y., Chan, W.K., Wong, P.C., and Bongso, A. (2002). Human feeders support prolonged undifferentiated growth of human inner cell masses and embryonic stem cells. Nat Biotechnol *20*, 933-936.

Riesewijk, A.M., Hu, L., Schulz, U., Tariverdian, G., Hoglund, P., Kere, J., Ropers, H.H., and Kalscheuer, V.M. (1997). Monoallelic expression of human PEG1/MEST is paralleled by parent-specific methylation in fetuses. Genomics *42*, 236-244.

Rinaudo, P., and Schultz, R.M. (2004). Effects of embryo culture on global pattern of gene expression in preimplantation mouse embryos. Reproduction *128*, 301-311.
Robertson, K.D. (2005). DNA methylation and human disease. Nat Rev Genet *6*, 597-610.

Rougeulle, C., Glatt, H., and Lalande, M. (1997). The Angelman syndrome candidate gene, UBE3A/E6-AP, is imprinted in brain. Nat Genet *17*, 14-15.

Rountree, M.R., Bachman, K.E., and Baylin, S.B. (2000). DNMT1 binds HDAC2 and a new co-repressor, DMAP1, to form a complex at replication foci. Nat Genet *25*, 269-277.

Rugg-Gunn, P.J., Ferguson-Smith, A.C., and Pedersen, R.A. (2005). Epigenetic status of human embryonic stem cells. Nat Genet *37*, 585-587.

Rugg-Gunn, P.J., Ferguson-Smith, A.C., and Pedersen, R.A. (2007). Status of genomic imprinting in human embryonic stem cells as revealed by a large cohort of independently derived and maintained lines. Hum Mol Genet *16 Spec No. 2*, R243-251.

Saito, Y., Kanai, Y., Sakamoto, M., Saito, H., Ishii, H., and Hirohashi, S. (2001). Expression of mRNA for DNA methyltransferases and methyl-CpG-binding proteins and DNA methylation status on CpG islands and pericentromeric satellite regions during human hepatocarcinogenesis. Hepatology *33*, 561-568.

Saito, Y., Kanai, Y., Sakamoto, M., Saito, H., Ishii, H., and Hirohashi, S. (2002). Overexpression of a splice variant of DNA methyltransferase 3b, DNMT3b4, associated with DNA hypomethylation on pericentromeric satellite regions during human hepatocarcinogenesis. Proc Natl Acad Sci U S A *99*, 10060-10065.

Salpekar, A., Huntriss, J., Bolton, V., and Monk, M. (2001). The use of amplified cDNA to investigate the expression of seven imprinted genes in human oocytes and preimplantation embryos. Mol Hum Reprod *7*, 839-844.

Santos, F., Hendrich, B., Reik, W., and Dean, W. (2002). Dynamic reprogramming of DNA methylation in the early mouse embryo. Dev Biol *241*, 172-182.

Sato, A., Otsu, E., Negishi, H., Utsunomiya, T., and Arima, T. (2007). Aberrant DNA methylation of imprinted loci in superovulated oocytes. Hum Reprod *22*, 26-35.

Sawada, M., Kanai, Y., Arai, E., Ushijima, S., Ojima, H., and Hirohashi, S. (2007). Increased expression of DNA methyltransferase 1 (DNMT1) protein in uterine cervix squamous cell carcinoma and its precursor lesion. Cancer Lett *251*, 211-219.

Schermelleh, L., Haemmer, A., Spada, F., Rosing, N., Meilinger, D., Rothbauer, U., Cardoso, M.C., and Leonhardt, H. (2007). Dynamics of Dnmt1 interaction with the replication machinery and its role in postreplicative maintenance of DNA methylation. Nucleic Acids Res *35*, 4301-4312.

Schieve, L.A., Meikle, S.F., Ferre, C., Peterson, H.B., Jeng, G., and Wilcox, L.S. (2002). Low and very low birth weight in infants conceived with use of assisted reproductive technology. N Engl J Med *346*, 731-737.

Schoenherr, C.J., Levorse, J.M., and Tilghman, S.M. (2003). CTCF maintains differential methylation at the Igf2/H19 locus. Nat Genet *33*, 66-69.

Schotta, G., Lachner, M., Sarma, K., Ebert, A., Sengupta, R., Reuter, G., Reinberg, D., and Jenuwein, T. (2004). A silencing pathway to induce H3-K9 and H4-K20 trimethylation at constitutive heterochromatin. Genes Dev *18*, 1251-1262.

Schumacher, A., and Doerfler, W. (2004). Influence of in vitro manipulation on the stability of methylation patterns in the Snurf/Snrpn-imprinting region in mouse embryonic stem cells. Nucleic Acids Res *32*, 1566-1576.

Schwienbacher, C., Gramantieri, L., Scelfo, R., Veronese, A., Calin, G.A., Bolondi, L., Croce, C.M., Barbanti-Brodano, G., and Negrini, M. (2000). Gain of imprinting at chromosome 11p15: A pathogenetic mechanism identified in human hepatocarcinomas. Proc Natl Acad Sci U S A *97*, 5445-5449.

Shamblott, M.J., Axelman, J., Wang, S., Bugg, E.M., Littlefield, J.W., Donovan, P.J., Blumenthal, P.D., Huggins, G.R., and Gearhart, J.D. (1998). Derivation of pluripotent stem cells from cultured human primordial germ cells. Proc Natl Acad Sci U S A *95*, 13726-13731.

Sharif, J., Muto, M., Takebayashi, S., Suetake, I., Iwamatsu, A., Endo, T.A., Shinga, J., Mizutani-Koseki, Y., Toyoda, T., Okamura, K., *et al.* (2007). The SRA protein Np95 mediates epigenetic inheritance by recruiting Dnmt1 to methylated DNA. Nature *450*, 908-912.

Shen, Y., Matsuno, Y., Fouse, S.D., Rao, N., Root, S., Xu, R., Pellegrini, M., Riggs, A.D., and Fan, G. (2008). X-inactivation in female human embryonic stem cells is in a nonrandom pattern and prone to epigenetic alterations. Proc Natl Acad Sci U S A *105*, 4709-4714.

Shibata, H., Ueda, T., Kamiya, M., Yoshiki, A., Kusakabe, M., Plass, C., Held, W.A., Sunahara, S., Katsuki, M., Muramatsu, M., *et al.* (1997). An oocyte-specific methylation imprint center in the mouse U2afbp-rs/U2af1-rs1 gene marks the establishment of allele-specific methylation during preimplantation development. Genomics *44*, 171-178.

Shirohzu, H., Kubota, T., Kumazawa, A., Sado, T., Chijiwa, T., Inagaki, K., Suetake, I., Tajima, S., Wakui, K., Miki, Y., *et al.* (2002). Three novel DNMT3B mutations in Japanese patients with ICF syndrome. Am J Med Genet *112*, 31-37.

Simon, C., Escobedo, C., Valbuena, D., Genbacev, O., Galan, A., Krtolica, A., Asensi, A., Sanchez, E., Esplugues, J., Fisher, S., *et al.* (2005). First derivation in Spain of human embryonic stem cell lines: use of long-term cryopreserved embryos and animal-free conditions. Fertil Steril *83*, 246-249.

Sleutels, F., Tjon, G., Ludwig, T., and Barlow, D.P. (2003). Imprinted silencing of Slc22a2 and Slc22a3 does not need transcriptional overlap between Igf2r and Air. EMBO J *22*, 3696-3704.

Sleutels, F., Zwart, R., and Barlow, D.P. (2002). The non-coding Air RNA is required for silencing autosomal imprinted genes. Nature *415*, 810-813.

Smilinich, N.J., Day, C.D., Fitzpatrick, G.V., Caldwell, G.M., Lossie, A.C., Cooper, P.R., Smallwood, A.C., Joyce, J.A., Schofield, P.N., Reik, W., *et al.* (1999). A maternally methylated CpG island in KvLQT1 is associated with an antisense paternal transcript and loss of imprinting in Beckwith-Wiedemann syndrome. Proc Natl Acad Sci U S A *96*, 8064-8069.

Smith, J.R., Maguire, S., Davis, L.A., Alexander, M., Yang, F., Chandran, S., ffrench-Constant, C., and Pedersen, R.A. (2008). Robust, persistent transgene expression in human embryonic stem cells is achieved with AAVS1-targeted integration. Stem Cells *26*, 496-504.

Smrzka, O.W., Fae, I., Stoger, R., Kurzbauer, R., Fischer, G.F., Henn, T., Weith, A., and Barlow, D.P. (1995). Conservation of a maternal-specific methylation signal at the human IGF2R locus. Hum Mol Genet *4*, 1945-1952.

Solter, D., and Knowles, B.B. (1975). Immunosurgery of mouse blastocyst. Proc Natl Acad Sci U S A *72*, 5099-5102.

Southern, E. (2006). Southern blotting. Nat Protoc *1*, 518-525.

Sparago, A., Cerrato, F., Vernucci, M., Ferrero, G.B., Silengo, M.C., and Riccio, A. (2004). Microdeletions in the human H19 DMR result in loss of IGF2 imprinting and Beckwith-Wiedemann syndrome. Nat Genet *36*, 958-960.

Sperger, J.M., Chen, X., Draper, J.S., Antosiewicz, J.E., Chon, C.H., Jones, S.B., Brooks, J.D., Andrews, P.W., Brown, P.O., and Thomson, J.A. (2003). Gene expression patterns in human embryonic stem cells and human pluripotent germ cell tumors. Proc Natl Acad Sci U S A *100*, 13350-13355.

Steele, W., Allegrucci, C., Singh, R., Lucas, E., Priddle, H., Denning, C., Sinclair, K., and Young, L. (2005). Human embryonic stem cell methyl cycle enzyme expression: modelling epigenetic programming in assisted reproduction? Reprod Biomed Online *10*, 755-766.

Stewart, C.L., Stuhlmann, H., Jahner, D., and Jaenisch, R. (1982). De novo methylation, expression, and infectivity of retroviral genomes introduced into embryonal carcinoma cells. Proc Natl Acad Sci U S A *79*, 4098-4102.

Stoger, R., Kubicka, P., Liu, C.G., Kafri, T., Razin, A., Cedar, H., and Barlow, D.P. (1993). Maternal-specific methylation of the imprinted mouse Igf2r locus identifies the expressed locus as carrying the imprinting signal. Cell *73*, 61-71.

Strelchenko, N., Verlinsky, O., Kukharenko, V., and Verlinsky, Y. (2004). Morula-derived human embryonic stem cells. Reprod Biomed Online *9*, 623-629.

Suetake, I., Shinozaki, F., Miyagawa, J., Takeshima, H., and Tajima, S. (2004). DNMT3L stimulates the DNA methylation activity of Dnmt3a and Dnmt3b through a direct interaction. J Biol Chem *279*, 27816-27823.

Sun, B.W., Yang, A.C., Feng, Y., Sun, Y.J., Zhu, Y., Zhang, Y., Jiang, H., Li, C.L., Gao, F.R., Zhang, Z.H., *et al.* (2006). Temporal and parental-specific expression of imprinted genes in a newly derived Chinese human embryonic stem cell line and embryoid bodies. Hum Mol Genet *15*, 65-75.

Surani, M.A. (2001). Reprogramming of genome function through epigenetic inheritance. Nature *414*, 122-128.

Sutcliffe, J.S., Nakao, M., Christian, S., Orstavik, K.H., Tommerup, N., Ledbetter, D.H., and Beaudet, A.L. (1994). Deletions of a differentially methylated CpG island at the SNRPN gene define a putative imprinting control region. Nat Genet *8*, 52-58.

Suzuki, S., Ono, R., Narita, T., Pask, A.J., Shaw, G., Wang, C., Kohda, T., Alsop, A.E., Marshall Graves, J.A., Kohara, Y., *et al.* (2007). Retrotransposon silencing by DNA methylation can drive mammalian genomic imprinting. PLoS Genet *3*, e55.

Szabo, P.E., Hubner, K., Scholer, H., and Mann, J.R. (2002). Allele-specific expression of imprinted genes in mouse migratory primordial germ cells. Mech Dev *115*, 157-160.

Tachibana, M., Sugimoto, K., Fukushima, T., and Shinkai, Y. (2001). Set domain-containing protein, G9a, is a novel lysine-preferring mammalian histone methyltransferase with hyperactivity and specific selectivity to lysines 9 and 27 of histone H3. J Biol Chem *276*, 25309-25317.

Tachibana, M., Sugimoto, K., Nozaki, M., Ueda, J., Ohta, T., Ohki, M., Fukuda, M., Takeda, N., Niida, H., Kato, H., *et al.* (2002). G9a histone methyltransferase plays a dominant role in euchromatic histone H3 lysine 9 methylation and is essential for early embryogenesis. Genes Dev *16*, 1779-1791.

Takada, S., Paulsen, M., Tevendale, M., Tsai, C.E., Kelsey, G., Cattanach, B.M., and Ferguson-Smith, A.C. (2002). Epigenetic analysis of the Dlk1-Gtl2 imprinted domain on mouse chromosome 12: implications for imprinting control from comparison with Igf2-H19. Hum Mol Genet *11*, 77-86.

Takahashi, K., Tanabe, K., Ohnuki, M., Narita, M., Ichisaka, T., Tomoda, K., and Yamanaka, S. (2007). Induction of pluripotent stem cells from adult human fibroblasts by defined factors. Cell *131*, 861-872.

Tamaru, H., and Selker, E.U. (2001). A histone H3 methyltransferase controls DNA methylation in Neurospora crassa. Nature *414*, 277-283.

Tang, L.Y., Reddy, M.N., Rasheva, V., Lee, T.L., Lin, M.J., Hung, M.S., and Shen, C.K. (2003). The eukaryotic DNMT2 genes encode a new class of cytosine-5 DNA methyltransferases. J Biol Chem *278*, 33613-33616.

Thomson, J.A., Itskovitz-Eldor, J., Shapiro, S.S., Waknitz, M.A., Swiergiel, J.J., Marshall, V.S., and Jones, J.M. (1998). Embryonic stem cell lines derived from human blastocysts. Science *282*, 1145-1147.

Thomson, J.A., Kalishman, J., Golos, T.G., Durning, M., Harris, C.P., Becker, R.A., and Hearn, J.P. (1995). Isolation of a primate embryonic stem cell line. Proc Natl Acad Sci U S A *92*, 7844-7848.

Thomson, J.A., and Odorico, J.S. (2000). Human embryonic stem cell and embryonic germ cell lines. Trends Biotechnol *18*, 53-57.

Thorvaldsen, J.L., Duran, K.L., and Bartolomei, M.S. (1998). Deletion of the H19 differentially methylated domain results in loss of imprinted expression of H19 and Igf2. Genes Dev *12*, 3693-3702.

Tsai, T.F., Jiang, Y.H., Bressler, J., Armstrong, D., and Beaudet, A.L. (1999). Paternal deletion from Snrpn to Ube3a in the mouse causes hypotonia, growth retardation and partial lethality and provides evidence for a gene contributing to Prader-Willi syndrome. Hum Mol Genet *8*, 1357-1364.

Tsou, A.P., Chuang, Y.C., Su, J.Y., Yang, C.W., Liao, Y.L., Liu, W.K., Chiu, J.H., and Chou, C.K. (2003). Overexpression of a novel imprinted gene, PEG10, in human hepatocellular carcinoma and in regenerating mouse livers. J Biomed Sci *10*, 625-635.

Tsumura, A., Hayakawa, T., Kumaki, Y., Takebayashi, S., Sakaue, M., Matsuoka, C., Shimotohno, K., Ishikawa, F., Li, E., Ueda, H.R., *et al.* (2006). Maintenance of self-renewal ability of mouse embryonic stem cells in the absence of DNA methyltransferases Dnmt1, Dnmt3a and Dnmt3b. Genes Cells *11*, 805-814.

Ueda, T., Abe, K., Miura, A., Yuzuriha, M., Zubair, M., Noguchi, M., Niwa, K., Kawase, Y., Kono, T., Matsuda, Y., *et al.* (2000). The paternal methylation imprint of the mouse H19 locus is acquired in the gonocyte stage during foetal testis development. Genes Cells *5*, 649-659.

Umlauf, D., Goto, Y., Cao, R., Cerqueira, F., Wagschal, A., Zhang, Y., and Feil, R. (2004). Imprinting along the Kcnq1 domain on mouse chromosome 7 involves repressive histone methylation and recruitment of Polycomb group complexes. Nat Genet *36*, 1296-1300.

Unger, C., Skottman, H., Blomberg, P., Dilber, M.S., and Hovatta, O. (2008). Good manufacturing practice and clinical-grade human embryonic stem cell lines. Hum Mol Genet *17*, R48-53.

Vallier, L., Alexander, M., and Pedersen, R.A. (2005). Activin/Nodal and FGF pathways cooperate to maintain pluripotency of human embryonic stem cells. J Cell Sci *118*, 4495-4509.

Vallier, L., Reynolds, D., and Pedersen, R.A. (2004a). Nodal inhibits differentiation of human embryonic stem cells along the neuroectodermal default pathway. Dev Biol *275*, 403-421.

Vallier, L., Rugg-Gunn, P.J., Bouhon, I.A., Andersson, F.K., Sadler, A.J., and Pedersen, R.A. (2004b). Enhancing and diminishing gene function in human embryonic stem cells. Stem Cells *22*, 2-11.

van de Stolpe, A., van den Brink, S., van Rooijen, M., Ward-van Oostwaard, D., van Inzen, W., Slaper-Cortenbach, I., Fauser, B., van den Hout, N., Weima, S., Passier, R., *et al.* (2005). Human embryonic stem cells: towards therapies for cardiac disease. Derivation of a Dutch human embryonic stem cell line. Reprod Biomed Online *11*, 476-485.

Venter, J.C., Adams, M.D., Myers, E.W., Li, P.W., Mural, R.J., Sutton, G.G., Smith, H.O., Yandell, M., Evans, C.A., Holt, R.A., *et al.* (2001). The sequence of the human genome. Science *291*, 1304-1351.

Vertino, P.M., Yen, R.W., Gao, J., and Baylin, S.B. (1996). De novo methylation of CpG island sequences in human fibroblasts overexpressing DNA (cytosine-5-)-methyltransferase. Mol Cell Biol *16*, 4555-4565.

Vu, T.H., and Hoffman, A.R. (1994). Promoter-specific imprinting of the human insulin-like growth factor-II gene. Nature *371*, 714-717.

Vu, T.H., Li, T., and Hoffman, A.R. (2004). Promoter-restricted histone code, not the differentially methylated DNA regions or antisense transcripts, marks the imprinting status of IGF2R in human and mouse. Hum Mol Genet *13*, 2233-2245.

Wang, Q., Curran, M.E., Splawski, I., Burn, T.C., Millholland, J.M., VanRaay, T.J., Shen, J., Timothy, K.W., Vincent, G.M., de Jager, T., *et al.* (1996). Positional cloning of a novel potassium channel gene: KVLQT1 mutations cause cardiac arrhythmias. Nat Genet *12*, 17-23.

Watt, F., and Molloy, P.L. (1988). Cytosine methylation prevents binding to DNA of a HeLa cell transcription factor required for optimal expression of the adenovirus major late promoter. Genes Dev *2*, 1136-1143.

Webster, K.E., O'Bryan, M.K., Fletcher, S., Crewther, P.E., Aapola, U., Craig, J., Harrison, D.K., Aung, H., Phutikanit, N., Lyle, R., *et al.* (2005). Meiotic and epigenetic defects in Dnmt3L-knockout mouse spermatogenesis. Proc Natl Acad Sci U S A *102*, 4068-4073.

Weksberg, R., Shen, D.R., Fei, Y.L., Song, Q.L., and Squire, J. (1993). Disruption of insulin-like growth factor 2 imprinting in Beckwith-Wiedemann syndrome. Nat Genet *5*, 143-150.

Weksberg, R., Smith, A.C., Squire, J., and Sadowski, P. (2003). Beckwith-Wiedemann syndrome demonstrates a role for epigenetic control of normal development. Hum Mol Genet *12 Spec No 1*, R61-68.

Wevrick, R., Kerns, J.A., and Francke, U. (1994). Identification of a novel paternally expressed gene in the Prader-Willi syndrome region. Hum Mol Genet *3*, 1877-1882.

Williams, R.L., Hilton, D.J., Pease, S., Willson, T.A., Stewart, C.L., Gearing, D.P., Wagner, E.F., Metcalf, D., Nicola, N.A., and Gough, N.M. (1988). Myeloid leukaemia inhibitory factor maintains the developmental potential of embryonic stem cells. Nature *336*, 684-687.

Wu, H., Kim, K.J., Mehta, K., Paxia, S., Sundstrom, A., Anantharaman, T., Kuraishy, A.I., Doan, T., Ghosh, J., Pyle, A.D., *et al.* (2008). Copy number variant analysis of human embryonic stem cells. Stem Cells *26*, 1484-1489.

Wu, R., Terry, A.V., Singh, P.B., and Gilbert, D.M. (2005). Differential subnuclear localization and replication timing of histone H3 lysine 9 methylation states. Mol Biol Cell *16*, 2872-2881.

Wutz, A., Smrzka, O.W., Schweifer, N., Schellander, K., Wagner, E.F., and Barlow, D.P. (1997). Imprinted expression of the Igf2r gene depends on an intronic CpG island. Nature *389*, 745-749.

Wylie, A.A., Murphy, S.K., Orton, T.C., and Jirtle, R.L. (2000). Novel imprinted DLK1/GTL2 domain on human chromosome 14 contains motifs that mimic those implicated in IGF2/H19 regulation. Genome Res *10*, 1711-1718.

Xiao, L., Yuan, X., and Sharkis, S.J. (2006). Activin A maintains self-renewal and regulates fibroblast growth factor, Wnt, and bone morphogenic protein pathways in human embryonic stem cells. Stem Cells *24*, 1476-1486.

Xin, Z., Tachibana, M., Guggiari, M., Heard, E., Shinkai, Y., and Wagstaff, J. (2003). Role of histone methyltransferase G9a in CpG methylation of the Prader-Willi syndrome imprinting center. J Biol Chem *278*, 14996-15000.

Xu, C., Inokuma, M.S., Denham, J., Golds, K., Kundu, P., Gold, J.D., and Carpenter, M.K. (2001). Feeder-free growth of undifferentiated human embryonic stem cells. Nat Biotechnol *19*, 971-974.

Xu, G.L., Bestor, T.H., Bourc'his, D., Hsieh, C.L., Tommerup, N., Bugge, M., Hulten, M., Qu, X., Russo, J.J., and Viegas-Pequignot, E. (1999). Chromosome instability and immunodeficiency syndrome caused by mutations in a DNA methyltransferase gene. Nature *402*, 187-191.

Xu, R.H., Chen, X., Li, D.S., Li, R., Addicks, G.C., Glennon, C., Zwaka, T.P., and Thomson, J.A. (2002). BMP4 initiates human embryonic stem cell differentiation to trophoblast. Nat Biotechnol *20*, 1261-1264.

Xu, R.H., Peck, R.M., Li, D.S., Feng, X., Ludwig, T., and Thomson, J.A. (2005). Basic FGF and suppression of BMP signaling sustain undifferentiated proliferation of human ES cells. Nat Methods *2*, 185-190.

Xu, Y., Goodyer, C.G., Deal, C., and Polychronakos, C. (1993). Functional polymorphism in the parental imprinting of the human IGF2R gene. Biochem Biophys Res Commun *197*, 747-754.

Yamazaki, Y., Mann, M.R., Lee, S.S., Marh, J., McCarrey, J.R., Yanagimachi, R., and Bartolomei, M.S. (2003). Reprogramming of primordial germ cells begins before migration into the genital ridge, making these cells inadequate donors for reproductive cloning. Proc Natl Acad Sci U S A *100*, 12207-12212.

Ying, Q.L., Nichols, J., Chambers, I., and Smith, A. (2003a). BMP induction of Id proteins suppresses differentiation and sustains embryonic stem cell self-renewal in collaboration with STAT3. Cell *115*, 281-292.

Ying, Q.L., Stavridis, M., Griffiths, D., Li, M., and Smith, A. (2003b). Conversion of embryonic stem cells into neuroectodermal precursors in adherent monoculture. Nat Biotechnol *21*, 183-186.

Yoder, J.A., Soman, N.S., Verdine, G.L., and Bestor, T.H. (1997a). DNA (cytosine-5)-methyltransferases in mouse cells and tissues. Studies with a mechanism-based probe. J Mol Biol *270*, 385-395.

Yoder, J.A., Walsh, C.P., and Bestor, T.H. (1997b). Cytosine methylation and the ecology of intragenomic parasites. Trends Genet *13*, 335-340.

Yoon, B.J., Herman, H., Sikora, A., Smith, L.T., Plass, C., and Soloway, P.D. (2002). Regulation of DNA methylation of Rasgrf1. Nat Genet *30*, 92-96.

Young, L.E., and Fairburn, H.R. (2000). Improving the safety of embryo technologies: possible role of genomic imprinting. Theriogenology *53*, 627-648.

Young, L.E., Fernandes, K., McEvoy, T.G., Butterwith, S.C., Gutierrez, C.G., Carolan, C., Broadbent, P.J., Robinson, J.J., Wilmut, I., and Sinclair, K.D. (2001). Epigenetic change in IGF2R is associated with fetal overgrowth after sheep embryo culture. Nat Genet *27*, 153-154.

Yu, J., Vodyanik, M.A., Smuga-Otto, K., Antosiewicz-Bourget, J., Frane, J.L., Tian, S., Nie, J., Jonsdottir, G.A., Ruotti, V., Stewart, R., *et al.* (2007). Induced pluripotent stem cell lines derived from human somatic cells. Science *318*, 1917-1920.

Zaragosi, L.E., Billon, N., Ailhaud, G., and Dani, C. (2007). Nucleofection is a valuable transfection method for transient and stable transgene expression in adipose tissue-derived stem cells. Stem Cells *25*, 790-797.

Zhang, X., Zhou, Y., Mehta, K.R., Danila, D.C., Scolavino, S., Johnson, S.R., and Klibanski, A. (2003). A pituitary-derived MEG3 isoform functions as a growth suppressor in tumor cells. J Clin Endocrinol Metab *88*, 5119-5126.

Zhao, Z., and Zhang, F. (2006). Sequence context analysis of 8.2 million single nucleotide polymorphisms in the human genome. Gene *366*, 316-324.

Zochbauer-Muller, S., Fong, K.M., Virmani, A.K., Geradts, J., Gazdar, A.F., and Minna, J.D. (2001). Aberrant promoter methylation of multiple genes in non-small cell lung cancers. Cancer Res *61*, 249-255.

Zwart, R., Sleutels, F., Wutz, A., Schinkel, A.H., and Barlow, D.P. (2001). Bidirectional action of the Igf2r imprint control element on upstream and downstream imprinted genes. Genes Dev *15*, 2361-2366.

8 Appendix 1

8.1 Buffers and media

8.1.1 General molecular works

8.1.1.1 10× TBE

Reagent	Volume	Supplier	Catalogue number
Tris Base	108g	Fisher	BPE152-5
Boric Acid	55g	Sigma	B1934
Ethylenediaminetetraacetic Acid (EDTA)	9.3g	Sigma	E5134

The volume was made up to 1 litre with distilled water. The solution was autoclaved and stored at room temperature.

8.1.1.2 LB medium

Reagent	Volume	Supplier	Catalogue number
LB Broth Power	12.50g	Fisher	BPE1426-500

The volume was made up to 500 ml with distilled water. The solution was autoclaved and stored at room temperature.

8.1.1.3 LB Agar

Reagent	Volume	Supplier	Catalogue number
LB Broth Power	12.50g	Fisher	BPE1426-500
Agar	7.50g	Fisher	BPE1423-500

The volume was made up to 500 ml with distilled water. The solution was autoclaved and stored at room temperature.

8.1.1.4 10% SDS

Reagent	Volume	Supplier	Catalogue number
Lauryl Sulfate (SDS)	10g	Sigma	L4390

The volume was made up to 100 ml with distilled water. The solution was autoclaved and stored at room temperature.

8.1.1.5 5 M NaCl

Reagent	Volume	Supplier	Catalogue number
Sodium Chloride	29.22 g	Fisher	BPE 358-1

The volume was made up to 100 ml with distilled water. The solution was autoclaved and stored at room temperature.

8.1.1.6 0.5 M EDTA (pH 8.0)

Reagent	Volume	Supplier	Catalogue number
EDTA	186.1g	Fluka	3677
Sodium Hydroxide	~ 20g	Fisher	S/4920/60

EDTA was dissolved in 800 ml of distilled water and the pH was adjusted to pH 8.0 with ~ 20g of NaOH (or with ~ 50 ml of 10N NaOH). Then, the volume was made up to 1 litre with distilled water. The solution was autoclaved and stored at room temperature.

8.1.1.7 1M Tris-HCl (pH 8.0)

Reagent	Volume	Supplier	Catalogue number
Tris base	24.2g	Fisher	BPE152-5
Hydrochloric acid	~ 9ml	Fisher	H/1200/PB17

Tris base was dissolved in 180 ml of distilled water and the pH was adjusted to pH 8.0 with ~ 9 ml of HCl. Then, the volume was made up to 200 ml with distilled water. The solution was autoclaved and stored at room temperature.

8.1.1.8 3M NaOH

Reagent	Volume	Supplier	Catalogue number
Sodium Hydroxide	12 g	Fisher	BPE359-500

The volume was made up to 100 ml with distilled water. The solution was autoclaved and stored at room temperature.

8.1.1.9 5× Gel loading solution

Reagent	Volume	Supplier	Catalogue number
Gel Loading Solution	-	Sigma	G2526

The solution was stored at room temperature.

8.1.1.10 DNA Ladder

Reagent	Volume	Supplier	Catalogue number
2-Log DNA Ladder	-	NEB	N3200S
1 kb DNA Ladder			N3232S
100 bp DNA Ladder			N3231S
50 bp DNA Ladder			N3236S

1 µl of DNA Ladder was mixed with 1 µl of 5× Gel loading solution (see 2.4.1.9) and 3 µl of RNase/DNase free water (see 2.4.1.20), and used as a molecular markers on the Agarose gel.

8.1.1.11 1 M DTT

Reagent	Volume	Supplier	Catalogue number
DL-Dithiothreitol	1.54 g	Sigma	D0632

The volume was made up to 10 ml with distilled water. The solution was filter-sterilised using a 10 ml syringe and a 0.2 µm minisart filter. 500 µl aliquots were stored at –20 ºC.

8.1.1.12 3M NaOAc (pH 5.5)

Reagent	Volume	Supplier	Catalogue number
3 M Sodium Acetate	-	Ambion	9740

This solution was stored at room temperature.

8.1.1.13 Phenol/chloroform/isoamyl alcohol

Reagent	Volume	Supplier	Catalogue number
Phenol:Chloroform:Isoamyl Alcohol	-	Sigma	P2069

Phenol/Chloroform/Isoamyl Alcohol was stored at 4 ºC.

8.1.1.14 2,000× Kanamycin

Reagent	Volume	Supplier	Catalogue number

Kanamycin	1 g	Sigma	K4000

The volume was made up to 10 ml with distilled water. The solution was filter-sterilised using a 10 ml syringe and a 0.2 µm minisart filter. 500 µl aliquots were stored at –20 ºC.

8.1.1.15 1,000× Ampicillin

Reagent	Volume	Supplier	Catalogue number
Ampicillin	500 mg	Sigma	A0166

The volume was made up to 10 ml with distilled water. The solution was filter-sterilised using a 10 ml syringe and a 0.2 µm minisart filter. 500 µl aliquots were stored at –20 ºC.

8.1.1.16 Ethanol

Reagent	Volume	Supplier	Catalogue number
Ethanol	-	Fisher	E/0650DF/17

The solution was stored at room temperature.

8.1.1.17 Methanol

Reagent	Volume	Supplier	Catalogue number
Methanol	-	Fisher	M/4056/17

The solution was stored at room temperature.

8.1.1.18 Isopropanol

Reagent	Volume	Supplier	Catalogue number
Propan-2-ol	-	Fisher	P/7507/PB17

The solution was stored at room temperature.

8.1.1.19 β-Mercaptoethanol

Reagent	Volume	Supplier	Catalogue number
β-Mercaptoethanol	-	Sigma	M3148

The solution was stored at room temperature.

8.1.1.20 RNase/DNase free water

Reagent	Volume	Supplier	Catalogue number
Water	-	Sigma	W4502

Water was stored at room temperature.

8.1.1.21 PBS

Reagent	Volume	Supplier	Catalogue number
PBS	-	Invitrogen	14190

PBS was stored at room temperature.

8.1.1.22 Lysis buffer (genomic DNA)

Reagent	Volume	Supplier	Catalogue number
1M Tris-HCl (pH 8.0)	100 µl	See 2.4.1.7	
5M NaCl	20 µl	See 2.4.1.5	
500mM EDTA	200 µl	See 2.4.1.6	
10% SDS	500 µl	See 2.4.1.4	

The volume was made up to 10 ml with distilled water. Proteinase K (Roche: 3115879001) was added into solution to give a final concentration of 50 $\mu g \cdot ml^{-1}$.

8.1.2 Western blotting works

8.1.2.1 10× Protein electrophoresis buffer

Reagent	Volume	Supplier	Catalogue number
Tris Base	30g	Fisher	BPE152-5
Glycine	144g	Fisher	BPE381-1

The volume was made up to 1 litre with distilled water. The solution was autoclaved and stored at room temperature.

8.1.2.2 10× Protein transfer buffer

Reagent	Volume	Supplier	Catalogue number
Tris Base	37.8g	Fisher	BPE152-5
Glycine	180g	Fisher	BPE381-1

The volume was made up to 1 litre with distilled water. The solution was autoclaved and stored at room temperature.

8.1.2.3 10× TBS

Reagent	Volume	Supplier	Catalogue number
Tris Base	12.11g	Fisher	BPE152-5
Sodium Chloride	87.66 g	Fisher	BPE 358-1

The volume was made up to 1 litre with distilled water. The solution was autoclaved and stored at room temperature.

8.1.2.4 TBST

Reagent	Volume	Supplier	Catalogue number
10X TBS	100 ml	See 2.4.2.3	
Tween 20	1 ml	Sigma	P9416

The volume was made up to 1 litre with distilled water.

8.1.2.5 Blocking buffer (5% Skim milk)

Reagent	Volume	Supplier	Catalogue number
Skim Milk Powder	5 g	Marvel	-
10X TBS	10 ml	See 2.4.2.3	

The volume was made up to 100 ml with distilled water. The solution was stored at 4 ^{o}C.

8.1.2.6 1M Tris-HCl (pH 6.8)

Reagent	Volume	Supplier	Catalogue number
Tris base	24.2 g	Fisher	BPE152-5
Hydrochloric acid (HCl)	~ 16 ml	Fisher	H/1200/PB17

Tris base was dissolved in 180 ml of distilled water and the pH was adjusted to pH 6.8 with HCl. Then, the volume was made up to 200 ml with distilled water. The solution was autoclaved and stored at room temperature.

8.1.2.7 1.5M Tris-HCl (pH 8.8)

Reagent	Volume	Supplier	Catalogue number
Tris base	36.3 g	Fisher	BPE152-5
Hydrochloric acid	~ 8 ml	Fisher	H/1200/PB17

Tris base was dissolved in 180 ml of distilled water and the pH was adjusted to pH 8.8 with ~ 8ml of HCl. Then, the volume was made up to 200 ml with distilled water. The solution was autoclaved and stored at room temperature.

8.1.2.8 Coomassie blue gel stain solution

Reagent	Volume	Supplier	Catalogue number
Coomassie Blue R-250	1g	Sigma	B0149
Methanol	450ml	See 2.4.1.17	
Glacial Acetic Acid	100ml	Fisher	A/0400/PB17

The volume was made up to 1 litre with distilled water. The solution was stored at room temperature.

8.1.2.9 Coomassie blue gel destain solution

Reagent	Volume	Supplier	Catalogue number
Methanol	100ml	See 2.4.1.17	
Glacial Acetic Acid	100ml	Fisher	A/0400/PB17

The volume was made up to 1 litre with distilled water. The solution was stored at room temperature.

8.1.2.10 50% Glycerol

Reagent	Volume	Supplier	Catalogue number
Glycerol	50 ml	Sigma	G5516

The volume was made up to 100 ml with distilled water. The solution was stored at room temperature.

8.1.2.11 1% Bromophenole blue

Reagent	Volume	Supplier	Catalogue number
Bromophenole Blue	100 mg	Sigma	B8026

The volume was made up to 10 ml with distilled water. The solution was filter-sterilised using a 10 ml syringe and a 0.2 µm minisart filter and stored at –20 ºC.

8.1.2.12 10% APS

Reagent	Volume	Supplier	Catalogue number
Amonium Persulfate (APS)	0.5 g	Fisher	BPE179-25

The volume was made up to 5 ml with distilled water. The solution was filter-sterilised using a 10 ml syringe and a 0.2 µm minisart filter. 500 µl aliquots were placed into eppendorf tubes and stored at –20 ºC.

8.1.2.13 5% NP40

Reagent	Volume	Supplier	Catalogue number
Igepal CA-630	5 ml	Sigma	I3021

The volume was made up to 100 ml with distilled water. The solution was filter-sterilised using a 50 ml syringe and a 0.2 µm minisart filter and stored at room temperature.

8.1.2.14 RIPA buffer

Reagent	Volume	Supplier	Catalogue number
1M Tris-HCl (pH 8.0)	2.5ml	See 2.4.1.7	
5M NaCl	4.2ml	See 2.4.1.5	
500mM EDTA	100µl	See 2.4.1.6	

5% NP40	2ml	See 2.4.2.13

The volume was made up to 50 ml with distilled water. The solution was stored at 4ºC.

8.1.2.15 Protein loading buffer

Reagent	Volume	Supplier	Catalogue number
1M Tris (pH 6.8)	600µl	See 2.4.2.6	
50% Glycerol	5ml	See 2.4.2.10	
10% SDS	2ml	See 2.4.1.4	
β-Mercaptoethanol	500µl	See 2.4.1.19	
1% Bromophenole Blue (BPB)	1ml	See 2.4.2.11	

The volume was made up to 10 ml with distilled water. The solution was filter-sterilised using a 10 ml syringe and a 0.2 µm minisart filter. 500 µl aliquots were stored at –20 ºC.

8.1.2.16 Protein maker

Reagent	Volume	Supplier	Catalogue number
Prestained Protein Marker, Broad Rindge	-	NEB	P7708S

18 µl aliquots were stored at -20 ºC.

8.1.2.17 Bradford solution

Reagent	Volume	Supplier	Catalogue number
Protein assay	-	Bio-Rad	500-0006

The solution was stored at 4 ºC.

8.1.2.18 Ponceau S solution

Reagent	Volume	Supplier	Catalogue number
Ponceau S	200 mg	Sigma	P3504
Glacial Acetic Acid	10 ml	Fisher	A/0400/PB17

The volume was made up to 200 ml with distilled water. The solution was filter-sterilised using a 50 ml syringe and a 0.2 µm minisart filter. The solution was stored at room temperature.

8.1.3 Immunostaining works

8.1.3.1 2% Blocking solution

Reagent	Volume	Supplier	Catalogue number
BSA	2g	Sigma	A2153

The volume was made up to 100 ml PBS. The solution was filter-sterilised using a 50 ml syringe and a 0.2 µm minisart filter and stored at –20 ºC.

8.1.3.2 0.2% Triton ×-100

Reagent	Volume	Supplier	Catalogue number
Triton X-100	200µl	Sigma	T8787

The volume was made up to 100 ml with PBS (see 2.4.1.21). The solution was filter-sterilised using a 50 ml syringe and a 0.2 µm minisart filter. The solution was stored at room temperature.

8.1.3.3 0.2% Tween20

Reagent	Volume	Supplier	Catalogue number
Tween20	200µl	Sigma	P9416

The volume was made up to 100 ml with PBS (see 2.4.1.21). The solution was filter-sterilised using a 50 ml syringe and a 0.2 µm minisart filter. The solution was stored at room temperature.

8.1.3.4 4 M HCl

Reagent	Volume	Supplier	Catalogue number
Hydrochloric acid	10 ml	Fisher	H/1200/PB17
Distilled water	30 ml	-	

The solution was stored at room temperature.

8.1.3.5 Mounting solution

Reagent	Volume	Supplier	Catalogue number
VECTASHIELD® Mounting Medium with DAPI	-	Vector	H-1200

The solution was stored at 4 ºC.

8.1.3.6 Hypotonic solution

Reagent	Volume	Supplier	Catalogue number
Potassium Chloride	200 mg	BDH	101985M
Sodium Citrate	200 mg	Fisher	BPE 327-500

Potassium chloride and Sodium citrate were respectively dissolved in each 50 ml of distilled water. Two solutions were mixed together to give a final volume of 100 ml.

8.1.3.7 Fixative solution

Reagent	Volume	Supplier	Catalogue number
Methanol	15 ml	Fisher	M/4056/17
Glacial Acetic Acid	5 ml	Fisher	A/0400/PB17

Two solutions were mixed together in a ratio of 1:3.

8.1.3.8 4% PFA

Reagent	Volume	Supplier	Catalogue number
Paraformaldehyde	4	Sigma	P6148

The volume was made up to 100 ml with PBS. The solution was incubated at 60ºC for 2 h with shaking. 5 ml aliquots were stored at -20ºC.

8.1.4 Southern blotting works

8.1.4.1 20× SSC

Reagent	Volume	Supplier	Catalogue number
Sodium Chloride	175.3	Fisher	BPE 358-1
Sodium Citrate	88.2	Fisher	BPE 327-500

Sodium Chloride and Sodium Citrate were dissolved in 800 ml of distilled water and the pH was adjusted up to pH 7.0 with HCl. Then, the volume was made up to 1 liter with distilled water. The solution was autoclaved and stored at room temperature.

8.1.4.2 2× SSC

Reagent	Volume	Supplier	Catalogue number
20x SSC	100 ml	See 2.4.4.1	
Distilled water	900 ml	-	

The solution was autoclaved and stored at room temperature.

8.1.4.3 10% PVP

Reagent	Volume	Supplier	Catalogue number
Polyvinylpyrrolidone	5 g	Sigma	P5288

The volume was made up to 50 ml with distilled water. The solution stored at room temperature.

8.1.4.4 10% Ficoll

Reagent	Volume	Supplier	Catalogue number
Ficoll	5 g	GE Healthcare	17-0300-10

The volume was made up to 50 ml with distilled water. The solution was stored at room temperature.

8.1.4.5 10% BSA

Reagent	Volume	Supplier	Catalogue number
BSA	5g	Sigma	A2153

The volume was made up to 50 ml with distilled water. The solution was filter-sterilised using a 50 ml syringe and a 0.2 µm minisart filter and stored at –20 ºC.

8.1.4.6 1mg·ml^{-1} Heparin

Reagent	Volume	Supplier	Catalogue number
Heparin	100 mg	Fluka	51550

The volume was made up to 100 ml with distilled water. The solution was filter-sterilised using a 50 ml syringe and a 0.2 µm minisart filter and stored at –20 ºC.

8.1.4.7 2mg·ml^{-1} ssDNA

Reagent	Volume	Supplier	Catalogue number
Salmon sperm DNA	1 g	Sigma	D1626

The volume was made up to 500 ml with distilled water. The solution was stored at –20 ºC.

8.1.4.8 Pre-hybridisation solution for LINE-1

Reagent	Volume	Supplier	Catalogue number
20X SSC	7.5 ml	See 2.4.4.1	
0.5M EDTA	1 ml	See 2.4.1.6	
10% PVP	1 ml	See 2.4.4.3	
10% Ficoll	1 ml	See 2.4.4.4	
10% BSA	1 ml	See 2.4.4.5	
10% SDS	0.5 ml	See 2.4.1.4	
1 mg/ml Heparin	0.5 ml	See 2.4.4.6	
2 mg/ml ssDNA	1 ml	See 2.4.4.7	

The volume was made up to 50 ml with distilled water.

8.1.4.9 Hybridisation solution for LINE-1

Reagent	Volume	Supplier	Catalogue number
20X SSC	3.75 ml	See 2.4.4.1	
0.5M EDTA	0.5 ml	See 2.4.1.6	
10% PVP	0.5 ml	See 2.4.4.3	
10% Ficoll	0.5 ml	See 2.4.4.4	
10% BSA	0.5 ml	See 2.4.4.5	
10% SDS	0.25 ml	See 2.4.1.4	

1 mg/ml Heparin	0.25 ml	See 2.4.4.6	
2 mg/ml ssDNA	0.5 ml	See 2.4.4.7	
Dextran Sulfate	2.25 g	Sigma	D8906

The volume was made up to 25 ml with distilled water.

8.1.4.10 0.4 M NaOH

Reagent	Volume	Supplier	Catalogue number
Sodium Hydroxide	16 g	Fisher	BPE359-500

The volume was made up to 1 liter with distilled water. The solution was autoclaved and stored at room temperature.

8.1.4.11 2× SSC/0.1% SDS

Reagent	Volume	Supplier	Catalogue number
20×SSC	100 ml	See 2.4.4.1	
10% SDS	10 ml	See 2.4.1.4	

The solution was autoclaved and stored at room temperature.

8.1.4.12 0.1× SSC/0.1% SDS

Reagent	Volume	Supplier	Catalogue number
20×SSC	5 ml	See 2.4.4.1	
10% SDS	10 ml	See 2.4.1.4	

The solution was autoclaved and stored at room temperature.

8.1.4.13 20× SSPE

Reagent	Volume	Supplier	Catalogue number
Sodium Chloride	175.3 g	Fisher	BPE 358-1
Sodium Phosphate Monobasic	27.6 g	Sigma	S8282
EDTA	9.4 g	Fluka	3677

Sodium Chloride, Sodium Phosphate Monobasic and EDTA were dissolved in 800 ml of distilled water and the pH was adjusted to pH 7.4 with NaOH (~ 27 ml/litre of 10 N NaOH). Then, the volume was made up to 1 liter with distilled water. The solution was autoclaved and stored at room temperature.

8.1.4.14 5× SSPE

Reagent	Volume	Supplier	Catalogue number
20× SSPE	250 ml	See 2.4.4.13	

The solution was autoclaved and stored at room temperature.

8.1.4.15 50× Denhardt's solution

Reagent	Volume	Supplier	Catalogue number
Polyvinylpyrrolidone	10 g	Sigma	P5288
Ficoll	10 g	GE Healthcare	17-0300-10
BSA	10 g	Fluka	3677

The volume was made up to 100 ml with distilled water. The solution was stored at room temperature.

8.1.4.16 Hybridisation solution for oligonucleotide probe

Reagent	Volume	Supplier	Catalogue number
20x SSPE	12.5 ml	See 2.4.4.13	
50x Denhardt's solution	10 ml	See 2.4.4.15	

10% SDS	0.5 ml	See 2.4.1.4
2 mg/ml ssDNA	1 ml	See 2.4.4.7

The volume was made up to 50 ml with distilled water.

8.1.5 Cell culture works

8.1.5.1 MEFs medium

Reagent	Volume	Supplier	Catalogue number
Dulbecco's Modifed Eagle Media (DMEM)	500ml	Invitrogen	21969-035
Fetal Bovine Serum (FBS)	50ml	Invitrogen	10106-169
100X MEM Non-Essential Amino Acids (NEAA)	5ml	Invitrogen	11140-050
200mM L-Glutamine	5ml	Invitrogen	25030-149

FBS, NEAA and L-Glutamine were added and mixed together in a universal tube. The mixture was added into DMEM by filter-sterilisation using a 50 ml syringe and a 0.2 µm minisart filter (Sartorius: SM16532K).

8.1.5.2 Mitomycin C

Reagent	Volume	Supplier	Catalogue number
Mitomycin C (MMC)	2mg	Sigma	M4287

2 mg of Mitomycin C was dissolved in 200 ml of MEFs medium (see 2.4.5.1) to give a final concentration of 10 $\mu g \cdot ml^{-1}$. The solution was filter-sterilised using a 50 ml syringe and a 0.2 µm minisart filter. 5 ml aliquots were stored at –20 ºC.

8.1.5.3 BG-K medium

Reagent	Volume	Supplier	Catalogue number
DMEM-12	500ml	Invitrogen	11320-058
Knockout Serum Replacement (KSR)	90ml	Invitrogen	10828-028
100X NEAA	6ml	Invitrogen	11140-035
200mM Glutamax-I supplement	6ml	Invitrogen	25030-024
1M β-Mercaptoethanol	60µl	Sigma	M7522
4 µg/ml Fibroblast Growth Factor (FGF)	600µl	Sigma	F0291

KSR, NEAA, Glutamax and 1M β-Mercaptoethanol were added and mixed together in a container. The mixture was added into DMEM-12 by filter-sterilisation using a 50 ml syringe and a 0.2 µm minisart filter (Sartorius: SM16532K). To make 1 M β-Mercaptoethanol, 1 ml of 14.3 M β-Mercaptoethanol was mixed with 13.3 ml of water (Sigma: W3500). The solution was filter-sterilised using a 50 ml syringe and a 0.2 µm minisart filter and stored at 4ºC. To make 4 $\mu g \cdot ml^{-1}$ bFGF, 1 mg bFGF was dissolved in 246.80 ml of PBS. 3.25 ml of 7.5% BSA was added into the bFGF solution. Then, the solution was filter-sterilised using a 0.20 µm filter (Sartorius: 17597K). 2 ml aliquots were stored at -80 ºC.

8.1.5.4 Matrigel

Reagent	Volume	Supplier	Catalogue number
Matrigel Basement Membrane Matrix	-	BD Biosciences	354234

The Matrigel was thawed on ice in the fridge overnight. 0.5 ml aliquots were placed into chilled tubes by a chilled 5 ml pipette. Immediately, aliquots were stored at –80 ºC.

8.1.5.5 Trypsin EDTA

Reagent	Volume	Supplier	Catalogue number

0.05% Trypsin EDTA	100ml	Invitrogen	25300-054

Trypsin EDTA was thawed in the fridge overnight. Once completely thawed, 20 ml aliquots were placed into universal tubes. They were stored at –20 ºC.

8.1.5.6 Cryopreservation medium

Reagent	Volume	Supplier	Catalogue number
Hyclone ES FBS	4 ml	Perbio	SH30070.03
DMSO	1 ml	Sigma	D5879

4 parts of Hyclone FBS and 1 part of DMSO were mixed together. The solution was filter-sterilised using a 10 ml syringe and a 0.2 µm minisart filter and stored at 4ºC.

8.1.5.7 0.1% Gelatine solution

Reagent	Volume	Supplier	Catalogue number
Gelatin	500mg	Sigma	G9391

Gelatin was dissolved in 500 ml of distilled water. The solution was autoclaved and stored at room temperature.

8.1.5.8 KaryoMax

Reagent	Volume	Supplier	Catalogue number
Karyo MAX® Colcemide®	-	Invitrogen	15212-046

This solution was stored at 4ºC.

8.1.5.9 GeneJammer® transfection reagent

Reagent	Volume	Supplier	Catalogue number
GeneJammer® transfection reagent	-	Stratagene	204132

The reagent was stored at 4ºC.

9 Appendix 2

List of Suppliers Details

Company	Website
Abcam, Plc.	http://www.abcam.com
Alpha Laboratories (UK)	http://www.alphalabs.co.uk
Amaxa AG	http://www.amaxa.com
Ambion, Inc. C/O Applied Biosystems	http://www.ambion.com
Applied Biosystems	http://www.appliedbiosystems.com
Axygen Scientific, Inc.	http://www.axygen.com
Beckman Coulter (UK), Ltd.	http://www.beckmancoulter.co.uk
BDH, C/O VWR International (UK), Ltd.	http://uk.vwr.com
Cambio (UK), Ltd.	http://www.cambio.co.uk
Charles River Laboratories, Inc.	http://www.criver.com
Chemicon Europe, Ltd.	http://www.chemicon.com
Clontech-Takara Bio Europe	http://www.clontech.com
Eppendorf (UK), Ltd.	http://www.eppendorf.co.uk
Fermentas	http://www.fermentas.com
Fisher Scientific (UK), Ltd.	http://www.fisher.co.uk
GE Healthcare	http://www.gehealthcare.com
Grant Instruments (UK), Ltd.	http://www.grant.co.uk
Hyclone	http://www.hyclone.com
Improvision	http://www.improvision.com
Invitrogen, Ltd.	http://www.invitrogen.com
Jackson Immunoresearch Laboratories, Inc.	http://www.jacksonimmuno.com
Leica Microsystems	http://www.leicamicrosystems.com
Menzel-Glaser	http://www.menzel.de
Merck Chemicals (UK), Ltd.	http://www.merckbiosciences.co.uk
NanoDrop Technologies	http://www.nanodrop.com
New England Biolabs (UK), Ltd.	http://www.neb.uk.com
Nikon Ltd.	http://www.europe-nikon.com
Nalge Nunc International	http://www.nuncbrand.com
Qiagen, Ltd.	http://www.qiagen.com
Raytek Scientific (UK), Ltd.	http://www.raytek.co.uk
Roche Diagnostics Ltd.	http://www.rocheuk.com
Sartorius (UK), Ltd.	http://www.sartorius.co.uk
Santa Cruz Biotechnology, Inc.	http://www.scbt.com
Scientific Laboratory Supplies, Ltd.	http://www.scientificlabs.eu
Sigma-Genosys/ Sigma-Aldrich Ltd.	http://www.sigmaaldrich.com
SPSS (UK), Ltd.	http://www.ssps.com/uk
Vector Laboratories, Ltd.	http://www.vectorlabs.com

10 Appendix 3

Post Hoc Tests

Multiple Comparisons

	(I) Group	(J) Group	Mean Difference (I-J)	Std. Error	Sig.	95% Confidence Interval	
			Lower Bound	Upper Bound	Lower Bound	Upper Bound	Lower Bound
Tukey HSD	TC	p336 #1	.08135	.07742	.969	-.2249	.3876
		p336 #9	.16691	.07742	.495	-.1394	.4732
		p388 #8	.09063	.07742	.945	-.2157	.3969
		p388 #9	.13804	.07742	.692	-.1683	.4443
		hESOD1 #1	.76784(*)	.07742	.000	.4616	1.0741
		hESDO1 #3	.42107(*)	.07742	.007	.1148	.7274
		hESOD1 #4	.65802(*)	.07742	.000	.3517	.9643
		hESOD1 #9	.78141(*)	.07742	.000	.4751	1.0877
	p336 #1	TC	-.08135	.07742	.969	-.3876	.2249
		p336 #9	.08557	.07742	.959	-.2207	.3919
		p388 #8	.00928	.07742	1.000	-.2970	.3156
		p388 #9	.05669	.07742	.997	-.2496	.3630
		hESOD1 #1	.68649(*)	.07742	.000	.3802	.9928
		hESDO1 #3	.33972(*)	.07742	.028	.0334	.6460
		hESOD1 #4	.57667(*)	.07742	.001	.2704	.8830
		hESOD1 #9	.70007(*)	.07742	.000	.3938	1.0064
	p336 #9	TC	-.16691	.07742	.495	-.4732	.1394
		p336 #1	-.08557	.07742	.959	-.3919	.2207
		p388 #8	-.07629	.07742	.978	-.3826	.2300
		p388 #9	-.02888	.07742	1.000	-.3352	.2774
		hESOD1 #1	.60092(*)	.07742	.001	.2946	.9072
		hESDO1 #3	.25415	.07742	.125	-.0521	.5604
		hESOD1 #4	.49110(*)	.07742	.002	.1848	.7974
		hESOD1 #9	.61450(*)	.07742	.000	.3082	.9208
	p388 #8	TC	-.09063	.07742	.945	-.3969	.2157
		p336 #1	-.00928	.07742	1.000	-.3156	.2970
		p336 #9	.07629	.07742	.978	-.2300	.3826
		p388 #9	.04741	.07742	.999	-.2589	.3537
		hESOD1 #1	.67721(*)	.07742	.000	.3709	.9835
		hESDO1 #3	.33044(*)	.07742	.033	.0242	.6367
		hESOD1 #4	.56739(*)	.07742	.001	.2611	.8737
		hESOD1 #9	.69079(*)	.07742	.000	.3845	.9971
	p388 #9	TC	-.13804	.07742	.692	-.4443	.1683
		p336 #1	-.05669	.07742	.997	-.3630	.2496
		p336 #9	.02888	.07742	1.000	-.2774	.3352
		p388 #8	-.04741	.07742	.999	-.3537	.2589
		hESOD1 #1	.62980(*)	.07742	.000	.3235	.9361
		hESDO1 #3	.28303	.07742	.075	-.0233	.5893
		hESOD1 #4	.51998(*)	.07742	.002	.2137	.8263
		hESOD1 #9	.64338(*)	.07742	.000	.3371	.9497
	hESOD1 #1	TC	-.76784(*)	.07742	.000	-1.0741	-.4616
		p336 #1	-.68649(*)	.07742	.000	-.9928	-.3802
		p336 #9	-.60092(*)	.07742	.001	-.9072	-.2946

		p388 #8	-.67721(*)	.07742	.000	-.9835	-.3709
		p388 #9	-.62980(*)	.07742	.000	-.9361	-.3235
		hESDO1 #3	-.34677(*)	.07742	.025	-.6531	-.0405
		hESOD1 #4	-.10982	.07742	.866	-.4161	.1965
		hESOD1 #9	.01358	.07742	1.000	-.2927	.3199
	hESDO1 #3	TC	-.42107(*)	.07742	.007	-.7274	-.1148
		p336 #1	-.33972(*)	.07742	.028	-.6460	-.0334
		p336 #9	-.25415	.07742	.125	-.5604	.0521
		p388 #8	-.33044(*)	.07742	.033	-.6367	-.0242
		p388 #9	-.28303	.07742	.075	-.5893	.0233
		hESOD1 #1	.34677(*)	.07742	.025	.0405	.6531
		hESOD1 #4	.23695	.07742	.167	-.0693	.5432
		hESOD1 #9	.36034(*)	.07742	.020	.0541	.6666
	hESOD1 #4	TC	-.65802(*)	.07742	.000	-.9643	-.3517
		p336 #1	-.57667(*)	.07742	.001	-.8830	-.2704
		p336 #9	-.49110(*)	.07742	.002	-.7974	-.1848
		p388 #8	-.56739(*)	.07742	.001	-.8737	-.2611
		p388 #9	-.51998(*)	.07742	.002	-.8263	-.2137
		hESOD1 #1	.10982	.07742	.866	-.1965	.4161
		hESDO1 #3	-.23695	.07742	.167	-.5432	.0693
		hESOD1 #9	.12339	.07742	.788	-.1829	.4297
	hESOD1 #9	TC	-.78141(*)	.07742	.000	-1.0877	-.4751
		p336 #1	-.70007(*)	.07742	.000	-1.0064	-.3938
		p336 #9	-.61450(*)	.07742	.000	-.9208	-.3082
		p388 #8	-.69079(*)	.07742	.000	-.9971	-.3845
		p388 #9	-.64338(*)	.07742	.000	-.9497	-.3371
		hESOD1 #1	-.01358	.07742	1.000	-.3199	.2927
		hESDO1 #3	-.36034(*)	.07742	.020	-.6666	-.0541
		hESOD1 #4	-.12339	.07742	.788	-.4297	.1829
Bonferroni	TC	p336 #1	.08135	.07742	1.000	-.2708	.4335
		p336 #9	.16691	.07742	1.000	-.1852	.5191
		p388 #8	.09063	.07742	1.000	-.2615	.4428
		p388 #9	.13804	.07742	1.000	-.2141	.4902
		hESOD1 #1	.76784(*)	.07742	.000	.4157	1.1200
		hESDO1 #3	.42107(*)	.07742	.015	.0689	.7732
		hESOD1 #4	.65802(*)	.07742	.000	.3059	1.0102
		hESOD1 #9	.78141(*)	.07742	.000	.4293	1.1336
	p336 #1	TC	-.08135	.07742	1.000	-.4335	.2708
		p336 #9	.08557	.07742	1.000	-.2666	.4377
		p388 #8	.00928	.07742	1.000	-.3429	.3614
		p388 #9	.05669	.07742	1.000	-.2955	.4088
		hESOD1 #1	.68649(*)	.07742	.000	.3343	1.0386
		hESDO1 #3	.33972	.07742	.063	-.0124	.6919
		hESOD1 #4	.57667(*)	.07742	.001	.2245	.9288
		hESOD1 #9	.70007(*)	.07742	.000	.3479	1.0522
	p336 #9	TC	-.16691	.07742	1.000	-.5191	.1852
		p336 #1	-.08557	.07742	1.000	-.4377	.2666
		p388 #8	-.07629	.07742	1.000	-.4284	.2759
		p388 #9	-.02888	.07742	1.000	-.3810	.3233
		hESOD1 #1	.60092(*)	.07742	.001	.2488	.9531
		hESDO1 #3	.25415	.07742	.342	-.0980	.6063
		hESOD1 #4	.49110(*)	.07742	.005	.1389	.8433

		hESOD1 #9	.61450(*)	.07742	.001	.2623	.9667
	p388 #8	TC	-.09063	.07742	1.000	-.4428	.2615
		p336 #1	-.00928	.07742	1.000	-.3614	.3429
		p336 #9	.07629	.07742	1.000	-.2759	.4284
		p388 #9	.04741	.07742	1.000	-.3047	.3996
		hESOD1 #1	.67721(*)	.07742	.000	.3251	1.0294
		hESDO1 #3	.33044	.07742	.075	-.0217	.6826
		hESOD1 #4	.56739(*)	.07742	.002	.2152	.9195
		hESOD1 #9	.69079(*)	.07742	.000	.3386	1.0429
	p388 #9	TC	-.13804	.07742	1.000	-.4902	.2141
		p336 #1	-.05669	.07742	1.000	-.4088	.2955
		p336 #9	.02888	.07742	1.000	-.3233	.3810
		p388 #8	-.04741	.07742	1.000	-.3996	.3047
		hESOD1 #1	.62980(*)	.07742	.001	.2776	.9820
		hESDO1 #3	.28303	.07742	.190	-.0691	.6352
		hESOD1 #4	.51998(*)	.07742	.003	.1678	.8721
		hESOD1 #9	.64338(*)	.07742	.001	.2912	.9955
	hESOD1 #1	TC	-.76784(*)	.07742	.000	-1.1200	-.4157
		p336 #1	-.68649(*)	.07742	.000	-1.0386	-.3343
		p336 #9	-.60092(*)	.07742	.001	-.9531	-.2488
		p388 #8	-.67721(*)	.07742	.000	-1.0294	-.3251
		p388 #9	-.62980(*)	.07742	.001	-.9820	-.2776
		hESDO1 #3	-.34677	.07742	.055	-.6989	.0054
		hESOD1 #4	-.10982	.07742	1.000	-.4620	.2423
		hESOD1 #9	.01358	.07742	1.000	-.3386	.3657
	hESDO1 #3	TC	-.42107(*)	.07742	.015	-.7732	-.0689
		p336 #1	-.33972	.07742	.063	-.6919	.0124
		p336 #9	-.25415	.07742	.342	-.6063	.0980
		p388 #8	-.33044	.07742	.075	-.6826	.0217
		p388 #9	-.28303	.07742	.190	-.6352	.0691
		hESOD1 #1	.34677	.07742	.055	-.0054	.6989
		hESOD1 #4	.23695	.07742	.488	-.1152	.5891
		hESOD1 #9	.36034(*)	.07742	.043	.0082	.7125
	hESOD1 #4	TC	-.65802(*)	.07742	.000	-1.0102	-.3059
		p336 #1	-.57667(*)	.07742	.001	-.9288	-.2245
		p336 #9	-.49110(*)	.07742	.005	-.8433	-.1389
		p388 #8	-.56739(*)	.07742	.002	-.9195	-.2152
		p388 #9	-.51998(*)	.07742	.003	-.8721	-.1678
		hESOD1 #1	.10982	.07742	1.000	-.2423	.4620
		hESDO1 #3	-.23695	.07742	.488	-.5891	.1152
		hESOD1 #9	.12339	.07742	1.000	-.2288	.4756
	hESOD1 #9	TC	-.78141(*)	.07742	.000	-1.1336	-.4293
		p336 #1	-.70007(*)	.07742	.000	-1.0522	-.3479
		p336 #9	-.61450(*)	.07742	.001	-.9667	-.2623
		p388 #8	-.69079(*)	.07742	.000	-1.0429	-.3386
		p388 #9	-.64338(*)	.07742	.001	-.9955	-.2912
		hESOD1 #1	-.01358	.07742	1.000	-.3657	.3386
		hESDO1 #3	-.36034(*)	.07742	.043	-.7125	-.0082
		hESOD1 #4	-.12339	.07742	1.000	-.4756	.2288

* The mean difference is significant at the .05 level.

Homogeneous Subsets

	Group	N	Subset for alpha = .05			
		1	2	3	4	1
Tukey HSD(a)	hESOD1 #9	2	4.0804			
	hESOD1 #1	2	4.0940			
	hESOD1 #4	2	4.2038	4.2038		
	hESDO1 #3	2		4.4408	4.4408	
	p336 #9	2			4.6949	4.6949
	p388 #9	2			4.7238	4.7238
	p388 #8	2				4.7712
	p336 #1	2				4.7805
	TC	2				4.8618
	Sig.		.788	.167	.075	.495
Tukey B(a)	hESOD1 #9	2	4.0804			
	hESOD1 #1	2	4.0940			
	hESOD1 #4	2	4.2038	4.2038		
	hESDO1 #3	2		4.4408		
	p336 #9	2			4.6949	
	p388 #9	2			4.7238	
	p388 #8	2			4.7712	
	p336 #1	2			4.7805	
	TC	2			4.8618	

Means for groups in homogeneous subsets are displayed.
a Uses Harmonic Mean Sample Size = 2.000.

Means Plots

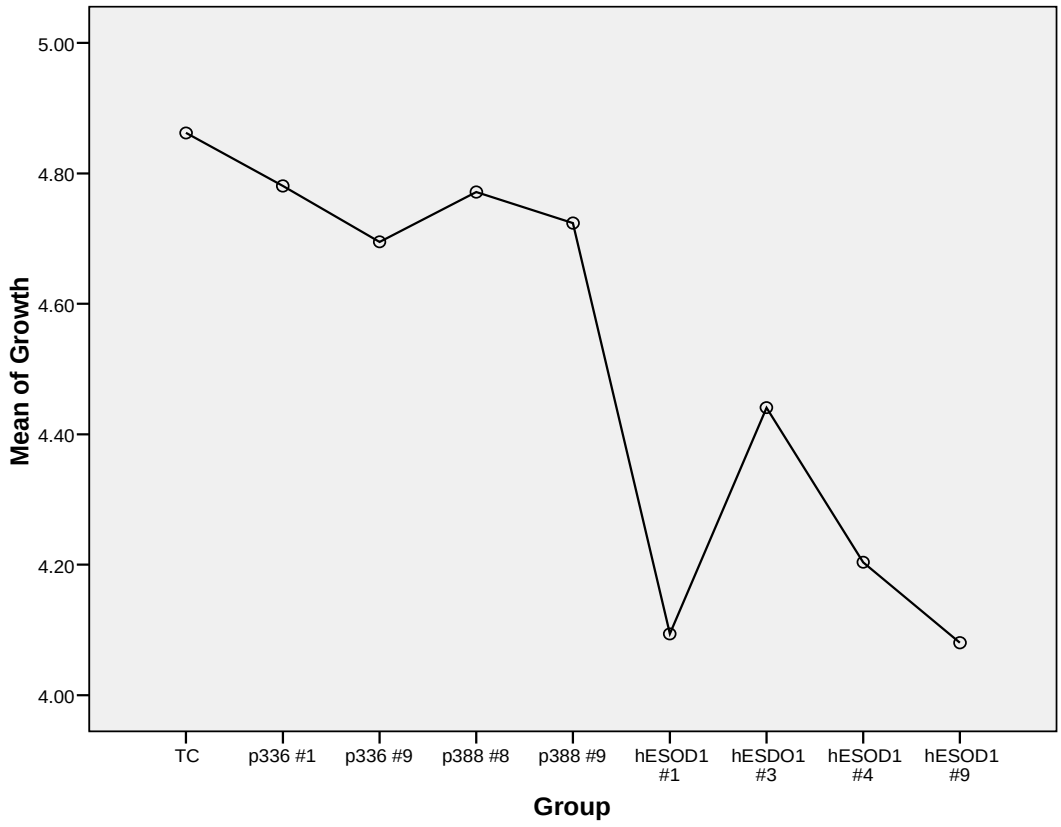

Kruskal-Wallis Test

Ranks

	Group	N	Mean Rank
Growth	TC	2	17.50
	p336 #1	2	14.50
	p336 #9	2	10.50
	p388 #8	2	13.50
	p388 #9	2	11.50
	hESOD1 #1	2	2.50
	hESDO1 #3	2	7.50
	hESOD1 #4	2	5.00
	hESOD1 #9	2	3.00
	Total	18	

Test Statistics(a,b)

	Growth
Chi-Square	15.825
df	8
Asymp. Sig.	.045

a Kruskal Wallis Test
b Grouping Variable: Group

Mann-Whitney Test

Ranks

	Group	N	Mean Rank	Sum of Ranks
Growth	1.00	2	1.50	3.00
	2.00	8	6.50	52.00
	Total	10		

Test Statistics(b)

	Growth
Mann-Whitney U	.000
Wilcoxon W	3.000
Z	-2.089
Asymp. Sig. (2-tailed)	.037
Exact Sig. [2*(1-tailed Sig.)]	.044(a)
Exact Sig. (2-tailed)	.044
Exact Sig. (1-tailed)	.022
Point Probability	.022

a Not corrected for ties.
b Grouping Variable: Group